Part A, Volume 1, No. 12, December 1963

Journal of Polymer Science

Part A: General Papers

Editorial Board: R. M. Fuoss • J. J. Hermans • H. Mark • H. W. Melville • C. G. Overberger • G. Smets

Contents

Editorial 3521

HAROLD SCHONHORN: Generalized Approach to Adhesion Via the Interfacial Deposition of Amphipathic Molecules. II. Adhesion of Polyethylene to Aluminum 3523

HISASHI UEDA, ZENICHIRO KURI, and SHOJI SHIDA: Electron Spin Resonance Studies of the Reaction of Gases with the Radicals Formed in Irradiated Polytetrafluoroethylene 3537

M. KHAIRY, S. MORSI, and CLARENCE STERLING: Crystallization in Starch: The Role of Ions in the Lyotropic Series 3547

JOSEPH PELLON: Polyamides Containing Phosphorus. II. Structural Effects on Softening and Glass Transition Temperatures 3561

G. NATTA, G. CRESPI, and U. FLISI: Thermodynamic Interpretations of the Elastic Properties of Rubbers Obtained from Ethylene–Propylene Copolymers 3569

BERNHARD WUNDERLICH, PETER SULLIVAN, TAMIO ARAKAWA, A. B. DICYAN, and J. F. FLOOD: Thermodynamics of Crystalline Linear High Polymers. III. Thermal Breakdown of the Crystalline Lattice of Polyethylene 3581

THOR L. SMITH: Ultimate Tensile Properties of Elastomers. I. Characterization by a Time and Temperature Independent Failure Envelope 3597

WILLIAM J. BURKE and HAROLD P. HIGGINBOTTOM: Nitrosation of Linear Phenol-Formaldehyde Polymers 3617

H. R. ALLCOCK and R. L. KUGEL: Ionic Polymerization of Diphenylvinylphosphine Oxide 3627

ARIEL OTTOLENGHI, SAMUEL BARZAKAY, and ALBERT ZILKHA: Anionic Polymerization of Acrylonitrile by Various Catalysts 3643

ROBERT H. HORROCKS and EUGENE C. WINSLOW: Oxine–Formaldehyde Polymers and Their Metallic Chelates 3655

continued inside

Published by INTERSCIENCE PUBLISHERS a division of John Wiley & Sons, Inc.

Journal of Polymer Science **Part A: General Papers**

Editorial Board:

R. M. Fuoss • J. J. Hermans • H. Mark • H. W. Melville • C. G. Overberger • G. Smets

Advisory Board:

T. Alfrey, Jr.	P. Debye	O. Kratky	G. V. Schulz
W. O. Baker	F. Eirich	M. Magat	H. M. Spurlin
H. Benoit	P. J. Flory	C. S. Marvel	A. J. Staverman
C. J. Bevington	J. Furukawa	G. Natta	J. K. Stille
J. W. Breitenbach	G. Gee	S. Okamura	W. H. Stockmayer
A. M. Bueche	A. Katchalsky	A. Peterlin	M. Szwarc
C. W. Bunn	A. Kelier	C. C. Price	A. V. Tobolsky
G. M. Burnett	G. M. Kline	Ch. Sadron	K. Ueberreiter
F. S. Dainton		N. G. Gaylord, Book Review Editor	

Contents (continued), Volume 1, No. 12

BOOK REVIEW

Makromolekulare Stoffe, Part II, Vol. XIV, Methoden der Organischen Chemie, (Houben-Weyl), E. MÜLLER, Ed., Reviewed by NORBERT M. BIKALES 3665

Errata

O. C. HANSEN, T. L. FABRY, L. MARKER, and O. J. SWEETING: Apparatus for Measuring the Dynamic Modulus of Thin Polymer Films (article in *J. Polymer Sci.*, A1, 1585–1600, 1963) 3666

M. WALES and S. J. REHFELD: Molecular Weight Distribution by Velocity Ultracentrifugation (article in *J. Polymer Sci.*, 62, 179–196, 1962) 3666

Author Index Volume 1 3667

Subject Index Volume 1 3678

Volume Title Page i

Volume Contents iii

The Journal of Polymer Science is published in three sections as follows: Part A, General Papers, monthly; Part B, Polymer Letters, monthly; Part C, Polymer Symposia, irregular.

Published semi-monthly by Interscience Publishers, a Division of John Wiley & Sons, Inc., covering one volume annually. Publication Office at 20th and Northampton Sts., Easton, Pa. Executive, Editorial, and Circulation Offices at 605 Third Avenue, New York 16, N. Y. Second-class postage paid at Easton, Pa. Subscription price, $154.00 per volume (including Part B: Polymer Letters; and Part C: Polymer Symposia). Foreign postage $3.50 per volume (including Parts B and C).

Copyright © 1963, by John Wiley & Sons, Inc. *Printed in U.S.A.*

EDITORIAL

The year of 1963 is the first in which the Journal was presented in its new format, i.e., divided into 3 parts; (A) General Papers, (B) Letters, and (C) Symposia. Papers related to biopolymers have been published in a companion journal, *Biopolymers*. The new mode of publication proved to be efficient and expedient and enabled us to fulfill the aims we outlined in our editorial of last year.

General Papers could be published in regular sequence, in the order of their acceptance by the editors, and the issues of Part A appeared at regular monthly intervals. Letters to the Editors could be published within 6 to 8 weeks. Symposia could be published whenever manuscripts were ready, without interrupting the flow of the general papers.

But our goal of reducing the time-lag between acceptance of papers and publication to 6–8 months could not be achieved. The reason was the unexpected increase in the submission of publishable papers. In an effort to improve this situation immediately, the following steps have been taken during 1963:

(*1*) The editors are turning back a larger percentage of manuscripts either because they are not of direct interest to the readers of the Journal, or because they do not fully meet quality requirements.

(*2*) The editors are systematically encouraging the authors to reduce the size of their manuscripts.

(*3*) The publishers are enlarging the 1963 Journal from the originally planned 4800 pages to 5800 pages (Part A—4300; Part B—600; Part C—900) *without additional charge*.

These measures will not be sufficient for 1964 when we expect at least 1000 additional pages consisting of original material and the following symposia: IUPAC Paris Symposium and the ACS Symposium on Thermal Analysis of Polymers and the Rheo-Optics Symposium held at the University of Massachusetts.

Editors and publishers are firmly convinced that the value of the Journal will be greatly enhanced for contributors and authors alike by the reduction of publication time to 6–8 months. To reach this goal, the editors will become more strict in accepting and reducing papers. But this will not be sufficient to enable us to publish approximately 9000 pages (Part A—5850; Part B—750; Part C—2400), which we need to reduce the publication time. We are therefore forced to raise our subscription price again.

We believe that this is a wiser course than to establish a page charge for contributors or their employers, a practice which has become customary among scientific societies.

We further wish to announce that we will publish at the beginning of 1964 a Cumulative Index (Author and Subject) for Volumes I to LXII (1946 to 1962). As you know, a substantial part of the research and development of polymer science has been published in our Journal. The Index will therefore become an indispensable source of information for all future research and will not only give the owner of the Journal access to the published material, but will become an important desk tool for everybody who is engaged in research and in publication in the polymer field.

We have the following plans for our companion journals for 1964: The *Journal of Applied Polymer Science* will be increased in size by 600 pages, and *Biopolymers* will be published in 2 Parts: General Papers and the Stanford Symposium on Quantum Aspects of Polypeptides and Polynucleotides.

Editorial Board and Publishers

JOURNAL OF POLYMER SCIENCE: PART A VOL. 1, PP. 3523–3536 (1963)

Generalized Approach to Adhesion Via the Interfacial Deposition of Amphipathic Molecules. II. Adhesion of Polyethylene to Aluminum

HAROLD SCHONHORN, *Bell Telephone Laboratories, Incorporated, Murray Hill, New Jersey*

Synopsis

Oriented monolayer adhesives of radioactive stearic acid have been employed to bond polyethylene to aluminum. Bonding time, bonding temperature, and rate of peel are several of the parameters that were varied to determine their effect on the final peel strength. Techniques for maximizing the resistance to peel are discussed and incorporated in this communication. Peel strengths in excess of 100 lb./in. width are reported with stearic acid as the monolayer adhesive. The peel forces obtained in the present investigation are more than two orders of magnitude greater than those reported in the literature. The only limitation being the cohesive strength of the thermoplastic adhered. Kaeble's peel force theory is described and adapted to our experimental data. Reasonably good agreement is obtained for low peel strengths ($\leq$25 lb./in. width).

I. INTRODUCTION

Previously,[1] it has been demonstrated that the adsorption of condensed monolayers of long chain amphipathic molecules between selected adherends afforded a bonding phase possessing a high degree of orientation, uniformity and specificity. Oriented condensed monolayers of these amphipathic molecules were employed as effective adhesives in bonding polyethylene to aluminum producing bond strengths exceeding the cohesive strength of the bulk polyethylene. Data obtained from contact angle and tracer experiments have helped to optimize the bonding conditions described in the previous communication.

Monolayer desorption data[1] indicated that chemisorption of the polar functional groups occurred when they came into contact with the sulfochromated aluminum surface. In addition, the aliphatic portion of the monomolecular layer has been shown to be mechanically encapsulated as well as chemically bonded to the hydrophobic polymer phase.

In this communication the peel strength data presented previously will be extended to illustrate further the degree of the adhesion of polyethylene to aluminum. As in the past, the 180° peel test corresponding to ASTM test D903-49 will be used exclusively. Bonding time, bonding temperature, and rate of peel are several of the parameters that were varied to determine their affect on the final peel strength.

The residual film thickness of polyethylene on the aluminum surface after peeling is determined by employing radiolabeled stearic acid as the oriented monolayer adhesive. When one considers the residual film after peeling as the adhesive thickness, reasonably good agreement is obtained with the existing theory up to 25 lb./in. width.

II. EXPERIMENTAL

A. Material

Stearic acid, labeled with C^{14} in the carboxyl group, of specific activity 8.3 mc./mmole, was obtained from Tracerlab Inc., Waltham, Massachusetts. The force–area isotherms of this radioactive species on deionized water and 0.0005*M* aluminum chloride produced extrapolated areas per molecule at zero compression of 20.5 and 29.6 A.,[2] respectively. The collapse pressure of the stearic acid on deionized water was 42.5 dynes/cm., while the collapse pressure of the stearic acid on 0.0005*M* aluminum chloride was 43 dynes/cm. The purity of this material was verified by Dr. L. H. Sharpe of the Bell Telephone Laboratories, Inc., using the technique of infrared spectroscopy involving frustrated total internal reflection.[2]

B. Peel Experiments

Sulfochromated Alclad aluminum 2024-T3 test specimens (5 × 1 × 1/16 in.), coated with a monolayer of stearic acid deposited at 30 dynes/cm. surface pressure, were bonded with sections of abraded and acetone-washed polyethylene 5 × 1 × 1/16 in. on a calibrated hot stage. They were cooled, then peeled at 180° according to ASTM D903-49 (test for peel or stripping strengths of adhesives) except that crosshead separation rates ranging from 0.2 to 20 in./min. were employed. Three bonded specimens were peeled for each reported value. The results are reproducible within ±5% of the recorded value.

For the remainder of the materials and the preparation and characterization of the monolayers, the reader is referred to Part I of this series.[1]

All experiments reported here were carried out at room temperature (21–23°C.) unless otherwise noted.

III. THEORY

A discussion of the theory is outlined in Part I of this series. The experimental data obtained in the present communication substantiate the theoretical analysis. The results of this analysis may be summarized in the following manner.

The adsorption energy of a mole of amphipathic molecules on a polar substrate would be

$$E_{ads} \cong -1440(n)$$

where n is the number of methylene groups in the hydrophobic portion of the molecule. The energy liberated in the adsorption of 1 cm.^{2} of surface would be 700 ergs, or $\Delta E_{ads} \cong -700$ ergs/cm.^{2}.

If we have the hydrocarbon portion of our amphipathic molecule dissolved in the polymer phase to which we are bonding, and possibly chemically bonded to this phase by a crosslinking phenomenon, the energy necessary to rupture the interface would be prohibitive. Therefore only failure of one or both of the adherends should result.

IV. RESULTS AND DISCUSSION

The effect of surface pressure as a function of peel force[1] has indicated that low surface coverage results in a decrease from the maximum bond strength which we can realize when a fully condensed monolayer is adsorbed onto our polar adherend. For this reason, in the present investigation 30 dynes/cm. were used as the plating pressure.

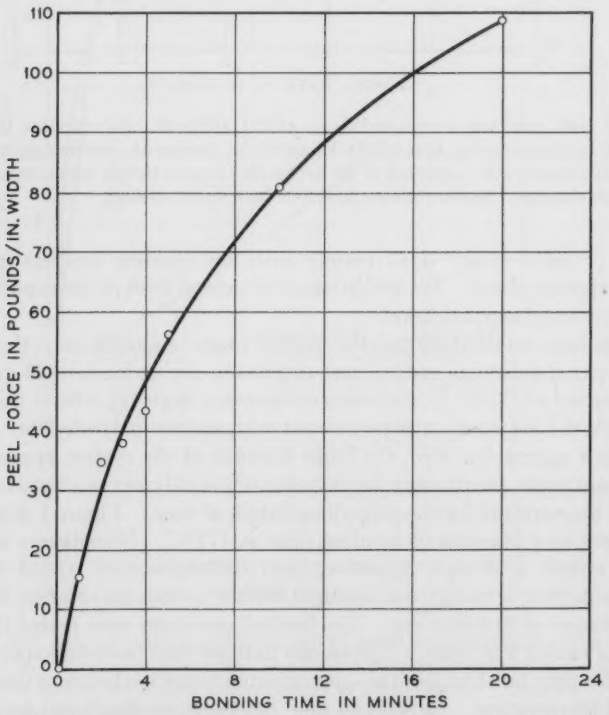

Fig. 1. 180° peel test corresponding to ASTM D903-49. Polyethylene bonded at 177°C. for varying lengths of time to sulfochromated Alclad 2024-T3 aluminum having an adsorbed monolayer of radioactive stearic acid deposited at 30 dynes/cm. from a trough containing 0.0005M aluminum chloride. Peel rate was 5 in./min. Specimens were peeled the day of preparation.

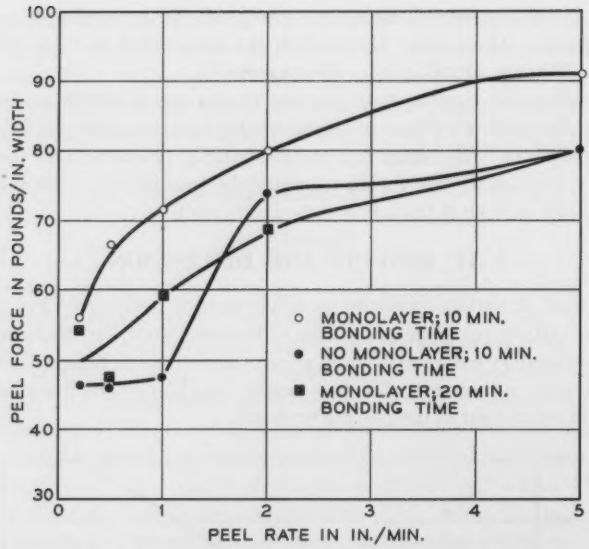

Fig. 2. 180° peel test corresponding to ASTM D903-49. Polyethylene bonded at 205°C. to sulfochromated Alclad 2024-T3 aluminum having an adsorbed monolayer of radioactive stearic acid deposited at 30 dynes/cm. from a trough containing 0.0005*M* aluminum chloride. Specimens were aged four days prior to testing.

The previous study[1] dealt mainly with low bonding temperatures and short exposure times. We will attempt to extend both of these parameters in the present communication.

It has been established that the contact angle of molten polyethylene on the prepared substrate goes to zero degrees in approximately 20 min. at a temperature of 175°C.[1] The observed contact angle (θ) reflects the extent to which the prepared substrate is wet with molten polyethylene. Moreover, as θ approaches zero, the bond strength of the system approaches a maximum value, barring any degradation of the polymer as a result of being at that temperature for the prescribed length of time. Figure 1 depicts the peel force as a function of bonding time at 177°C. Monolayers of radioactive stearic acid were deposited onto sulfochromated Alclad 2024-T3 aluminum from a trough containing 0.0005*M* aluminum chloride at a surface pressure of 30 dynes/cm. The bonded specimens were peeled the same day at a rate of 5 in./min. The results indicate that the whole spectrum of peel force may be obtained, the only criterion being the bonding time at the desired temperature. Beyond 20 min. exposure, no significant increase in peel force was noticed. Peel force for 30 min. exposure is the same as that for 20 min. These data further substantiate our contact angle experiments. For a particular application only a few pounds per inch of width peel force may be satisfactory. This can be achieved readily by short time exposures.

Specimens exhibiting a high peel resistance (>50), always had a visible thin film of residual polyethylene remaining on the metal substrates. As the peel force increased, this residual film increased in thickness. It is

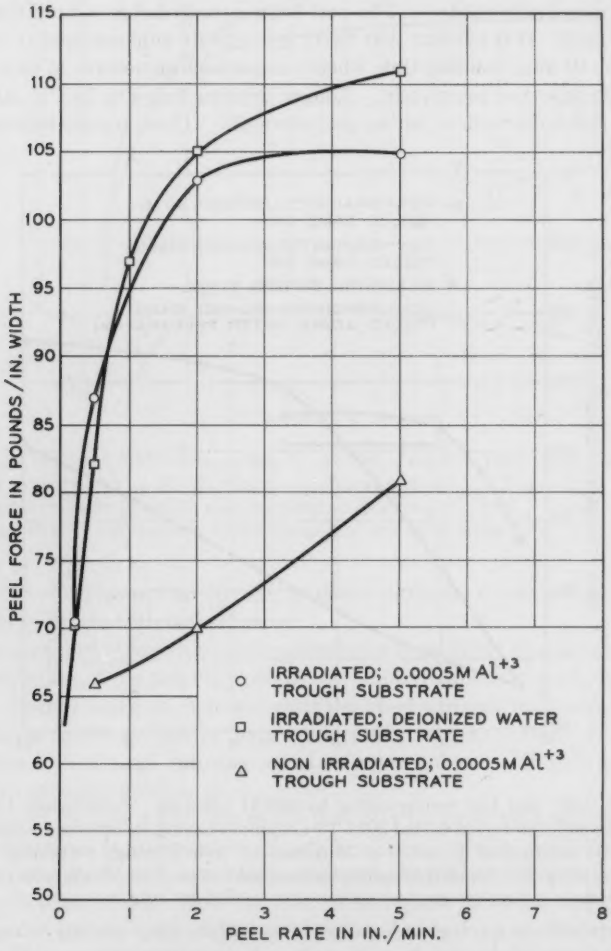

Fig. 3. 180° peel test corresponding to ASTM D903-49. Polyethylene bonded for 10 min. at 177°C. to sulfochromated Alclad 2024-T3 aluminum having an adsorbed monolayer of radioactive stearic acid deposited at 30 dynes/cm. Specimens received a dose of 10 Mrads prior to testing.

important to note that in all the experiments reported in this communication no pressure was exerted to form any of the bonds, beyond the weight of the polyethylene. Pressure may have an advantageous effect by hastening

the wetting of the substrate surface, thereby increasing the peel force for similar bonding times.

Figure 2 illustrates the effect of bonding time at 205°C. with and without an oriented condensed monolayer adsorbed onto the sulfochromated Alclad aluminum surface. The peel force is recorded as a function of the rate of peel. It is evident that there is a definite enhancement of the peel force for 10 min. bonding time when a condensed monolayer of stearic acid has been adsorbed previously. Longer bonding times at 205°C. appear to have a deleterious effect on the peel strength. These results indicate that

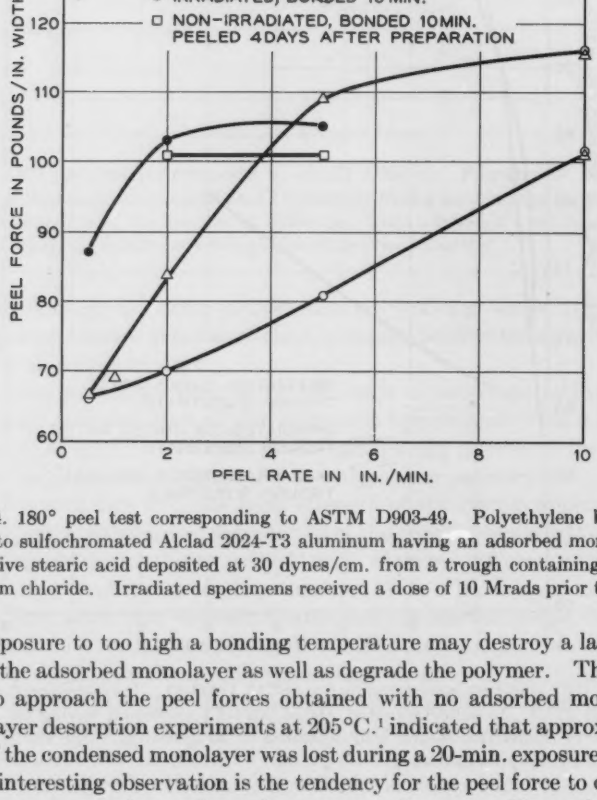

Fig. 4. 180° peel test corresponding to ASTM D903-49. Polyethylene bonded at 177°C. to sulfochromated Alclad 2024-T3 aluminum having an adsorbed monolayer of radioactive stearic acid deposited at 30 dynes/cm. from a trough containing 0.0005*M* aluminum chloride. Irradiated specimens received a dose of 10 Mrads prior to testing.

long exposure to too high a bonding temperature may destroy a large fraction of the adsorbed monolayer as well as degrade the polymer. The values tend to approach the peel forces obtained with no adsorbed monolayer. Monolayer desorption experiments at 205°C.[1] indicated that approximately 35% of the condensed monolayer was lost during a 20-min. exposure.

One interesting observation is the tendency for the peel force to converge to some common value as the peel rate approaches zero. Presently, we are extending our peel force data in this region.

Although we have not determined the contact angle as a function of time

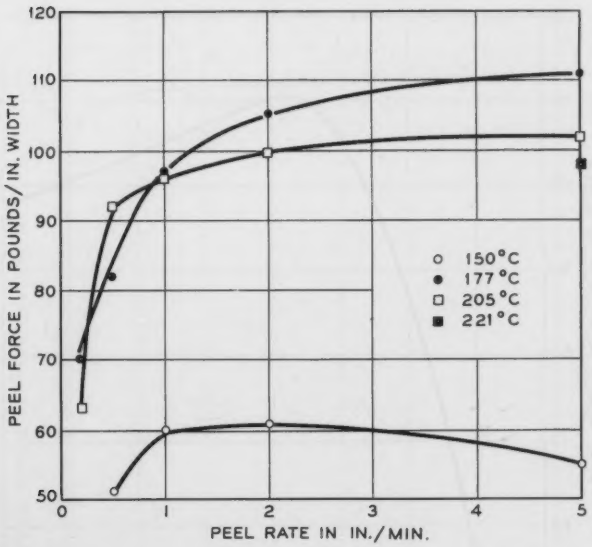

Fig. 5. 180° peel test corresponding to ASTM D903-49. Polyethylene bonded at various temperatures for 10 min. to sulfochromated Alclad 2024-T3 aluminum having an adsorbed monolayer of stearic acid deposited at 30 dynes/cm. from a trough containing deionized water. Specimens were irradiated at a dose of 10 Mrads.

at 205°C., it appears that 10 min. or less is sufficient to wet completely the substrate surface with polyethylene.

The high peel force without the monolayer is probably due to mechanical encapsulation of the polyethylene in the porous sulfochromated Alclad surface. Recent work on polished stainless steel surfaces indicates that the monolayer gives markedly improved peel strengths. Here mechanical adhesion is precluded, the only agent acting to enhance adhesion being the oriented monolayer adhesive.

The peel force as a function of the peel rate for irradiated and nonirradiated specimens is presented in Figure 3. These samples were bonded for 10 min. at 177°C. The surface pressure on the radioactive stearic acid, as in previous cases, was 30 dynes/cm. The trough substrate was 0.0005*M* aluminum chloride. Specified samples were irradiated at a total dose of 10 Mrads. For comparison purposes, samples prepared at the same time but not irradiated showed considerably less peel force than the irradiated specimens. Once again the values at low rates of peel tend to converge. The trough substrate does not appear to affect greatly the peel force when we consider irradiated samples. One possible reason for the greater peel forces when we employed deionized water as our trough substrate, would be the larger number of stearic acid molecules on our metal substrate. This is apparent when we observe the force-area isotherms and the area occupied

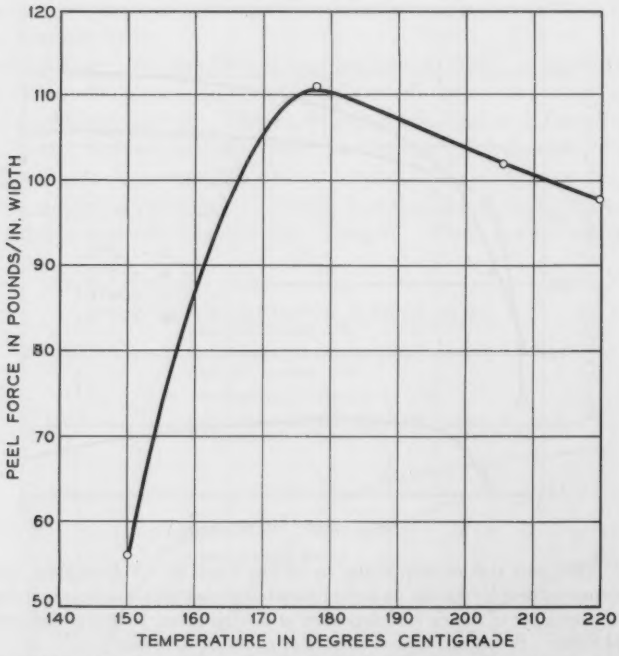

Fig. 6. 180° peel test corresponding to ASTM D903-49. Polyethylene bonded at various temperatures for 10 min. to sulfochromated Alclad 2024-T3 aluminum having an adsorbed monolayer of stearic acid deposited at 30 dynes/cm. from a trough containing deionized water. Specimens were irradiated at a dose of 10 Mrads and peeled at 5 in./min.

per molecule at zero compression of the monolayer. Moreover, the actual count of our substrates before bonding indicates a 5% greater surface coverage with deionized water as our trough substrate.

Irradiation causes the hydrocarbon matrix of the polymer to become crosslinked to itself and apparently to the hydrophobic portion of our amphipathic adsorbed molecules. In addition, there is probably some crosslinking of the stearic acid to itself.

Figure 4 presents data concerning the peel force as a function of aging of the bonded specimens. Nonirradiated specimens were prepared by bonding polyethylene at 177°C. for 10 min. to sulfochromated aluminum with an adsorbed monolayer of radioactive stearic acid deposited at 30 dynes/cm. from a trough substrate of 0.0005M aluminum chloride. A remarkable enhancement of peel force upon aging is apparent from Figure 4. Irradiation at 10 Mrads further increases the peel force of the system. Once again we note the effect of 20 min. bonding time. When the contact angle of molten polyethylene on the monolayer covered substrate attains an equilibrium value of zero, we obtain maximum adhesion of our adherends.

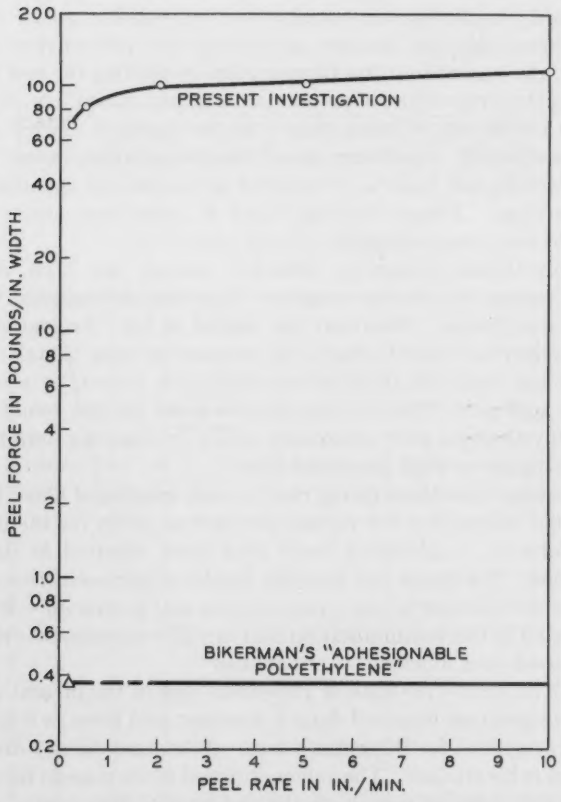

Fig. 7. Peel force of Bikerman's "adhesionable polyethylene" compared to typical results from the present investigation.

In Figure 5, the peel force as a function of bonding temperature and rate of peel is illustrated. All the specimens have been exposed to 10 Mrads irradiation prior to peeling to maximize the peel force. In these instances, the stearic acid was deposited from a trough containing deionized water and peeled about one week after preparation. We have demonstrated earlier that the peel forces are essentially the same for a trough substrate containing aluminum chloride or deionized water when the specimens are irradiated with 10 Mrads. Although we do not have the maximum peel force because we bonded for only 10 min. rather than 20 min., the time necessary to wet completely the substrate, the effect of bonding temperature becomes quite apparent. Above 177°C. there is a tendency for the peel force to decrease, probably due to disruption and solubilization of the monolayer in the polymer matrix. At 150°C. insufficient wetting of the substrate surface occurred to enable one to obtain respectable peel forces. There

was obviously insufficient time to allow the hydrophobic tails of the stearic acid to diffuse into and become anchored in the polyethylene network. Figure 6 further points out this phenomenon by plotting the peel force as a function of the temperature of preparation at a peel rate of 5 in./min. The maximum for 10 min. bonding time is in the region of 177°C. There is nothing particularly significant about this temperature except that the degree of wetting and monolayer retention are maximized apparently under these conditions. Longer bonding times at lower temperatures should produce the same bond strengths.

The polyethylene–aluminum adhesive system has been considered primarily because previous investigators[3,4] have had difficulties in obtaining good adhesive bonds. Bikerman has argued in his "rheological theory" that poor adherence must be due to the presence of weak boundary layers.[4] Bikerman has used the polyethylene–aluminum system to promote his particular approach. The two alternatives posed by him would be either making polyethylenes more chemically active or removing from them substances giving rise to weak interfacial films.

By removing substances giving rise to weak interfacial films, Bikerman has reported values of a few pounds per inch of width for the peel force. These results are considerably lower than those reported in the present investigation. Bikerman has actually employed surface-active materials to *decrease* the adhesion between polyethylene and aluminum. It has been demonstrated in this communication that oriented monolayers can *increase* adhesion of selected adherends to one another.

Figure 7 illustrates the data of Bikerman[4] and of the present investigation. Extrapolating from our data, a constant peel force as a function of peel rate is assumed for Bikerman's data. Bikerman did not consider the rate of peel in his studies. The values obtained in the present investigation exceed by two orders of magnitude the peel force of Bikerman's "adhesionable" polyethylene.

No attempt has been made in this study to alter the properties of the polyethylene as obtained from the manufacturer. If a weak boundary layer existed in the bonded system by virtue of not extracting substances giving rise to weak interfacial films, poor adhesion should have resulted. It can be concluded that it is not the impurities in the polyethylene that are contributing to poor adhesion, but rather, the lack of intermolecular forces between the adherends. Oriented monolayer adhesives act as a bridge between adherends. They are attached to both phases by virtue of chemisorption and mechanical encapsulation.

It is perhaps instructive to attempt to correlate the peel force data with the theory presently available. The several analyses currently available treat simple one dimensional stress distributions in the vicinity of the bond boundary. From this elementary viewpoint the bond stresses are considered uniform through the thickness and across the width of the bond and variable only as a function of distance from the advancing boundary. We will attempt to correlate our data with the theory as presented by

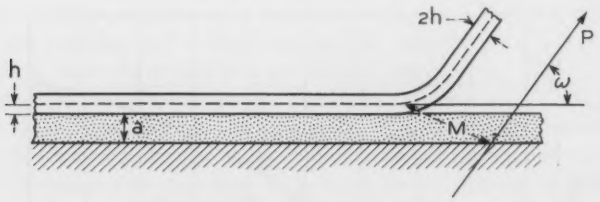

Fig. 8. Bond boundary during peel.

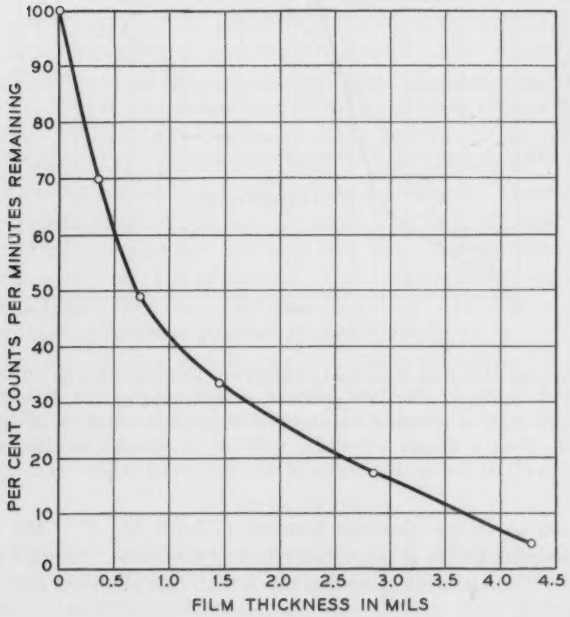

Fig. 9. Per cent of counts per minute of C^{14} remaining as a function of the average residual film thickness of polyethylene on sulfochromated Alclad 2024-T3 aluminum having an adsorbed monolayer of radioactive stearic acid deposited at 30 dynes/cm. from a trough containing 0.0005M aluminum chloride. Specimens were bonded at 177°C. for varying lengths of time and peeled at 5 in./min.

Kaelble.[5,6] Figure 8 is a schematic of an idealized bond comprising a flexible member of thickness $2h$ and width b, an adhesive interlayer of thickness a, and a fixed and rigid substrate. Kaelble's analysis yields,

$$P = ba\left[\frac{K\sigma_0}{(2Y)^{1/2}} + \frac{3^{1/2}\cos\omega\lambda_0}{(2G)^{1/2}}\right]^2 (1 - \cos\omega)^{-1}$$

where P is the peel force, σ_0 and λ_0 are the cleavage and shear stress respectively, K is a dimensionless factor which relates the cleavage bond force

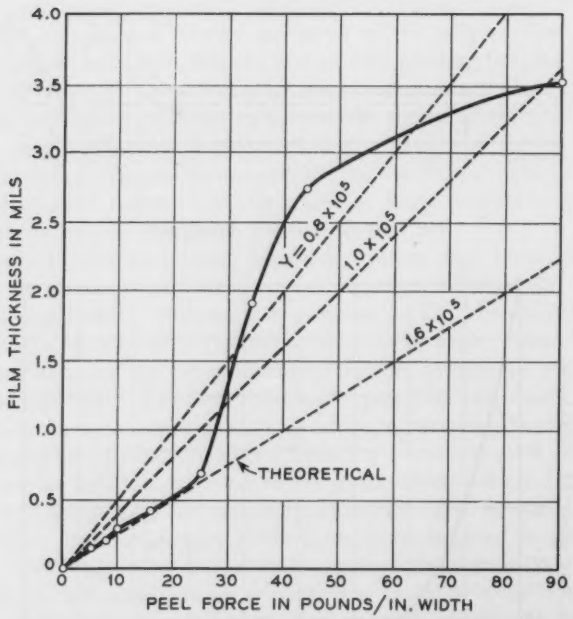

Fig. 10. Average thickness of residual polyethylene film remaining on sulfochromated Alclad 2024-T3 aluminum after 180° peel test corresponding to ASTM D903-49. The metal substrate had an adsorbed monolayer of radioactive stearic acid deposited at 30 dynes/cm. from a trough containing 0.0005M aluminum chloride. Specimens were bonded at 177°C. for varying lengths of time and peeled at 5 in./min.

($P_c = P \sin \omega$) to the cleavage moment of force M_c, Y is the adhesive Young's modulus and G is the adhesive shear modulus. At high angles of peel (90–180°), the above expression takes with fair precision the following form:

$$P \cong baK^2\sigma_0^2/[2Y(1 - \cos \omega)]$$

where the cleavage stress mechanism is the dominating process of failure and the shear stress contribution becomes negligible. At 180°, the angle at which we perform our analyses, $K = 1.0$ and the expression is further reduced to

$$P_{\omega=180} = ba\sigma_0^2/4Y$$

If the assumption is made that the polyethylene remaining on the metal substrate after peeling corresponds to an adhesive interlayer in the Kaelble sense, then a method is available for the testing of his theory. Employing radioactive stearic acid as the monolayer, the per cent activity as a function of peel strength and residual film thickness on specimens bonded for various times at 177°C. was determined.

Figure 1 illustrates the peel force as a function of the bonding time employing radiolabeled stearic acid as the monolayer adhesive. Short intervals of exposure results in a spectrum of peel forces. The activity on the peeled aluminum surfaces was measured and related to a thickness of polyethylene remaining on the substrate. The counting procedure, was standardized by employing several thicknesses of aluminum and Mylar. As the thickness was increased, a decrease in the number of counts was recorded. Knowledge of the density of these materials made it possible to relate a loss in activity with a definite thickness of polyethylene. Figure 9 depicts the film thickness of polyethylene remaining on the metal substrate covered with a monolayer of stearic acid deposited at 30 dynes/cm. from a trough containing 0.0005M aluminum chloride. After peeling, the polyethylene sections of all the specimens showed essentially no count. Approximately 50% of the counts are lost for a thickness of only 0.75 mils of polyethylene. Considerably greater thicknesses of polymer are needed to stop the higher energy particles in the C^{14} decay spectrum. The average energy of the β particles is only 40% of the maximum. The peel forces of these specimens obtained at a rate of peel of 5 in./min. are plotted as function of residual film thickness in Figure 10. For values of the peel force up to 25 lb./in. width, σ_0^2/Y is invariant. This is related to the storage energy factor in Kaelble's theory. A reasonably good fit to the data is obtained at low peel strengths when $\sigma_0^2/4Y$ is equal to 1.6×10^5 lb./in.^{2}.

In future experiments we will employ a lower rate of peel in the region where the peel force is no longer a linear function of the peel rate. This may tend to bring the deviations above 25 lb./in. width peel force closer to the theoretical curve.

V. CONCLUSION

The adsorption of condensed monolayers of radioactive stearic acid between selected adherends affords a bonding phase possessing a higher degree of orientation, uniformity and specificity. The generalized approach to adhesion which has been presented should be adaptable, in principle, to the bonding of any pair of adherends without regard to their surface polarities.

The force necessary to peel polyethylene from a properly bonded aluminum surface has been demonstrated to be orders of magnitude greater than the values previously recorded in the literature.

In future communications the systems, stainless steel–polyethylene, copper–polyethylene, aluminum–polypropylene, and stainless steel–polypropylene will be discussed. It will be shown that for a properly prepared substrate, the final bond strengths are independent of the substrate phase, since the polymer makes intimate contact only with the monolayer.

We sincerely thank Dr. J. Struthers, Dr. R. Salovey, Dr. L. H. Sharpe and the members of the Adhesives Group for their kind assistance in the experimental phase of this work.

References

1. Schonhorn, H., *J. Polymer Sci.*, **A1**, 2343 (1963).
2. Sharpe, L. H., *Proc. Chem. Soc.*, **1961**, 461.
3. Bikerman, J. J., *Science of Adhesive Joints*, Academic Press, New York, 1961.
4. Bikerman, J. J., *J. Appl. Chem.*, **11**, 81 (1961).
5. Kaelble, D. H., *Trans. Soc. Rheol.*, **3**, 161 (1959).
6. Kaelble, D. H., *Trans. Soc. Rheol.*, **4**, 45 (1960).

Résumé

Des adhésifs en couches monomoléculaires orientées à base d'acide stéarique radioactifont été employés pour lier le polyéthylène à l'aluminium. Le temps de liaison, température de liaison et la vitesse d'écaillement sont les différents paramètres qui ont été variés afin de déterminer leur effet sur la résistance finale à l'écaillement. Des techniques pour augmenter la résistance à l'écaillement sont discutées et incorporées dans ce mémoire. Des résistances à l'écaillement au-dessus de 100 lb./in. d'épaisseur sont reportées employant de l'acide stéarique comme adhésif en couche monomoléculaire. Les résistances à l'écaillement obtenues dans cette étude sont plus grandes de deux ordres de granduer que celles reportées dans la littérature. La seule limitation consiste dans la force cohésive de l'adhésif thermoplastique. La théorie de Kaelble sur la résistance à l'écaillement est décrite et adaptée à nos résultats expérimentaux. Un accord raisonable est obtenu pour des résistances basses à l'écaillement (25 lb./in. width).

Zusammenfassung

Zur Verbindung von Polyäthylen mit Aluminium wurden orientierte monomolekulare Schichten von radioaktiver Stearinsäure als Klebemittel verwendet. Bindungsdauer, Bindungstemperatur und Abziehgeschwindigkeit gehören zu den Parametern, deren Einfluss auf die Endabziehfestigkeit durch Variierung bestimmt wurde. Verfahren zur Erreichung einer maximalen Abziehfestigkeit werden im vorliegenden Bericht angegeben und diskutiert. Mit Stearinsäure als Monoschichtenklebestoff wird eine Abziehfestigkeit von mehr als 100 lb./in. Breite erreicht. Die hier erhaltenen Abziehkräfte liegen um mehr als zwei Grössbnordnungen höher als die Literaturwerte. Die einzige Beschränkung ist die Köhäsionsfestigkeit des verklebten Thermoplasten. Die Theorie der Abziehkraft von Kaelble wird beschrieben und für die Versuchsergebnisse verwendet Bei niedriger Abziehfestigkeit (25 lb./in. Breite) wird recht gute Übereinstimmung erhalten.

Received September 19, 1962

JOURNAL OF POLYMER SCIENCE: PART A VOL. 1, PP. 3537–3545 (1963)

Electron Spin Resonance Studies of the Reaction of Gases with the Radicals Formed in Irradiated Polytetrafluoroethylene

HISASHI UEDA,* ZENICHIRO KURI, and SHOJI SHIDA, *Tokyo Laboratories, Japanese Association for Radiation Research on Polymers, Bunkyoku, Tokyo, Japan*

Synopsis

The effect of O_2, SO_2, NH_3, H_2S, and NO on the ESR of irradiated PTFE were studied. Radicals were produced by (*1*) irradiation of PTFE in an atmosphere of one of these gases and (*2*) by the postirradiation reaction of PTFE with this same gas. These radicals were subsequently reacted with each of the remaining four gases, and the resulting spectra were studied. The radical produced in PTFE by the irradiation in vacuum is quenched by NO. In this reaction, the relation between the number of quenched radicals and the pressure of NO was measured, showing that the relation can be expressed by Freundlich's equation for adsorption equilibria. From these data, the bonds formed by the reaction between the gases and the radicals, the classification of the radical and the structure of these radicals were discussed.

INTRODUCTION

Previous electron spin resonance (ESR) studies have been made of the effects of gases on irradiated PTFE (polytetrafluoroethylene), but only a few gases were studied.[1–3]

We undertook the present study with the hope of learning more about the reactions of the radicals produced in PTFE with H_2S or NH_3 by the method of ESR. The effects of these two gases have not been reported yet. Rexroad and Gordy reported that the radical formed by the reaction between oxygen and the radical produced in PTFE after irradiation in vacuum, viz. $RO_2\cdot$, is reduced to the $RO\cdot$ radical by CO gas. This is the only reported case in which successive gas reactions were studied. We, therefore, also hoped to learn about other such successive gas reactions.

The gases chosen as reactants were those which showed some interesting effects with irradiated polyvinyl chloride.[4]

EXPERIMENTAL

Our measurements were made at 20°C. at a frequency of 9400 Mcycles/sec. with an automatic recording spectrometer which displays the first

* Present address: Department of Chemistry, The University of British Columbia, Vancouver, British Columbia, Canada.

derivatives of the true absorption curve. The irradiation was done with a kilocurie Co^{60} γ-ray source at 20°C. The gases used were O_2 (air), SO_2, NO, H_2S, and NH_3, they were purified by drying and repeated distillation.

RESULTS

A. Radicals Produced with Oxygen

There is a small but distinct difference between the two spectra obtained by the irradiation in oxygen and postirradiation reaction of oxygen with PTFE, shown in Figures 1*a* and 1*b*, respectively. The reactivities of these two radicals are the same. In the reaction with NH_3, some change is observed, as shown in Figure 2*a*. When SO_2 is introduced into the sample, the ESR spectrum changes to that shown in Figure 2*b*. With NO, the signal is quenched, but is not affected by H_2S.

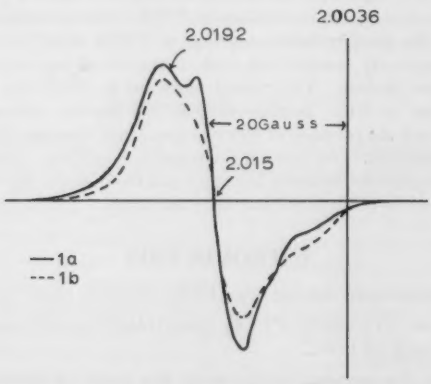

Fig. 1. The ESR spectra of irradiated PTFE reacted with O_2: (*a*) spectrum given by irradiation with O_2 present; (*b*) spectrum given by the postirradiation reaction. The arrows pointing downwards and the numbers above them show the g factors corresponding to those values of the resonant magnetic field. The ordinate is located to show the resonant point for DPPH, i.e., $g = 2.0036$. There are at least two radicals giving the spectra, $R^1O_2\cdot$ ($g = 2.0192$) and $R^2O_2\cdot$ ($g =$ various values).

B. Radicals Produced with Sulfur Dioxide

No difference between the radicals produced by irradiation in SO_2 and the postirradiation reaction with SO_2 is observed, and Figure 3*a* shows the spectrum thus obtained. These radicals react with O_2, and the resulting spectrum is the same as that in Figure 2*b*. With NH_3 introduced, the spectrum changes to that shown in Figure 3*b*. With NO, only the central component of the spectrum shown in Figure 3*a* is not quenched, and the resulting spectrum is shown in Figure 3*c*. With H_2S no change is observed.

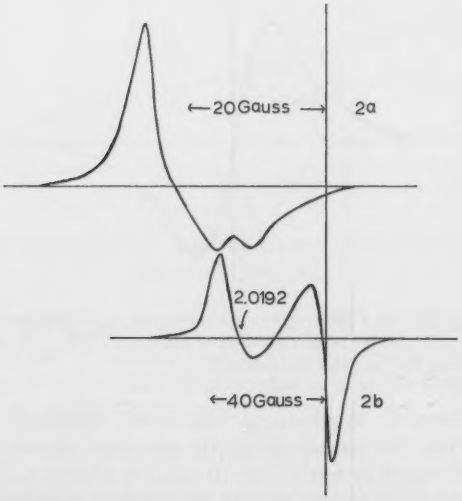

Fig. 2. ESR spectra of (*a*) sample giving Fig. 1*a* or 1*b* but after reaction with NH_3; (*b*) the sample giving Fig. 1*a* or 1*b* but after reaction with SO_2. The spectrum is also obtained by the sample giving Fig. 3*a* after reaction with O_2. This spectrum shows two radicals: $R^1O_2\cdot$ ($g = 2.0192$) and $R^2SO_2\cdot$ ($g = 2.004$).

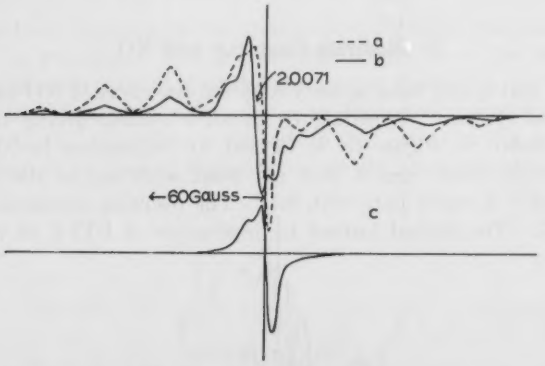

Fig. 3. ESR spectra of (*a*) irradiated PTFE in SO_2 (the central anisotropic component is due to $R^2SO_2\cdot$ and the components appearing on either side are due mainly to $R^1\cdot$); (*b*) the sample giving Fig. 3*a* after reaction with NH_3 (the central component may be produced by the reaction $R\text{—}SO_2\cdot + NH_3 \rightarrow R\text{—}SO\cdot + NH_2OH\cdot$; the peaks on either side are due to $R^1\cdot$); (*c*) sample of Fig. 3*b* after reaction with NO.

C. Radicals Produced with Ammonia

No difference between the spectra of the radicals produced by the irradiation in NH_3 and the postirradiation reaction with NH_3 is observed, as shown in Figure 4*a*. This radical reacts with O_2 and a partial change of the

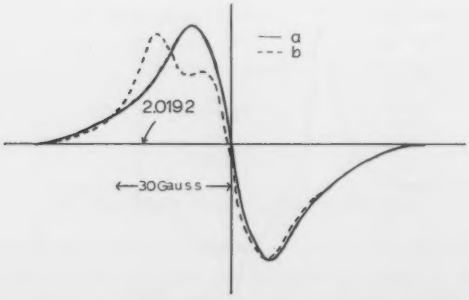

Fig. 4. Effect of NH_3 on ESR spectra: (*a*) spectrum of PTFE irradiated in the presence of NH_3 present or by the postirradiation reaction with NH_3; (*b*) spectrum obtained by the sample giving Fig. 4*a* after reaction with O_2.

spectrum is observed, as shown in Figure 4*b*. However, this change is reversible. When the sample giving the spectrum shown in Figure 4*b* is evacuated and heated at 150°C. for 10 min., it reverts to the form giving the spectrum shown in Figure 4*a*. In the reaction with NO, the radical is destroyed, but by subsequent evacuation and heating, as described above, this sample gives a spectrum coinciding with that of Figure 9. In the reaction with H_2S, a spectrum coinciding with that of Figure 8 is obtained. In the reaction with SO_2, a spectrum coinciding with that of Figure 3*c* is obtained.

D. Radicals Produced with NO

Rexroad and Gordy have already reported the effect of NO on the ESR of irradiated Teflon. According to them, a radical giving the triplet spectrum shown in Figure 5*a* is formed by irradiation in NO.[1] This radical is very stable, and it does not react with any of the gases O_2, NH_3, or H_2S;[1] it reacts only with SO_2. The resulting spectrum is shown in Figure 5. The radical formed by irradiation of PTFE in vacuum is

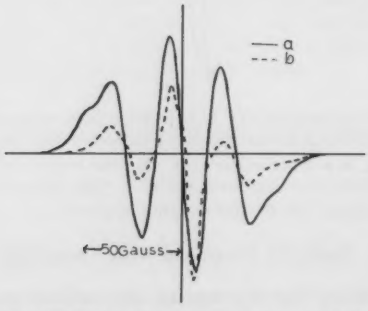

Fig. 5. ESR spectra of (*a*) PTFE irradiated in the presence of NO; (*b*) the same sample after reaction with SO_2.

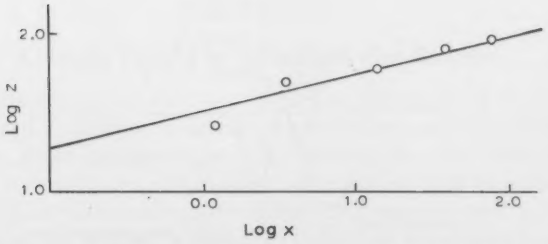

Fig. 6. Log–log plot of the relation between the pressure of NO, X and the amount of the destroyed radical Z.

destroyed when NO is introduced.[1] The relation between the pressure of NO and the number of radicals destroyed after equilibrium is reached is shown in Figure 6. An experimental relation may be deduced from the graph of Figure 6. This relation is,

$$Z = Y_0 - Y = 32X^{1/4.15}$$

where Z is the quantity of the destroyed radical, Y_0 is the initial amount of radical, and Y is the remaining amount of radical at an NO pressure of X. This is in the form of Freundlich's[5] equation of adsorption equilibria, except that the exponent of X is smaller than 1.0.

E. Radicals Produced with H_2S

The spectrum obtained by the irradiation of PTFE in vacuum, as shown in Figure 7*a*, is different only in its central portion from that obtained by the postirradiation reaction with H_2S as shown in Figure 7*b*. On irradiation of PTFE in H_2S, the spectrum shown in Figure 8*a* is obtained. In the reaction with O_2, the spectrum changes to that shown in Figure 8*b*. This changes further to that of Figure 8*c* when the sample is evacuated and

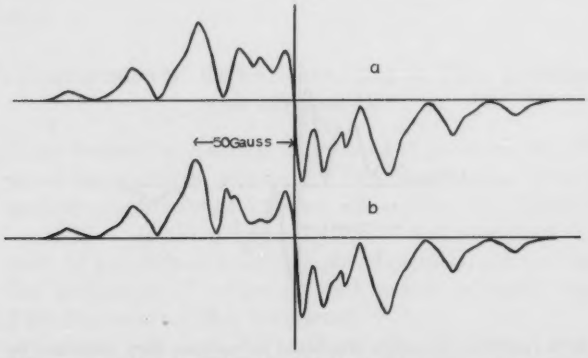

Fig. 7. ESR spectra of (*a*) PTFE irradiation in vacuum (spectrum of R·); (*b*) the same sample after reaction with H_2S. The partial effect is seen at the center.

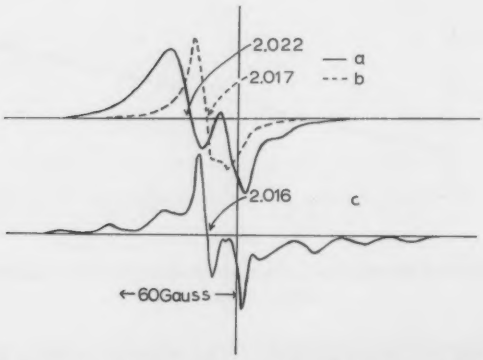

Fig. 8. ESR spectra of (*a*) PTFE irradiated with H_2S present: (*b*) the sample giving Fig. 8*a* after reaction with O_2. (*c*) the same sample after evacuation and heat treatment at 150°C. for 10 min. (after prolonged heating in vacuum this sample gave a spectrum coinciding with that of Fig. 3). The spectrum of curve *a* is due to R^2—$S\cdot$; *b* is due to R^2—$SOO\cdot$ and $R^1O_2\cdot$, and *c* is due to R^2—$SO_2\cdot$ (g = 2.004), $R^1O_2\cdot$ (g = 2.016), and $R^1\cdot$ (peaks on either side).

heated at 160°C. for 10 min., and it finally becomes that of Figure 3*a*. In the reaction with SO_2 a spectrum almost coinciding with that of Figure 3*c* is obtained. In the reaction with NH_3, no change is observed. In the reaction with NO, decay of radical is observed.

F. Regeneration of the Radical Quenched by NO

When we heated in vacuum at 150°C. for 10 min., a sample, which had been irradiated in vacuum and in which the radical had been destroyed by NO, the spectrum shown in Figure 9 was obtained. This is different from that of Figure 7, but is the same as that obtained by Levedev et al.[6] when they introduced NO to a PTFE sample irradiated in vacuum at 150°C.

Fig. 9. ESR spectrum of sample irradiated in vacuum, then quenched by NO, and subsequently after evacuated and heated at 150°C. for more than 10 min. If the second heating in vacuum is not carried out, the samples give no signal.

DISCUSSION

A. Bonds Formed by the Radical–Gas Reaction

Matsugashita[7] reported that most of the oxygen could be removed from the oxygenated radicals by evacuation and heating, and that for the most part, these radicals changed from $RO_2\cdot$ back to $R\cdot$. He concluded that this was a reversible reaction.[7] He also reported that evacuation and heating of irradiated samples treated with NO accomplished a reversible regeneration of the original radical $R\cdot$. However, we obtained a different result in the case of NO.

This reaction, if it is completely reversible, might suggest that it is an adsorption process.

However, if all the existing reactions are adsorption processes, there are many things difficult to understand. It is true that if the sample giving the spectrum of Figure 1*a* is evacuated and heated at 150°C., the spectrum reverts to that of Figure 7. This is a very slow change. This slow change is not compatible with the concept of adsorbed oxygen. Of course, it is possible that there is a large activation energy for adsorption, but if it is so, the change from Figure 7 to Figure 1*a* must be slow. The reaction of oxygen with irradiated PTFE as observed by ESR is, on the contrary, very rapid. The case of NO is also like this. Only a portion of the original radical or something different from them can be regenerated.

Therefore, there are at least two steps of radical–gas reactions involved. The first is adsorption and the next is some chemical reaction. The adsorption is reversible, but the chemical reaction is not. The regeneration of the original radical after a prolonged heating of the oxygenated radical will be a decomposition process of the oxygenated radical, something like the thermal decomposition of alkyl hydroperoxides. The radicals formed by SO_2, NH_3, or H_2S cannot be decomposed by evacuation and heating. In these cases, therefore, the transformed radicals are stable at higher temperatures.

B. Classification of Radicals According to Their Reaction with SO_2 and O_2

The radicals formed by reaction with O_2 react partially with SO_2, and give the spectrum shown in Figure 2. This means that there are two kinds of radicals, each having different affinity for O_2. These may be called $R^{1}\cdot$ and $R^{2}\cdot$. In the previous section it was concluded that there are two types of gas–radical reactions, an adsorption and a chemical reaction. The adsorption of oxygen by each radical is equally rapid, but the rate of the chemical reaction is different:

$$R^{1}\cdot + O_2 \rightarrow R^{1}O_2(\text{ad})\cdot \rightarrow R^{1}O_2\cdot$$

$$R^{2}\cdot + O_2 \rightarrow R^{2}O_2(\text{ad})\cdot$$

Here (ad) means that the oxygen molecules are adsorbed. The $R^2O_2(ad)\cdot$ readily reacts with SO_2, which is an exchange reaction,

$$R^2O_2(ad)\cdot + SO_2 \rightarrow R^2SO_2(ad)\cdot + O_2$$

$$R^2SO_2(ad)\cdot \xrightarrow{\text{very rapid}} R^2SO_2\cdot$$

The reaction

$$R^1\cdot + SO_2 \rightarrow R^1SO_2(ad)\cdot$$

seems to be very slow, while

$$R^2\cdot + SO_2 \rightarrow R^2SO_2(ad)\cdot$$

is very rapid, so the radicals formed by the irradiation in SO_2 are a mixture of $R^2SO_2\cdot$, $R^1\cdot$, and $R^1SO_2\cdot$. Then if oxygen is reacted with these radicals, the products will be $R^2SO_2\cdot$, $R^1SO_2\cdot$, and $R^1O_2\cdot$. The ESR spectrum of Figure 2*b* agrees well with these. The radical $R^1O_2\cdot$, in which oxygen is more strongly bonded to the radical than in $R^2O_2(ad)\cdot$, has less anisotropy in the *g* factor, which is near 2.0192, while $R^2O_2\cdot(ad)$ has a large anisotropy in its *g* factor. Both $R^1SO_2\cdot$ and $R^2SO_2\cdot$ have a *g* factor of 2.004.

In the case of H_2S, the radicals giving the ESR spectrum of Figure 8*a*, obtained by irradiation in H_2S, seem to consist of $R^1\cdot$ and $R^1S\cdot$. After oxidation and heat treatment they should give $R^1O_2\cdot$, $R^1\cdot$, and $R^2SO_2\cdot$. Since after a long heat treatment only $R^1\cdot$ and $R^2SO_2\cdot$ were obtained, it is concluded that H_2S has the same reactive tendency as SO_2.

In the case of NO, the quenching reaction occurs at the same rate for each radical except $R^2SO_2\cdot$; therefore, NO does not distinguish between $R^1\cdot$ and $R^2\cdot$. This is also the case for NH_3. The $O_2 \rightarrow NH_3$ reaction (meaning the irradiation in vacuum followed by the O_2 reaction and then the NH_3 reaction), and the $SO_2 \rightarrow NH_3$ reaction both occur to a considerable extent. Therefore, it cannot be determined whether NH_3 is more reactive with $R^1\cdot$ or its related radicals or with $R^2\cdot$ or its related radicals.

3. Structure of Various Radicals

The radical produced by the irradiation of PTFE in H_2S can be converted by heat treatment into a radical having the ESR spectrum shown in Figure 3*a*. Therefore, it is concluded that the radical produced by the irradiation in H_2S is the R—S· radical and that it was transformed into R—SO_2· by the raction with O_2 at 150°C. Alternatively, it can be said that for the radical produced by the irradiation in SO_2, the linkage between the polymer and SO_2 group is not a C—O bond, but a C—S bond.

The chemical structure of the radical produced by the reaction with NH_3 is unknown as yet. However, it can be said that NH_3 does react somewhat with the free radicals and transforms them into different ones. It also seems that NH_3 reacts only with radicals produced in irradiated halide polymers, although we have observed only two cases, PTFE and polyvinyl chloride.[8]

It is to be noted that H_2S and NO have peculiar radical transforming powers when they are reacted under irradiation. Postirradiation reactions with them either quench the resonance or have no effect. The radicals given off by the polymer under irradiation may react with the gas. The reaction between these intermediate radicals and the polymer radicals or the polymer itself should also be considered.

The authors' thanks to Dr. Raymond Patten, who kindly read their manuscript.

References

1. Rexroad, H. N., and W. Gordy, *J. Chem. Phys.*, **30**, 399 (1959).
2. Matsugashita, T., and K. Shinohara, *J. Chem. Phys.*, **32**, 954 (1960).
3. Abraham, R. J., and D. H. Whiffen, *Trans. Faraday Soc.*, **54**, 1291 (1958).
4. Kuri, Z., H. Ueda, and S. Shida, *J. Chem. Phys.*, **32**, 371 (1960).
5. Nernst, H. W., *Theoretical Chemistry*, McMillan, London, 1923, p. 578.
6. Levedev, Ya. S., H. D. Tsvedev, and V. V. Voerdskil, *Opt. Spektroskopiya*, **8**, 426 (1960).
7. Matsugashita, T., private communication.
8. Ueda, H., Z. Kuri, and S. Shida, *J. Appl. Polymer Sci.*, **5**, 478 (1961).

Résumé

On a étudié l'effet de O_2, SO_2, NH_3, H_2S et NO sur le ESR du PTFE irradié. On produit des radicaux: (*1*) en irradiant le PTFE sous atmosphère d'un de d'un de ces gaz, (*2*) par post-irradiation du PTFE avec ces mêmes gaz. Ces radicaux ont ensuite réagi avec chacun de ces quatre gaz résiduaires, et on a étudié les spectres qui en résultent. Le radical produit sur le PTFE par irradiation sous vide est capté par NO. Lors de cette réaction, on a mesuré la relation entre le nombre de radicaux captés et la pression en NO; on a montré que la relation peut s'exprimer par l'équation de Freundlich pour les équilibres d'adsorption. On a discuté, à partir de ces données, des liens formés par réaction entre les gaz et les radicaux, de la classification du radical et de la structure de ces radicaux.

Zusammenfassung

Der Einfluss von O_2, SO_2, NH_3, H_2S und NO auf die ESR von bestrahltem PTFE wurde untersucht. Radikale wurden (*1*) durch Bestrahlung von PTFE in einer Atmosphäre eines dieser Gase und (*2*) durch die Nachreaktion nach der Bestrahlung von PTFE mit dem gleichen Gas erzeugt. Diese Radikale wurden dann mit jedem der restlichen vier Gase zur Reaktion gebracht und die auftretenden Spektren untersucht. Das in PTFE durch Bestrahlung im Vakuum erzeugte Radikal wird durch NO zerstört. Bei dieser Reaktion wurde die Abhängigkeit der Zahl der gebundenen Radikale vom NO-Druck gemessen; es zeigte sich dass die Abhängigkeit durch die Freundlichsche Adsorptionsisotherme ausgedrückt werden kann. Auf Grund der Ergebnisse wurde die Art der durch die Reaktion zwischen den Gasen und den Radikalen gebildeten Bindungen, die Klassifizierung des Radikals und die Struktur dieser Radikale diskutiert.

Received October 1, 1962

JOURNAL OF POLYMER SCIENCE: PART A VOL. 1, PP. 3547–3559 (1963)

Crystallization in Starch: The Role of Ions in the Lyotropic Series*

M. KHAIRY S. MORSI and CLARENCE STERLING, *Department of Food Science and Technology, University of California, Davis, California*

Synopsis

The crystallization (retrogradation) of starch from solution has been investigated as a function of electrolyte composition and concentration. The anion effects follow a lyotropic series which causes retrogradation in the approximate descending order: CNS^-, ($PO_4^{\equiv}$, $CO_3^{=}$), I^-, NO_3^-, Br^-, Cl^-, $C_2H_3O_2^-$, F^-, $SO_4^{=}$. Cations also tend to follow the lyotropic series of Ba^{++}, Sr^{++}, Ca^{++}; K^+, Na^+, Li^+. Increasing concentrations of most salts (except for NaF and $MgSO_4$) result in decreased precipitation of starch. The descending order of ions in the lyotropic series is best explained in terms of the decreasing polarity and decreasing relative intensity of electric charge, due either to increasing ion symmetry or to increasing area of charge distribution as a result of resonance among several configurations. It is suggested that the polar, higher charge intensity in ions at the upper end of the series brings about charging of the starch molecule, which leads to solubilization because of (*1*) the repulsion of the similarly charged molecules and (*2*) the aggregation of a water mantle about each molecule.

Introduction

The spontaneous crystallization ("retrogradation") of starch from solution has been related to temperature,[1–4] hydrogen ion concentration,[5–8] length of the starch molecule,[9] and various other factors. However, despite the intriguing relationships of electrolytes in the hydration of biological polymers, few studies have reported the rôle of salts in the crystallization of starch. Samec[10] found that crystallization, as measured by precipitation of amylose from sols, was retarded by increasing concentrations of different salts. These salts were decreasingly effective in the order: Na_2HPO_4, $Na_2B_4O_7$, $Na_4P_2O_7$, NH_4CNS, NH_4Cl. In some cases, lower concentrations retarded precipitation more than higher ones. Increasing concentrations of $(NH_4)_2SO_4$, on the other hand, appeared to accelerate precipitation. Using a different set of salts, Loewus and Briggs[11] studied changes in iodine-binding capacity of amylose solutions at low salt concentrations (0.1*M* or less). Aside from noting that, in general, monovalent ions tended to retard crystallization as the size of the anion increased and as the size of the cation increased, they found little consistency in salt effects. Moreover, the number of salts used was limited, as was also the range of concen-

* This investigation was supported by grant EF-155 from the U.S. Public Health Service.

trations. An investigation[12] of the crystalline nature of precipitates of amylodextrin in salt solutions showed that while sulfates always brought about crystallization of the *B* type, the alkali halides, according to their concentration and their position in the lyotropic series, tended to produce *C* or *A* crystals.

Because the physicochemical rôle of electrolytes in polymer crystallization and solubilization is still in the realm of speculation, it seemed desirable to characterize more carefully the relative effect of salts on these events in starch sols. The presumption was implicit that an evaluation of the results with a greater range of salts and salt concentrations might provide clues to the rôles of the ions. The present study deals with the effects on starch crystallization of 40 salts, used in a range of concentrations from 0.01 to 1.0*m*.

Experimental

An acid-modified cornstarch, which has a large proportion of short-chain amylose[13,14] that can be readily dispersed at lower than autoclave temperatures, was employed. This material will crystallize more readily than native cornstarch. The salts used included the halides of sodium and potassium; the chlorides of ammonium, calcium, iron, zinc, barium, magnesium, lithium, cobalt, copper, strontium, aluminum, manganese, and antimony; the acetates of sodium, potassium, ammonium, barium, copper, and magnesium; the sulfates of sodium, potassium, ammonium, iron, and lithium; the nitrates of sodium, potassium, ammonium, iron, and strontium; and the thiocyanates, carbonates, and phosphates of sodium and potassium.

For most of the salts used, the pH range varied from 6.5 to 7.5. Although it might seem reasonable to bring all the solutions to the same (neutral) pH

TABLE I

Soluble Starch in Sols Stored at 3°C. (in Weight of Equivalent Glucose, Based on Total Possible 2000 mg.)

Salt (0.1*m*)	pH	Soluble starch, mg.			
		0 weeks	1 week	2 weeks	4 weeks
KCNS	6.8	730	670	670	660
KI	7.0	730	660	660	640
KNO_3	7.0	700	680	680	570
KBr	6.8	690	660	650	480
KCl	6.8	650	570	550	410
K_2SO_4	6.7	710	610	480	370
$KC_2H_3O_2$	7.5	680	540	440	320
K_3PO_4	12.4	710	—[a]	—[a]	660
K_2CO_3	11.5	750	680	680	670
None	7.0	665	580	395	390

[a] Sample lost.

level, several series of experiments indicated that this was not practicable: with salt solutions of very low pH, upward adjustment of the pH value led to the prompt precipitation of the metal hydroxide; with salt solutions of very high pH, adjustment gave the acid anion. In all cases, the salt solutions had different amounts of the added buffer salts. Consequently, it was decided to use unbuffered salt solutions in the final experiments, with notations of large departures from neutrality (cf. Table I). Those salts with very large deviations in pH are considered separately in the discussion.

In the first two experiments, solutions were made of 1 g. air-dry starch in 100 ml. distilled water, and the appropriate amount of salt necessary for a final concentration of 0.1*m* was added either before or after heating. Until the start of boiling, the solution was stirred continually over an electric hot plate. Boiling continued for 5 min., with the agitation of the process being sufficient to keep the solution well mixed. (Amylose is completely dispersed by this treatment: the undispersed material is amylopectin.) At the finish of boiling, the water in the solution was made up to 100 g. with added hot water (or added salt and water when the salt was to be added after the heating).

In the third experiment, salt solutions were prepared before heating in concentrations of 0.01, 0.02, 0.05, 0.1, 0.2, 0.5, 0.7, and 1.0*m*. The manner of preparation of the sols is as described above. However, those salts which are strongly hydrolytic or which are insoluble at higher concentrations (chlorides of copper, cobalt, and manganese and the iron salts) were not used. For four salts (NaCl, $CaCl_2$, $Ca(NO_3)_2$, and $MgSO_4$), the electrolyte was also added after heating. Not all the salts were available in sufficient quantity for this experiment.

Following preparation of the sols, 30 ml. were removed for analysis. Toluene (2 ml.) was added to the remaining 70 ml. of hot solution, which were then stored at 3°C. Samples were taken again at 1, 2, and 4 weeks in the first two experiments and at 4 weeks in the third experiment. (At each intermediate sampling, the toluene was removed; and then 2 ml. of fresh toluene were added afterwards, before the samples were replaced in refrigerated storage.)

Relative solubility of starch, in the first two experiments and in the solutions of the above-mentioned four salts of the third experiment, was determined by adding 10 ml. of phosphate buffer (pH 7) to 1 ml. of sol and centrifuging 5 ml. of the mixture for 15 min. at 3°C. and at 11,300 *g*. A 2-ml. portion of the supernatant was combined with 0.2 ml. of 37% HCl and held in a boiling water bath 1.5 hr. After cooling, the volume was made up to 10 ml.; of this 5 ml. was added to 10 ml. of ferricyanide solution, made up according to the method of Schales and Schales.[15] After 15 min. boiling and 3 min. cooling, the mixture was diluted to 25 ml. Optical density was read at 420 mμ and converted to a glucose equivalent on the basis of a standard calibration curve for glucose. The average error for this method is 4.2%.

Indirect measurements of solubility were made by the methods of (*1*)

iodine sorption, in which 1 ml. of the centrifuged supernatant described above was diluted with 10 ml. of iodine solution (0.01% I_2 and 0.02% KI in water) and the optical density read at 590 mμ as an index of the amount of soluble amylose (estimated for thiocyanates, in which the color disappears rapidly), with an average error of 1.9%; (*2*) in experiment 3, centrifuging the sol 15 min. at 11,300*g* and measuring roughly the volume of the precipitate to the nearest 0.5 ml. (10% error); and (*3*) recording photographically the heights of the precipitates in experiment 3.

The starch sols were tested by enzymatic hydrolysis: the remainder of the buffered sol served as a substrate. To 6 ml. of the sol, 1 ml. of enzyme solution (25 mg. bacterial α-amylase and 12.5 mg. $CaCl_2 \cdot 2H_2O$ in 50 ml. water) was added and mixed in gently. A 2-ml. portion of the mixture was placed immediately in 10 ml. of ferricyanide solution,[15] which was then boiled, cooled, and completed to 25 ml., as described above. The glucose equivalent was determined in the manner previously given. The remaining 5 ml. of the enzyme–starch mixture were held at 30°C. for 2 hr., after which 2 ml. was placed in 10 ml. of ferricyanide solution and treated in the same way as the control. The difference in reducing power between the digested sol and the control gave the amount of amorphous starch susceptible to enzymatic attack. Because this appeared to be a relatively insensitive measure of crystallization, it was not used in the comparison.

It is important to note that the measurement of reducing power of the control provided a significant index for possible starch hydrolysis during pasting and possible microbial activity during storage. Whenever the latter was found, the results were discarded. However, because of the precautions taken, microbial contamination was rare.

Results

A typical series of results for solutions of 0.1*m* salt concentration is represented by the different potassium salts. Table I shows the changes in soluble starch content (in terms of glucose equivalent, based on acid hydrolysis of the supernatant solutions) for sols in which the salt was added before heating. It is apparent that the amount of soluble starch decreases with time in all cases, but at different rates. Note that the classical lyotropic series is followed, in general, with respect to the different anions. Thus, in the order of decreasing solubility of starch, the series is $PO_4^{\equiv}$, CNS^-, $CO_3^{=}$, I^-, NO^-_3, Br^-, Cl^-, $SO_4^{=}$, $C_2H_3O_2^-$. For iodine sorption, in relative terms, the results are essentially similar.

With most salts, there are only slight differences in starch solubility as a result of the difference in the time at which the salt is added. However, in two cases, there are pronounced differences between adding the salt before heating and adding it afterwards: (*1*) when the salt solution has a low pH value (ferric salts, $AlCl_3$) the glucose equivalent of the sol is greater if the salt is added before heating, presumably as a result of greater hydrolysis during heating; and (*2*) when the salt is an acetate or a sulfate,

the glucose equivalent of the sol tends to be greater if the salt is added after heating.

To compare the effects of the salts (0.1*m*) on crystallization, it seemed reasonable to use a solubility index, expressed as the percentage relationship of the amount of soluble starch in the supernatant after 4 weeks to the amount present initially, as determined by hydrolysis with concentrated HCl. For salts added before heating, this index is shown in Table II. The values may be compared with the value for starch sols with no added salt (53). On the basis of this comparison, it is to be observed that acetates and sulfates generally cause an acceleration of the crystallization process, whereas the bromides, iodides, nitrates, thiocyanates, carbonates, and phosphates appear to retard that process. Note also that the usual lyotropic anion series is found among the sodium salts. In the halides and most other salts, the customary cation relationships obtain: sodium causes less crystallization than lithium, and potassium less than sodium. Similarly, the series, $CaCl_2$, $SrCl_2$, and $BaCl_2$, follows this relationship.

When the concentration is varied, the solubility indices also change, as is shown for NaCl, $CaCl_2$, $Ca(NO_3)_2$, and $MgSO_4$ in Table III. Increasing concentrations of the first three salts bring about decreasing crystallization. However, increasing concentrations of $MgSO_4$ cause greater crystallization. These relationships are readily perceived in Figure 1 (*1–4*). Under the force of gravity alone, no precipitate is visible with NaCl solutions at concentrations of 0.7*m* and higher, with $CaCl_2$ solutions 0.5*m* and higher, or with $Ca(NO_3)_2$ solutions 0.1*m* and higher.

TABLE II

Solubility Indices for Starch Sols with Salt added before Heating (0.1*m* Concentration)[a]

	Anion									
Cation	F^-	Cl^-	Br^-	I^-	NO_3^-	CNS^-	$CO_3^=$	$PO_4^=$	$C_2H_3O_2^-$	$SO_4^=$
Li^+		51			72	87	97	89	41	—[b]
Na^+	49	60	68		81	90	89	93	47	49
K^+		63	69	88	76				42	48
NH_4^+		58								
Cu^+		86								
Ca^{++}		58			91					
Sr^{++}		59			87					
Ba^{++}		75							66	
Mg^{++}		53							39	50
Cu^{++}		64							35	
Zn^{++}		34								
Mn^{++}		64								
Co^{++}		55								
Fe^{++}										42
Fe^{+++}		94			91					
Al^{+++}		79								

[a] Solubility index for starch in water only: 53.

[b] Doubtful data; insufficient salt available to repeat the experiment.

Fig. 1. The effect of salt concentration on starch precipitation over a period of 28 days at 3°C. Except where noted, the concentrations of salt, from left to right, are 0.01, 0.02, 0.05, 0.1, 0.2, 0.5, 0.7, and 1.0*m*, respectively. (*1*) Solutions of starch with NaCl. Note that the volume of precipitate decreases as the concentration increases. At concentrations of 0.7*m* and higher, the starch does not precipitate. (*2*) Solutions of starch with $CaCl_2$. At concentrations of 0.5*m* and higher, no precipitate appears. (*3*) Solutions of starch with $Ca(NO_3)_2$. At concentrations of 0.1*m* and higher, no precipitate is visible at the bottom of the tubes. (*4*) Solutions of starch with $MgSO_4$. A continuous increase in the volume of precipitated starch follows the increase in salt concentration. (*5*) Solutions of starch with NaF. Note the relatively minor effect of increasing concentrations of salt. (*6*) Solutions of starch with LiCl. (*7*) Solutions of starch with $NaC_2H_3O_2$ at concentrations of 0.01, 0.05, 0.1, 0.5, 0.7, and 1.0*m* (*8*) Solutions of starch with $KC_2H_3O_2$. Note the contrast, at higher concentrations, with $NaC_2H_3O_2$.

TABLE III
Solubility Indices when Salts are added before Heating, with Concentrations varied

Concentration, molal	Salt			
	NaCl	$CaCl_2$	$Ca(NO_3)_2$	$MgSO_4$
0.01	57	61	70	57
0.02	67	64	73	65
0.05	64	64	80	62
0.1	63	72	91	50
0.2	76	100	91	41
0.5	100	98	95	5
0.7	95	100	91	1
1.0	100	85	90	1
2.0	100	—[a]	—[a]	—[a]

[a] Solutions of this concentration were not prepared.

Other salts, whose increasing concentration brings about decreasing crystallization are: all the potassium salts; the chlorides of ammonium, barium, calcium, magnesium, zinc, and aluminum; most of the sodium salts, save the fluoride, sulfate, and acetate; barium acetate; and ammonium nitrate.

No salts are as strongly precipitant as $MgSO_4$. The remaining salts tested seem to be indifferent, in that changing concentrations do not notably affect the volume of starch precipitate. These salts include LiCl (Fig. 1, *5*), NaF (Fig. 1, *6*), $NaC_2H_3O_2$ (Fig. 1, *7*), Na_2SO_4, and $(NH_4)_2SO_4$. In contrast to solutions of $NaC_2H_3O_2$, higher concentrations of $KC_2H_3O_2$ (Fig. 1, *8*) cause solubilization of starch. Table IV shows the amounts of precipitate for the different sodium salts.

TABLE IV
Volume of Starch Precipitate for the Sodium Salts as a function of Concentration

Salt	Volume of starch precipitate, ml.							
	0.01 *m*	0.02 *m*	0.05 *m*	0.1 *m*	0.2 *m*	0.5 *m*	0.7 *m*	1.0 *m*
NaF	3.5	3.0	2.5	4.0	3.0	3.0	3.0	4.0
NaCl	2.5	2.5	1.5	1.0	1.0	0.5	0.5	0.5
NaBr	2.0	2.0	2.0	1.5	0.5	0.5	0.5	0.5
$NaNO_3$	2.5	2.0	1.0	1.5	0.5	0.5	0.5	0.0
NaCNS	2.5	2.5	2.5	2.0	1.0	1.0	0.5	0.0
Na_2CO_3	2.5	2.0	1.5	1.0	0.5	0.5	0.5	1.0
Na_3PO_4	4.0	3.0	3.0	1.0	1.0	0.5	0.0	0.0
$NaC_2H_3O_2$	3.0	3.0	2.5	2.0	2.0	2.0	2.0	2.0
Na_2SO_4	2.5	2.5	2.5	2.5	2.0	2.0	2.0	2.0

Table V provides an overview of the general crystallizing effect of increasing concentrations of electrolytes. The numerical values represent the relative amount of starch which is soluble at a salt concentration of

1.0*m*, expressed as a percentage of the amount precipitated at a salt concentration of 0.01*m*. Despite the roughness of the volumetric data, the results obviously agree qualitatively with the solubility indices reported in Table III. It is evident that even for acetates, some sulfates, and lithium chloride, crystallization is inhibited to some extent at higher salt concentrations. Only with NaF and $MgSO_4$ does the 1.0*m* concentration cause increasing crystallization; and, because of the limitations of the method of measurement, it is quite possible that the small presumptive increase with NaF is not real.

TABLE V

Starch in Solution in 1.0*M* Salts, as a Percentage of Precipitated Starch at 0.01*m* Concentration (see text)

	Anion, %									
Cation	F^-	Cl^-	Br^-	I^-	NO_3^-	CNS^-	$CO_3^=$	$PO_4^{\equiv}$	$C_2H_3O_2^-$	$SO_4^=$
Li^+		33								
Na^+	−14[a]	80	75		100	100	60	100	33	20
K^+		83	83	86	88	100	86		75	50
NH_4^+		80			75					14
Ca^{++}		75			100					
Ba^{++}		90							80	
Mg^{++}		80								−180[a]
Zn^{++}		71								
Al^{+++}		80								

[a] Negative numbers indicate increased amount of precipitate over that at 0.01*m*.

Discussion

The results of the present investigation pose two questions of paramount interest: (*1*) what chemical differences among these salts will explain the different crystallizing effects; and (*2*) how do increasing concentrations of most salts inhibit crystallization?

The progressive effects of the classical lyotropic anion series (CNS^-, I^-, NO_3^-, Br^-, Cl^-, F^-, $SO_4^=$) and cation series (K^+, Na^+, Li^+, Ba^{++}, Sr^{++}, Ca^{++}) have been described for the swelling and gelatinization of native starch.[11,16–22] For the alkali halides and monatomic ions generally, these series are obviously related to the ionic radius. According to Fajans,[23] ion hydration is an inverse function of ion size. Fajans suggested that, because of its smaller size, a smaller ion has a more concentrated charge at its surface and therefore is more highly hydrated than a larger one of the same charge. Subsequently, Katz and Muschter[21] postulated that anions are adsorbed on the surface of the starch micelle inversely according to the size of their water shell. (Earlier, Hoeve, Bungenberg de Jong, and Kruyt[19] had demonstrated that salt adsorption on starch followed the lyotropic series.) They further related ion adsorption to the preferential migration of anions to the starch–water interface. (In this

instance, it is known that anions follow the lyotropic series in their ability to lower interfacial tension.[24-26])

It has also been found[27] that anions tend to break down the 4-coordinated structure of liquid water as a direct function of their radius and charge. Other work has supported the concept that ions higher in the lyotropic series tend to be more "structure-breaking" than those lower in the series.[28] No explanation has been provided for the relationship between specific physical chemical properties of the anions and the degree of breakdown of water structure.

Other questions are unanswered: How is the structure of water broken? If ionic radius and ionic charge alone are involved and the ionic radius of NO_3^- is smaller than the ionic radius of $SO_4^=$,[27] the markedly solubilizing effect of the former on starch is inexplicable *vis-à-vis* the precipitating effect of the latter. Moveover, none of these explanations accounts for the rôles of the acetate ion or the ions of other organic acids, of ions such as the thiocyanates, or of cations.

Nevertheless, there is an important physical chemical difference among these ions, which can be related to their positions in the lyotropic series. Larger monatomic ions (both anions and cations) have an electron cloud of greater diameter, and with a larger number of electrons, than do smaller ones. In addition, the larger cloud is more easily distorted or polarized in an electric field.[29] Polarization of the electron cloud leads to the creation of a dipole moment in the ion, in which the centers of gravity of the electric charges tend to be separated and the charges thereby concentrated at relatively small poles. The greater the polarization, the more concentrated are the charges. For polyatomic ions, presumably the more polar the construction of the ion, the more localized and concentrated are the charges.

In this light, it seems possible to view the descent in the lyotropic series as related not to a decreasing ion radius but to a decreasing local charge intensity, generally as a result of increasing symmetry of charge distribution at the ionic surface. At the upper end of the series, the polar confinement of progressively larger electric charges to smaller surface areas makes those charges relatively more intense. Polarization will be enhanced by the presence of a large electric field due to a highly polarized, large ion of opposite charge. An intense field alone or the close proximity within an ion of two opposite charges of high intensity could be reasonable sources of the destruction of the 4-coordinated structure of water.[27,28]

The marked difference between the effects of sulfates and nitrates can then be related to the polarity of the anion structure. The sulfate ion is a tetrahedron,[30,31] with sulfur at the center and the four oxygens at the apices. Its charge is stabilized by resonance among 6 configurations.[32] Because of the radial symmetry, the charge per unit surface is quite low. The nitrate ion, on the other hand, is planar, and an axis of 2-fold symmetry lies in the plane. The $N—O_1$ distance for the unique oxygen is slightly different from the $N—O_{23}$, distance for the two symmetrical oxygens, and angle $O_1—N—O_2 \neq$ angle $O_2—N—O_3$:[33,34]

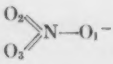

The charge thus tends to be confined to one end of the ion, whose resonance is limited, and the solvating effect is pronounced. It may be pointed out that the structure of thiocyanate shows a more marked asymmetry. Consequently, that ion would be expected to have a more intense charge concentration:

Indeed, as should be anticipated, the cyanide ion, which also has a polar structure:

has been found to retard starch crystallization.

Virtual lack of anion polarization then can account for the ineffectiveness of LiCl and NaF in retarding starch retrogradation. The small fluoride ion is spherically symmetrical and essentially unpolarized, even in the presence of Na^+; its charge tends to be evenly distributed over its surface. Although the larger chloride ion is more readily polarized than the fluoride ion, the small lithium ion tends to be unpolarized and does not provide a strong enough electric field for polarization of the chloride ion. Both these alkali halides are poor solubilizing agents and do not retard retrogradation.

The form of the acetate ion appears to be polar:

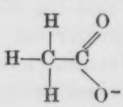

However, there is resonance among two configurations. The total charge is spread over the two oxygens, hence over a surface larger than is the case with nitrate but not as large as that of the sulfate. Because of this charge distribution, the antiretrogradative effect of the acetate ion is intermediate between that of the nitrate and that of the sulfate. Except for the relative solubility of the hydrocarbon residue, any organic acid ion should then be expected to act similarly to the acetate ion. Indeed, Hofmeister[35] ranked tartrate and citrate ions close to the acetate ion in the lyotropic series.

In the present experiments, phosphates and carbonates generally retard the precipitation of starch. Since the anions form weak acids, their solutions with alkali cations are alkaline. The solubilizing role of these salts is then definitely due to the creation of a high pH, in which the quite polar base ion (OH^-) is the active agent. (It is well known that low concentrations of bases will solubilize starch, even in the cold.[7,16,17]) However, both these ions are symmetrical. Like the sulfate anion, the phosphate anion is tetrahedral, with the phosphorus centrally situated.[36,37] Four resonating configurations are possible. The carbonate ion is planar,

but a three-fold axis—perpendicular to the plane—passes through the centrally located carbon;[38,39] resonance occurs among three configurations. It is not surprising, then, that in neutral solutions, carbonate and phosphate rank with sulfate at the lower end of the lyotropic series.[21,35]

It has been represented here that the descending order of the lyotropic series of ions essentially is related to a decreasing polarity (and intensity) of charge on the surface of the ion. We propose that the most reasonable explanation of the solubilizing effect on starch is that it is similar to the effect of the ions on water: the electric field of the negative pole of the ion causes a separation of the hydrogen from the oxygen, thus giving each an increased charge and giving the water molecule an enhanced dipolar character. The water dipoles and the ion poles tend to be attracted to each other. The starch molecule may be viewed as consisting substantially of a carbon–oxygen core, coated by a layer of hydrogen atoms. A negative charge will then attract the protons on the surface of the molecule, causing them to separate somewhat, leaving the molecule core negatively charged. (This charging in salt solutions has been demonstrated experimentally for other nonelectrolytes by Longsworth.[40]) Thus, in solutions of salts with ions high in the lyotropic series, the starch molecule will have a higher negative charge than normally, due to this proton separation. Statistically, the anions of the electrolyte will tend to be attached (adsorbed) at the surface of the starch molecule[21] and help increase the negative charge. Higher solubility results from both the repulsion between similarly charged starch molecules and the aggregation of water dipoles about these charged molecules.

The rôle of electrolyte concentration in solubilizing starch is explicable in the above terms. The higher the ionic concentration, the greater the proportional amount of charging of the starch molecule by more or less polarized ions. The less polar the ion charge, the less the solubilizing effect and the less the ion hydration. When the anion is completely symmetrical and of relatively small superficial charge density ($SO_4^=$, F^-), charging is much diminished, and the ion is surrounded only by a narrow shell of immobilized water molecules;[28] the larger amount of electrolyte precipitates starch by lowering the water activity, i.e., by a dehydration effect.[21] Presumably this effect of the salt is enhanced if the salt is added before heating, thus restricting the extent of gelatinization. (It has been shown that retrogradation will ensue more rapidly in starch which has been gelatinized to a smaller degree by the use of lower heating temperatures.[4])

References

1. Itallie, Th. B. van, Dissertation, Amsterdam, 1930.
2. Katz, J. R., and A. Weidinger, *Z. physik. Chem.*, **A171**, 181 (1934).
3. Maquenne, L., *Compt. Rend.*, **137**, 797 (1903).
4. Kalb, A. J., and C. Sterling, *J. Food Sci.*, **26**, 587 (1961).
5. Fouard, E., *Compt. Rend.*, **144**, 501, 1366 (1907).
6. Paschall, E. F., and J. F. Foster, *J. Am. Chem. Soc.* **75**, 1177 (1953).
7. Kalb, A. J., and C. Sterling, *J. Appl. Polymer Sci.*, **23**, 571 (1962).

8. Holló, J., J. Szejtli, and G. S. Gantner, *Periodica Polytech.*, **3**, 95 (1959).
9. Whistler, R. L., and C. Johnson, *Cereal Chem.*, **25**, 418 (1948).
10. Samec, M., *Kolloid-Beih.*, **43**, 272 (1936).
11. Loewus, F. A., and D. R. Briggs, *J. Am. Chem. Soc.*, **79**, 1494 (1957).
12. Hizukuri, S., M. Fujii, and Z. Nikuni, *Biochim. Biophys. Acta*, **40**, 346 (1960).
13. Kerr, R. W., *Stärke*, **4**, 39 (1952).
14. Cowie, J. M. G., and C. T. Greenwood, *J. Chem. Soc.*, **1957**, 516, 2658.
15. Schales, O., and S. S. Schales, *Arch. Biochem. Biophys.*, **8**, 285 (1945).
16. Reychler, A., *Bull. Soc. Chim. Belges*, **29**, 118, 309 (1920).
17. Mangels, C. E., and C. H. Bailey, *J. Am. Chem. Soc.*, **55**, 1981 (1933).
18. Kruyt, H. R., and H. J. Edelman, *Kolloid-Beih.*, **36**, 350 (1932).
19. Hoeve, J. A. van der, H. G. Bungenberg de Jong, and H. R. Kruyt, *Kolloid-Beih.*, **39**, 105 (1933).
20. Meyer, A., *Untersuchungen über die Stärkekörner*, G. Fischer, Jena, 1895.
21. Katz, J. R., and F. J. F. Muschter, Jr., *Biochem. Z.*, **257**, 385 (1933).
22. Katz, J. R., J. Seiberlich, and A. Weidinger, *Biochem. Z.*, **298**, 320 (1938).
23. Fajans, K., *Naturwissenschaften*, **9**, 729 (1921).
24. Cheesman, D. F., and A. King, *Trans. Faraday Soc.*, **36**, 241 (1940).
25. McBain, J. W., *Colloid Science*, Heath, Boston, 1950.
26. Clayton, W. E., *The Theory of Emulsions and Their Technical Treatment*, 5th ed. C. G. Sumner, Ed., Blakiston, New York, 1954.
27. Buswell, A. M., R. C. Gore, and W. H. Rodebush, *J. Phys. Chem.*, **45**, 543 (1941).
28. Frank, H. S., and W.-Y. Wen, *Discussions Faraday Soc.*, **24**, 133 (1957).
29. Fajans, K., and G. Joos, *Z. Physik.*, **23**, 1 (1924).
30. Lipson, H., and C. A. Beevers, *Proc. Roy. Soc.* (*London*), **A148**, 664 (1935).
31. Mazzi, F., *Acta Cryst.*, **8**, 137 (1955).
32. Pauling, L., *The Nature of the Chemical Bond*, 3rd ed., Cornell Univ. Press, Ithaca, N. Y., 1960.
33. Duke, J. R. C., and F. J. Llewellyn, *Acta Cryst.*, **3**, 305 (1950).
34. Luzzati, V., *Acta Cryst.*, **4**, 239 (1951).
35. Hofmeister, F., *Arch. Exptl. Pathol. Pharmakol.*, **24**, 247 (1888).
36. Ito, T., and H. Mori, *Acta Cryst.*, **4**, 412 (1951).
37. Smith, J. P., W. E. Brown, and J. R. Lehr, *J. Am. Chem. Soc.*, **77**, 2728 (1955).
38. Brown, C. J., H. S. Peiser, and A. Turner-Jones, *Acta Cryst.*, **2**, 167 (1949).
39. Nitta, I., Y. Tomiie, and C. H. Koo, *Acta Cryst.*, **5**, 292 (1952).
40. Longsworth, L. G., *J. Am. Chem. Soc.*, **69**, 1288 (1947).

Résumé

La cristallisation (rétrogradation) de l'amidon en solution a été étudiée en fonction de la composition et de la concentration en électrolyse. Les effets anioniques suivent une série lyotrope qui occasionne une rétrogradation approximativement suivant l'ordre décroissant: CNS^-, ($PO_4^=$, $CO_3^=$), I^-, NO_3^-, Br^-, Cl^-, $C_2H_3O_2^-$, F^-, $SO_4^=$. Les cation, ont également tendance à suivre une série lyotrope de Ba^{++}, Sr^{++}, Ca^{++}, K^+, Na^+, Li^+s Une augmentation des concentrations de la plupart des sels (excepté pour NaF et $MgSO_4$) donne lieu à une diminution de la précipitation de l'amidon. L'ordre décroissant des ions dans la série lyotrope peut s'expliquer le mieux en considérant la polarité décroissante et la diminution relative de l'intensité de charge électrique, qui sont dues soit à l'augmentation de la symétrie de l'ion, soit à l'augmentation de la surface de distribution de charge résultant de la résonance entre diverses configurations. On a suggéré que la polarité, l'intensité de charge supérieure dans les ions de l'extrémité supérieure de la série apporte une charge autour de la molécule d'amidon qui occasionne la solubilisation du fait de (1) la rèpulsion entre les molécules de charge identique et de (2) la formation d'un écran de molécules d'eau autour de chaque molécule d'eau.

Zusammenfassung

Die Kristallisation (Retrogradierung) von Stärke aus Lösung wurde als Funktion der Elektrolytzusammensetzung und Konzentration untersucht. Die Anioneneffekte befolgen eine lyotrope Reihe, welche Retrogradierung etwa in der absteigenden Reihe: CNS^-, (PO_4^{3-}, CO_3^{2-}), J^-, NO_2^-, Br^-, Cl^-, $C_2H_3O_2^-$, F^-, SO_4^{2-} bewirkt. Kationen bilden ebenfalls die lyotrope Reihe Ba^{2+}, Sr^{2+}, Ca^{2+}; K^+, Na^+, Li^+. Zunehmende Salzkonzentration führt meist (mit Ausnahme von NaF und $MgSO_4$) zu einer Herabsetzung der Stärkefällung. Die Reihenfolge der Ionen in der lyotropen Reihe wird am besten durch ihre abnehmende Polarität und die durch die zunehmende Ionensymmetrie oder den aus der Resonanz zwischen mehreren Konfigurationen folgenden grösseren Bereich für die Ladungsverteilung bewirkte Abnahme der relativen elektrischen Ladungsintensität erklärt. Es wird angenommen, dass die höhere Ladungsintensität der Ionen am oberen Ende der Reihe eine Aufladung des Stärkemoleküls bewirkt, welche (1) wegen der Abstossung gleichgeladener Moleküle und (2) wegen der Ausbildung einer Wasserhülle um jedes Molekül zur Solubilisierung führt.

Received June 18, 1962
Revised August 20, 1962

JOURNAL OF POLYMER SCIENCE: PART A VOL. 1, PP. 3561–3567 (1963)

Polyamides Containing Phosphorus. II. Structural Effects on Softening and Glass Transition Temperatures

JOSEPH PELLON, *Chemical Research Department, Central Research Division, American Cyanamid Company, Stamford, Connecticut*

Synopsis

Glass transition temperatures as a function of structure for phosphorus-containing polyamides and polyamides containing other heteroatoms are analyzed in terms of the effect of polarity, steric behavior, and bond flexibility differences. The side-chain alkyl or aryl group carried by phosphorus was expected to increase chain mobility (lower glass transition temperatures) by separating chains and reducing intermolecular interaction. This general effect is offset by decreased mobility due to the greater polarity of the phosphorus groups, and the intramolecular steric hindrance to rotation caused by the alkyl or aryl group on phosphorus. Glass transition temperatures indicate the following order of bond flexibility: ($CH_2NCH_2 \approx CH_2SCH_2 \approx CH_2OCH_2$) > $CH_2P(R)CH_2 \approx CH_2CH_2CH_2$. The phosphorus-to-carbon bond showed no enhanced flexibility over a carbon-to-carbon bond.

INTRODUCTION

The preceding paper[1] in this series describes the preparation of polyamides containing phosphine [C—P(R)—C] and phosphine oxide [C—O‖P(R)—C] units in their backbone structure. The phosphorus-containing polymers generally were low-softening amorphous solids. A brief comparison with regular nylon analogs disclosed no major differences in terms of thermal stability or mechanical behavior. It was of interest to more clearly define structural effects on a molecular level by examination of glass transition temperatures.

RESULTS AND DISCUSSION

Softening temperatures and glass transition temperatures for the series of phosphorus-containing polyamides and related materials are summarized in Table I. The preparation of these polymers was described in the previous paper.[1] Glass transition temperatures were obtained by the differential thermal technique previously described by Keavney and Eberlin.[2]

TABLE I
Polyamide Softening Temperatures

No.	Amine comonomer	Softening temp., °C.	Glass transition temp. T_g, °C.	Melting points, °C.[a]
	I. Polyadipamides			
1	$H_2N(CH_2)_3—\underset{\displaystyle CH_3}{\overset{\displaystyle |}{N}}—(CH_2)_2NH_2$	70–75	5	NX
2	$H_2N(CH_2)_3—\underset{\displaystyle C_8H_{17}}{\overset{\displaystyle |}{P}}—(CH_2)_3NH_2$	—	12	X, 135
3	$H_2N(CH_2)_3—\underset{\displaystyle CH_3}{\overset{\displaystyle \overset{\displaystyle O}{\overset{\displaystyle \|\|}{|}}}{P}}—(CH_2)_3NH_2$	90–100	33	NX
4	$H_2N(CH_2)_3—CH_2—(CH_2)_3NH_2$	—	45	X, 245
5	$H_2N(CH_2)_3—(CH_2)_3NH_2$	220	47,[b] 65[c]	X, 268
6	$H_2N(CH_2)_3—\underset{\displaystyle \bigcirc}{\overset{\displaystyle |}{P}}—(CH_2)_3NH_2$	72	49	NX
7	$H_2N(CH_2)_3—\underset{\displaystyle \bigcirc}{\overset{\displaystyle \overset{\displaystyle O}{\overset{\displaystyle \|\|}{|}}}{P}}—(CH_2)_3NH_2$	100	55	NX
8	$H_2N(CH_2)_3—\overset{\displaystyle O}{\overset{\displaystyle \|\|}{P}}CH_2—(CH_2)_3NH_2$	70–80	59	NX
9	$H_2N(CH_2)_3—\underset{\displaystyle CH_2}{\overset{\displaystyle |}{P}}—(CH_2)_3NH_2$ CH_3CHCH_3	100–110	71	NX
	II. Hexamethylenediamine Polyamides			
10	$HOOC(CH_2)_2—S—(CH_2)_2COOH$	—	14–27	X, 215–216
11	$HOOCCH_2—\underset{\displaystyle CH_3}{\overset{\displaystyle |}{CH}}—(CH_2)_2COOH$	—	17	X, 230
12	$HOOC(CH_2)_2—\underset{\displaystyle \bigcirc}{\overset{\displaystyle \overset{\displaystyle O}{\overset{\displaystyle \|\|}{|}}}{P}}—(CH_2)_2COOH$	50–60	29	NX
13	$HOOC(CH_2)_2—\underset{\displaystyle \bigcirc}{\overset{\displaystyle \overset{\displaystyle S}{\overset{\displaystyle \|\|}{|}}}{P}}—(CH_2)_2COOH$	65–70	43	NX
14	$HOOC(CH_2)_2—\underset{\displaystyle CH_3}{\overset{\displaystyle |}{CH}}—(CH_2)_2COOH$	—	50[c]	X
15	$HOOC(CH_2)_2—CH_2—(CH_2)_2COOH$	202[d]	58[c]	X

[a] X = crystalline, NX = noncrystalline.
[b] Data of D'Alelio.[3]
[c] Data of Schmieder and Wolf.[5]
[d] Data of Coffmann et al.[4]

The polyamides listed in Table I can first be differentiated according to whether they possess crystallinity. The polymers having $\rangle P-R$ (except when R is octyl), $\begin{matrix} | \\ RP \\ | \end{matrix}$ $\begin{matrix} \| \\ =O, \\ | \end{matrix}$ C_6H_5P $\begin{matrix} \| \\ =S, \\ | \end{matrix}$ and $\rangle N-CH_3$ groups are amorphous. Nylon 66, nylon 76, the methyl-substituted nylons, and the polyamide having a S group are crystalline. A major effect of introducing phosphorus or amine groups is the elimination of crystallinity associated with a regular polyamide such as nylon 66. The packing disorder introduced by the phosphine group (—RP—) and the amine group (—RN—) could result both from the presence of the substituent R which must reside outside the plane of the $—CH_2—$ groups and also from the fact that the pyrimidally directed valences may introduce an additional three-dimensional aspect to the chain. The phosphine oxide group, with tetrahedrally directed valences, also presents a situation in which attached groups must reside outside the plane of the methylene groups. Similar explanation was advanced for the amorphous character of the polyadipamide derived from 4,4-dimethyl-1,7-heptanediamine.[6] In the latter case the authors consider this to result from the extension of the side-chain methyl groups in a plane perpendicular to the plane of the backbone, i.e.,

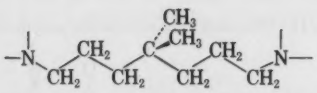

The polyadipamide containing the $\begin{matrix} | \\ P—C_8H_{17} \\ | \end{matrix}$ group was found to be crystalline from its appearance and x-ray pattern. However the crystalline melting point was much lower than that exhibited by regular nylons, and it is believed that the crystallinity is related only to the octyl side chain. Side-chain crystallinity has previously been advanced to explain the reversal of the trend toward lower softening points for increasing chain lengths of straight-chain acrylates at the C_{12} ester.[7]

In addition to its effect on crystallinity, bulk character and polymer melt temperature, replacement of one group for another in a given polymer system can also affect the mobility of segments of an individual polymer chain by reason of differences in steric behavior, polarity, and bond flexibility. Glass transition temperatures T_g, which can be considered to be internal polymer softening points, are measures of segmental mobility.[8]

Before discussing the data it is worthwhile to consider what effects one could expect on replacing a methylene group by a phosphorus group.

It is expected that the alkyl and phenyl groups on phosphorus could exert two types of steric effects on chain mobility. First by keeping polymer chains apart they could reduce intermolecular interactions and

enhance chain mobility. This would result in lower glass transition temperatures. This steric effect is intermolecular. Secondly, however, elements of the alkyl or aryl groups, such as hydrogen atoms, could interfere with adjacent backbone hydrogen atoms of the same chain to hinder chain rotations and give a subsequent increase in glass transition temperature. This is an intramolecular steric hindrance to rotation. Increased polarity of the heteroatom and decreased flexibility of the carbon to heteroatom bond over a carbon to carbon bond would also tend to reduce rotational freedom and give higher glass transition temperatures.

The glass transition temperatures for the series of polymers listed in Table I were found to increase in the order listed in Table II.

TABLE II

Order

Series I (Polyadipamides)

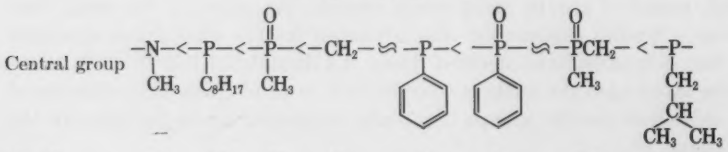

Series II (Hexamethylenediamine polyamides)

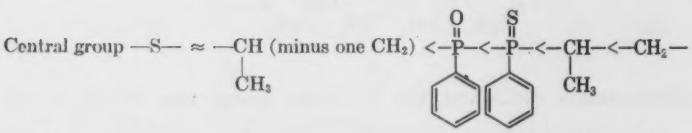

The results demonstrate the interplay of these various factors. If we imagine replacement of a methylene group by any other groups listed, we find that the methyl phosphorus oxide, the octyl phosphorus, and the methyl nitrogen give progressively lower glass transition temperatures in series I, while the methyl carbon, the phenylphosphorus sulfide, the phenylphosphorus oxide show lower glass transitions in series II. Reduction in intermolecular interactions by the steric effects of the side-chain alkyl and aryl groups provides an explanation for this trend. The glass transition temperatures would presumably be even lower in some cases except for the opposing influence resulting from the greater polarity of the heteroatoms over a methylene group, and possible effects of steric hindrance. For the central groups of series I which show glass transition temperatures above the methylene group the intermolecular steric effect is overshadowed by factors of enhanced polarity and steric hindrance. In particular, the isobutyl group appears to present a dramatic example of steric hindrance.

These results show no evidence of any difference in the flexibility of the carbon to phosphorus bond over a carbon to carbon bond. The lower values for $\diagdown N-CH_3$ and —S— would indicate that these groupings $\diagup$ contribute increased chain flexibility, i.e., that the $—CH_2—N—CH_2—$ and $—CH_2—S—CH_2$ bond have more rotational freedom than a $—CH_2—CH_2—CH_2—$ system. Bis(3-aminopropyl)ether adipamide is reported[9] to have a T_g of 34°C., some 15°C. below that of the corresponding nylon 76. This points to a similarly enhanced flexibility of $—CH_2—O—CH_2—$ over $—CH_2—CH_2—CH_2$.

Hill and Walker[10] have previously noted that the presence of a —S— linkage in polyamides does not greatly affect melting points. Korshak and co-workers[11] have stated that the introduction of sulfide sulfur greatly increases the flexibility of the polymer chain by increasing the possibilities of free rotation. It is not certain to which other polyamide they actually refer, since the reported melting points would tend to confirm the opinion of Hill and Walker. Actually the melting point of the sulfur containing polyamide would seem to be higher than the corresponding hydrocarbon polymer. That is, the melting point reported by the Russian workers for the hexamethylenediamine polyamide of $S[(CH_2)_4COOH]_2$ is 185–190°C.,[4] while Coffmann et al.[5] give the same melting point of 185°C. for $CH_2[(CH_2)_3COOH]_2$, i.e., nylon 69. Presumably the carbon analog of the

TABLE III
Softening Temperatures of Hexamethylenediamine *p*-Carboxyphenyl-Type Polyamides

No.	Diacid	Softening temp., °C.
1	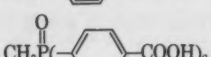	130–132[a]
2	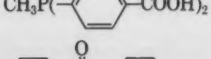	202–205[a]
3	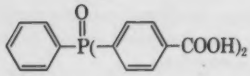	230–231[a]
4	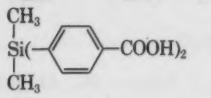	190[b]
5	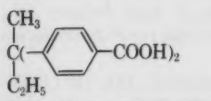	210–219

[a] Data of Frunze et al.[14]
[b] Data of Speck.[16]

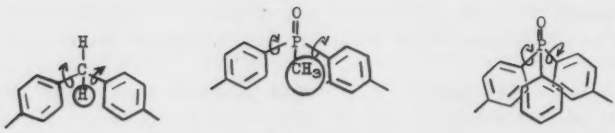

Figure 1.

sulfur polymer (nylon 611) would have an even lower melting point. The glass transition temperatures presented here however, being more sensitive to chain flexibility, do point to a greater swivel action around a CH_2—S—CH_2 linkage than around a CH_2—CH_2—CH_2 linkage.

Frunze, Korshak, and Kurashev[12–15] have attributed increased softening points in a series of bis(*p*-carboxyphenyl)phosphine oxide polyamides prepared by them to result from an increased group polarity. The concept of steric hindrance has been used here to explain, in part, the higher glass transition temperature for example of the polymer containing the C_4H_9P group. It is instructive to consider the possible influence of a similar steric hindrance in the *p*-carboxyphenylphosphine oxide series. Softening point data are summarized in Table III for this purpose. All compounds listed are amorphous, so that their softening temperatures can be compared directly.

The order of increasing softening points for the hexamethylenediamine polyamides of $CH_2 < CH_3P{=}O < C_6H_5P{=}O$ (Nos. 1, 2, 3 in Table III) considered by Korshak et al. to be a result of polarity increases in the same order. It is shown by Table III that increasing softening temperatures are also displayed in the order $CH_2 < Si(CH_3)_2 < C(CH_3)C_2H_5$ (Nos. 1, 4, 5 in Table III). This order can be ascribed to increased steric hindrance to rotation. It is felt that similar considerations can account, in part, for the order found in the phosphine oxide series.

Examination of models of the polymers of the carboxyphenyl type tend to confirm the concept that the rotational freedom around the central atom becomes increasingly more restricted in going from CH_2 to $CH_3P{=}O$ to C_6H_5—$P{=}O$, as illustrated in Figure 1.

The author wishes to acknowledge significant contributions to this work by Miss E. C. Eberlin in the determination of glass transition data. Acknowledgment is also given to Dr. W. M. Thomas for helpful discussions.

References

1. Pellon, J., and W. G. Carpenter, *J. Polymer Sci.*, **A1**, 863 (1963).
2. Keavney, J. J., and E. C. Eberlin, *J. Appl. Polymer Sci.*, **3**, 47 (1960).
3. D'Alelio, G. F., *Fundamental Principles of Polymerization*, Wiley, New York, 1952, Table 18, p. 124.
4. Schmieder, K., and K. Wolf, *Kolloid-Z.*, **134**, 149 (1953).
5. Coffmann, D. D., G. J. Berchet, W. R. Peterson, and E. W. Spanagel, *J. Polymer Sci.*, **2**, 306 (1947).
6. Yu, A. J., and R. D. Evans, *J. Polymer Sci.*, **42**, 249 (1960).

7. Overberger, C. G., L. H. Arond, R. H. Wiley, and R. R. Garrett, *J. Polymer Sci.*, **7**, 431 (1951).

8. For a general discussion see C. W. Bunn, in *Fibers from Synthetic Polymers*, R. Hill, Ed., Elsevier, New York, 1953, Chapter 12.

9. Cramer, F. B., and R. G. Beaman, *J. Polymer Sci.*, **21**, 237 (1956).

10. Hill, R., and E. E. Walker, *J. Polymer Sci.*, **3**, 615 (1948).

11. Frunze, T. M., and V. V. Korshak, *Vysokomol. Soedin.*, **1**, 293 (1959).

12. Korshak, V. V., *J. Polymer Sci.*, **31**, 319 (1958).

13. Frunze, T. M., V. V. Korshak, V. V. Kurashev, G. S. Kolesnikov, and B. A. Zhubanov, *Izv. Akad. Nauk SSSR, Otd. Khim. Nauk*, **1958**, 783.

14. Frunze, T. M., V. V. Korshak, and V. V. Kurashev, *Vysokomol. Soedin.*, **1**, 670 (1959).

15. Frunze, T. M., V. V. Korshak, L. V. Kozlov, and V. V. Kurashev, *Vysokomol. Soedin.*, **1**, 677 (1959).

16. Speck, S. B., *J. Org. Chem.*, **18**, 1689 (1953).

Résumé

On a étudié les température de transition vitreuse de polyamides contenant du phosphore et de polyamides contenant d'autres hétéro-atomes en fonction de leur structure au point de veu de l'effet de la polarité, du comportement stérique et des différences dans la flexibilité de la liaison. La chaîne latérale portée par le phosphore et contenant les groupements alcoyles ou aryles augment la mobilité de la chaîne (température de transition vitreuse plus basse) par séparation des chaînes et réduction de l'interaction intermoléculaire. Cet effet géneral est réduit par une diminution de la mobilité due à la plus grande polarité des groupes phosphorés et à l'empêchement stérique intramoléculaire due à la rotation provoquée par le groupement alcoyle ou aryle sur le phosphore. Les températures de transition vitreuse indiquent l'ordre suivant quant à la flexibilité de la liaison: ($CH_2NCH_2 \approx CH_2SCH_2 \approx CH_2OCH_2$) > $CH_2P(R)CH_2 \approx CH_2CH_2CH_2$. La liaison phosphore–carbone ne présente pas de flexibilité supérieure à une liaison carbone–carbone.

Zusammenfassung

Die Glasumwandlungstemperatur von phosphor-hältigen Polyamiden und Polyamiden mit anderen Heteroatomen wird in bezug auf ihre Strukturabhängigkeit anhand des Einflusses von Unterschieden der Polarität, des sterischen Verhaltens und der Bindungssteifigkeit untersucht. Es wurde eine Erhöhung der Kettenbeweglichkeit (niedrigere Glasumwandlungstemperatur) durch die am Phosphor befindlichen Seitenketten-Alkyl- oder Arylgruppen wegen der grösseren Trennung der Ketten und der Herabsetzung der zwischenmolekularen Wechselwirkung erwartet. Diesem allgemeinen Einfluss wirkt die Verminderung der Beweglichkeit durch die grössere Polarität der Phosphorgruppen und die intramolekulare sterische Hinderung der Rotation durch die Alkyl- order Arylgruppen am Phosphor entgegen. Aus der Glasumwandlungstemperatur ergibt sich folgende Reihenfolge für die Deformierbarkeit der Bindung: ($CH_2NCH_2 \approx CH_2SCH_2 \approx CH_2OCH_2$) > $CH_2P(R)CH_2 \approx CH_2CH_2CH_2$. Die Phosphor–Kohlenstoffbindung zeigt keine höhere Deformierbarkeit als die Kohlenstoff–Kohlenstoffbindung.

Received October 23, 1961

JOURNAL OF POLYMER SCIENCE: PART A VOL. 1, PP. 3569–3580 (1963)

Thermodynamic Interpretations of the Elastic Properties of Rubbers Obtained from Ethylene–Propylene Copolymers

G. NATTA, G. CRESPI, and U. FLISI, *Istituto Chimica Industriale del Politecnico di Milano* and *Istituto Ricerche Divisione Petrolchimica, Società Montecatini, Milan, Italy*

Synopsis

Stress–temperature coefficients have been measured for a high-molecular-weight ethylene–propylene copolymer, containing 45 mole-% of ethylene, chlorinated and vulcanized with a cure system based on sulphur and accelerators. From the relationships:

$$f = \left[\frac{\partial E}{\partial l}\right]_T - T\left[\frac{\partial S}{\partial l}\right]_T \text{ and } \left[\frac{\partial S}{\partial l}\right]_T = -\left[\frac{\partial f}{\partial T}\right]$$

the thermodynamic functions $[\partial E/\partial L]_T$ and $-T[\partial S/\partial L]_T$ have been determined in a range of the extension ratio up to $\alpha = 6.9$. A good agreement has been found between the experimental data and the stress–strain theoretical curve obtained for a non-Gaussian type network.

Introduction

Extensive research work on the production of linear, amorphous, high molecular weight copolymers of ethylene with α-olefins and on their use in the field of elastomers has been carried out in this laboratory for several years.[1] Beside studying the most suitable catalysts for obtaining copolymers with a random distribution of monomeric units, vulcanization was studied as well as the properties of the vulcanizates.[2]

The considerable interest aroused by these new rubbers, which are already being produced on a commercial scale, is not only due to the low cost of the olefinic monomers, as compared with that of the diolefinic used for the production of the unsaturated rubbers, but also to their peculiar properties.

Unlike natural rubber and many other synthetic rubbers, these elastomers do not contain unsaturation in the macromolecules; as a consequence of this their resistance to oxidation and to aging is far higher than that of unsaturated rubbers. These properties, as well as the good mechanical and elastic properties, make these copolymers of particular interest.

The copolymers with a fairly high ethylene content, even if prevailingly amorphous, show stress–strain curves which are similar to those of natural

rubber; in fact, an increase of the elastic moduli versus the degree of stretching follows the rather low initial moduli.

We had previously attributed these properties both to the presence of polymethylenic chain segments, even if rather short, and to their parallelization under stretching that causes an association of these chain segments with an effect comparable to a crystallization.

In order to interpret better the shape of such stress–strain diagrams and the other properties of the rubbers based on ethylene–propylene copolymers, we have carried out researches in two directions: (*1*) we tried to produce copolymers with a higher ethylene content, and such that the presence of longer methylenic chains might be foreseen, so as to favor crystallization under stretching; (*2*) we have prepared copolymers as much as possible amorphous and lacking regular chain segments, which will favor crystallization under stretching.

The runs carried out according to (*1*) for the amorphous copolymers showed that the increase in ethylene content causes a decrease of the temperature of the second order transition, but only a slight increase, at room temperature, of resilience with respect to the copolymers with an ethylene content of 50%. Copolymers containing more than 80 mole-% of ethylene show a crystallinity of the ethylenic type also in the unstretched state with a slight increase of the equatorial lattice constants, but have poorer elastomeric properties. Those copolymers of such ethylene contents that they yield a clear crystallinity by x-rays show an increase of the initial elastic modulus and on the whole less valuable elastomeric properties of the amorphous copolymers.

In research carried out according to (*2*) we tried to prepare definitely amorphous copolymers; for this purpose, we studied copolymers with a content of 50 mole-% of ethylene prepared with the aid of homogeneous catalyst systems that favor the random distribution of the monomeric units. The stress–strain curve of these copolymers shows only a slight decrease in mechanical properties, with respect to that of copolymers with a higher ethylene content. Such a decrease may be attributed to the more irregular structure of the chain. Consequently, and in order to study its effect devices have been adopted to increase the disorder in the structure of the macromolecules. Therefore, amorphous copolymers have been chlorinated, taking into account that chlorination causes, also in crystalline polymers such as polyethylene, an amorphization that is higher, the higher the chlorine content introduced.

The lack of unsaturation in the ethylene–propylene copolymers makes their vulcanization with the ingredients normally used for unsaturated rubber impossible; in fact, these rubbers are usually vulcanized with the aid of organic peroxides as crosslinking agents.[3] However, other crosslinking systems have been investigated in order to study the properties of these elastomers.[2]

In particular, we wish to refer here to the crosslinking system based on the dehydrochlorination reaction of chlorinated copolymers,[4] which

allows the use in the vulcanization of those ingredients normally used for unsaturated rubbers. In fact, this paper describes the results obtained from investigations on the mechanical properties of amorphous ethylene–propylene copolymers previously chlorinated up to a chlorine content of 15 wt.-%. Chlorination was performed in solution in order that the introduction of the chlorine atoms might be as much disordered as possible. Since the stress–strain curves of these chlorinated and vulcanized copolymers show behavior very similar to that of the rubbers crystallizable under stretching, we have started a thermodynamic study of such elastomers in order to understand better the nature of the phenomenon and to interpret it.

A chlorine content of 15% corresponds to 8 chlorine atoms for 100 carbon atoms. Also considering that in the subsequent vulcanization a part of chlorine is removed from the polymeric chains by dehydrochlorination, it must be assumed that no more than 6–7 chlorine atoms per 100 carbon atoms are bound to the polymeric chain. Such an amount can influence the completion of the amorphization of the polymer, but practically it exerts little influence on the mobility of the chain itself.

Obviously, chlorination causes an increase in the transition temperature, which could be foreseen on the basis of the Cl content: the nonchlorinated copolymer has a transition temperature of about −60°C., that of polyvinyl chloride is +77°C. The calculated value (−25°C.) corresponds to that found experimentally.

For rubbers crystallizing under stretching, some relationships exist between mechanical properties and crystallization phenomena:[5] the latter can be studied by means of stress–temperature measurements at constant length.[6,7]

In rubbers, crystallization under stretching is accompanied by a strong negative variation of internal energy; this variation, added to that of entropy, gives rise to a considerable increase in the retractive force, thus contributing to increase the tensile strength of the elastomer. In rubbers that do not crystallize under stretching, the variation of internal energy at high stretching ratios can be hardly determined because test pieces in general break before reaching the equilibrium conditions; therefore, it is impossible to determine the values of stress versus temperature within a wide range of the stretching ratio.

The thermodynamic properties versus the stretching ratio of a chlorinated and vulcanized ethylene–propylene copolymer are examined in this paper. For this rubber, unlike those rubbers that do not crystallize under stretching, it is possible to perform the stress–temperature measurements at high elongation values also.

Experimental

A high molecular weight ethylene–propylene copolymer containing 45 mole-% of ethylene and prepared with the aid of homogeneous catalysts based on soluble vanadium compounds and aluminum alkyls, was used

for these runs.[8] This copolymer was subsequently chlorinated by addition of chlorine to a solution of the copolymer in carbon tetrachloride under the conditions described in a previous paper,[9] until in the final product, a chlorine content of 15 wt.-% was attained.

The chlorinated ethylene–propylene copolymer was then mixed, in a laboratory roll mixer, with the vulcanization ingredients reported in Table I. The amount of zinc oxide is higher than that normally used for recipes of this type; however, it allows regular crosslinking to be obtained, the hydrochloric acid evolved being absorbed by the chlorinated polymer on vulcanization.

TABLE I
Recipe Used for Vulcanization of the Chlorinated Ethylene–Propylene Copolymer

Component	Parts
Polymer	100
Stearic acid	2
Zinc oxide	10
2-Mercaptobenzathiazole (MBT)	1
Tetramethylthiuram disulfide (TMT)	2
Sulfur	2

The recipe was then vulcanized in a parallel plate press at 150°C. for 30 min, and the vulcanized product thus obtained had the properties reported in Table II.

TABLE II
Properties of the Vulcanizates

Property	
Tensile strength, kg./cm.^{2}	148
Elongation at break, %	840
300% Modulus, kg./cm.^{2}	10
700% Modulus, kg./cm.^{2}	38
Resilience at 20°C., %	31
Degree of swelling at equilibrium	5.71
Degree of crosslinking, moles/cc.	0.55×10^{-4}

The degree of crosslinking was determined by measuring the retractive force at equilibrium on test pieces swollen in benzene at 30°C. For these runs test pieces of the type described in ASTM D 412 type C were used. The apparatus used was the same as that adopted by us to perform analogous measurements on cured *cis*-1,4-polybutadiene; it has been described in a previous paper.[7]

Temperature control was obtained by circulating ethyl alcohol in the tube containing the test piece; this allowed temperatures lower than

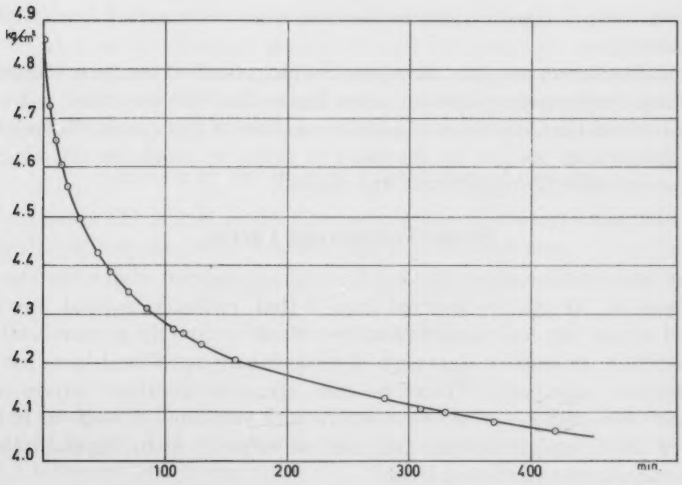

Fig. 1. Relaxation curve at 40°C. with $\alpha = 1.82$.

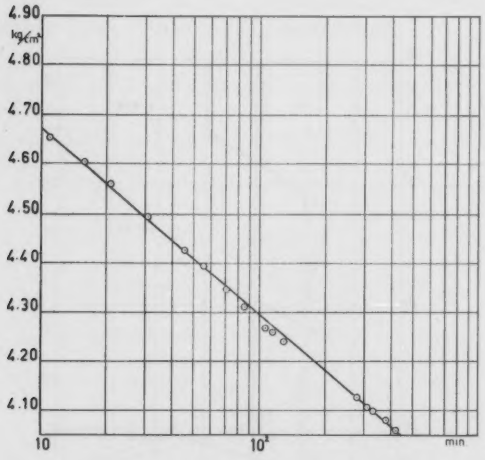

Fig. 2. Relaxation curve at 40°C. with $\alpha = 1.82$ (logarithmic scale of time).

0°C. to be attained. For these measurements the temperature was kept constant within ±0.3°C. The technique used for these runs was the same as that used by us for *cis*-1,4 polybutadiene. The test piece was stretched at the highest test temperature and left under these conditions until the stress did not appreciably decrease any longer with time (generally 3–5 hr. was enough); after that the temperature was lowered at intervals. Figures 1 and 2 show two relaxation curves obtained at the highest test

temperature. In the two figures the time scale is linear and logarithmic, respectively.

It has been observed that, after prestretching, stress at the lower temperatures remained constant also for times higher than the test time. It was also observed that, on increasing the elongation of test pieces, the relaxation temperature had to be decreased in order to avoid the breaking of test pieces before the equilibrium was reached.

Stress–Temperature Curves

The stress–temperature curves obtained as reported above are shown in Figure 3. It can be observed from it that, contrary to what was observed by us[7] for *cis*-1,4-polybutadiene, stress is directly proportional to temperature, at least in the range of temperature considered here, for all elongations examined. Therefore, the stress–temperature curves are straight lines and do not show curvature with variations in slope as in the case of *cis*-1,4-polybutadiene and natural rubber, when crystallization phenomena under stretching occur.[7]

At high stretching ratios, the slope of the stress–temperature lines are very steep; this indicates a strong variation of entropy with respect to the elongation.

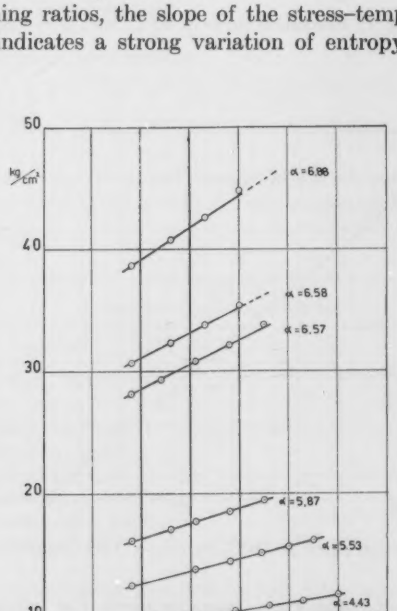

Fig. 3. Stress–temperature curves at constant length.

By extrapolating these lines to absolute zero, negative values are obtained also for low elongation values; from this point of view, the chlorinated copolymer behaves in an analogous way to crosslinked polyethylene,[10] whereas SBR shows rather low positive values, which however change their sign rapidly[11] with the increase of the stretching ratio.

Variation of the Internal Energy and of Entropy

As known, the relationships that permit the thermodynamic functions to be drawn from the stress–temperature measurements are

$$f = (\partial E/\partial l)_{T,V} - T\,(\partial S/\partial l)_{T,V} \tag{1}$$

$$-(\partial S/\partial l)_{T,V} = (\partial f/\partial T)_{l,V} \tag{2}$$

$$f = (\partial E/\partial l)_{T,V} + T(\partial f/\partial T)_{l,V} \tag{3}$$

where f is the stress exerted on the test piece in order to maintain it at a constant length, E is the internal energy, S is the entropy, l is the length, and T is the absolute temperature.

By using relation (3) it is possible to obtain the term $(\partial E/\partial l)_{T,V}$ from the stress–temperature plots by extrapolation to absolute zero. Figures 4 and 5 report the values of $(\partial E/\partial l)$ $(\partial S/\partial l)$ and of f versus the stretching ratio at the temperatures of 15 and 0°C., respectively.

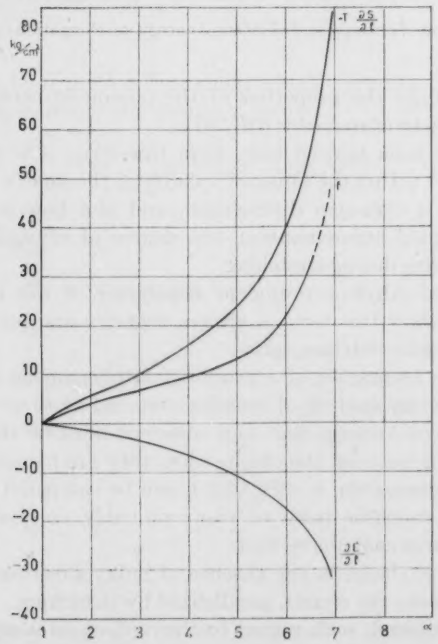

Fig. 4. Variation of entropy and of internal energy vs. elongation (values at 15°C.).

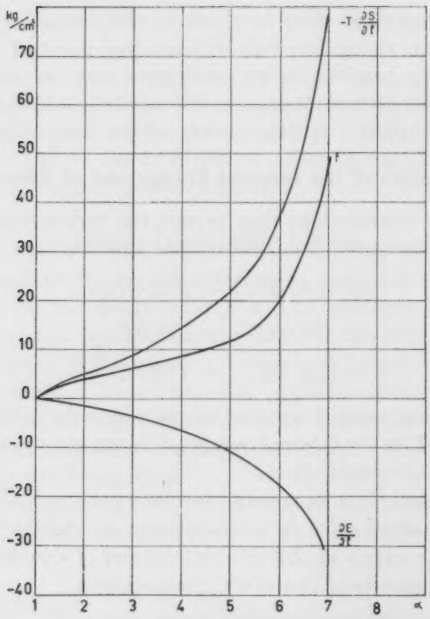

Fig. 5. Variation of entropy and of internal energy vs. elongation (values at 0°C.).

In order to study the properties of the polymeric network, the most important term to be examined is $(\partial E/\partial l)_{T,V}$.

It has already been noticed how, from this term, it is possible to obtain $d \ln \bar{r}_0^2/dT$,[12] within the limits of validity of the kinetic theory of elasticity, based on a Gaussian distribution, and also how it is possible to evaluate, to a good approximation, the degree of crystallization of the rubbers crystallizing during stretching.[7]

For chlorinated ethylene–propylene copolymer, it can be observed in Figures 4 and 5 how this term is always negative and assumes high absolute values at high stretching ratios.

If the possible occurrence of crystallization phenomena is excluded, as is seen from the x-ray analysis of samples stretched up to $\alpha = 7$, the strong variations of internal energy that were observed must be attributed to the interaction arising between the chains when they are parallelized owing to stretching; this interaction is such that it can be compared to a change of state, from the energetic point of view; probably an association of the polar groups present contributes to it.

The linearity of chains in the absence of bulky substituents favors the associations between the chains, parallelized by stretching. These associations can be compared, with regard to their effect, to a crystallization of lower degree, which cannot be detected by x-ray analysis.

Theoretical Stress–Strain Curves and Comparision between Them and the Experimental Data

It is known that the theory of elasticity based on the Gaussian network is valid only for a narrow range of the stretching ratio, and that the theoretical curves are quite different from the experimental ones for values of α higher than $^1/_3\ R_{max}/\bar{r}_0^2$, where R_{max} is the length of the chain fully extended and $\bar{r}_0^2$ is the mean-square length of the unstretched chain.

A theoretical stress–strain relation that does not introduce the approximations assumed for the Gaussian network was obtained independently by Kuhn and Grün[13] and by James and Guth[14] treating the non-Gaussian network, and is given in eq. (5):

$$f = \frac{NKT}{3} n^{1/2}[\mathfrak{L}^{-1}(\alpha n^{-1/2}) - \alpha^{-3/2}\,\mathfrak{L}^{-1}(\alpha^{-1/2}\, n^{-1/2})] \tag{5}$$

In this equation N is the total number of chains, K is the Boltzmann constant, T is the absolute temperature, n is the number of links of the chains, α is the stretching ratio, and $\mathfrak{L}^{-1}$ is the inverse Langevin function.

If the contribution to stress of the internal pressure is small, eq. (5) can be simplified to:

$$f = \frac{NKT}{3k}\,[\mathfrak{L}^{-1}(\alpha k) - (3k/\alpha^2)] \tag{6}$$

where $k = n^{-1/2}$.

By indicating by G the NKT product, which is constant at a given temperature, eq. (6) becomes the simple equation:

$$f = \frac{G}{3k}\,[\mathfrak{L}^{-1}(\alpha k) - (3k/\alpha^2)] \tag{7}$$

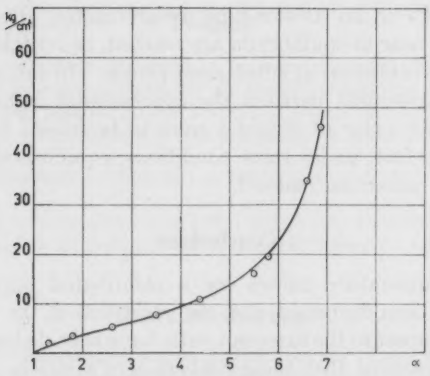

Fig. 6. Curve obtained from eq. (7) for $G = 1.95$ and $k = 0.13$ and stress values (⊙) obtained from Fig. 3.

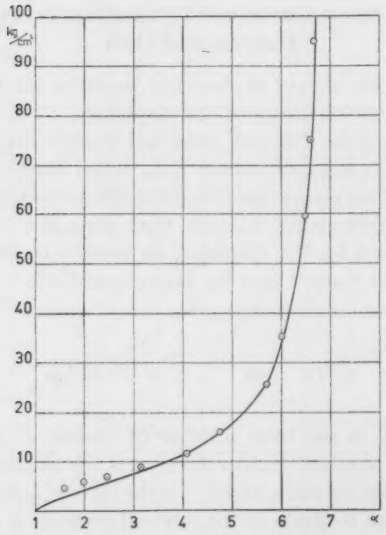

Fig. 7. Curve obtained from eq. (7) or $G = 2.25$ and $k = 0.14$ and values of the stress (⊙) obtained on the dynamometer.

In Figure 6, relation (7), calculated for the values $G = 1.95$ kg./cm.^{2} and $k = 0.13$, is compared with the experimental values of stress at equilibrium versus elongation, obtained from the diagram of Figure 3, at a temperature of 15°C.

The perfect agreement between the actual values of stress measured at equilibrium conditions and the theoretical curve demonstrates the validity of eq. (7) for the whole elongation range. In Figure 7 a comparison is also made between relation (7) and the stress–elongation curve obtained at 15°C. on an Amsler-type dynamometer, after several cycles when conditions near to equilibrium are reached, as revealed by the superposition of curves obtained at subsequent cycles. In this case, in order to obtain a good agreement between the experimental values and the theoretical curve, the value of G and k were to be varied to 2.25 and 0.14 respectively. In fact, under these conditions, equilibrium for low values of the stretching ratio is not reached.

Conclusions

The stress–temperature curves for a chlorinated ethylene–propylene copolymer have been examined, and the variations of the thermodynamic functions with respect to the extension ratio have been deduced.

It has been observed that these rubbers give a strong variation of the internal energy, of the same order as that of rubbers that crystallize during stretching. This notwithstanding that the stress–temperature relations

are linear and that the copolymer used has a composition excluding the crystallization under stretching.

On the contrary it was observed that the stress–elongation curves at equilibrium can be represented with excellent agreement, by the theoretical relation between stress and elongation derived for the non-Gaussian network. This relation foresees a strong upward curvature of the stress–elongation curve for values of the stretching ratio which are near the highest extensibility of the chains. This phenomenon, observed here under equilibrium conditions, was difficult to be appreciated in rubbers that do not crystallize under stretching and is masked by the effect of crystallization for rubbers with structure regularity.

References

1. Natta, G., *Rubber Plastics Age*, **39**, 493 (1957); G. Natta, G. Mazzanti, A. Valvassori, and G. Pajaro, *Chim. Ind. (Milan)*, **39**, 733 (1957).
2. Natta, G., and G. Crespi, *Chim. Ind. (Milan)*, **41**, 123 (1959); G. Natta, G. Crespi, and M. Bruzzone, *Kautschuk Gummi*, **14**, 3, 54 (1961).
3. Natta, G., G. Crespi, E. DiGiulo, G. Ballini, and M. Bruzzone, *Rubber Plastics Age*, **42**, 43 (1961).
4. Crespi, G., and M. Bruzzone, *Chim. Ind. (Milan)*, **43**, 137 (1961).
5. Treloar, L. R. G., *The Physics of Rubber Elasticity*, Clarendon, Oxford, 1958, p. 270.
6. Boonstra, B. B. S. T., *Ind. Eng. Chem.*, **43**, 361 (1951).
7. Crespi, G., and U. Flisi, *Chim. Ind. (Milan)*, **43**, 993 (1961).
8. Mazzanti, G., A. Valvassori, and G. Pajaro, *Chim. Ind. (Milan)*, **39**, 743 (1957); G. Mazzanti, A. Valvassori, and G. Pajaro, *ibid.*, **39**, 825 (1957); G. Natta, A. Valvassori, G. Mazzanti, and G. Sartori, *ibid.*, **40**, 717 (1958).
9. Bruzzone, M., and G. Crespi, *Chim. Ind. (Milan)*, **42**, 1226 (1960).
10. Ciferri, A., C. A. J. Hoeve, and P. J. Flory, *J. Am. Chem. Soc.*, **83**, 1015 (1961).
11. Roth, F. L., and L. A. Wood, *J. Appl. Phys.*, **15**, 749 (1944).
12. Flory, P. J., A. Ciferri, and C. A. Hoeve, *J. Polymer Sci.*, **45**, 235 (1960).
13. Kuhn, W., and F. Grün, *Kolloid-Z.*, **101**, 248 (1942).
14. James, H. M., and E. Guth, *J. Chem. Phys.*, **11**, 455 (1943).

Résumé

On a mesuré les coefficients thermiques de tension d'un copolymère éthylène–propylène de poids moléculaire élevé, contenant 45 mole-%, d'éthylène, chloré et vulcanisé au moyen d'un système basé sur du soufre et des accélérateurs. Les fonctions thermodynamiques $[\partial E/\partial l]_T - T[\partial S/\partial l]_T$ et sont déterminés en partant des relations

$$f = [\partial E/\partial l]_T - T[\partial S/\partial l]_T \text{ et } [\partial S/\partial l]_T = -(\partial f/\partial T)_l$$

dans un domaine de rapports d'extension jusqu' à $\alpha = 6.9$. On constate un bon accord entre les courbes de tension-élongation théoriques obtenues pour un réseau d'un type non-Gaussien.

Zusammenfassung

Es wurden die Spannungs-Temperatur-Koeffizienten eines Äthylen–Propylen-Copolymeren hohen Molekulargewichtes mit einem Äthylengehalt von 45 Mol% gemessen, das chloriert und mit einem aus Schwefel und Beschleuniger bestehenden Vulkanisationssystem vulkanisiert wurde. Aus den Gleichungen

$$f = [\partial E/\partial l]_T - T[\partial S/\partial l]_T \text{ und } [\partial S/\partial l]_T = -[\partial f/\partial T]_l$$

wurden die thermodynamischen Funktionen $[\partial E/\partial l]_T$ und $-[\partial S/\partial l]_T$ in einem Bereich des Dehnungsverhältnisses bis hinauf zu $\alpha = 6{,}9$ berechnet. Die Ergebnisse stimmen mit den für ein Netzwerk vom Nicht-Gauss'schen Typ berechneten theoretischen Spannungs-Dehnungs-Kurven gut überein.

Received June 10, 1963

JOURNAL OF POLYMER SCIENCE: PART A VOL. 1, PP. 3581–3596 (1963)

Thermodynamics of Crystalline Linear High Polymers. III. Thermal Breakdown of the Crystalline Lattice of Polyethylene*

BERNHARD WUNDERLICH, PETER SULLIVAN, TAMIO ARAKAWA, A. B. DICYAN, and J. F. FLOOD, *Department of Chemistry, Cornell University, Ithaca, New York*

Synopsis

The thermal breakdown of the crystalline lattice of polyethylene grown by quenching from solution (dendrites) and by cooling slowly from solution (single crystals) and melt has been investigated as a function of heating rate. The dendrites showed strong reorganizations at temperatures only little above the crystallization temperatures. Heating rates as fast as 20°C./min. could not avoid this reorganization. Heating rates between 10 and 20°C./min. were necessary to have a constant melting point for single crystals grown from solution. The measured melting points were proportional to the thickness and perhaps the density of the samples as determined by interference microscopy and by the density gradient column method. Surface free energy values calculated from the lowering of the melting points range from 81–96 ergs./cm.^{2}. Literature values on specific heats and specific volumes of bulk samples allowed a discussion of the premelting behavior of semicrystalline polyethylene. It is found that the defects frozen-in below the glass transition temperature "grow" above 250°K. depending upon the overall crystallinity. This destroys the additivity of the specific heat as well as the specific volume. Correlation with NMR and dynamic mechanical loss measurements are attempted. The difference between melting and dissolution temperature in toluene (0.5–8.0 mg. polyethylene/g. toluene) for slowly cooled bulk as well as solution crystals was found to be 26°C., placing the maximum dissolution temperature of polyethylene crystals in toluene at 111°C.

A. INTRODUCTION

Three characteristic morphological structures of polyethylene are known. When melt is crystallized some 20–50°C. below the melting point, spherulitic growth arises. The spherically ordered aggregates may have a size up to 1 mm. They are made up of twisting, ribbonlike crystals radiating spherically from the center.[1]

From solution, dendrites arise[2,3] under similar crystallization conditions as are necessary for the growth of spherulites. Their morphology is similarly spherical when floating in solution.[3] On flattening out on the microscope slide the structures represented in Figure 6 are observed. Their size also reaches the order of magnitude millimeters.

* For previous articles of this series see Wunderlich et al.[12,25]

By cooling very slowly single crystal platelets grow[4] from solution. These can also have lateral dimensions up to 1 mm.; however, they are thin lamellae of about 150 A. thickness. A thickening mechanism of the platelets is based on a screw dislocation leading to growth spirals. Similar growth spirals have been found in slowly cooled melts.[5]

On a molecular scale all these structures can be built up with the orthorhombic unit cell[6] and a series of defects.[7] The unit cell dimensions are dependent upon temperature[8] and to some degree also on the defects.[9]

The normal modes of vibration of the all-*trans* chains in perfect crystalline arrangement are also known.[10] Comparison with specific heat measurements[11] has shown that the molecules in large perfect crystals of polyethylene show no motion outside of vibrations up to 400°K. All rotational motion is concentrated in the defects.

To describe the thermodynamic state of the three characteristically different structures, the fraction of material forming perfect unit cells and the amount and type of surfaces and defects must be known.[12] The general expression for the total free energy of the polymer is given by[7]

$$F = \sum_i F_i \tag{1}$$

where F_i is the free energy of the subsystems making up the whole sample. The subsystem is thought to be small enough to be homogeneous, but also large enough to neglect inhomogeneities due to the molecular structure. Each F_i can be represented[7] by

$$F_i = m_i^0 \mu_{\text{cryst.}}^0 + \sum_d m_i^d \mu_d + \sum_s m_i^s \mu_s \tag{2}$$

where m_i^0 is the weight of polymer contained in perfect unit cells and $\mu_{\text{cryst.}}^0$ the corresponding chemical potential at the temperature in question. The two sums contain analogously defined terms for the internal defects, d, and the different surfaces, s.

For the slowly crystallized samples, interference microscopy can give the thickness of the crystal platelets. In this way the surface area is determined. The only term not known in eq. (2) would be the sum of defect effects. Every crystal platelet visible under the microscope is treated as a single subsystem.

At room temperature all the structures described above are metastable, so that the course of thermal breakdown on heating will depend upon heating rate.[7] In this paper the effect of rate will be analyzed experimentally, in order to gain information on the structures present at low temperatures in the metastable state.

B. EXPERIMENTAL

Samples

All experiments were performed with unfractionated linear polyethylene (Marlex 50 type, kindly supplied by the Phillips Petroleum Co., Bartlesville, Oklahoma). The bulk samples were cooled from approximately

20°C. above their melting point down to room temperature. The cooling rate used was 0.3°C./min. Dendritic polyethylene was obtained by crystallization of a 0.61 wt.-% solution in toluene under the given conditions. Single crystalline polyethylene was obtained by crystallizing from solutions of specified concentration and solvent. The temperature was dropped from 2°C. above the crystallization temperature (previously determined approximately) to 5°C. below this temperature. This procedure was found necessary to obtain large usable crystals for observation under the interference microscope. Isothermal crystallization usually gives only very much smaller crystals often covered with irregularly arranged overgrowth.

DTA Melting

The DTA apparatus was described in detail in a previous publication of this series.[12] A 0.5-g. portion of material was employed. The heating rate was varied between 1.8 and 3.4°C./min.

Hot-Stage Melting

Dendrites and single crystals can easily be observed with the help of an interference microscope.[13] Figure 6 gives typical examples. The complete breakdown of the structure is easily recognizable as the point where the dendrite or single crystal growth spiral changes to a droplet. A condition for this observation is that enough material is concentrated in the crystal under observation. Single lamellae will usually not form droplets, but stick to the glass in small, hardly resolvable separated specks and maintain the overall shape of the crystal. To find the melting point of single crystal lamellae, growth spirals were used. Single growth spirals of heights between 4,000 and 30,000 A. of the samples were measured. The different heights showed no influence on the melting point. It was, however, noted that less perfect growth spirals, recognized by their secondary growth spirals, always melted earlier. The dendrites used for melting had the same thickness range. All samples were dried 8–16 hr. in vacuum at 55–

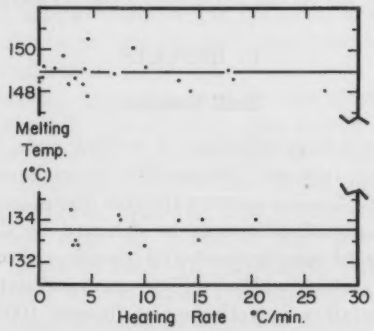

Fig. 1. Melting temperature of two standard melting point compounds as a function of heating rate.

60°C. before melting to assure complete removal of trapped solvent. For the measurements Reichert Normarski incident light interference optics with an 11 × objective and a Leitz hot stage were used.

To calibrate the hot stage as a function of heating rate two standard melting point compounds were measured. The thermometer was graduated in steps of 0.5°C. Figure 1 shows that up to at least 20°C./min. there was no lag in the thermometer system with the standard compounds. All measurements were made with a coverglass and shielding. The calibration with standard melting point compounds showed a standard deviation of a single measurement of ±0.7°C. The given melting point range of the standard compounds fell within one standard deviation. The observed changes in structure are thus fixed to within ±0.7°C.

Dissolution of Samples

The dissolution of bulk, dendrites, and single crystals was undertaken in a regulated bath under the heating condition given below. For dendrite dissolution, samples were withdrawn at constant time and temperature intervals and observed under the A. O. Baker interference microscope.[13] In this way two observations could be made. The structure could be checked for possible changes, and the residue left after evaporation of the solvent could be observed for secondary crystallization. This secondary crystallization is indicative of dissolution (see Fig. 6).

Bulk sample dissolution was measured by immersing a Pt wire basket with approximately 6 g. of sample in a controlled bath of toluene and measuring the total immersed weight (~0.8 g.) continuously. The temperature was raised 1–2°C. when constant weight was obtained after the previous temperature increase. After complete dissolution, the concentration of the solution was 8.2 mg. polyethylene/g. toluene. The accuracy was sufficient to detect changes of −0.5% in the amount of polymer in the wire basket.

The single crystalline sample was observed visually on heating to detect the disappearance of the turbidity caused by the crystalline lamellae.

C. RESULTS

Bulk Samples

For bulk samples a large selection of melting data is available in the literature, including detailed information throughout the melting region.[11,12,14] The two facts of interest for this discussion are the temperature where first recrystallization can be detected by slow heat evolution and the first increased specific heat and specific volume beyond the extrapolated semicrystalline values. First recrystallization was observed for 82 and 92% crystalline polyethylene at 390 and 400°K., respectively.[14] The time scale of these experiments was hours.

Figure 2 shows collected data from the literature on specific heats in

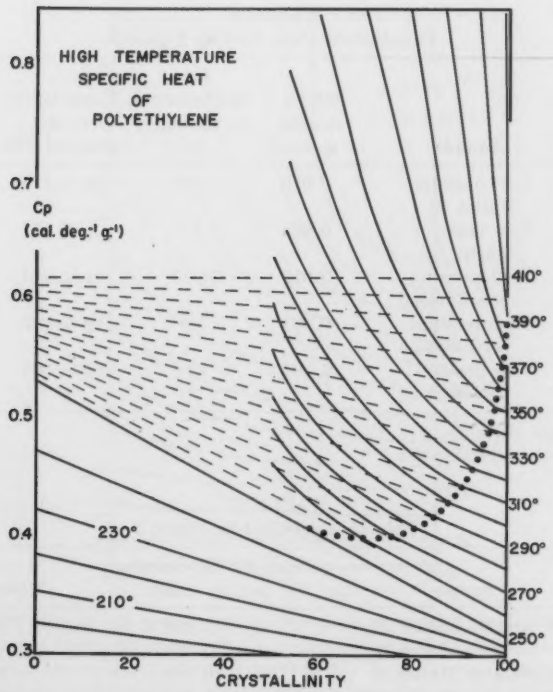

Fig. 2. Specific heat of polyethylene as a function of crystallinity at various temperatures. The dotted line separates the linear region from the nonlinear one.

the melting range plotted as a function of crystallinity at low temperature. The characteristics of the data used are given in Table I.

In the straight-line portion of the graph all experimental values are within 0.5% error. The curved portions represent all data to within 2% or better up to 350°K. and to within 5% or better up to 410°K. Deviations from linear crystallinity dependence are clearly evident even far below recognizable recrystallization.

A similar comparison was attempted by use of specific volume data. These data are inherently less accurate than specific heat data. Figure 3 shows the deviation of the measured specific volume from a specific volume calculated assuming linear addition of the volume contribution of amorphous and crystalline content. The normalization was done at 300°K. because most data are available only down to 300°K. The samples used are listed in Table II. The most striking result is that deviations start at 300°K., indicating that there is no additivity even at these low temperatures. The specific volume of the crystalline polyethylene was calculated from Swan's data[22] on the expansion of the unit cell. The amorphous specific volume was calculated from values by Richardson.[23]

TABLE I
Polyethylene Data Used for Figure 2

Sample No.	Sample	300°K. density, g./cm.³	Low temperature crystallinity, %	Temperature range measured, °K.	Reference
1	Low pressure Marlex 50	0.975	92[a]	up to 420	14
2	Low pressure Marlex 50	0.965	82[a]	up to 415	14
3	High pressure polyethylene	0.915	50–55[a]	up to 470	15
4	High pressure polyethylene	0.921	58[b]	up to 300	16
5	Low pressure polyethylene	0.964	79[b]	up to 300	16

[a] From heat of fusion.
[b] From x-ray crystallinities.

TABLE II
Polyethylenes Used for Figure 3

Sample	300°K. density, g./cm.³	Reference
Low pressure Marlex 50	0.968	20
Low pressure Marlex 50	0.960	17,18
Low pressure Marlex 50	0.951	19
Low pressure Ziegler polyethylene	0.937	19
High pressure polyethylene	0.907	19
High pressure polyethylene	0.921	21
High pressure polyethylene	0.918	21
High pressure polyethylene	0.922	21
High pressure polyethylene	0.928	21
High pressure polyethylene	0.902	21
Completely amorphous polyethylene	0.850	23
Completely crystalline polyethylene	0.999	22

Deviations of the experimental points from the smooth curves of Figure 3 are less than 0.005 g./cm.³ up to 350°K. and up to 0.02 g./cm.³ above 350°K.

Experimental maximum melting points[7] on linear high polymers with a noncrystallizable copolymer content of 0.005 mole fraction were determined by DTA[12] and calorimetry.[14] For slow crystallization, corresponding to cooling rates of 0.003–0.3°C./min., the experimental maximum melting point was constant over a wide range of heating rates: 134–135°C. was the value found for rates of heating between 3.4 and 0.3°C./min. This leads to a calculated value of 136–137°C. for pure polymethylene

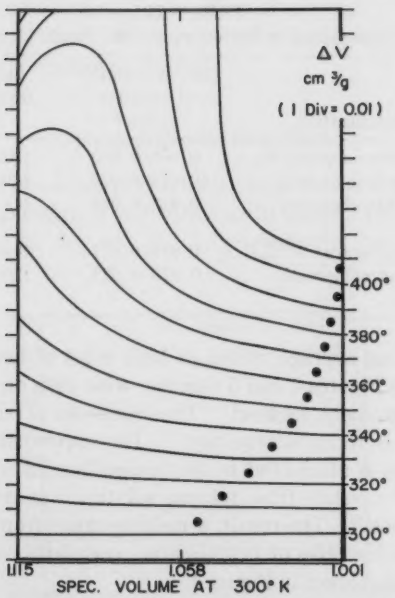

Fig. 3. Deviation of the specific volume of polyethylene from the calculated specific volume assuming additivity of amorphous specific volume and crystalline specific volume as a function of the measured specific volume at 300°K. at various temperatures. The dotted line separates the region of strict additivity from the region of deviations. Successive temperature curves are shifted by 0.01 cm.³/g.

crystallized in the same fashion.[12] This is in accord with measurements by Mandelkern.[24]

The results of dissolution experiments in toluene on two bulk polyethylene samples, one carefully crystallized as for the calorimetry data above and one quickly cooled are summarized in Table III.

TABLE III
Dissolution of Bulk Polyethylene in Toluene

Sample	300°K. density, g./cm.³	Temperature of solution, °C. 1% dissolved	50% dissolved	99% dissolved
Slowly crystallized	0.979	104	105	106.5
Fast crystallized	~0.960	100	101.5	105

Solution-Grown Single Crystals

The rate-dependent melting points of solution-grown single crystal growth spirals is shown in Figures 4 and 5. The different samples show differences in melting point as well as in rate dependence. Table IV

TABLE IV
Solution-Grown Linear Polyethylene (PE) Single Crystal Data

Mode of crystallization	300°K. density of crystals, g./cm.^{3}	Lamella thickness, A.	Limiting melting point, °C.
6.0 mg. PE/g. decane at 101°C.	0.969–0.973	132 ± 11	117.4
0.5 mg. PE/g. xylene at 90°C.	0.972–0.977	149 ± 17	122.8
0.4 mg. PE/g. chlorobenzene at 89°C.	0.983–0.988	144 ± 13	122.4
4.0 mg. PE/g. toluene at 91°C.	0.976–0.977	144 ± 13	121.2
2.5 mg. PE/g. tetrachloroethylene at 81°C.	0.973–0.978	129 ± 15	118.5

collects the limiting average values at high rates of heating indicated by horizontal lines in Figures 4 and 5 together with data on densities obtained by the density gradient method. The thickness of single lamellae was measured by interference microscopy.[13] The somewhat large variation of the thickness data is attributed to the nonisothermal crystallization.

DTA on single crystals from toluene solution was reported in the first article of this series.[25] The result, a melting range from 121°C. to a peak of 129°C. for heating rates of 1–2°C./min., correlates nicely with the data on that heating rate shown in Figure 4.

Dissolution of the single crystals grown from toluene solution was done by reheating the suspension of single crystals obtained on crystallization. At rates varying between 0.1 and 1.6°C./min. the dissolution was observed visually to occur at 94–96°C., independent of rate. Reduction of the

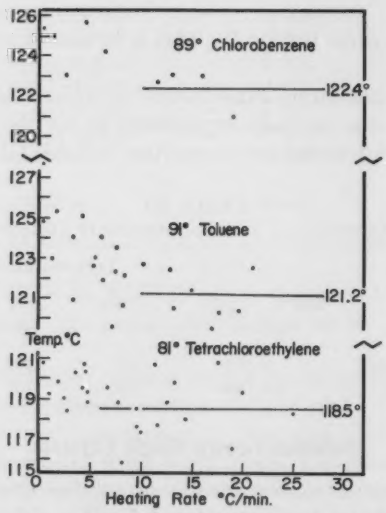

Fig. 4. Melting temperatures of different samples of polyethylene as a function of heating rate. For additional information see Table IV.

heating rate to 0.01°C./min. leads after dissolution of a large fraction of the starting material to some recrystallized polyethylene which has a final dissolution temperature of 97–98°C.

Solution-Grown Dendrites

Four samples of increasingly dendritic character were grown by quenching a 0.61 wt.-% solution of polyethylene in toluene from 110°C. Three were quenched to 75, 70, and 65°C., respectively, by immersion into a

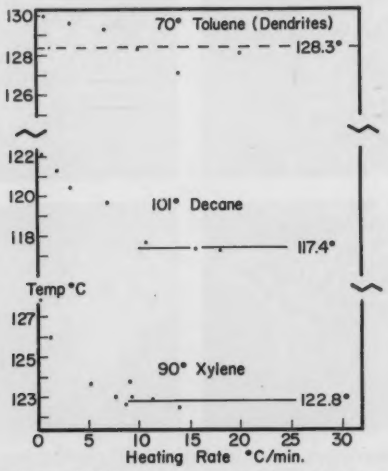

Fig. 5. Melting temperatures of different samples of polyethylene as a function of heating rate. For additional information see Tables IV and V.

TABLE V
Dendrite Dissolution

Sample	300°K. density, g./cm.³	Temperature of first clear change in dendrite and appearance of some dissolved polyethylene, °C.	Temperature at which no recognizable dendritic shapes left most material dissolved, °C.	Temperature of complete dissolution, °C.
75° dendrites	0.969–0.970	87	93–95	97
70° dendrites	0.967–0.970	85	93	95–96
65° dendrites	0.963–0.968	81–85°C.	89–90	95
Liq. N_2 dendrites	0.953–0.961	78–83°C.	—	96

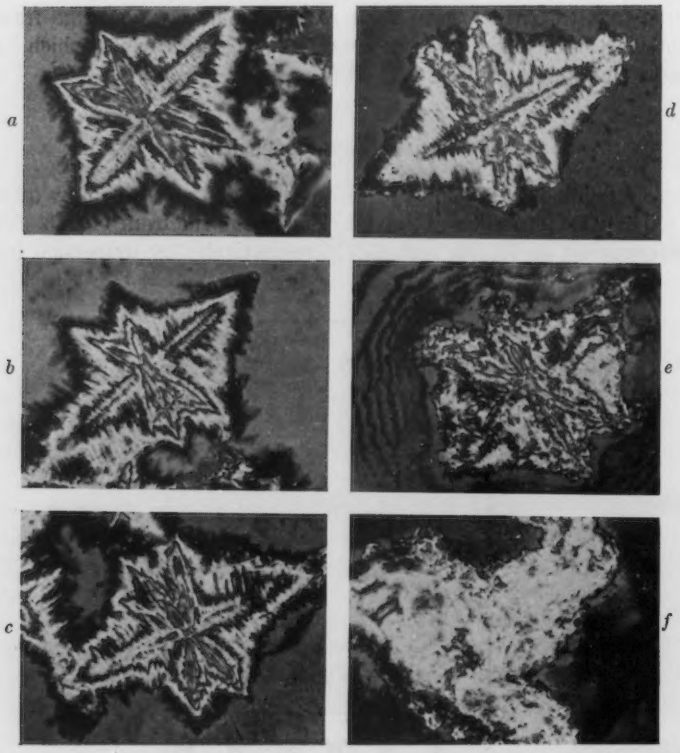

Fig. 6. Stages in dissolution of dendrites of polyethylene grown from toluene solution at 70°C. as observed on samples withdrawn at the various temperatures from the dissolution bath: (*a*) room temperature; (*b*) 76°C.; (*c*) 83.5°C.; (*d*) 85.4°C.; (*e*) 89.3°C.; (*f*) 92.8°C. Interference micrographs, A.O. Baker 10× shearing type objective. The long side of each photograph is 0.14 mm. in length.

regulated waterbath of the proper temperature. The fourth sample was quenched from 110°C. by pouring the hot solution into liquid N_2. The time needed to quench the solution in the waterbath to within 4–5°C. of the final temperature was 4–7 min., whereas the appearance times of the first visible dendrites were 6, 2, and 0.5, min., respectively. This means the lower temperature crystallizations started sometime before the equilibrium temperature was reached. At least in the higher temperature crystallizations most dendrites were formed at the constant temperature. The dendrites decreased in size and increased in feathery character on lowering of the crystallization temperature, as was observed before.[26] The dendrites grown at decreasing temperatures should in this way show increasing amounts of defects.

Melting experiments with single dendrites on a microscope slide were performed as in the case of growth spirals. Figure 5 shows values for the

70°C. dendrites, indicating only little variation with heating rate and a considerably higher melting point than the single crystals. In fact, the melting point is close to the slow rate melting point of toluene-grown single crystals, which may be taken as an indication that the heating rates employed were not fast enough for melting without extensive recrystallization.

Dissolution experiments are better suited in this case to obtain an indication of the rearrangements on heating. The dendrites were heated in contact with the mother liquor in steps of 2°C./10 min. and 2°C./60 min. Samples for microscopic observation were taken after each temperature increase. The two heating rates showed no significant differences. Figure 6 shows the characteristic changes in 70°C. dendrites as observed by the interference microscope. Increased partial dissolution parallels the reorganization, as is indicated by the background material which deposited on the slide on evaporation of the solvent. Table V summarizes the results on all dendrites.

D. DISCUSSION

1. Bulk Melting

Figure 2 shows that deviations from the linearly extrapolated specific heats occur as low as 260°K. for low crystallinities. The lower limit of the deviations as a function of crystallinity is marked by the dotted curve, which approaches the glass transition specific heats at low crystallinities and the 100% crystallinity vertical line at high crystallinities. The deviations become larger and less reproducible at higher temperatures and finally go over smoothly into the melting peak. To compare with the final melting, the scale of Figure 2 would have to be expanded considerably. The specific heat melting peak measured for sample 1 (Table I) was 18 cal./deg. g. at 406°K. A similar picture is offered by the plot of the deviation from additive specific volumes. Figure 3 contains values of this difference from 35 to 100% crystallinity (specific volume at 300°K. = 1.115–1.001 cm.^{3}/g.). The volume deviations start to be noticeable at a somewhat higher temperature and show a long, almost linear decrease in ΔV before going over into the horizontal lines at high crystallinities, which indicate strict additivity.

Since both completely amorphous as well as completely crystalline polyethylene exhibit no deviation from specific heats extrapolated down from the melt of the amorphous and up from the low temperature solid for crystalline materials, this additional contribution must be attributed to the presence of ordered and disordered polymer chain segments in the immediate vicinity, so that an interaction between the two states of order can occur.

The description offered here is, that below the dotted line of Figures 2 and 3, the defects present in bulk polyethylene can be represented by assigning fractional order to them, based on the amorphous polymer as zero and the x-ray crystalline material as 1.0. This leads to the well known one param-

eter (weight fraction crystallinity ^cw) description of semicrystalline polymers, which satisfactorily predicts specific heats, specific volumes, and related quantities. Above the dotted line this additivity breaks down, the disorder and/or size of the defects must increase by changing some of the completely or partially ordered chain segments in or near the defects into a less ordered configuration. This "growth" of the defects causes the enthalpy and volume increase indicated in Figures 2 and 3. The growth of the defects is reversible over a limited temperature range. Only at considerably higher temperatures have the defects acquired enough motion to reorganize into thermodynamically more stable, ordered configurations. In specific heat measurements this ordering (recrystallization) is detected as prolonged negative drifts after heat addition.[14] For a sample of 82% crystallinity at low temperature (Marlex 50), for example, the first growth of defects occurs according to Figure 2 at about room temperature, while the first noticeable recrystallization was discovered at 115°C.[14]

Supporting evidence for the above description comes from measurements of dynamic mechanical properties of semicrystalline bulk polyethylene. A loss peak α' is found in semicrystalline polyethylene between the upper glass transition peak β and the high temperature peak α'' which is attributed to final melting.[27-31] A loss peak indicates a maximum in the molecular relaxation time spectrum at the same frequencies as was used for the measurements. Not enough measurements on samples of varying crystallinities and over a wide enough range of frequencies are known to attempt a more quantitative correlation between specific heats and dynamical mechanical measurements. Qualitatively, the intermediate α' loss peak[32] behaves in the proper way. The α' peak shifts to lower temperatures for lower crystallinities[27-31] and becomes less intense for higher crystallinities,[27] in accord with a reversible motional process which causes a change in order in or near a defect.

Nuclear magnetic resonance measurements also indicate an additional process in the temperature range between the upper end of the glass transition interval (250°K.) and the final melting. The broad component of the resonance signal which in completely crystalline material narrows only at the melting point starts narrowing at about 300°K. for high pressure polyethylene and at increasingly higher temperatures for more highly crystalline samples.[33] The narrowing process finally leads to a disappearance of the broad component as is expected on complete melting. Determinations of the fraction of rigid polymer[34] in a sample are not numerous and accurate enough so that a separation of the intensity of the narrow component of the NMR signal according to increase in mobility of amorphous frozen chains and increase of disordered material could be made. It must be kept in mind that the effect discussed here is a second-order effect compared against the final melting peak. Taking again the 82% crystalline Marlex 50 as an example, the first detectable deviation comes at about 20°C. At 70°C. the increase of the specific heat above that of 82% crystalline and 18% amorphous material is only 0.016 cal./deg. g., which has led to an enthalpy

increase of no more than 0.2–0.4 cal./g. over this range, which corresponds to a crystallinity change of 0.3–0.6%.

Turning now to the relatively sharp melting peak it has been long recognized that determination of the disappearance of the last trace of crystallinity, the maximum melting point, is rate-dependent.[14,24,35–39] Recrystallizations after a large enough fraction of the metastable structure has collapsed allows the formation of more perfect structures with correspondingly higher melting points. As a result measurements performed at slow rates of heating[24,35–39] are made with samples of continuously varying crystalline order and cannot be used to draw conclusions about the material which was on hand at the lower temperatures.[12] Using heating rates which are considerably faster than the rate allowed for cooling (crystallization) minimizes this reorganization and does allow conclusions about the structures on hand at room temperature and below. Experimentally it was found that for polyethylene a ten times faster heating than cooling rate practically eliminates recrystallizations.[25,12]

The experimental maximum melting point[7] of 136–137°C. for the given rate of cooling has to be compared with theoretical maximum melting points of the thermodynamic equilibrium crystals. The most recent extrapolation[40] of paraffin melting points leads to 141 ± 2.4°C., a 4.5°C. higher value. This lowering must be attributed mainly to surface effects. Dissolving the same polymer instead of melting, leads to a further reduction in the temperature of the breakdown of the crystalline lattice, due to the lowering of the chemical potential of the amorphous polyethylene in solution. The measurements (part C) indicate that samples crystallized at different cooling rates, similar to the bulk experiments,[14] show a shift of the 50% dissolution temperature to higher temperatures on slower cooling, while the experimental maximum dissolution temperature, T_D, stays relatively constant for the cooling rates used. More accurate experiments are in progress and will be reported on in a later article of this series. The assumption that the presence of the solvent gives only an additional term to eq. (2) leads to the modified dissolution equation at the given concentration:

$$(1/T_D) - (1/T_D^0) = \text{const.} \tag{3}$$

Since the defect free energy will not change considerably in going from a melt to a solution T_D^0, the dissolution temperature of a perfect crystal can be estimated to be about 4.5°C. higher or 111°C., a value close to the T_D^0 assumed previously.[26] The uncertainty expected is 2–3°C.

2. Single Crystals

Experiments on solution-grown single crystals at elevated temperatures are even more involved, since these crystals are grown at a relatively low temperature and on heating above the crystallization temperature of 70–100°C. considerable reorganization has been found.[41,42] The most prominent one is a thickening of the crystal lamellae leading to a decrease in sur-

face area which as all reorganizations increases the melting point. Figures 4 and 5 show, however, that increasing the heating rate beyond 10°C./min. leads to a plateau in melting points and the exclusion of at least one, if not all of the reorganization processes. Since there is no superheating in such crystals[43] this temperature has been recorded in Table IV, together with density and average lamella thickness data. The thickest crystal shows clearly the highest melting point, while the two thinnest crystals show the lowest melting points using the limiting fast rate melting points. The melting points are thus shown to depend mainly upon the surface area. Minor deviations like between the decane and tetrachloroethylene crystallized samples are traceable to the difference in density, which should be a measure of the internal defects, although this correlation is on the borderline of experimental accuracy. Assuming that the internal defects contribute little to the melting point and neglecting all but the fold surfaces gives eq. (2) the form

$$T = T_0[1 - (2\sigma_e/\Delta h_f l)] \tag{4}$$

where T is the experimental melting point, T_0 the maximum melting point for the given copolymer content (139°C.), Δh_f is the heat of fusion at the temperature in question (66 cal./cm.^{3}), l is the thickness (in centimeters), and σ_e is the surface free energy per square centimeter. The data in Table IV lead to values of 81 to 96 ergs./cm.^{2} for σ_e, a range of values which coincides with the surface free energies derived previously from crystallization kinetics.[26]

Another point of interest is that there is no correlation between thickness and crystallization temperature. The thickness seems to be dependent mainly on the degree of supercooling.[26]

The dissolution experiments on the toluene crystallized crystals are not quite as accurate as the melt experiments which were done on single identified growth spirals. The difference between melting temperature (121.2°C. and dissolution temperature (95°C.) is 26°C., which is within the experimental error of the difference in experimental maximum melting temperature (134.8°C.)[14] and maximum dissolution temperature (106.5) of sample 1 (Table I).

3. Solution-Grown Dendrites

The melting of the solution-grown dendrites (Fig. 5) indicates that the rates employed were not fast enough to arrest extensive reorganization. The conclusion which must be drawn is that in the case of dendrites the larger defect concentration (indicated by lower density) allows a much faster reorganization than in the relatively well packed single crystals. Experiments are under way to increase the heating rates by at least a factor of 10 to get some information on the defect structure of dendrites.

From Table V at least some indication can be gained that reorganization of dendrites occurs not far above the temperature of their crystallization. On slow heating in solution the dendrites reorganize as well as the single crystals into a structure (Fig. 6*f*) which cannot be resolved into any struc-

ture detail by optical techniques and appears similar to the high temperature growth obtained from solution at temperatures where no single crystals could be grown over extended periods (days) of time.[26]

Financial support from the Advanced Research Projects Agency is gratefully acknowledged.

References

1. Keller, A., *J. Polymer Sci.*, **17**, 291, 351, 447 (1955).
2. Till, P. H., Jr., *J. Polymer Sci.*, **24**, 301 (1957).
3. Wunderlich, B., and P. Sullivan, *J. Polymer Sci.*, **61**, 195 (1962).
4. Fischer, E. W., *Z. Naturforsch.*, **12a**, 753 (1957); A. Keller, *Phil. Mag.*, **2**, 1171 (1957).
5. Geil, P. H., to be published.
6. Bunn, C. W., *Trans. Faraday Soc.*, **35**, 482 (1939).
7. Wunderlich, B., presented to the Polymer Division, 142nd Meeting of the American Chemical Society, Atlantic City, September, 1962.
8. Bunn, C. W., and T. C. Alcock, *Trans. Faraday Soc.*, **41**, 317 (1945); E. R. Walter and F. P. Reding, *J. Polymer Sci.*, **21**, 561 (1956).
9. Cole, E. A., and D. R. Holmes, *J. Polymer Sci.*, **46**, 245 (1960).
10. Wunderlich, B., *J. Chem. Phys.*, **37**, 1207 (1962).
11. Wunderlich, B., *J. Chem. Phys.*, **37**, 1203 (1962).
12. Wunderlich, B., and D. Poland, *J. Polymer Sci.*, **A1**, 357 (1963).
13. Wunderlich, B., and P. Sullivan, *J. Polymer Sci.*, **56**, 19 (1962); *Polymer*, **3**, 247 (1962).
14. Wunderlich, B., and M. Dole, *J. Polymer Sci.*, **24**, 201 (1957).
15. Dole, M., W. P. Hettinger, Jr., N. R. Larson, and J. A. Wethington, Jr., *J. Chem. Phys.*, **20**, 781 (1952).
16. Dainton, F. S., D. M. Evans, and T. P. Melia, *Polymer*, **3**, 263 (1962).
17. Quinn, F. A., Jr., and L. Mandelkern, *J. Am. Chem. Soc.*, **80**, 3178 (1958).
18. Swan, P. R., *J. Polymer Sci.*, **42**, 525 (1960).
19. Gubler, M. G., and A. J. Kovacs, *J. Polymer Sci.*, **34**, 551 (1959).
20. Matsuoka, S., *J. Appl. Polymer Sci.*, **4**, 116 (1960).
21. Hunter, E., and W. G. Oakes, *Trans. Faraday Soc.*, **41**, 49 (1945).
22. Swan, P. R., *J. Polymer Sci.*, **56**, 403 (1962).
23. Unpublished, quoted by R. Chiang and P. J. Flory, *J. Am. Chem. Soc.*, **83**, 2857 (1961).
24. Mandelkern, L., M. Hellmann, D. W. Brown, D. E. Roberts, and F. A. Quinn, Jr., *J. Am. Chem. Soc.*, **75**, 4093 (1953).
25. Wunderlich, B., and W. Kashdan, *J. Polymer Sci.*, **50**, 71 (1961).
26. Wunderlich, B., *J. Polymer Sci.*, **A1**, 1245 (1963).
27. Flocke, H. A., *Kolloid-Z.*, **180**, 118 (1962).
28. Deeley, C. W., D. E. Kline, J. A. Sauer, and A. E. Woodward, *J. Polymer Sci.*, **28**, 109 (1958).
29. Hellwege, K. H., R. Kaiser, and K. Kuphal, *Kolloid-Z.*, **157**, 27 (1958).
30. Kline, D. E., J. A. Sauer, and A. E. Woodward, *J. Polymer Sci.*, **22**, 455 (1956).
31. Schmieder, K., and K. Wolf, *Kolloid-Z.*, **134**, 149 (1953).
32. Wolf, K. A., *Z. Electrochem.*, **65**, 605 (1961).
33. See for example, J. A. Sauer and A. E. Woodward, *Rev. Mod. Phys.*, **32**, 88 (1960) (also for earlier references).
34. Thurn, H., *Kolloid-Z.*, **179**, 11 (1961).
35. Quinn, F. A., Jr., and L. Mandelkern, *J. Am. Chem. Soc.*, **80**, 3178 (1958).
36. Chiang, R., and P. J. Flory, *J. Am. Chem. Soc.*, **83**, 2857 (1961).
37. Matsuoka, S., *J. Appl. Polymer Sci.*, **4**, 116 (1960).
38. Willbourn, A. H., *J. Polymer Sci.*, **34**, 569 (1959).
39. Charlesby, A., and L. Callaghan, *J. Phys. Chem. Solids*, **4**, 227 (1958).

40. Broadhurst, M. G., *J. Chem. Phys.*, **36**, 2578 (1962).
41. Statton, W. O., and P. H. Geil, *J. Appl. Polymer Sci.*, **3**, 357 (1960).
42. Slichter, W. P., *J. Appl. Phys.*, **32**, 2339 (1961).
43. Ubbelohde, A. R., *Quart. Revs.*, **4**, 356 (1950).

Résumé

La destruction thermique du réseau cristallin du polyéthylène, obtenu par refroidissement brutal de la solution (dendrites) et par refroidissement lent de solutions (simples cristaux) et de la masse fondue, a été étudiée en fonction de la vitesse de chauffage. Les dendrites montrèrent de fortes réorganisations à des températures légèrement supérieures aux températures de cristallisation. Des vitesses de chauffage aussi rapides que 20°C/min. ne pouvaient pas éviter cette réorganisation. Des vitesses du chauffage entre 10 et 20°C/min étaient nécessaires pour voir un point de fusion constant pour des mono-cristaux croissant à partir des solutions. Les points de fusion mesurés étaient proportionnels à l'épaisseur et peut-être à la densité des échantillons déterminés par microscopie interférentiel et par la méthode à colonne de gradient de densité. Des valeurs de l'énergie libre de surface calculées par abaissement des points de fusion se rangent de 81 à 96 ergs/cm². Les valeurs de la littérature pour les chaleurs spécifiques et les volumes spécifiques d'échantillons permettent une discussion du comportement du polyéthylène semi-cristallin avant la fusion. On a trouvé que les imperfections gelées en-dessous de la température de transition vitreuse croissent au-dessus de 250°K suivant la cristallinité globale. Ceci détruit l'additivité de la chaleur spécifique aussi bien que cells du volume spécifique. On a essayé de mettre en corrélation des mesures de NMR et de pertes mécaniques dynamiques. La différence entre la température de fusion et de dissolution dans le toluène (0.5–8.0 mg polyéthylène/g toluène) par refroidissement lent de cristaux obtenus en masse ou aux dépens de solutions, a été trouvée être de 26°C; la température maximum de dissolution de cristaux de polyéthylène dans le toluène s'élève à 110°C.

Zusammenfassung

Der thermische Zusammenbruch des Kristallgitters von Polyäthylen, das durch Abschrecken aus Lösung (Dendrite) und durch langsames Abkühlen aus Lösung (Einkristalle) und Schmelze gebildet worden war, wurde als Funktion der Erhitzungsgeschwindigkeit untersucht. Die Dendrite zeigten bei Temperaturen knapp oberhalb der Kristallisations-temperature starke Reorganisation, die auch durch eine Erhitzungsgeschwindigkeit bis hinauf zu 20°C/min nicht verhindert werden konnte. Zur Erreichung eines konstanten Schmelzpunktes waren für aus Lösung gewonnene Einkristalle Erhitzungsgeschwindigkeiten zwischen 10 und 20°C/min notwendig. Die gemessenen Schmelzpunkte waren der Dicke und veilleicht auch der Dichte der Proben, wie sie interferenz-mikroskopisch und nach der Dichtegradienten-Säulenmethode bestimmt wurden, proportional. Die aus der Schmelzpunktserniedrigung berechneten Werte der freien Grenzflächenenergie liegen im Bereich von 81 bis 96 erg/cm². Literaturwerte für die spezifische Wärme und das spezifische Volumen von grösseren Proben ermölichen eine Diskussion des Vorschmelzverhaltens von semikristallinem Polyäthylen. Es zeigt sich, dass die unterhalb der Glasumwandlungstemperatur eingefrorenen Defekte oberhalb 250°K, abhängig von der Bruttokristallinität "wachsen." Dadurch wird die Additivität der spezifischen Wärme und des spezifischen Volumens zerstört. Eine Korrelation mit NMR- und dynamisch-mechanischen Verlustmessungen wird versucht. Der Unterschied zwischen Schmelz- und Lösungstemperatur in Toluol (0,5–8,0 mg Polyäthylen/g Toluol) beträgt sowohl für langsam gekühlte Kristalle aus Substanz als auch aus Lösung 26°C. Die maximale Lösungstemperatur für Polyäthylenkristalle in Toluol liegt bei 111°C.

Received October 2, 1962

JOURNAL OF POLYMER SCIENCE: PART A VOL. 1, PP. 3597–3615 (1963)

Ultimate Tensile Properties of Elastomers. I. Characterization by a Time and Temperature Independent Failure Envelope*.

THOR L. SMITH, *Stanford Research Institute, Menlo Park, California*

Synopsis

The tensile stress at break (σ_b) and the associated ultimate strain (ϵ_b) of an elastomer depend on (1) the chemical and topological characteristics of the polymeric network, and (2) the test conditions under which rupture is observed. To separate these effects, the ultimate tensile properties can often be characterized by a "failure envelope" defined by values of σ_b and ϵ_b determined at various strain rates over a wide temperature range. Provided time–temperature superposition is applicable, such data superpose on a plot of log $\sigma_b T_0/T$ versus log ϵ_b, where T is the test temperature (absolute) and T_0 is an arbitrarily selected reference temperature. The resulting failure envelope is independent of time (strain rate) and temperature and thus it depends only on basic characteristics of the polymeric network. To illustrate the characterization method, data on two styrene–butadiene gum vulcanizates, SBR-I and SBR-II, were analyzed. For SBR-I, values of σ_b and ϵ_b obtained over extensive ranges of strain rate and temperature superposed to give a failure envelope. Data at elevated temperatures also gave a reliable value for the equilibrium modulus. For SBR-II, data obtained at various temperatures under conditions of constant strain and constant strain rate yielded identical failure envelopes; this strongly suggests that the failure envelope is independent of the test method. A theoretical consideration of the time-to-rupture associated with different test methods showed that for given values of σ_b and ϵ_b the time-to-rupture from the following types of tests should increase in the order: constant strain < constant stress < constant strain rate < constant stress rate.

I. INTRODUCTION

The tensile stress at break (σ_b) and the associated ultimate strain (ϵ_b) of an elastomer depend markedly on the test conditions. Within the range of rubbery behavior, a variation in test temperature or in experimental time scale may change σ_b by a hundredfold or more and ϵ_b by nearly tenfold. Because of this marked variation, it has been difficult to relate unambiguously the ultimate properties of different elastomers to their molecular structures. The ambiguity has existed because differences observed in the ultimate properties of various elastomers are normally the result of two types of factors: (*1*) those related to structural characteristics and (*2*) those related only to experimental conditions. To obtain basic

* Most of the material in this paper was presented before the Division of Organic Coatings and Plastics Chemistry at the 140th Meeting of the American Chemical Society, Chicago, September 1961.

information, the dependence of the ultimate properties on these two factors must be evaluated separately.

In this paper, a basic method for characterizing the ultimate tensile properties of amorphous elastomers is considered. Characterization is effected by a "failure envelope" which is independent of time and temperature effects. Also, the failure envelope appears to be independent of the type of test used to determine the ultimate properties. Thus, differences observed in the failure envelopes for various elastomers are not the result of factors which stem from chain interactions and mobilities but are primarily the result of differences in the topological characteristics of the networks. In addition to giving a basic characterization, the failure envelope also provides criteria for predicting when rupture will occur in a specimen that is subjected to different types of tests and to different test conditions.

II. BACKGROUND INFORMATION

The most common method for determining ultimate tensile properties consists of subjecting a specimen to a constant strain rate* and observing the stress and the strain at the moment of rupture. A similar but seldom used method consists of subjecting a specimen to a stress which increases at a constant rate until the specimen breaks. These methods provide values† of σ_b, ϵ_b, and t_b, where t_b is the time to break, i.e., the elapsed time from the beginning of a test until rupture occurs. For tests at a constant strain rate $\dot{\epsilon}$, $t_b = \epsilon_b/\dot{\epsilon}$; and for those at a constant rate of stress increase $\dot{\sigma}$, $t_b = \sigma_b/\dot{\sigma}$.

When tests are made at either a constant strain rate or a constant rate of stress increase, none of the quantities σ_b, ϵ_b, and t_b is known prior to the termination of a test. However, values of the ultimate properties can often be determined by subjecting a specimen at zero time to either a strain or a stress which subsequently is held constant until rupture occurs. In conducting such tests, t_b is determined along with values of either σ_b or ϵ_b, depending on whether the strain or stress is fixed throughout the test. Such tests provide values of σ_b, ϵ_b, and t_b, where either σ_b or ϵ_b is prescribed by the initial test conditions. Although a specimen subjected to either a constant strain or a constant stress can exhibit delayed rupture only under certain conditions, there appears to be a rather wide range of conditions under which rupture can be obtained.

Phenomenologically, the problem of characterizing ultimate tensile prop-

* Unfortunately, the majority of data reported in the literature have been obtained by subjecting a dumbbell-shaped specimen to a test in which the grips are separated at a constant rate. During such a test, the strain rate imposed on the specimen decreases considerably, especially after the elongation exceeds 100–200%.

† In this paper, the stress at any temperature is defined as the retractive force divided by the cross-sectional area of the unstressed specimen at room temperature; likewise, the strain is defined as the increase in length of a specimen at any temperature divided by the length of the unstressed specimen at room temperature.

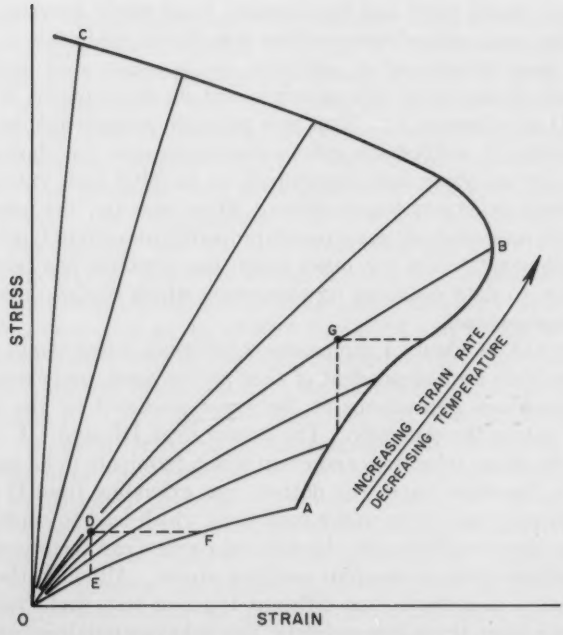

Fig. 1. Schematic representation of the dependence of stress–strain curves on strain rate and temperature.

erties requires a determination of functional relations among σ_b, ϵ_b, and t_b and how these quantities depend on test conditions and the type of test conducted. The results, presented subsequently, strongly suggest that for each value of σ_b there exists a unique value of ϵ_b which is independent of the test method and the test conditions; in other words, the functional relation between σ_b and ϵ_b is independent of t_b. If this theory is correct, not only can the ultimate properties be readily characterized, but also certain methods can be proposed for interrelating values of t_b observed in different types of tests.

Certain important aspects of the ultimate tensile properties of elastomers which remain amorphous until rupture occurs can be considered in terms of the schematic diagram shown in Figure 1. (This diagram has been discussed previously[1,2] and in light of results presented in this paper, as well as more recent ones,[3] it should be modified slightly to represent more precisely the nature of real elastomers.) The lines emanating from the origin of the diagram represent stress–strain curves determined at various strain rates and temperatures; the envelope ABC connects the rupture points. The rupture point moves counterclockwise around the envelope, called the failure envelope, either as the strain rate is increased or as the test temperature is decreased. Such a failure envelope, which is independ-

ent of time (strain rate) and temperature, must result provided the well known time–temperature superposition principle is applicable to ultimate property data determined at different temperatures and strain rates. (A detailed discussion of this principle and its development is given in Chapter 11 of reference 4.) That this principle is applicable to ultimate property data for unfilled amorphous elastomers was first shown[5] several years ago by analyzing data determined on an SBR gum vulcanizate at various strain rates and temperatures. More recently, the principle has been used to interrelate ultimate tensile properties for certain types of highly filled elastomers.[6–8] On the other hand, the principle has been shown[9] inapplicable to data obtained on elastomers which contain a reinforcing filler like carbon black.

The line OA in Figure 1 represents equilibrium stress–strain behavior, that is, the data are independent of time and temperature, except for the small temperature dependence of the stress predicted by the statistical theory of rubberlike elasticity. The dotted lines DE and DF represent, respectively, stress relaxation and creep which terminate in an equilibrium state. On the other hand, the dotted lines extending from G represent stress relaxation and creep under conditions which lead to rupture. The latter lines show qualitatively why delayed rupture can occur under conditions of either constant strain or constant stress. Although the diagram is constructed to indicate that different types of tests yield values of σ_b and ϵ_b which lie on the failure envelope, this behavior requires experimental verification; a convincing, although incomplete, verification is provided by data in this paper.

The diagram does not indicate whether the rupture point moves along OA toward the origin as tests are made progressively at either higher temperatures or lower strain rates; it is assumed that such tests can be carried out without the occurrence of chemical degradation during the test periods. However, results discussed below, as well as those of more extensive studies,[3] show conclusively that rupture can occur along the equilibrium curve OA. As a result, the sharp corner A shown on the failure envelope does not exist.

III. MATERIALS AND EXPERIMENTAL METHODS

The data discussed in this paper were obtained during the course of two previous investigations of styrene–butadiene (SBR) gum vulcanizates. The first study[5] included the testing of an SBR vulcanizate (hereafter called SBR-I) at various strain rates and temperatures with an Instron tester. Time–temperature superposition was found applicable for constructing composite curves from values of σ_b and ϵ_b determined at different strain rates and temperatures. A recent analysis[10] of the stress–strain curves, for strains up to ϵ_b, showed that the dependence of the stress on time and temperature is independent of its dependence on strain over a wide range of test conditions. For the second study,[1] the stress-relaxation properties of another SBR vulcanizate (hereafter called SBR-II) were

determined at various strains and temperatures. The study was made to demonstrate that delayed rupture will occur in a specimen maintained at a fixed strain and to determine the dependence of σ_b and t_b on the temperature and the magnitude of the strain. For comparison, values of σ_b and ϵ_b were determined at a limited number of strain rates and temperatures.

Both vulcanizates, supplied by F. L. Roth of the National Bureau of Standards, were prepared from SBR gum stock which contained 23.5% bound styrene. The compounding recipes, which were nearly identical for both vulcanizates, and the cure conditions are given elsewhere.[1,5] Values of the average molecular weight M_c between junction points were obtained from both equilibrium swelling and equilibrium modulus data. The swelling data gave an M_c of 8020 for SBR-I and 15,800 for SBR-II; corresponding values from the equilibrium modulus are 8,500 and 13,100. (The value 8,500 was calculated from the modulus reported previously.[10])

Tensile data were obtained by testing rings cut from sheets of the vulcanizates. Methods for preparing the rings and for conducting the tests are described in previous publications.[1,5] Values of ϵ_b were obtained from crosshead displacement and the inside circumference of the unstretched rings; use of the average circumference would have given an average value for the strain existing at rupture. [Although the strain is uniform around a ring, it varies across a ring because of the variation in the initial gage length (circumference) from the inside to the outside diameter of a ring.] On the other hand, values of σ_b were erroneously taken to equal the tensile force divided by twice the cross-sectional area of the unstretched rings. Consequently, a reported value of σ_b is not the stress at break but is the average stress existing across a stretched ring at the moment of rupture. A computational method has recently been devised and evaluated[3] for obtaining the value of stress existing around the inside circumference of a ring at the moment of rupture. The method involves extrapolating an observed stress–strain curve beyond the rupture point. However, for purposes of this paper, it did not appear necessary to compute the correct values of σ_b from the original data obtained several years ago.

The magnitude of the error in σ_b depends on the shape of a stress–strain curve immediately prior to rupture and on the ratio of the initial average diameter of a ring to its initial inside diameter; this ratio for rings of SBR-I was about 1.07 and for rings of SBR-II was about 1.09. For SBR-I, the maximum error in σ_b occurs in values at −34.4°C., at which temperature the largest values of ϵ_b were observed. The previously reported values of σ_b at this temperature were estimated to be low by about 20%. On the other hand, values at 71°C. were estimated to be in error by about 10% or less.

IV. ANALYSIS OF EXPERIMENTAL DATA

Typical Failure Envelope

The failure envelope for SBR-I is shown in Figure 2. The envelope is defined by values of σ_b and ϵ_b which were determined at 12 temperatures

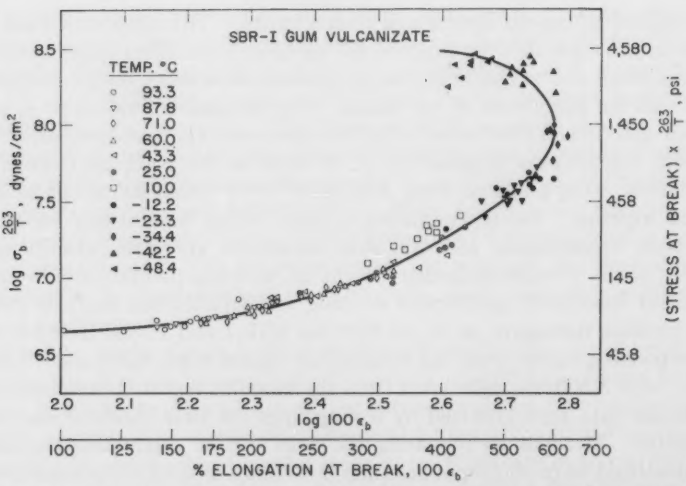

Fig. 2. Failure envelope for SBR-I from data determined at various strain rates and temperatures.

between −48.4 and 93.3°C. and at 8–11 strain rates at each temperature; the range of strain rate was from about 0.0095 to 9.5 min.$^{-1}$ and was obtained by conducting tests at crosshead speeds between 0.02 and 20 in./min. To define the failure envelope, the data are plotted as log σ_b 263/T versus log 100ϵ_b. Values of σ_b are multiplied by the ratio 263/T, where T is the test temperature in degrees Kelvin, to reduce all values of σ_b to the arbitrary reference temperature 263°K. The reason and justification for including this ratio are given in a subsequent section.

Figures 2 shows that data determined at different temperatures overlap and define the failure envelope quite precisely. Essentially no point deviates from the curve by more than 0.05 logarithmic unit, which corresponds to a 12% deviation; the majority of the points lie even closer. The greatest scatter occurs in data determined at −42.2 and −48.4°C. Data obtained at temperatures below −48.4°C. (not shown in Fig. 2) scatter considerably as a result of necking of the specimens during test.

The rupture point should move counterclockwise around the failure envelope as either the strain rate is increased or as the test temperature is decreased. An inspection of tabulated data shows that the opposite behavior occurs at times because of scatter in the experimental data. Even when such behavior is observed, the values of σ_b and ϵ_b usually lie on or close to the failure envelope even though their dependence on strain rate and temperature is opposite to that expected. Thus, the failure envelope is defined more precisely than the temperature and strain rate dependence of either σ_b or ϵ_b.

A detailed analysis[10] of the stress–strain curves showed quite conclusively that those determined at 87.8 and 93.3°C. were equilibrium ones. At

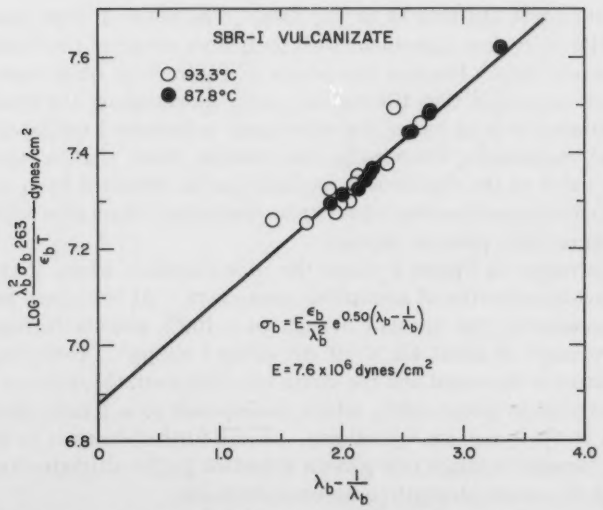

Fig. 3. Ultimate property data for SBR-I determined at different strain rates at 87.8 and 93.3°C. plotted according to the Martin-Roth-Stiehler equation.

these temperatures, however, the ultimate properties varied considerably with strain rate and temperature even though neither viscous relaxation nor chemical degradation occurred to a detectable degree during the test periods. For example, at 93.3°C. and a strain rate of 0.0095 min.$^{-1}$, ϵ_b was 1.00, while at 87.8°C. and a strain rate of 9.5 min.$^{-1}$, ϵ_b was 2.75; the corresponding values of σ_b were 4.5×10^6 and 8.4×10^6 dynes/cm.^{2} (65 and 122 psi), respectively.

Previously[10] it was found that the equilibrium stress–strain curves could be represented by the equation of Martin, Roth, and Stiehler:[11]

$$\sigma = E(\epsilon/\lambda^2)\exp A\{\lambda - (1/\lambda)\} \quad (1)$$

where E is equilibrium tensile modulus, λ is the extension ratio which equals $\epsilon + 1$, and A is an adjustable parameter. Data at 87.8°C. showed that $A = 0.47$ and $E = 1.04 \times 10^7$ dynes/cm.^{2} (151 psi). However, an analysis of extensive isochronal stress–strain data gave $A = 0.49$. To verify that values of σ_b and ϵ_b determined at 87.8 and 93.3°C. lie along the equilibrium stress–strain curve, such values were fitted to eq. (1) as shown in Figure 3. (For constructing Fig. 3, values of ϵ_b and λ_b were based on the average instead of the inside diameter of the rings. Thus, the values of ϵ_b shown in Fig. 3 are smaller by a factor of 1.07 than the corresponding ones in Fig. 2.) Because values of $\sigma_b 263/T$ were used, the intercept should correspond to the equilibrium modulus at 263°K. As the modulus at 87.8°C. has been found[10] to be 1.04×10^7 dynes/cm.^{2}, the value at 263°K. should be $(1.04 \times 10^7)(263/361) = 7.6 \times 10^6$ dynes/cm.^{2}. This modulus value was used to define the intercept in Figure 3 and then the slope of the line was

adjusted to give the best fit to the data. The selected slope gives $A = 0.50$ which is in close agreement with the values obtained previously from stress–strain data. Because the points in Figure 3 lie quite close to the line, it is concluded that the rupture point moves along the equilibrium stress–strain curve as either the strain rate is increased or the test temperature decreased. Conversely, the results show that a reasonably reliable value of the equilibrium modulus can be obtained from values of the ultimate properties determined under conditions which give equilibrium stress–strain data prior to rupture.

The envelope in Figure 2 shows the wide variation which is typical of the ultimate properties of amorphous elastomers. At low strain rates and high temperature, the ultimate elongation is 100% and the corresponding tensile strength is about 4.5×10^6 dynes/cm.^{2} (65 psi). However, as the temperature is decreased and the strain rate increased, the ultimate elongation increases to about 600% which corresponds to a tensile strength of about 1×10^8 dynes/cm.^{2} (1450 psi). A still further decrease in temperature or increase in strain rate gives a reduction in the ultimate elongation, although the tensile strength continues to increase.

Uniqueness of Failure Envelope

A key question that requires careful exploration is whether or not the failure envelope is unique, i.e., independent of the type of test. The results discussed in the previous section only show that the ultimate properties of a typical amorphous elastomer determined at various constant strain rates yield a failure envelope that is independent of test conditions.

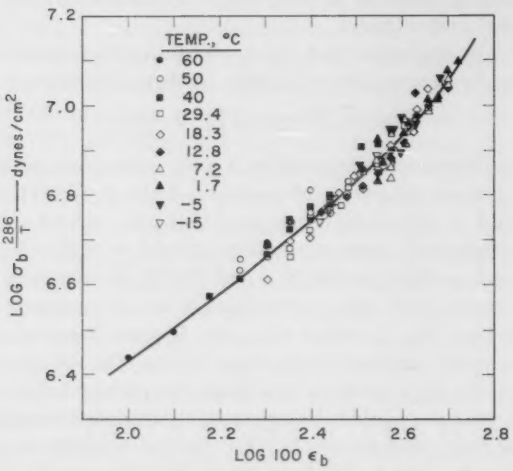

Fig. 4. Failure envelope for SBR-II from data determined under conditions of constant strain at different temperatures.

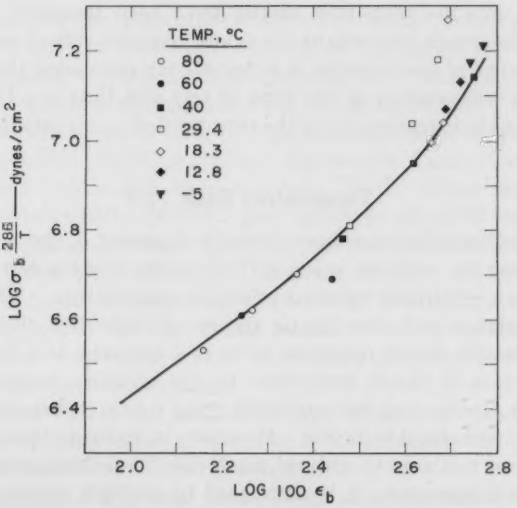

Fig. 5. Failure envelope for SBR-II from data determined at various strain rates and temperatures. Envelope drawn identical to one in Fig. 4.

That is, a change in either strain rate or temperature only shifts the rupture point along the envelope. If values of σ_b and ϵ_b determined under conditions of constant strain rate, constant strain, constant stress, and constant stress rate lie on the same envelope, then it can be concluded that the envelope provides a basic characterization of the ultimate tensile properties and depends only on certain topological and physical aspects of the polymeric network.

Evidence for the uniqueness of the failure envelope results from analyzing the data on SBR-II reported previously.[1] Ultimate properties of SBR-II were determined at a number of constant strains at ten temperatures between −15 and 60°C. and also at several strain rates at seven temperatures between −5 and 80°C. The failure envelope defined by results from the constant strain tests is shown in Figure 4; the points show remarkably little scatter about the curves. Even the −15 and −5°C. data, which previously[1] were not presented because of erratic variations in the rupture times, fall on the failure envelope. Figure 5 shows the data obtained under constant strain rate conditions. The curve in this figure has purposely been drawn identical to that in Figure 4, and the individual points, with few exceptions, are seen to lie extremely close to the curve. This agreement shows that the failure envelope which results from the constant strain rate data is identical with the one from the constant strain data.*

*** Note Added in Proof.** Recent results described by the author at the Fourth International Congress on Rheology, Brown University, August 1963, show that values of σ_i and ϵ_b determined under constant loads on a Viton A-HV elastomer yield the same failure as do data obtained from constant strain rate tests.

Ideally, ultimate properties should have been measured under other test conditions such as constant stress and constant rate of stress increase. In the absence of such results, it is tentatively concluded that the failure envelope is independent of the type of test and thus is a basic material property which depends only on the structural characteristics of the elastomer.

Temperature Ratio T_0/T

To obtain the failure envelopes shown in Figures 2, 4, and 5, the quantity plotted along the ordinate is log $\sigma_b T_0/T$, where T is the test temperature and T_0 is an arbitrarily selected reference temperature. This procedure is in accordance with the kinetic theory of rubberlike elasticity, which predicts that the elastic retractive force in a specimen at a fixed extension ratio increases in direct proportion to the absolute temperature, even though the theory does not explicitly treat rupture phenomena or time-dependent mechanical behavior. However, in applying time–temperature superposition methods to reduce[4] small-deformation viscoelastic data to a reference temperature, it is customary to multiply values of the stress relaxation and dynamic moduli by the temperature factor before shifting plotted data along the time or frequency axis to effect superposition. Thus, when time–temperature superposition was first applied[5] to superpose values of σ_b and ϵ_b determined at different strain rates and temperature, σ_b was multiplied by the temperature ratio, although no direct experimental evidence was presented to justify the procedure.

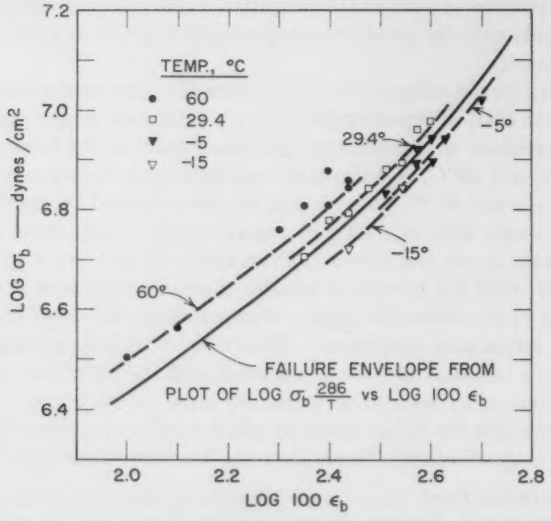

Fig. 6. Plot to show that σ_b from constant strain tests must be multiplied by temperature ratio T_0/T to obtain superposition. Data from Fig. 4.

Results can now be presented which show rather conclusively that values of σ_b at different temperatures should be multiplied by T_0/T before they are compared or used in the preparation of a failure envelope or a reduced plot. To show the important role of the factor $286/T$ in effecting the smooth superposition of data in Figure 4, individual values obtained at 60, 29.4, −5, and −15°C. have been replotted in Figure 6, except that the temperature factor has been omitted. Those values measured at temperatures above 13°C. (286°K.) now fall above the solid curve, which is the failure envelope shown in Figure 4, and those measured at −5 and −15°C. fall below the solid curve. The dotted lines have been drawn parallel to the failure envelope but displaced by the amount log $T/286$. As the dotted lines fit the appropriate points quite closely, this behavior shows the necessity of using $\sigma_b T_0/T$ to obtain a smooth failure envelope from data at different temperatures.

That the factor T_0/T is also needed to obtain a failure envelope from data determined at constant strain rates can be seen reasonably well by examining closely the results in Figure 2, although recent results[3] provide more convincing evidence. The need for T_0/T can also be shown by examining the data of Greensmith,[9] who determined the ultimate tensile properties of an SBR gum vulcanizate over a wide range of strain rate at 25 and 90°C. Figure 7 shows that his data overlap and yield a smooth failure envelope on a plot of σ_b (298/363) versus $100\epsilon_b$. (Values of σ_b and $100\epsilon_b$ were obtained from the smoothed curves published by Greensmith; the original data appear to be quite precise and were obtained by testing 3–6 ring

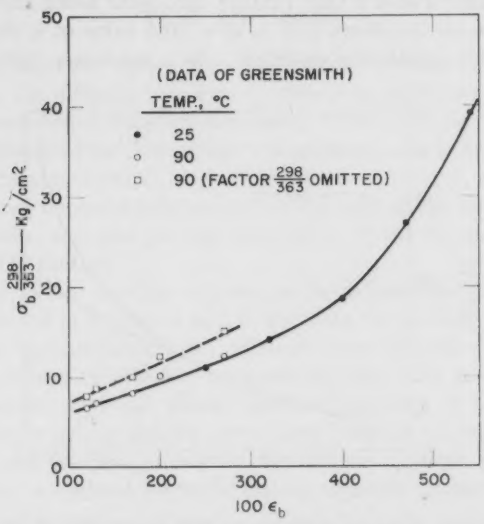

Fig. 7. Plot to show that σ_b from constant strain rate tests must be multiplied by temperature ratio T_0/T to obtain superposition.

specimens at each of 9 strain rates at each temperature.) However, when the factor (298/363) is omitted, the 90°C. results, shown by the squares in Figure 7, lie appreciably above the solid curve.

For constructing the failure envelope, a precise application of time–temperature superposition methods[4] requires the use of $(\sigma_b)_c T_0\rho_0/T\rho$, where ρ_0 and ρ are the respective densities at temperatures T_0 and T and $(\sigma_b)_c$ is the stress at break based on the cross-sectional area of the unstressed specimen at temperature T. The density ratio ρ_0/ρ is required to correct for the change in stress (at a fixed extension ratio) which a temperature change produces, owing to thermal expansion (or contraction), in the number of effective network chains per unit volume.

As mentioned earlier, values of σ_b and ϵ_b used throughout this paper were based on the dimensions of an unstressed specimen at room temperature (ca. 298°K.) Thus, $(\sigma_b)_c = \sigma_b A_0/A$, where A and A_0 are the cross-sectional areas of an unstressed specimen at T and T_0 = 298°K., respectively. Likewise, the correct value of strain is $(\epsilon_b)_c = \epsilon_b L_0/L$, where L_0 and L are the lengths of an unstressed specimen at T and T_0 = 298°K., respectively. Thus, if T_0 = 298°K. had been selected for constructing the failure envelopes, the correct plot would have been log $(\sigma_b T_0 L/TL_0)$ versus log $(\epsilon_b L_0/L)$. However, because log (L/L_0) equals about 0.01 when $T-T_0$ = 100, a negligible error was introduced in the failure envelopes by omitting the (L/L_0) factor.

Comparison of Failure Envelopes

Because Figure 3 shows that rupture can occur along the equilibrium stress–strain curve, it follows that σ_b at a fixed value of ϵ_b should be proportional to the equilibrium modulus. As a minimum, this dependence

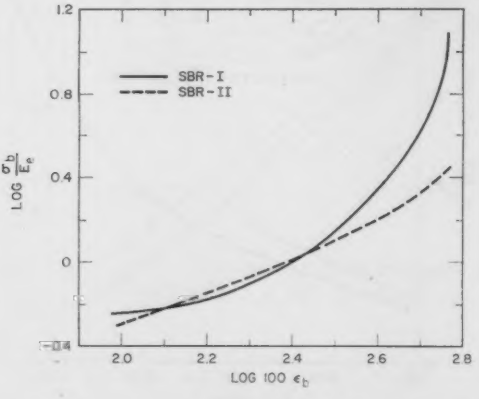

Fig. 8. Comparison of failure envelopes for SBR-I and SBR-II; E_e = 7.6 × 10⁶ dynes/cm.² for SBR-I at 263°K. and E_e = 5.33 × 10⁶ dynes/cm.² for SBR-II at 286° K.

must exist for values of σ_b obtained when the stress–strain curves prior to rupture are equilibrium ones. Thus, the high-temperature portions of failure envelopes for different elastomers should superpose on a plot of log (σ_b/E_e) versus log ϵ_b, where E_e is the equilibrium modulus at the temperature at which the value of σ_b is determined. Recent unpublished results[3] have verified this expected behavior.

The failure envelopes for SBR-I and SBR-II are compared in Figure 8 on a plot of log σ_b/E_e versus log ϵ_b. As the reference temperatures for the failure envelopes for SBR-I in Figure 2 and for SBR-II in Figure 4 are 263 and 286°K., respectively, the required values of E_e at these temperatures were obtained by multiplying those determined previously[1,10] at elevated temperatures. For SBR-I, E_e is 7.6×10^6 dynes/cm.^{2} at 263°K., and for SBR-II, the value is 5.33×10^6 dynes/cm.^{2} at 286°K.

Figure 8 indicates that the failure envelopes for the two vulcanizates are probably identical within experimental error for values of ϵ_b less than about 300%. However, at greater values of the ultimate strain, σ_b for SBR-I increases more rapidly with ϵ_b than that for SBR-II. This behavior* seems reasonable because the maximum value for ϵ_b would be expected to decrease with an increase in degree of crosslinking; the degree of crosslinking in SBR-I is about 50% greater than in SBR-II. On the other hand, the maximum value of ϵ_b undoubtedly depends to a greater degree on the distribution of chain lengths in the molecular network than on the average degree of crosslinking.

V. RELATIONS AMONG RUPTURE TIMES FROM DIFFERENT TEST METHODS

Thus far it has been shown that the failure envelope can be used for characterizing the ultimate tensile properties of an elastomer and for comparing the properties of different elastomers. The relatively high precision with which experimental data define the envelope results largely because values of the time to break (t_b) are not required. However, considerations of how t_b depends on test conditions and on the type of test lead to relations of practical value and may provide information about the molecular processes that lead to rupture.

Because the failure envelope appears to be independent of the type of test, as illustrated in Figures 4 and 5, methods can possibly be developed for predicting rupture times when different types of tests are conducted. For example, it may be possible to predict rupture times under conditions of constant strain, constant stress, and constant rate of stress increase from the failure envelope and the stress–time behavior observed at various strain rates and temperatures prior to rupture. Before pursuing this matter further, a method for interrelating ultimate properties of linear

*** Note Added in Proof.** Recent data obtained by the author show that the failure envelopes for elastomers whose M_c differ superpose on a plot of log $(1 + \epsilon_b)\sigma_b T_0/T$ versus log (ϵ_b/M_c). On this type of plot, the envelopes for SBR-1 and SBR-II superpose

viscoelastic materials must be discussed. As real elastomers do not exhibit linear viscoelastic behavior except at small strains, this discussion is given only to illustrate certain principles and to provide a basis for subsequent considerations of real elastomers.

Linear Viscoelastic Materials

For linear viscoelastic materials, the relaxation of stress in a sample maintained at a constant strain ϵ is given by the equation

$$\frac{\sigma(t,\epsilon)}{\epsilon} = E(t) \tag{2}$$

where $\sigma(t,\epsilon)$ is the stress which depends on time and strain and $E(t)$ is the stress-relaxation modulus which is independent of strain. Stress–strain curves measured at constant strain rates can be represented by

$$\frac{\sigma(t,\epsilon)}{\epsilon} = F(t) \tag{3}$$

where $F(t)$ is the constant strain rate modulus which depends only on time and ϵ increases in direct proportion to the time. The stress-relaxation modulus is related[10] to $F(t)$ by the equation

$$E(t) = F(t)\left[1 + \frac{d \log F(t)}{d \log t}\right] \tag{4}$$

Likewise, the strain in a specimen maintained under a constant stress is given by

$$\frac{\epsilon(t,\sigma)}{\sigma} = D(t) \tag{5}$$

where $D(t)$ is the creep compliance. When a specimen is subjected to a stress which increases at a constant rate, the resulting stress–strain behavior can be represented by

$$\frac{\epsilon(t,\sigma)}{\sigma} = U(t) \tag{6}$$

where σ increases in direct proportion to the time and $U(t)$ is a function of time alone which can be called the constant stress rate compliance. The creep compliance is related[3] to $U(t)$ by the equation

$$D(t) = U(t)\left[1 + \frac{d \log U(t)}{d \log t}\right] \tag{7}$$

The above six equations are exact and apply to any material within the range of linear viscoelastic behavior.

Let us now assume that $F(t)$ can be represented over some range of time by the equation

$$F(t) = at^{-b} \qquad b \geq 0 \tag{8}$$

where a and b are constants. By the application of eq. (4), the following is obtained:

$$E(t) = a(1 - b)t^{-b} \tag{9}$$

When $E(t)$ can be represented by eq. (9), the creep compliance is given exactly by[12]

$$D(t) = \frac{\sin \pi b}{ab\pi(1 - b)} t^b \tag{10}$$

To obtain $U(t)$, $D(t)$ from eq. (10) can be substituted in eq. (7) and the resulting differential equation solved subject to the boundary condition $U(0) = 0$. The solution is

$$U(t) = \frac{\sin \pi b}{ab\pi(1 - b^2)} t^b \tag{11}$$

As we have assumed that linear viscoelastic behavior exists up to the rupture point, eqs. (8)–(11) can be applied to determine differences in rupture times under the test methods being considered. For this purpose, let us assume that a specimen subjected to a constant strain rate ruptures in time $t_b^{(2)}$ at σ_b^* and ϵ_b^*. Now suppose that a specimen is subjected initially to the strain ϵ_b^*. Because the failure envelope is independent of the test method, rupture will occur under the constant strain ϵ_b^* when the stress has relaxed to the value σ_b^*. Thus, immediately prior to rupture $E(t)$ must equal $F(t)$. Consequently, from a comparison of eq. (9) with eq. (8), it follows that $t_b^{(1)}$, the time to break under constant strain, is related to $t_b^{(2)}$ by the equation

$$\log t_b^{(1)} = \log t_b^{(2)} + \frac{1}{b} \log (1 - b) \tag{12}$$

Similarly, if a specimen is subjected to the constant stress σ_b^*, rupture will occur when the strain reaches ϵ_b^*. A comparison of eq. (8) with eq. (10) shows that under the constant stress the time to break $t_b^{(4)}$ is given by the equation

$$\log t_b^{(4)} = \log t_b^{(2)} + \frac{1}{b} \log \left[\frac{\pi b(1 - b)}{\sin \pi b} \right] \tag{13}$$

Now suppose that a specimen is subjected to a stress which increases at a constant rate and that the rate is selected such that σ_b^* and ϵ_b^* will be reached at the time of rupture. Under these conditions, the time to break $t_b^{(3)}$, obtained by equating eqs. (8) and (11), is given by

$$\log t_b^{(3)} = \log t_b^{(2)} + \frac{1}{b} \log \left[\frac{\pi b(1 - b^2)}{\sin \pi b} \right] \tag{14}$$

Thus, for given values of σ_b and ϵ_b, we have found interrelations among the rupture times obtained from the different types of tests. The dif-

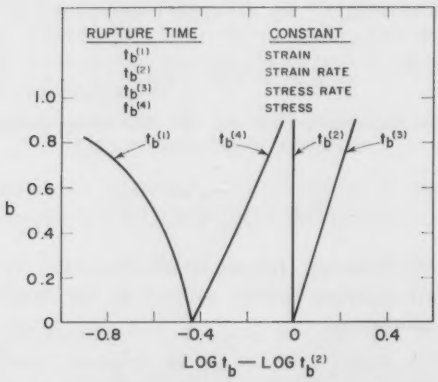

Fig. 9. Differences in logarithms of rupture times from different test methods for a linear viscoelastic material whose stress-relaxation modulus is $E(t) = a(1 - b)t^{-b}$.

ferences in the logarithms of the rupture times are functions of the parameter b and these differences are shown as a function of b in Figure 9. When b is near zero, Figure 9 shows that rupture times under constant strain rate and constant stress rate are essentially identical. Also, the rupture times under constant strain and constant stress are identical for $b = 0$ but are lower by a factor of about 2.7 than rupture times observed under conditions of constant strain rate and constant stress rate. As b increases in magnitude, appreciable differences develop among the rupture times from the four types of tests.

Real Elastomers

A possible modification of linear viscoelastic theory can now be proposed for predicting how different types of tests affect the rupture times of real elastomers.

For certain elastomers, stress-relaxation data can be represented by the equation

$$\frac{g(\epsilon)\sigma(\epsilon,t)}{\epsilon} = E(t) \tag{15}$$

where $g(\epsilon)$ is a strain function which approaches unity as ϵ approaches zero. In order for eq. (15) to fit experimental data, stress-relaxation data must yield parallel curves on a plot of log σ versus log t. Some years ago, this behavior was found over certain regions of the time scale at elongations up to 100% for SBR[13] and for polyisobutylene.[14] Recently,[15] such behavior was found for SBR at elongations up to 500%. It has been postulated by Tobolsky[12b] that other amorphous elastomers show similar behavior in certain regions of the time-scale. Apparently, however, no extensive study has been made to determine the ranges of temperature, time, and strain in which $g(\epsilon)$ is a function of strain alone.

When stress-relaxation results can be represented by eq. (15), stress–strain curves determined at constant strain rates can probably be represented by the equation

$$g(\epsilon)\,\frac{\sigma(\epsilon,t)}{\epsilon} = F(t) \tag{16}$$

The recent analysis[10] of the stress–strain curves of SBR-I showed that eq. (16) was applicable and that $g(\epsilon)$ was independent of time and temperature at temperatures between −34.4 and 93°C. and at strains up to rupture. Further, at each temperature, $F(t)$ could be represented by $F(t) = at^{-b}$. It thus appears that eq. (12) can be applied over a wide range of temperature to predict the difference in rupture times under conditions of constant strain and constant strain rate.

At temperatures between −5 and 60°C., the stress-relaxation data for SBR-II can be represented[15] by eq. (15), and in turn $E(t)$ can be represented by eq. (9) with b approximately equal to 0.027. For this value of b, eq. (12) predicts that rupture times under constant strain should be lower than those under constant strain rate by a factor of 0.36 (−0.44 logarithmic unit). Although the experimental data reported previously[1] are not inconsistent with this prediction, the uncertainties in the test data preclude an adequate evaluation. However, some of the data are in rather good agreement with the prediction. (See Figs. 10 and 11 in reference 1 for a comparison of results obtained at 29.4, 40, 50, and 60°C.)

The creep compliance of elastomers can often be represented by

$$h(\epsilon)\,\frac{\epsilon(\sigma,t)}{\sigma} = D(t) \tag{17}$$

where $h(\epsilon)$ is a function only of the strain. A recent discussion of problems associated with determining an appropriate strain function has been given by Leaderman,[16] who has tested several possible functions by analyzing creep and creep recovery data. If eq. (17) represents creep data for a material, we shall assume for present purposes that stress–strain curves determined at a constant rate of stress increase can be represented by

$$h(\epsilon)\,\frac{\epsilon(\sigma,t)}{\sigma} = U(t) \tag{18}$$

where σ increases in direct proportion to the time. Now suppose that rupture occurs at $t_b^{(4)}$ under a constant stress and that it occurs at $t_b^{(3)}$ under the stress rate needed to effect rupture at the same values of σ_b and ϵ_b as observed under the constant stress. Thus, the two tests are conducted such that $D(t_b^{(4)})$ must equal $U(t_b^{(3)})$. If $D(t)$ can be represented by eq. (10), then the differences in the rupture times can be obtained by equating eq. (10) with eq. (11). The result is

$$\log t_b^{(3)} = \log t_b^{(4)} + \frac{1}{b}\log(1+b) \tag{19}$$

Further, if we assume that $h(\epsilon)$ in eqs. (17) and (18) is identically equal to $g(\epsilon)$ in eqs. (15) and (16) and that $E(t)$, $F(t)$, $D(t)$, and $U(t)$, as defined for representing large-deformation behavior, depend on time according to eqs. (8)–(11), then the differences in t_b are given by eqs. (12)–(14).

Data for testing eq. (19) and eqs. (13)–(14) apparently are not available. It is interesting to observe, however, that Turner[17] determined the ultimate tensile properties of a polyvinyl chloride material by subjecting specimens to constant loads at temperatures between 95 and 125°C. and found that the data gave a smooth failure envelope. However, until the failure envelope for a single material has been determined by employing several different type of tests, it cannot be stated conclusively that the envelope is independent of the type of test. Likewise, to determine whether or not eq. (19) and eqs. (12)–(14) are applicable, extensive studies will be required. These studies should be designed to determine if eqs. (17)–(18) are correct and if $h(\epsilon) = g(\epsilon)$. Thus, the equations presented in this section are now quite speculative; they have been presented primarily to suggest basic approaches to the overall problem of understanding ultimate properties and to indicate needed experimental studies.

References

1. Smith, T. L., and P. J. Stedry, *J. Appl. Phys.*, **31**, 1892 (1960); *Rubber Chem. Technol.*, **34**, 897 (1961).

2. Smith, T. L., *SPE Journal*, **16**, No. 11, 1 (1960).

3. Smith, T. L., unpublished results.

4. Ferry, J. D., *Viscoelastic Properties of Polymers*, Wiley, New York, 1961.

5. Smith, T. L., *J. Polymer Sci.*, **32**, 99 (1958); *Rubber Chem. Technol.*, **32**, 992 (1959).

6. Landel, R. F., and T. L. Smith, *ARS Journal*, **31**, 599 (1961); *Rubber Chem. Technol.*, **35**, 291 (1962).

7. Bills, K. W., Jr., K. H. Sweeny, and F. S. Salcedo, *J. Appl. Polymer Sci.*, **4**, 259 (1960); *High-Speed Testing*, Vol. II, A. G. H. Dietz and F. R. Eirich, Eds., Interscience, New York, 1961, p. 3.

8. Brettschneider, H. D., in *High-Speed Testing*, Vol. I, A. G. H. Dietz and F. R. Eirich, Eds., Interscience, New York, 1960, p. 41.

9. Greensmith, H. W., *J. Appl. Polymer Sci.*, **3**, 175 (1960); *Rubber Chem. Technol.*, **34**, 76 (1961).

10. Smith, T. L., *Trans. Soc. Rheology*, **6**, 61 (1962).

11. Martin, G. M., F. L. Roth, and R. D. Stiehler, *Trans. Inst. Rubber Ind.*, **32**, 189 (1956); also, L. A. Wood, *J. Res. Natl. Bur. Std.*, **60**, 193 (1958).

12. MacLeod, A. A., *Ind. Eng. Chem.*, **47**, 1319 (1955); also, H. Leaderman, in *Rheology*, Vol. II, F. R. Eirich, Ed., Academic Press, New York, 1958, Chap. I.

13. (a) Tobolsky, A. V., and R. D. Andrews, *J. Chem. Phys.*, **13**, 3 (1945); (b) A. V. Tobolsky, *Properties and Structure of Polymers*, Wiley, New York, 1960, p. 106.

14. Andrews, R. D., N. Hofman-Bang, and A. V. Tobolsky, *J. Polymer Sci.*, **3**, 669 (1948).

15. Landel, R. F., and P. J. Stedry, *J. Appl. Phys.*, **17**, 1885 (1960).

16. Leaderman, H., *Trans. Soc. Rheology*, **6**, 361 (1962).

17. Turner, L. W., in *Physical Properties of Polymers*, Macmillan, New York, 1959.

Résumé

La force de tension à la rupture (σ_b) et la tension interne maximum qui en résulte (ϵ_b) dépendent dans un élastomère (1) des caractéristiques chimiques et topologiques du réseau polymérique, et (2) des conditions expérimentales pour lesquelles la rupture a été observée. Afin de séparer ces deux effets, on peut souvent caractériser les propriétés de la tension extrême par une "enveloppe de rupture" qui est définie par des valeurs de σ_b et ϵ_b déterminées à différentes vitesses de tension dans un large domaine de température. Etant donné que l'on peut appliquer la superposition temps-température, ces données se superposent dans un diagramme log $\sigma_b T_0/T$ un fonction de log ϵ_b où T est la température d'expérience en °K. et T_0 une température de référence choisie arbitrairement. L'"enveloppe de rupture" qui en résulte est indépendante du temps (vitesse de tension) et de la température et ne dépend donc uniquement que de caractéristiques essentielles du réseau polymérique. Afin d'illustrer la méthode de caractérisation on a étudié les données de deux gommes de styrène-butadiène vulcanisé, le SBR-I et le SBR-II. Dans le cas du SBR-I, les valeurs σ_b et ϵ_b qui ont été obtenues dans de larges domaines de vitesse de tension et de température se superposent pour donner une "enveloppe de rupture." Á des températures plus élevées les résultats donnent également une valeur en relation avec le module à l'équilibre. Dans le cas du SBR-II, on obtient une "enveloppe de rupture" équivalente à des températures variables et avec une tension et une vitesse d'étirement constantes. Ceci paraît fortement suggérer que l'enveloppe de rupture est indépendante de la méthode expérimentale. Une considération théorique temps-rupture, associée à différentes méthodes expérimentales nous montre que pour de valeurs données de σ_b et ϵ_b la relation temps-rupture augmente dans l'ordre des différents facteurs: tension interne constante < force constante < vitesse de tension constante < vitesse d'étirement constante.

Zusammenfassung

Die Zugspannung beim Bruch (σ_b) und die entsprechende Bruchdehnung (ϵ_b) hängen (1) von den chemischen und topologischen Eigenheiten des Polymernetzwerkes und (2) von den experimentellen Bedingungen beim Bruch ab. Zur Trennung dieser Effekte können die Zugeigenschaften beim Bruch häufig durch eine "Bruchenvelope" charakterisiert werden, die durch die bei verschiedenen Dehnungsgeschwindigkeiten über einen weiten Temperaturbereich bestimmten Werte von σ_b und ϵ_b definiert ist. Unter der Voraussetzung, dass eine Zeit-Temperatur-Superposition anwendbar ist, bilden solche Daten beim Auftragen von log $\sigma_b T_0/T$ gegen log ϵ_b eine gemeinsame Kurve, wobei T die Versuchs-temperatur in °K und T_0 eine willkürlich gewählte Bezugstemperatur ist. Die resultierende Bruchenvelope ist unabhängig von Zeit (Dehnungsgeschwindigkeit) und Temperatur und hängt somit nur von Grundeigenschaften des Polymernertzwerkes ab. Zur Illustration dieser Charaktersierungsmethode werden die an zwei Styrol–Butadien-Kautschukvulkanisaten, SBR-I und SBR-II, ermittelten Daten analysiert. Bei SBR-I bildeten die über ausgedehnte Dehnungsgeschwindigkeits- und Temperaturbereiche erhaltenen Werte von σ_b and ϵ_b eine gemeinsame Bruchenvelope. Die bei erhöhten Temperaturen ermittelten Daten ergaben auch einen auverlässigen Wert für den Gleichgewichtsmodul. Für SBR-II ergaben die bei verschiedenen Temperaturen unter Bedingungen konstanter Dehnung und Dehnungsgeschwindigkeit ermittelten Daten identische Bruchenvelopen. Dies weist deutlich darauf hin, dass die Bruchenvelope von der Prüfmethode unabhängig ist. Eine theoretische Betrachtung der Bruchzeit bei verschiedenen Prüfmethoden ergibt, dass bei gegebenen Werten von σ_b und ϵ_b die nach den folgenden Testmethoden ermittelte Bruchzeit in der Reihenfolge konstante Dehnung < konstante Spannung < konstante Dehnungsgeschwindigkeit < konstante Spannungsgeschwindigkeit ansteigen sollte.

Received March 13, 1963

JOURNAL OF POLYMER SCIENCE: PART A VOL. 1, PP. 3617–3625 (1963)

Nitrosation of Linear Phenol-Formaldehyde Polymers

WILLIAM J. BURKE and HAROLD P. HIGGINBOTTOM,
Department of Chemistry, University of Utah, Salt Lake City, Utah

Synopsis

The nitrosation of *o,o*-linked linear phenol-formaldehyde polymers was readily affected in aqueous *N,N*-dimethylformamide to give products containing *p*-benzoquinone monoxime repeating units. Elemental analyses and infrared spectra indicated the presence of nitrophenol moieties also. Factors influencing the nature of the nitrosation reaction were studied.

INTRODUCTION

Several types of linear phenol-formaldehyde polymers with recurring units of known structure have been prepared in this laboratory.[1–3] The physical and chemical properties of such isomeric polymers were shown to be strikingly different. Further substantial modifications in properties were noted in chloro substituted polymers of this type.[2]

The availability of *o,o*-linked phenol-formaldehyde polymers having a highly reactive free *para* position in each repeating unit[1] offers an attractive source of other polymers through chemical modification. The simplicity of such a polymer structure also offers important advantages in the interpretation of results in any system having potentially complicated side reactions.

Nitrosation of phenols occurs readily under mild conditions to give nitroso derivatives which in the solid form at least have been shown to exist almost exclusively as the *p*-benzoquinone monoxime tautomer.[4] In view of this, the nitrosation of *o,o*-linked phenol-formaldehyde polymers appeared to offer an attractive approach to polymeric products having novel repeating units.

EXPERIMENTAL APPROACH

In the nitrosation of phenols in aqueous acidified solutions of sodium nitrite, NO^+ or a carrier of this ion, NOX, is presumed to be the nitrosating agent.[5] Little information, however, is available concerning the nature of the nitrosonium ion carrier in organic solvent–acid systems.

Since the use of an aqueous nitrosating system with the phenolic polymers was not practical, several types of solvents were considered. These included *N,N*-dimethylformamide (DMF), acetone, and dioxane as well as mixed solvents. DMF was selected on the basis of high polarity, good

solvent power, miscibility with water, low freezing point, and stability. In general a mineral acid was added dropwise with good agitation to a cooled solution of the polymer and sodium nitrite in DMF.

RESULTS

The series of runs outlined in Table I was made in order to determine the influence of selected reaction variables. The properties of the resulting polymers are summarized in Table II.

TABLE I
Preparation of Nitrosated *o,o*-Linked Phenol-Formaldehyde Polymers

Polymer No.	DMF, ml.[a]	$NaNO_2$, moles[a]	Acid	Amt. acid, moles[a]	Temp., °C.	Time, hr.	Reaction atmos.[b]
1	500	0.11	H_2SO_4	0.1	−5	4	Air
2	500	0.125	H_2SO_4	0.63	−5	5.5	Air
3	310	0.075	HOAc	4.0	0	6	N_2
4	600	0.11	H_3PO_2	0.2	0	22	N_2
5	1000	0.20	H_3PO_3	1.2	0	2	N_2

[a] Per 0.1 mole of polymer repeating unit.

[b] Atmosphere in contact with reaction medium. Nitrogen was added in a continuous stream during reaction period.

TABLE II
Properties of Nitrosated *o,o*-Linked Phenol-Formaldehyde Polymers

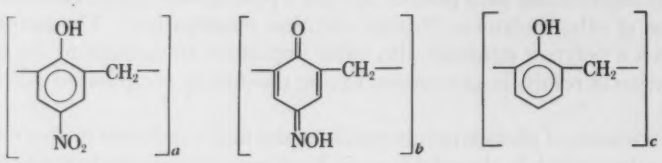

Polymer No.[a]	Solubility in DMF, %[b]	Inherent viscosity[c]	Formula *a b c*	Calculated, % C	H	N	O	Found.[d] C	H	N	O
1	100	0.38	5 4 5	64.4	4.1	6.9	24.5	64.1	4.3	6.9	24.5
2	90	0.25	– – –[e]	57.5	4.0	7.3	31.2	57.4	4.0	7.3	31.3
3	90	0.37	5 9 16	68.7	4.6	5.3	21.4	68.4	4.9	5.4	21.3
4	100	0.37	2 5 7	68.4	4.5	5.7	21.4	68.4	4.8	5.8	21.0
5	80	—	3 3 3	64.3	4.1	7.1	24.5	64.2	4.4	7.2	24.2

[a] Polymer number indicates method of preparation in Table I.

[b] At 25°C. in excess DMF.

[c] In DMF at 25°C. at a concentration of 0.5 g./100 ml.

[d] Reported on an anhydrous basis. Oxygen values are by difference.

[e] Calculated for $(C_{147}H_{122}N_{16}O_{60})_n$. High oxygen value did not permit evaluation of *a*, *b*, and *c*.

Infrared spectra, viscosity measurements, and elemental analyses were used to characterize the resulting nitrosated polymers. It was noted that the polymers prepared under certain conditions dissolved with difficulty and had a high solution viscosity. In each case the polymeric products had an oxygen content which was higher than that calculated for simple nitrosation. Infrared data indicated the presence of nitro and diazo groups in addition to the desired *p*-benzoquinone oxime units.

The formulas given in Table II are calculated on the basis of a principal contribution by the three indicated structures. A random order of these residues is assumed to be present along the chain. In general the contribution of diazo and other possible impurities, as well as end groups, was believed to be small.

The side reactions which appeared to have the greatest influence on the nature of the modified product were oxidation to the nitrophenol (III) and diazonium salt formation (IV) followed by azo coupling (V) with the unreacted phenol residues.

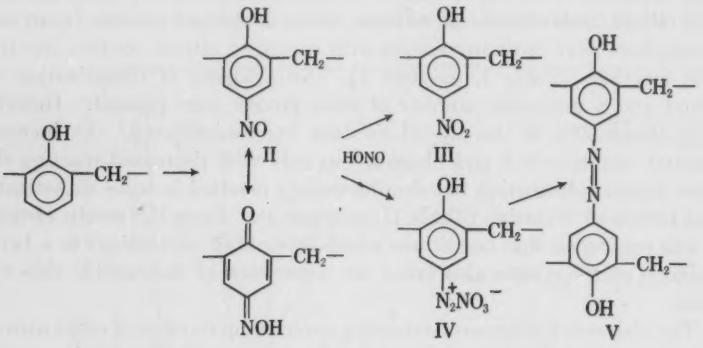

Jaeger[6] noted that nitrosophenol will react with excess nitrous acid to produce *p*-hydroxybenzene diazonium nitrate. More recently[7] excess nitrous acid has been used to effect a direct preparative diazotization of activated aromatic compounds. The mechanism is obscure but probably proceeds through an intermediate nitrosophenol. Obviously, excess nitrous acid in a nitrosating medium will favor this side reaction. The diazotization is also favored by the presence of certain oxides of nitrogen. It has been shown that *p*-nitrosophenol will react with nitric oxide in acetic acid to give the diazonium compound.[8]

In most instances the nitrosation reaction mixture remained homogeneous during the entire reaction period. This indicated that coupling did not occur to any significant extent. Upon isolation and neutralization of the polymeric product, coupling could more reasonably take place with a resulting decrease in solubility.

In order to obtain a maximum of benzoquinone oxime residues with a minimum of side reactions, several reaction variables were controlled. The presence of various oxides of nitrogen appeared to favor both oxidation and diazotization. These oxides can form by the decomposition of nitrous acid through a disproportionation reaction.[5]

$$3HONO \rightleftharpoons HNO_3 + 2NO + H_2O$$

The presence of these oxides was minimized by maintaining the temperature below 0°C. and by passing a stream of nitrogen through the system during the entire course of the reaction. Control of the molar ratio of nitrous acid to the phenolic residues was critical. Keeping the ratio at or below unity definitely reduced the diazotization side reaction. The oxidation of the benzoquinone oxime groups to nitrophenol units was also strongly dependent on nitrous acid concentration.

A noticeable change in the nature of the reaction product was observed when phosphorous acid was used in place of sulfuric acid to liberate free nitrous acid. The lower acidity and reducing properties of phosphorous acid appeared to be important. Use of small amounts of this acid and a very slight molar excess of sodium nitrite to phenol residue in an inert atmosphere gave optimum results with regard to nitroso content free from side reactions (Table I, polymer 4). No evidence of diazotization was found and a minimum number of nitro groups were present. However, only about 50% of the phenol residues were substituted. An increased amount of nitrite salt and phosphorous acid with decreased reaction time gave higher substitution but simultaneously resulted in some diazotization and increased oxidation (Table II, polymer 5). From the results obtained it was concluded that conditions which favor high conversions to a benzoquinone oxime system also favor the occurrence of undesirable side reactions.

The nitrosated polymers containing a minimum number of other nitrogen containing functional groups were bright canary-yellow amorphous solids. An increase in the number of diazo and nitro groups led to darker products. Polymers with a high quinone diazide impurity content changed to a dark reddish-brown upon heating. All of the modified polymers darkened and charred when gradually heated on a melting point block and displayed no distinct softening or decomposition points. When dropped on a preheated block, however, they decomposed violently in the region of 260–270°C.

The freshly isolated polymers which had reduced solubility exhibited a weak but distinct infrared band at 4.75 μ. This band is characteristic of a diazophenol in the high resonance form of a quinone diazide.[9,10] If the —N=N— group displayed itself in the infrared spectra,[10] it probably did so in the same region where the benzoquinone oxime group has a very strong carbonyl absorption band.[4] The spectrum of the nitrosated polymer 5 in Table II showed a distinct band at 4.75 μ. When exposed to direct sunlight or heated, the polymer darkened appreciably and the band disappeared from the spectrum. This behavior is characteristic of quinone diazides.[11]

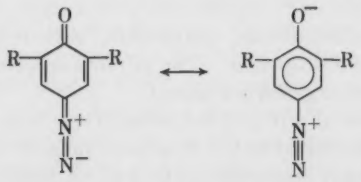

The band at 4.75 μ in quinone diazides is very strong. The weak band that appeared at this position in the spectra of the nitrosated polymers indicated that the number of these residues in the polymer was small. The partly soluble polymer products generally contained only a small amount of insoluble material. This denoted that there were very few —N=N— crosslinks between chains.

The infrared spectra of the model compound 2,6-dimethyl-4-benzoquinone oxime was used in conjunction with the spectral data obtained by Philbrook and Getten[4] on a number of *p*-benzoquinone oximes to provide a basis for specific band assignments. The infrared bands are believed to arise from quinoid structural features since bands characteristic of aromatic

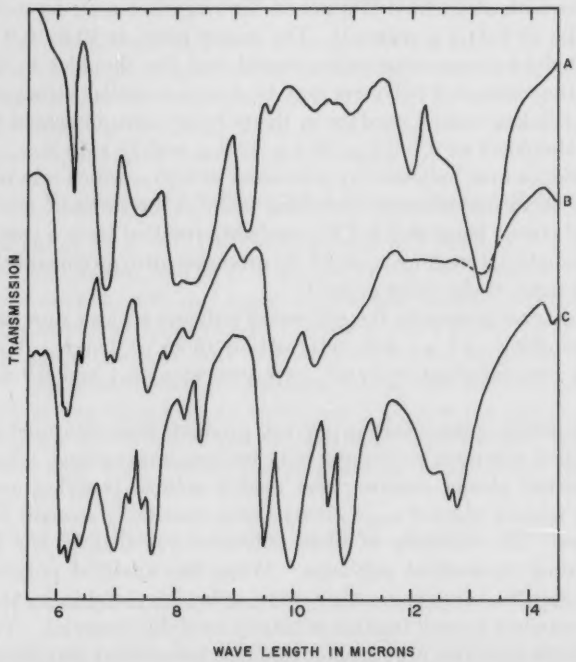

Fig. 1. Infrared spectra of: (*A*) *o,o*-linked phenol-formaldehyde polymer; (*B*) nitrosated *o,o*-linked phenol-formaldehyde polymer 5 in Table II; (*C*) 2,6-dimethyl-4-benzoquinone oxime.

structures were not found.[4] Further, there is a close overall similarity to the spectra of *p*-benzoquinones, particularly with respect to the strong carbonyl and olefinic absorptions. The infrared spectrum of 2,6-dimethyl-4-benzoquinone oxime is given in Figure 1.

The small inflection at 6.10 μ in the infrared spectrum of nitrosated polymers (Fig. 1) was attributed to C=N absorption and was almost obscured by the intense carbonyl absorption at 6.14 μ. A small band at 6.4 μ indicated the presence of conjugated C=C groups. The positions of these absorption bands in the polymer spectra corresponded almost exactly to those in the 2,6-dimethyl-4-benzoquinone oxime model (Fig. 1).

The majority of the bands in the 6.5–15 μ region in the spectra of *p*-benzoquinone oximes have not been assigned to any definite structures. Evidence brought out in the present study indicated that the broad strong band in the 9.7 μ region is due to the presence of *p*-benzoquinone oxime residues in the polymer. Each of the monomeric *p*-benzoquinone oximes studied by Philbrook and Getten[4] contained a strong unassigned band in the 9.4–9.7 μ region. Although the specific vibrational mode responsible for this band is not known, it was useful in detecting benzoquinone oxime residues, particularly at low concentrations.

Quinones with an isolated H atom on the ring show a moderately strong band in the 10.8–11.4 μ region.[12] The strong band at 10.8–10.9 μ in the 2,6-dimethyl-4-benzoquinone oxime model and the shoulder in the same region in the nitrosated polymers may be due to a similar structure. Unreacted *o,o*-linked phenol residues in the polymer were indicated by small bands or shoulders at 9.1–9.2 μ, 10.4 μ, 12.0 μ, and 13.1–13.3 μ. *p*-Nitrophenol residues were indicated by a shoulder at 6.55 μ, which is in the region attributed to the asymmetric stretching mode of an aromatic nitro group. The broad strong band at 7.4–7.6 μ probably resulted from a combination of the symmetric stretching mode of the aromatic nitro group and the N—O stretching mode of the oxime group.[13]

Other features present in the nitrosated polymer spectra were associated —OH stretching (3.1 μ) and deformation (8.25 μ) bands. Weak CH_2 stretching and deformation bands were present at 3.4 and 6.9 μ, respectively.

The viscosities of the resulting polymer products were measured in DMF. The modified polymers containing only benzoquinone oxime, nitrophenol, and unreacted phenol residues were readily soluble in either acetone or DMF. Viscosity plots of η_{sp}/c versus c gave essentially straight lines with zero slopes. The viscosity of these polymers was slightly less than the corresponding unmodified polymers. When the modified polymers contained —N=N— crosslinks, they were difficultly soluble in DMF and usually contained a small fraction of totally insoluble material. Viscosities on the soluble fractions were greater than the unmodified polymers in some cases. Plots of η_{sp}/c versus c were nonlinear with negative slopes as $c \rightarrow 0$ in such cases.

The benzoquinone oxime residues did not react with phenol in concen-

trated sulfuric acid to give the color test characteristic of the Liebermann reaction.[14] A qualitative test to detect the presence of such residues was developed by employing reactions described by Burmistrov et al.[15] The test was made in pyridine or DMF and consisted of forming the sulfonate ester followed by basic hydrolysis of the ester in the presence of phenol. The resulting indophenol salt was an intense green and turned red upon addition of concentrated H_2SO_4. All of the polymers listed in Table I gave a positive modified Burmistrov color test for the benzoquinone oxime residue. The test is extremely sensitive with monomers. A very low benzoquinone oxime residue content in a polymer is difficult to detect, however, because of bulk polymer precipitation.

EXPERIMENTAL

Infrared Absorption Spectra

Infrared spectra of the products were determined in potassium bromide disks with a Beckman Model IR-4 recording spectrophotometer with sodium chloride optics. A potassium bromide disk was used as a reference.

Determination of Intrinsic Viscosity

Relative viscosities of polymers were determined at two or more concentrations so chosen as to give values in the range from about 1.05 to 1.50. The measurements were carried out in DMF at 25°C. and in No. 50 and 100 Cannon-Fenske viscometers. Plots of η_{sp}/c against c were prepared and extrapolated graphically to zero concentrations.

Synthesis of 2,6-Dimethyl-4-benzoquinone Oxime

A solution of 61 g. of 2,6-dimethylphenol (0.5 moles), 20 g. of sodium hydroxide (0.5 moles), and 36 g. of sodium nitrite (0.52 moles) in 800 ml. of water was cooled to 0°C. and maintained at this temperature for the duration of the reaction. Aqueous 48% sulfuric acid (98 ml.; 0.66 moles) at 0°C. was added dropwise with stirring over a 2-hr. period to the phenol solution. An orange solid precipitated during the addition of the acid. The solution was stirred for an additional 2 hr. and the orange solid was then removed by filtration and washed with cold distilled water. The crude yield was 83%. After recrystallization from water, the product melted at 160–161°C.

ANAL. Calcd. for $C_9H_9NO_2$: C, 63.56%; H, 6.00%; N, 9.27%. Found: C, 63.84%; H, 6.04%; N, 9.21%.

Nitrosation of *o,o*-Linked Phenol-Formaldehyde Polymer

A solution of 2.12 g. of *o,o*-linked phenol-formaldehyde polymer (0.02 moles of C_7H_6O unit, $\eta_i = 0.40$) and 1.52 g. of sodium nitrite (0.022 moles) in 60 ml. of DMF was cooled to 0°C. and maintained at this temperature for the duration of the reaction. A solution of 3.3 g. of phosphorous acid

(0.04 moles) in 60 ml. of DMF was cooled to 0°C. and added dropwise with stirring to the polymer solution over a 2-hr. period. During the entire reaction period a stream of nitrogen was passed through the reaction vessel in order to sweep out any oxides of nitrogen which might be evolved and the mixture was agitated constantly with strict temperature control. At the end of a total reaction period of 22 hr., the solution was added slowly with stirring to one liter of distilled water and ice containing 10 ml. of 37% hydrochloric acid. The canary-yellow solid was removed by filtration, washed thoroughly with distilled water, and dried at 60°C./0.5 mm. over Drierite for 24 hr., $\eta_i = 0.37$.

ANAL. Calcd. for $[(C_7H_5O_3N)_2\ (C_7H_5O_2N)_5\ (C_7H_6O)_7]_n$: C, 68.40%; H, 4.51%; N 5.70%. Found: C, 68.38%; H, 4.80%; N, 5.77%.

The results obtained in modifications of this reaction are summarized in Table I.

Qualitative Test for the Detection of *p*-Benzoquinone Oxime Residues

A solution composed of 0.05 to 0.2 g. of the material being tested in dry pyridine or DMF was treated with 5 to 10 drops of benzenesulfonyl chloride. The solution was allowed to stand at room temperature for two or more hours and was then treated with 2 ml. of freshly prepared 10% NaOH containing 1 g. of phenol/10 ml. The tube was shaken and allowed to stand until a color change was observed. In the case of a positive test, an intense green coloration appeared within minutes with monomeric *p*-benzoquinone oximes. Polymers, on the other hand, often had to stand for several hours before giving a positive test. Addition of concentrated sulfuric acid to the green solution yielded an intense red coloration. Quinones, phenols, and nitrophenols do not interfere with the test.

This work was supported in part by the Army Research Office (Durham). We wish to express appreciation to the University of Utah Research Committee for a fellowship (to H. P. H.). This material was abstracted from a thesis submitted by H. P. Higginbottom in partial fulfillment of the requirements for the Ph.D. degree at the University of Utah.

References

1. Burke, W. J., S. H. Ruetman, C. W. Stephens, and A. Rosenthal, *J. Polymer Sci.*, **22**, 477 (1956).
2. Burke, W. J., S. H. Ruetman, and H. P. Higginbottom, *J. Polymer Sci.*, **38**, 513 (1959).
3. Burke, W. J., G. A. Short, and H. P. Higginbottom, *J. Polymer Sci.*, **43**, 49 (1960).
4. Philbrook, G. E., and T. C Getten, *J. Org. Chem.*, **24**, 569 (1959).
5. Turney, T. A., and G. A. Wright, *Chem. Revs.*, **59**, 497 (1959).
6. Jaeger, C., *Ber.*, **8**, 894 (1875).
7. Tedder, J. N., *J. Chem. Soc.*, **1957**, 4003.
8. Nesmeyanov, N., and S. T. Ioffe, *J. Gen. Chem. (U.S.S.R.)*, **11**, 392 (1941).
9. Le Fevre, R. J. W., J. B. Sousa, and R. L. Werner, *J. Chem. Soc.*, **1954**, 4686.
10. Bellamy, L. J., *The Infra-Red Spectra of Complex Molecules*, 2nd Ed., Methuen, London, 1958, p. 95.

11. Kraaljeveld, A., and E. Havinga, *Rec. Trav. Chim.*, **73,** 537 (1954).
12. Yates, P., M. A. Ardao, and L. Fieser, *J. Am. Chem. Soc.*, **78,** 650 (1956).
13. Boll, P. M., *Acta Chem. Scand.*, **12,** 1777 (1958).
14. Turney, T. A., *J. Org. Chem.*, **22,** 1692 (1957).
15. Burmistrov, S. I., and E. A. Titov, *Ukr. Khim. Zh.*, **22,** 223 (1956); *C A.*, **51,** 272 (1957).

Résumé

La nitrosation des polymères, phénol-formaldéhyde linéaires, liés en *o,o-*, a été effectuée facilement en solution aqueuse de *N,N*-diméthylformamide; elle donne des produits contenant des unités périodiques mon-oxime de *p*-benzoquinone. L'analyse élémentaire et les spectres infarouges indiquent également la présence de moitiés de nitrophénol. Les facteurs influencant la nature de la réaction de nitrosation ont été étudiés.

Zusammenfassung

Die Nitrosierung *o,o*-verknüpfter, linearer Phenolformaldehydpolymerer unter Bildung von Produkten mit *p*-Benzochinonmonoximbausteinen konnte leicht in wässrigem *N,N*-Dimethylformamid durchgeführt werden. Elementaranalyse und Infrarotspektren sprachen auch für die Anwesenheit von Nitrophenolgruppen. Die für den Verlauf der Nitrosierung verantwortlichen Faktoren wurden untersucht.

Received August 1, 1962

JOURNAL OF POLYMER SCIENCE: PART A VOL. 1, PP. 3627–3642 (1963)

Ionic Polymerization of Diphenylvinylphosphine Oxide*

H. R. ALLCOCK and R. L. KUGEL, *Chemical Research Department, Central Research Division, American Cyanamid Company, Stamford, Connecticut*

Synopsis

Grignard reagents, organolithium compounds, sodium naphthalene and aluminum alkyl–metal halide catalysts were examined as initiators for the polymerization of diphenylvinylphosphine oxide. The most effective catalysts studied were Grignard reagents and sodium naphthalene. With Grignard catalysis, polymers of molecular weight up to ~10,000 were produced although the yield, molecular weight, and crystallinity of the products were influenced by the organic and halide components of the catalyst and by the reaction solvent. Copolymerization studies indicated that the anionic reactivity of diphenylvinylphosphine oxide is between those of styrene and methyl methacrylate. For Grignard catalysis an anionic-type polymerization mechanism is proposed which requires the formation of polymer–organomagnesium halide adducts in the transition state.

INTRODUCTION

Recent publications have described the free-radical polymerization behavior of diphenylvinylphosphine oxide. Berlin and Butler[1] and Rabinowitz and Pellon[2] reported free-radical solution and bulk polymerizations of this monomer which yielded mainly oligomers. The latter authors found that the compound also showed a low reactivity in copolymerization with styrene and methyl methacrylate. This behavior was ascribed to the electronic and steric properties of the diphenylvinylphosphine oxide molecule[1] and to the lack of radical stabilization by the diphenylphosphine oxide group.[3] Tsetlin et al.[4] reported the preparation of a polymer of molecular weight 30,000 by x-ray irradiation of the molten monomer.

We have examined the use of several organometallic initiators to effect the polymerization of diphenylvinylphosphine oxide. These include Grignard reagents, organolithium compounds, sodium naphthalene, and Ziegler-Natta type initiators. Catalysis by Grignard reagents was studied in more detail, and these results are interpreted in terms of a polymerization mechanism. The role of diphenylvinylphosphine oxide in ionic copolymerization reactions is also discussed in this paper.

* Presented, in part, at the Eleventh Canadian High Polymer Forum, Windsor, Ontario, September 5–7, 1962.

RESULTS AND DISCUSSION

Properties of Diphenylvinylphosphine Oxide Polymers

The polymers prepared from diphenylvinylphosphine oxide in the presence of organometallic initiators formed a range of products with molecular weights between 2,000 and 10,000 and with reduced specific and intrinsic viscosities between 0.02 and 0.10. Melting points of products within this range varied from 150°C. to over 300°C. Polymer solubility in solvents such as toluene, tetrahydrofuran (THF), and chloroform decreased with increasing chain length. Oligomers (MW < 2,000) were soluble in these solvents, but higher polymers (MW 4,000–10,000) were soluble only in polar solvents, such as dimethylformamide (DMF), dimethyl sulfoxide, pyridine, nitrobenzene, aliphatic carboxylic acids, and hot alcohols. Both oligomers and polymers were insoluble in aqueous liquids although hydrate formation occurred in both the solid state and in solution. Removal of water from the solid hydrates was achieved by prolonged drying in a vacuum oven. When dried in this manner the materials gave satisfactory analyses for diphenylvinylphosphine oxide polymers. The absence of 1,4-addition products was suggested by the infrared spectra of the polymers, which showed no peaks due to P-O-C absorption and which resembled that of the monomer except for the absence of a vinyl peak at 972 cm.$^{-1}$

Polymers prepared with the use of Grignard reagents as initiators were examined by x-ray diffraction, and both crystalline and amorphous modifications were detected, the degree of order being dependent on the polymerization conditions employed.

Polymerization by Grignard Reagents

When solutions of diphenylvinylphosphine oxide in toluene, tetrahydrofuran, or pyridine were treated with catalytic amounts of Grignard reagents, a color change from colorless to yellow or orange occurred immediately, and a polymerization reaction was initiated. Reactions in toluene or tetrahydrofuran were generally heterogeneous from the time of catalyst addition, with solid polymer separating continuously from the mixtures. Polymerizations were usually performed for 20 hr., and after this time the polymer was isolated and fractionated according to solubility in tetrahydrofuran, toluene and heptane. The yields, molecular weight range and crystallinity of the products were dependent on a number of factors, and the influence of initiator concentration, organomagnesium halide, and solvent were examined.

Initiator Concentration. The data in Table I describes the effects of a tenfold variation in the catalyst/monomer ratio on the yield of polymer. There appeared to be a lower limit in the catalyst/monomer ratio below which no yellow color formation or polymerization occurred. The failure of polymerizations below this limit was attributed to a reaction of the catalyst or monomer anion with traces of water or impurity in the monomer

TABLE I
Variation of Polymer Yield with Catalyst/Monomer Ratio[a]

[Catalyst]/[Monomer] × 10^2	Conversion, %[b]	$[\eta]^{\text{ethanol}}_{30^\circ}$, dl./g.
1.5	0	—
3.0	8	0.05
7.5	35	0.03–0.06[c]
15.0	94	0.03–0.09[c]

[a] Polymerization method B; Grignard, *tert*-BuMgBr; $(C_6H_5)_2P(O)CH{=}CH_2$ (0.022 moles); toluene (100 ml.); temp., 25°C.; reaction time, 20 hr.
[b] Toluene-insoluble products (m.w. ~ over 2,000).
[c] Intrinsic viscosity range of fractionated products.

or solvent. The threshold varied with the polymerization technique employed, being lower for reactions within a vacuum system, and also varied slightly for different solvents and from batch to batch of the same solvent. Comparative reactions were performed with the use of the same supply of solvent for polymerizations of the same series, and with a standardized drying technique for the monomer prior to each reaction. For the series described in Table I, conversion to polymer in a given time was proportional to the catalyst/monomer ratio. The intrinsic viscosities of the products showed no significant dependence on the catalyst to monomer ratio over the concentration range studied.

Changes in Structure of Grignard Reagents. The polymerizations were sensitive to the type of Grignard reagent used as initiator, and the influence of several organomagnesium halides was examined. A measure of the relative effectiveness of different catalysts was obtained from the percentage conversions to tetrahydrofuran-insoluble polymer, as shown in Tables II and III.

In both toluene and tetrahydrofuran solvents the polymer yields varied with both the organic and halide components of the organomagnesium halides. Under the conditions described, the conversion varied with R in RMgBr in the order, *tert*-butyl> phenyl> *n*-butyl, and with X in *n*-BuMgX in the order I>Br>Cl.

TABLE II
Influence of Grignard Reagent on Conversion to Polymer in Toluene Solvent[a]

Grignard	THF-insoluble product, %	Reduced specific viscosity (1% solution in DMF), dl./g.
t-BuMgBr	93	0.038
n-BuMgI	66	0.080
n-BuMgBr	53	0.050
n-BuMgCl	26	0.050
C_6H_5MgBr	63	0.050

[a] Polymerization method A; Grignard (1.56×10^{-3} moles); $(C_6H_5)_2P(O)CH{=}CH_2$ (2.2×10^{-2} moles); toluene (100 ml.); temp. 25–26°C., reaction time, 20 hr.

TABLE III
Influence of Grignard Reagent on Conversion to Polymer in Tetrahydrofuran Solvent[a]

Grignard	[Grignard]/[Monomer] × 10^2	THF-insoluble product, %	Reduced specific viscosity (1% solution in DMF), dl./g.
t-BuMgBr	10.3	76	0.100
t-BuMgBr[b]	35.0	94	0.040
n-BuMgBr	7.0	22	0.085
n-BuMgCl	7.0	0	[c]
C_6H_5MgBr	7.0	25	0.090

[a] Polymerization method A; $(C_6H_5)_2P(O)CH{=}CH_2$ (2.2×10^{-2} moles); THF (100 ml.); temp. 25–26°C.; reaction time, 20 hr.

[b] In 120 ml. THF.

[c] For THF-soluble product $[\eta_{sp}/C] = 0.055$ (C = 1% in ethanol).

Solvent Changes. The data in Tables II and III indicate that replacement of toluene by tetrahydrofuran as a reaction solvent generally resulted in lower yields of higher molecular weight polymers. Comparisons of catalyst/monomer ratios with molecular weights computed from viscosity data revealed that, with the exception of *n*-butylmagnesium iodide catalysis, reactions in toluene yielded polymers of chain length corresponding to approximately one catalyst molecule per chain. In tetrahydrofuran the highest polymers contained a greater ratio of monomer units for each initiator molecule. This evidence may reflect partial catalyst deactivation or destruction in tetrahydrofuran.

Another contributing factor for the formation of higher molecular weight polymers in tetrahydrofuran is, probably, the fact that poly(diphenylvinylphosphine oxide) is more soluble in tetrahydrofuran than in toluene. In this system it appeared possible that precipitation of polymer

TABLE IV
Polymerization of Diphenylvinylphosphine Oxide in Toluene, Tetrahydrofuran and Pyridine[a]

Solvent	Temperature, °C.	[Catalyst]/[Monomer] × 10^2	Product A, %[b]	Product B, %[c]
Toluene	25–26	7.1	63	25
THF	"	7.1	25	50
Pyridine	"	7.0	0	25
"	0	"	0	30
"	−40	"	0	32

[a] Polymerization method A; catalyst, C_6H_5MgBr; reaction time, 20 hr.; solvent (100 ml.); $(C_6H_5)_2P(O)CH{=}CH_2$ (2.2×10^{-2} moles).

[b] Insoluble in THF and toluene.

[c] Soluble in THF, insoluble in toluene.

retarded further chain growth and limited the degree of polymerization. It was, therefore, of interest to carry out polymerizations in pyridine in which the polymer is soluble. Table IV describes the results of polymerization reactions in toluene, tetrahydrofuran, and pyridine.

At a comparable catalyst/monomer ratio and temperature, higher molecular weight polymer was not produced in pyridine than in toluene or tetrahydrofuran, and decreases in reaction temperature from 25°C. to −40°C. in pyridine did not change the polymerization behavior significantly. A decrease in the catalyst/monomer ratio in pyridine served to increase the yield of higher molecular weight products. However, analysis of the products demonstrated the presence of nitrogen (0.4 to 0.8%). Furthermore, the reduced specific viscosities of products prepared in pyridine were similar to those prepared in toluene, although the former were soluble in tetrahydrofuran and the latter were insoluble. These results suggest the participation of a pyridine anion, formed by reaction of the Grignard or polymer anion with the solvent, and indicate that the reaction mechanism in pyridine differs from that in toluene or tetrahydrofuran.

Changes in the polymerization solvent resulted in differences in the crystallinity of the polymers. Polymers prepared in tetrahydrofuran, pyridine, or in toluene containing more than 5% diethyl ether gave amorphous x-ray diffraction patterns. Polymers prepared in toluene solvent (except with *n*-butylmagnesium chloride) were crystalline when isolated directly from the reaction mixtures, were amorphous when reprecipitated, and recovered crystallinity when heated below the softening point or when swelled by chloroform and dried.

Polymerization Mechanism. Recent publications on the nature of Grignard reagents suggest that a halogen-bridged complex between diorganomagnesium and magnesium halide is a likely structure, and that in donor solvents, such as ethers or pyridine, coordinated adducts are formed between the organomagnesium halide and the solvent.[5,6]

Initiation of diphenylvinylphosphine oxide by Grignard reagents probably involves the prior formation of a monomer–magnesium halide or monomer–Grignard complex (I) followed by conversion to a colored monomeric anion (II):

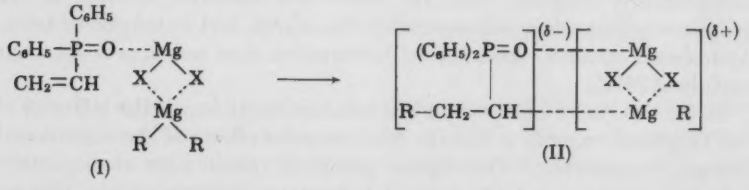

Formation of (I) would be retarded in donor solvents because of solvent coordination with the catalyst. In the formation of (I) a beta-addition of the organic anion is tentatively assumed in view of the evidence of related nucleophilic additions.[7] The adducts I and II are believed to be

the initial precipitate formed when Grignard reagents are added to solutions of diphenylvinylphosphine oxide, since rapid isolation of the precipitate yielded a product which appeared to contain monomer, oligomers, and magnesium halide. An adduct of diphenylvinylphosphine oxide with magnesium bromide was prepared separately, and although the material formed a yellow colored species with Grignard reagents, it did not polymerize. The initiation mechanism depicted requires that the organic group from the catalyst should be present in the polymer as an endgroup, and infrared evidence was obtained for *tert*-butyl endgroups in oligomers prepared with the use of *tert*-butylmagnesium bromide as a catalyst.

Chain propagation is believed to take place by insertion of monomer molecules into the polymer catalyst bond as in III, in which coordination of the entering phosphine oxide group with the catalyst precedes addition of the vinyl group.

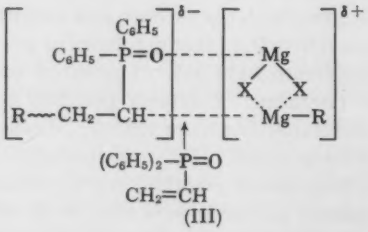

(III)

This process is similar to the one proposed by Natta[12] for the Grignard-catalyzed polymerization of 2-vinylpyridine. Since polymerizations in toluene and tetrahydrofuran are generally heterogeneous, this step may also be analogous to many polymerizations of the Ziegler-Natta type. Propagation is probably a fast step compared to formation of II, since addition of diphenylvinylphosphine oxide solution to an excess of phenylmagnesium bromide solution yields polymer but no monomeric Grignard addition product.

Chain growth probably continues until the rate is reduced by polymer insolubility in the solvent. However, in the absence of protonating or chain-transfer reagents, both the colors and initiation activity of the polymers persist when polymerization has ceased, and in toluene or tetrahydrofuran solvents, spontaneous termination does not appear to occur rapidly at 25°C.

In the absence of kinetic data it is not possible to assign the influence of the Grignard reagents to specific steric or polar effects of the organic and halogen components. The organic group, R, would play an important role in initiation, and the ease of heterolytic cleavage of the organomagnesium bond and the ease of carbanion, R^-, attack on the vinyl group would affect the initiation step. The effects of the magnesium halide component of the catalyst may reflect changes in the rate of propagation. An increasing polarity of magnesium halides in the order MgI_2

$< MgBr_2 < MgCl_2$ would be expected to retard polymerization by increasing the delocalization of the terminal carbanionic charge.

The role of the solvent in this reaction may be ascribed to the effect on polymer solubility and solvation of the propagating complex. Solvation of the polymer–catalyst complex by ethers or other donor solvents could influence the stereochemistry of propagation. If polymer crystallinity is due to a stereospecific mode of monomer addition, it is likely that the phosphine oxide–Grignard complex is responsible for the orientation. The stereoregulating properties of the complex may originate from polar, steric, or purely surface effects, but the absence of crystallinity in polymers prepared in tetrahydrofuran or pyridine suggests that, in these donor solvents, solvation of the catalyst–polymer complex interferes with the orienting effect of this adduct.

Other Ionic Initiators

In this series of reactions, as in those described previously, the choice of solvent and temperature was limited by the low solubility of the monomer. The preferred low temperature conditions frequently required for ionic polymerizations were not practicable for most of the suitable solvents.

TABLE V
Polymerization of Diphenylvinylphosphine Oxide by Various Catalysts

Catalyst	Polymerization method	[Catalyst]/[Monomer] × 10^2	Solvent	Temperature, °C.	THF-insoluble polymer, %
$TiCl_4.3AlBu_3$	B	7.0	Toluene	110	0
$TiCl_3.5Al(i\text{-}Bu)_3$	B	2.3	Heptane	75	0
$CrCl_3.3THF.3AlBu_3$	B	7.0	Toluene	110	3
n-BuLi	A	7.1	"	25	0
"	A	7.0	Pyridine	−40	9.6
9-Fluorenyllithium	A	5.0	THF	−50	0
"	A	1.0	"	0	0
Na-Naphthalene	A	10.0	"	10	3
"	A	12.7	"	−20	6
"	A	1.3	"	−30	30
"	A	1.8	"	−70	16

Diphenylvinylphosphine oxide was only sparingly soluble in toluene below room temperature and in heptane below 75°C., while 5% solutions in tetrahydrofuran and pyridine were heterogeneous below −30°C. and −40°C., respectively.

As with Grignard reagent catalysis, a measure of the effectiveness of each initiator was deduced from the percentage conversion to tetrahydrofuran-insoluble polymer (MW > 4000), although oligomers were produced by all the catalyst systems described. The data in Table V summarize the

effects of different catalysts in polymerizing diphenylvinylphosphine oxide.

Tributylaluminum–Transition Metal Halide Catalysts. Catalysts prepared from triisobutylaluminum or tri-*n*-butylaluminum and titanium tri- or tetrachloride yielded only oligomers of molecular weight below 2000. Evidence was obtained that the polymerizations were complicated by the formation of metal halide–phosphine oxide complexes since the oligomeric products were isolated in the form of yellow crystalline materials which were shown, by analysis, to contain titanium. It is interesting to note that boron trifluoride and aluminum trichloride also form adducts with the monomer, from which the latter can be regenerated unchanged by treatment with water. However, treatment of diphenylvinylphosphine oxide solutions with a catalyst prepared from tri-*n*-butylaluminum and trichlorotris (tetrahydrofuran) chromium(III)* yielded polymer, 30% of the products having intrinsic viscosities in dimethylformamide of 0.05 and above. It is possible that the chromium trichloride tritetrahydrofuran structure is sterically unable to form a complex with the phosphine oxide groups and polymerization is facilitated.

Organo lithium Initiators. *n*-Butyllithium proved to be a more effective polymerization catalyst in pyridine at −40°C. than in toluene at 25°C. The failure of 9-fluorenyllithium to produce high molecular weight polymers, even in tetrahydrofuran at −50°C., may be the result of a retardation of initiation due to steric hindrance to the addition of a fluorenyl anion.

Sodium Naphthalene. This initiator is effective for the polymerization of diphenylvinylphosphine oxide in tetrahydrofuran. The data in Table V indicate that conversion to polymer is increased by decreases in both initiator concentration and reaction temperature. Insolubility of the monomer and polymer in tetrahydrofuran at temperatures below −30°C. is probably a limiting factor in the exploitation of this system, since a decrease in reaction temperature from −30°C. to −70°C. lowers the yield of polymer.

Reaction Mechanisms. Polymerizations by *n*-butyllithium and by sodium naphthalene presumably proceed through an anionic chain mechanism of a similar type to that postulated for Grignard-catalyzed reactions. However, in these systems there is the possibility of 1-4 additions since the phosphine oxide terminal groups are not complexed with a metal halide. The oligomers prepared with *n*-butyllithium in toluene solution produced amorphous x-ray diffraction patterns, and this is further evidence that stereoregular polymerization of this monomer requires the formation of phosphine oxide–catalyst complexes.

* Samples of this compound were kindly provided by Dr. R. A. Krause and Dr. J. R. Leto.

IV. Ionic Copolymerization of Diphenylvinylphosphine Oxide

Diphenylvinylphosphine oxide and methyl methacrylate both polymerize under the influence of Grignard reagents. It was of interest, therefore, to study the effect of adding Grignard reagents to mixed solutions of the two monomers and to determine the effects, if any, of variations in the monomer ratios. The results obtained with the use of *n*-butylmagnesium bromide and phenylmagnesium bromide are shown in Table VI.

TABLE VI
Copolymerization of Diphenylvinylphosphine Oxide and Methyl Methacrylate[a]

	n-Butylmagnesium bromide			Phenylmagnesium bromide	
[MMA]/[DPVPO]	Conversion, %[b]	DPVO in copolymer, %	[η] $CHCl_3$, dl./g.	Conversion, %[b]	DPVPO in copolymer, %
9	11.1	74	0.04	11.2	75
3	17.8	83	"	23.2	82
2	12.3	82	"	—	—
1	—	—	—	13.6	80
0.33	—	—	—	12.6	86

[a] Polymerization method A; Grignard (1.56×10^{-3} moles); $(C_6H_5)_2P(O)CH{=}CH_2$ (4.4×10^{-2} moles); toluene (100 ml.); temp. 25°C.; reaction time, 1 hr.
[b] Based on diphenylvinylphosphine oxide (DPVPO).

Addition of these Grignard reagents to mixtures of diphenylvinylphosphine oxide and methyl methacrylate in toluene brought about the formation of low molecular weight copolymers which contained a high proportion of the phosphine oxide. The intrinsic viscosities of the products suggest chain lengths of about twenty monomer units containing only three or four molecules of methyl methacrylate. The copolymer composition and yield were not changed significantly by large variations in the monomer ratio or by changes in Grignard reagent. No methyl methacrylate homopolymer was isolated from these reactions, although, in the absence of diphenylvinylphosphine oxide, methyl methacrylate yields homopolymer having a molecular weight of 670,000 ($[\eta]_{benzene} = 2.2$ dl./g.), under identical conditions.

In an anionic copolymerization process of this type between two monomers, A and B, it is necessary to establish if anion $A^{\ominus}$ will initiate monomer B, and conversely if anion $B^{\ominus}$ will initiate monomer A. Accordingly, methyl methacrylate and diphenylvinylphosphine oxide were each initiated with phenylmagnesium bromide at 25°C. Immediately after initiation, the alternate comonomer was added. The methyl methacrylate anion did not initiate diphenylvinylphosphine oxide, but the diphenylvinylphosphine oxide formed a copolymer with methyl methacrylate.

Thus, in a mixture of the two monomers at 25°C., block copolymerization is limited to the addition of methyl methacrylate monomer to poly(diphenylvinylphosphine oxide) anions.

The evidence indicates that addition of an organomagnesium halide to a mixture of the two monomers brings about initiation of the phosphine oxide only. This may be due to the stronger complexing power of the phosphine oxide with the catalyst. Following initiation, the phosphine oxide probably polymerizes independently of the second monomer until the homopolymerization is retarded by polymer insolubility or until all the diphenylvinylphosphine oxide is consumed. Addition of a few methyl methacrylate units to the chain ends can then occur. It appears that methyl methacrylate addition is essentially a termination reaction, and this may be due to the inability of the catalyst to transfer from the phosphine oxide group to the carbonyl group of methyl methacrylate. Under these conditions, the charge separation required for the addition of more than two or three methyl methacrylate units would be too great to allow propagation to occur. Furthermore, since the terminal methyl methacrylate anion cannot initiate addition of phosphine oxide monomer molecules, the chains are effectively terminated. Confirmation of such a process is provided by the ability of sodium naphthalene-initiated poly(diphenylvinylphosphine oxide) anion to yield high molecular weight copolymers with methyl methacrylate. In this reaction, catalyst transfer is not involved in each monomer addition step, and methyl methacrylate addition to the poly(diphenylvinylphosphine oxide) anion can occur without hindrance.

In the absence of air or protonating agents, polymerization mixtures of diphenylvinylphosphine oxide initiated by Grignard reagents retained a yellow or orange color for several days. If the color is due to polymer anions, such species appear to be essentially non-terminating at 25°C. and may initiate the anionic block polymerization of other vinyl monomers. An unterminated oligomer of diphenylvinylphosphine oxide was prepared, therefore, from phenylmagnesium bromide, and aliquots of the mixture were added to solutions of acrylonitrile, methyl methacrylate, and styrene. The results are shown in Table VII.

TABLE VII
Treatment of Vinyl Monomers With Unterminated Poly(diphenylvinylphosphine) Oxide[a]

$Monomer_2$[b]	$Monomer_2$ in Final Product, %	$[\eta]_{DMF}$, dl./g.
Methyl methacrylate	43	0.01
Acrylonitrile	93	0.08
Styrene	0	—

[a] Initiating mixture = 17.7 ml. of a mixture prepared from C_6H_5MgBr (1.09×10^{-2} moles) and $(C_6H_5)_2P(O)CH{=}CH_2$ (4.4×10^{-2} moles) in 124 ml. of a 50% THF in toluene mixture. After 1 hr. reaction at 25°C., aliquots were transferred by hypodermic syringe.
[b] $[C_6H_5MgBr]/[Monomer_2] = 0.03$; in toluene (100 ml.); 20 hr. reaction at 25°C.

The behavior of unterminated poly(diphenylvinylphosphine oxide) anions with methyl methacrylate is in agreement with the data in Table VI. Although addition of methyl methacrylate occurs, extensive polymerization does not take place. With acrylonitrile, block copolymerization occurs to a greater extent to give a product which is predominantly polyacrylonitrile. However, under identical conditions, styrene undergoes no reaction with poly(diphenylvinylphosphine oxide) although it was demonstrated that sodium naphthalene-initiated polystyrene forms a copolymer with diphenylvinylphosphine oxide. In this reaction, at −70°C., addition of the phosphine oxide monomer to the red polystyrene solution brought about an immediate color change to yellow. The final product contained 7 mole-% of the phosphine oxide ($[\eta]_{\text{benzene}} = 0.33$ dl./g.).

The block copolymerization data is consistent with the concept that the poly(diphenylvinylphosphine oxide) anion will not initiate copolymerization with a less-polar monomer such as styrene, but will undergo copolymerization with more activated monomers such as acrylonitrile or methyl methacrylate. The anionic reactivity of the three comonomers is known to be in the order, acrylonitrile > methyl methacrylate > styrene, and the results described, indicate that diphenylvinylphosphine oxide falls between methyl methacrylate and styrene in this reactivity scale. This is consistent with the half-wave polarographic reduction potentials of the monomers (acrylonitrile = −2.10 e.v., methyl methacrylate = −2.22 e.v., diphenylvinylphosphine oxide = −2.40 e.v.. and styrene = −2.53 e.v.). but not with the dipole moments (acrylonitrile = 3.51 D.[10], methyl methacrylate = 1.77 ± 0.05 D., diphenylvinylphosphine oxide = 4.57 ± 0.07 D., and styrene = 0.37 D.[11]) (Here $\epsilon_{1/2}$ values are versus a saturated calomel electrode in dimethylformamide or acetonitrile (for styrene); dipole moments quoted are for benzene solutions.)

Dipole moment is a measure of ground-state polarity, while anionic reactivity is a transition-state phenomenon which responds to both the inductive and conjugative properties of the molecule. The half-wave reduction potential of a monomer represents the ease with which that monomer can accept an electron. It is, thus, a convenient measure of monomer reactivity which responds to the ground-state and transition state influences in a similar manner to the e values used by Graham et al.[13] For diphenylvinylphosphine oxide, the conjugative electron withdrawal by the phosphine oxide group cannot be transmitted readily through phosphorus,[14] and this molecule thus shows a lower anionic reactivity than acrylonitrile or methyl methacrylate in spite of the higher dipole moment.

EXPERIMENTAL

Monomers

Diphenylvinylphosphine oxide was prepared by the two methods described by Rabinowitz and Pellon.[2] Since ionic polymerizations of this

material were sensitive to trace impurities and water, a rigorous purification procedure was required. This was accomplished by several recrystallizations from *n*-heptane–acetone and *n*-heptane–toluene mixtures, followed by prolonged drying in a vacuum oven at 50–60°C., to yield a white, crystalline product, m.p. 117–117.5°C.

Methyl methacrylate (Rohm and Haas, uninhibited) was distilled at reduced pressure from calcium hydride and was stored at −10°C. under nitrogen in a flask sealed by a rubber serum-cap stopper. Transfers of this material and other liquid monomers were effected by hypodermic syringe.

Styrene (Dow H 99) was purified and dried by passage through a chromatography tube containing activated alumina and calcium hydride.

Acrylonitrile was dried over magnesium sulfate and was distilled through an 18 in. glass helix-packed column to give a fraction boiling at 77°C.

Solvents

Toluene (Baker and Adamson, Reagent Grade) was dried by distillation from sodium and from calcium hydride and was stored over calcium hydride at reduced pressure on a vacuum system. *Tetrahydrofuran* (Fisher Certified Reagent) was dried by distillation under argon from sodium and from lithium aluminum hydride. Sodium naphthalene was prepared in the solvent to complete the drying process and the green mixture was stored in a darkened flask attached to a vacuum system. *Pyridine* was refluxed for 2 hr. over potassium hydroxide pellets, before distillation into a flask containing barium oxide, and was stored at reduced pressure on a vacuum system.

Catalyst

Grignard Reagents. *n*-Butyl chloride, *n*-butyl bromide, *n*-butyl iodide, *tert*-butyl bromide, and bromobenzene (Eastman Organic Chemicals) were used to prepare Grignard reagents by dropwise addition of the organic halide to magnesium turnings in tetrahydrofuran (for polymerizations in that solvent), in diethyl ether, or in 50% diethyl ether in toluene. The Grignard reactions were carried out under an atmosphere of dry nitrogen or argon, with stirring by a glass-covered magnetic stirrer bar. After completion of the organic halide addition the mixtures were refluxed for 1 hr., and cooled to 25°C before use. Organomagnesium halide concentrations were estimated by the acid–base titration method of Gilman,[8] with the exception that the mixtures were not boiled with water before titration. *tert*-Butylmagnesium bromide presented a special case since, in the event of incomplete Grignard formation, residual *tert*-butyl bromide would be hydrolyzed rapidly during titration, thus causing partial neutralization of the titratable magnesium salts. (*n*-Alkylmagnesium bromides and iodides would be subject to the same error in hot aqueous mixtures.) Compensation for this effect with *tert*-butylmagnesium bromide was made by computing the actual Grignard concentration from the mean of the

theoretical and observed titration figures, assuming that, after hydrolysis, 1 mole of alkyl halide is equivalent to 1 mole of Grignard.

Ziegler-Natta-Type Catalysts. A solution of titanium tetrachloride (3.7×10^{-4} moles) in cyclohexane was introduced by syringe through a serum cap stopper into toluene (100 ml.) contained in an argon-filled, 250 ml. flask. To this mixture was added a heptane solution of tri-*n*-butylaluminum (2.5×10^{-3} moles) (obtained from Orgmet Chemicals). The black suspension was stirred at 25°C. for 30 min. before addition to the monomer solution.

A heptane solution of triisobutylaluminum (25 vol.-%) (Ethyl Corporation) was prepared under nitrogen atmosphere. A 20-ml. sample of this solution was added by syringe to a stirred suspension of titanium trichloride (5×10^{-3} moles) in heptane (200 ml.). The mixture was then heated to 75°C. for 15 min. before addition of the monomer.

A heptane solution of tri-*n*-butylaluminum (2.5×10^{-3} moles) was added by syringe to a solution of trichlorotris(tetrahydrofuran) chromium-(III) (8×10^{-4} moles) in toluene (100 ml.). The violet color changed to brown, and the mixture was stirred at 25°C. for 30 min. before removal of an aliquot by hypodermic syringe.

Other Catalysts. *n*-Butyllithium (1 *M* solution in pentane) was obtained from Orgmet Chemicals. The concentration of this catalyst was determined by acid–base titration to a phenolphthalein endpoint.

9-Fluorenyllithium was prepared from excess fluorene by treatment with *n*-butyllithium in tetrahydrofuran by a method similar to that described by Goode et al.[9] The catalyst concentration was computed from the amount of *n*-butyllithium employed.

Sodium naphthalene solutions were prepared by reaction of naphthalene with metallic sodium in dry tetrahydrofuran, in a flask attached to a vacuum system. The catalyst concentration was estimated from the naphthalene concentration.

Polymerization Techniques

Polymerization reactions were carried out in the absence of air and moisture by one of two techniques, designated methods A and B.

Method A was used for the majority of polymerizations, and involved solvent transfer and monomer polymerization within a glass vacuum system. In a typical example a weighed amount of diphenylvinylphosphine oxide (5 g.) was placed in a 250 ml., three-necked flask which was fitted with a glass-covered magnetic stirrer bar and a serum-cap stopper. The flask was then attached to the vacuum system and the monomer was dried at 50–60°C. under vacuum. Solvent (100 ml.) was then condensed into the flask to a calibration mark, and the mixture was stirred and warmed to room temperature (25–26°C.). A measured amount of catalyst solution was transferred by argon-filled hypodermic syringe, and was added to the stirred monomer solution through the serum-cap stopper. A colored suspension usually formed immediately after catalyst addition, and each

reaction mixture was then stirred at room temperature for the required time (usually 20 hr.).

Method B differed from the first method in that the monomer was dried within the reaction flask in a vacuum oven at 50–60°C. The flask was then swept by a stream of dry nitrogen or argon as it was fitted to a distillation assembly, and solvent was then distilled in. Polymerizations were then performed under an atmosphere of the inert gas.

Isolation of Polymers

At the conclusion of each reaction, air was admitted to the reaction vessel and the color was bleached. Insoluble polymer was removed by filtration, and inorganic salts were removed by treatment with aqueous acid. A separation of the products into fractions of different molecular weights was affected according to insolubility in tetrahydrofuran (MW > 4000), toluene (MW > 2000), and heptane (monomer and oligomers). In an example reaction, diphenylvinylphosphine oxide (5 g., 2.2×10^{-2} moles) was polymerized in toluene (100 ml.) by *n*-butylmagnesium iodide (1.50×10^{-3} moles) for 20 hr. at 25–26°C. The toluene-insoluble products were separated into THF-insoluble (3.3 g., m.p. 200–300°C.) and THF-soluble (0.9 g., m.p. 110–145°C.). The toluene-soluble material was precipitated by *n*-heptane and consisted of oligomers (0.3 g., m.p. 110–135°C.). The polymers were purified by washing with hydrochloric acid followed by precipitation from dimethylformamide into water and were subsequently dried in a vacuum oven.

Measurements

Solution viscosities were measured in Cannon viscometers at 30°C. using benzene, chloroform, ethanol, or dimethylformamide as solvents. In the latter two solvents the measurements were complicated by reduced specific viscosity increases with increasing dilution.

Molecular Weights. A number of different methods were used in attempts to estimate molecular weights. Products of molecular weight below 2500–3000 were soluble in chloroform, and number-average values were obtained by a vapor pressure thermistor technique using this solvent. Attempts to obtain molecular weights of oligomers by boiling point elevation in ethanol or acetic acid gave low values which indicated the existence of strong solvent–oligomer interactions. This was consistent with the ease of hydrate formation and the solution viscosity behavior. Molecular weights of oligomers were obtained by melting point depression of camphor, which corresponded satisfactorily with those obtained by lowering of vapor pressure. Oligomers, prepared using *tert*-butylmagnesium bromide as initiator showed a weak infrared absorption at 1250 cm.$^{-1}$ which appeared to result from *tert*-butyl endgroups. The absorption intensity of this peak for a representative oligomer (MW 2300 by vapor-pressure thermistore technique, $[\eta]^{30°C.}_{benzene} = 0.025$) was used to estimate the

molecular weight, and the results agreed well with the alternative data. Light-scattering measurements of a polymer in dimethylformamide at 25°C. indicated that material of reduced specific viscosity 0.1 (1% concentration) corresponded to a weight-average molecular weight of 9000.

Crystallinity. Polymer crystallinity was detected by means of x-ray diffraction patterns of powdered polymer, according to the relative sharpness of the diffraction rings. Polymers designated as amorphous gave diffuse diffraction patterns, while the crystalline modifications displayed a marked sharpening of the diffraction features which was indicative of an increase in crystal order.

The authors wish to thank Dr. Joseph Pellon for suggesting the topic and for his interest and helpful comments. We also thank Dr. L. A. Siegel for performing the x-ray crystallinity tests, Mr. W. Jura for the polarographic data, Dr. R. Best for dipole moment data, Mrs. R. R. Fiala for solution viscosity work, and Dr. R. Rabinowitz for advice concerning the monomer synthesis. The assistance of various members of the Research Service Deprtaments of these laboratories in obtaining molecular weight data is also gratefully acknowledged.

References

1. Berlin, K. D., and G. B. Butler, *J. Org. Chem.*, **26**, 2537 (1961).
2. Rabinowitz, R., and J. Pellon, *J. Org. Chem.*, **26**, 4623 (1961).
3. Rabinowitz, R., and J. Pellon, paper presented at 140th National Meeting, American Chemical Society, Chicago, Ill., September 1961.
4. Tsetlin, B. L., et al., *Vysokomol. Soedin.*, **3**, 1117 (1961).
5. Dessy, R. E., G. S. Handler, J. H. Wotiz, and C. A. Hollingsworth, *J. Am. Chem. Soc.*, **79**, 3476 (1957); R. E. Dessy, and G. S. Handler, *J. Am. Chem. Soc.*, **80**, 5824 (1958).
6. Hamelin, R., *Bull. Soc. Chim. France*, **1961**, 684.
7. Kabachnik, M. I., E. N. Tsveykov, and C. C. Yu, *Tetrahedron Letters, No. 1*, 5 (1962); P. T. Keough and M. Grayson, *J. Org. Chem.*, **27**, 1817 (1962).
8. Gilman, H., E. A. Zoellner, and J. B. Dickey, *J. Am. Chem. Soc.*, **51**, 1576 (1929).
9. Goode, W. E., F. H. Owens, R. P. Fellman, W. H. Snyder, and J. E. Moore, *J. Polymer Sci.*, **46**, 317 (1960).
10. Rogers, M. T., *J. Am. Chem. Soc.*, **69**, 2544 (1947).
11. Gorman, M., R. M. Davis, and P. M. Gross, *Physik. Z.*, **39**, 181 (1938).
12. Natta, G., G. Mazzanti, P. Longi, G. Dall'asta, and F. Bernardini, *J. Polymer Sci.*, **51**, 487 (1961).
13. Graham, R. K., J. R. Panchak, and M. J. Kampf, *J. Polymer Sci.*, **44**, 411 (1960).
14. Jaffé, H. H., and L. D. Freedman, *J. Am. Chem. Soc.*, **74**, 1069 (1952).

Résumé

On a examiné les réactifs de Grignard, les composés organolithiques, le naphtalène sodium ainsi que les catalyseurs alcoylaluminium–halogénure métallique comme initiateurs de polymérisation d'oxyde de diphénylvinylphosphine. Les catalyseurs les plus efficaces furent les réactifs de Grignard et le naphtalène-sodium. Avec le catalyseurs de Grignard, es poids moléculaires des polymères supérieur à 10.000 sont produits bien que la quantité, le poids moléculaire et la cristallinité des produits soient influencées par les composants organiques et halogènés du catalyseur et par le solvant de la réaction. Les études de copolymérisation indiquent que la réactivité anionique de l'oxyde de diphénylvinylphosphine est intermédiaire entre le styrène et le méthacrylate de méthyle. Pour la catalyse par réactif de Grignard un mécanisme de polymérisation du type

anionique est proposé et suppose à l'état de transition la formation d'un composé d'addition polymère–halogénure d'organo-magnésium.

Zusammenfassung

Grignard-Verbindungen, Organolithiumverbindungen, Natriumnaphthalin und Aluminiumalkyl–Metallhalogenid-Katalysatoren wurden auf ihre Brauchbarkeit als Starter für die Polymerisation von Diphenylvinylphosphinoxyd untersucht. Am wirksamsten erwiesen sich Grignard-Verbindungen und Natriumnaphthalin. Mit Grignard-Katalysatoren wurden Polymere mit einem Molekulargewicht bis zu 10.000 gebildet, wobei Ausbeute, Molekulargewicht und Kristallinität der Produkte von der organischen und der Halogen-Komponente des Katalysators sowie vom Lösungsmittel abhängig waren. Copolymerisationsversuche zeigten, dass die anionische Reaktivität von Diphenylphosphinoxyd zwischen der von Styrol und Methylmethacrylat liegt. Für die Grignard-Katalyse wird ein anionischer Polymerisationsmechanismus mit Bildung eines Polymer–Organomagnesium-halogenidaddukts im Übergangszustand angenommen.

Received November 13, 1962

JOURNAL OF POLYMER SCIENCE: PART A VOL. 1, PP. 3643–3654 (1963)

Anionic Polymerization of Acrylonitrile by Various Catalysts

ARIEL OTTOLENGHI, SAMUEL BARZAKAY,*
and ALBERT ZILKHA, *Department of Organic Chemistry, The Hebrew University, Jerusalem, Israel*

Synopsis

The polymerization of acrylonitrile was studied using cyclopentadienyllithium, cyclopentadienyl sodium, fluorenylithium, and phenyllithium, and was compared to polymerization with butyllithium. With phenyllithium and fluorenyllithium in tetrahydrofuran, termination was found to be by chain transfer to monomer. The homogeneous polymerization in dimethylformamide carried out at both high and low catalyst concentrations showed that at high catalyst concentrations the molecular weights of polymer increased sharply with monomer concentration using cyclopentadienyllithium and cyclopentadienyl sodium, unlike the case of polymer obtained with butyllithium and fluorenyllithium. The increase in molecular weight is due to what has been previously found that the cyclopentadienyl anion acts as a polyfunctional catalyst leading to initiation of polymerization at various places on the ring. The basic strength of the catalyst investigated, as determined from the ability to polymerize monomers of decreasing acidity, was as follows: butyl $\simeq$ phenyl > fluorenyl > cyclopentadienyl.

INTRODUCTION

In continuation of previous works on the anionic polymerization of acrylonitrile by cyclopentadienylsodium,[1] and by butyllithium[2] at low catalyst concentrations, we have studied its polymerization in different solvents by other catalysts such as: phenyllithium, fluorenyllithium, cyclopentadienyllithium, and cyclopentadienyl sodium.

The results are compared to these obtained with the classical anionic catalyst butyllithium on a wide range of catalyst concentrations.

The order of the basic strength in this series of catalysts was obtained by comparing their reactivity in the polymerization of acrylonitrile, methyl methacrylate and styrene.

EXPERIMENTAL CONDITIONS

The purification of materials and the polymerization procedure was described previously.[1] The preparation of phenyllithium,[3] cyclopentadienylsodium,[1] and butyllithium[2] has been described.

*Present address: Polymer Department, The Weizmann Institute of Science, Rehovoth, Israel.

Cyclopentadienyllithium

The general procedure for the preparation of cyclopentadienylsodium[1] in tetrahydrofuran was followed. Excess lithium in the form of wire was used (2.3 g. lithium for 5 ml. cyclopentadiene). The reaction was carried out for 4 hr. at 0°C. The catalyst solution was centrifuged and kept in the cold under nitrogen. The yield as determined by titration was 90%.

Fluorenyllithium

The general procedure for the preparation of cyclopentadienyllithium in tetrahydrofuran was followed. The fluorene used (m.p. 116–117°C.), was recrystallized twice from methanol and twice from hexane and kept in a vacuum desiccator. The yield of fluorenyllithium was 90%.

Molecular Weight Determinations

Polymer samples were further purified and dried for molecular weight determinations. Viscosities of polymer solutions in dimethylformamide were measured in an Ostwald viscometer. Average molecular weights of the polymers were calculated from intrinsic viscosities using the equation of Cleland and Stockmayer[4]

$$[\eta] = 2.33 \times 10^{-4} M_w^{0.75}$$

RESULTS

The heterogeneous polymerization of acrylonitrile in tetrahydrofuran was studied using fluorenyllithium and phenyllithium as catalysts, and the homogeneous polymerization in dimethylformamide was investigated using fluorenyllithium, cyclopentadienyllithium, and cyclopentadienyl sodium.

Effect of Monomer Concentration

The dependence of molecular weight on monomer concentration in tetrahydrofuran was studied using fluorenyllithium (Table I) and phenyllithium

TABLE I
Polymerization by Fluorenyllithium
Dependence of Molecular Weight on Monomer Concentration[a]

Run No.	[Monomer], mole/l.	Yield, %	$[\eta]$, dl/g.	$\bar{M}_w$
715	0.45	35	0.113	3800
723	0.45	40	0.085	2600
703	0.90	35	0.098	3150
712	0.90	40	0.101	3300
720	0.90	35	0.089	2750
716	1.80	35	0.122	4200
725	1.80	40	0.115	3900

[a] Experimental conditions: catalyst 1.2 mmole (24 mmole/l.) dissolved in tetrahydrofuran, was added in one portion to a solution of acrylonitrile in tetrahydrofuran. The total volume of the polymerization mixture was kept constant (50 ml.) polymerization temp. 0 ± 2°C., time 15 min.

(Table II). The molecular weights obtained were independent of monomer concentration in the range investigated. The effect of monomer concentration was also studied in dimethylformamide as solvent using cyclopenta-

TABLE II
Polymerization by Phenyllithium
Dependence of Molecular Weight on Monomer Concentration[a]

Run No.	[Monomer], mole/l.	Yield, %	$[\eta]$, dl/g.	$\bar{M}_w$
419	0.45	75	0.095	3000
420	0.45	65	0.087	2700
401	0.90	65	0.095	3000
402	0.90	60	0.106	3500
417	0.90	70	0.113	3800
418	0.90	70	0.101	3300
421	1.80	55	0.111	3700
422	1.80	60	0.115	3900

[a] Experimental conditions: catalyst 4.2 mmole (84 mmole/l.) dissolved in 3 ml. ether, was added in one portion to a solution of acrylonitrile in tetrahydrofuran. The total volume of the polymerization mixture was kept constant (50 ml.), polymerization temp. 0 ± 2°C., time 15 min.

TABLE III
Polymerization by Various Catalysts at High Catalyst Concentrations
Dependence of Molecular Weight on Monomer Concentration[a]

Run No.	Type of catalyst	[Monomer], mole/l.	Yield, %	$[\eta]$, dl/g.	$\bar{M}_w$
524	Cyclopentadienylsodium[b]	0.45	90	0.077	2300
505		0.45	95	0.080	2400
506		1.80	95	0.180	7100[d]
507		1.80	100	0.190	7600[d]
508	Cyclopentadienyllithium[b]	0.45	100	0.097	3100
509		0.45	90	0.092	2900
510		1.80	90	0.210	8700[d]
511		1.80	95	0.221	9300[d]
756	Fluorenyllithium[b]	0.45	85	0.090	2800
757		0.45	85	0.085	2600
758		1.80	90	0.095	3000
759		1.80	85	0.100	3250
624	Butyllithium[c]	0.45	95	0.085	2600
625		0.45	100	0.078	2350
626		1.80	100	0.106	3500
627		1.80	100	0.099	3200

[a] Experimental conditions: catalyst solution 3.4 mmole (68 mmole/l.) was added in one portion to a solution of acrylonitrile in dimethylformamide. The total volume of the monomer, the catalyst solvent (held always constant 2 ml.) and the solvent were kept constant, (50 ml.). Polymerization temp. 0 ± 2°C., time 15 min.

[b] Catalyst solvent was tetrahydrofuran.

[c] Catalyst solvent was petroleum ether.

[d] These molecular weights are only a rough approximation as the polymers are branched.

dienyllithium, cyclopentadienyl sodium, and fluorenyllithium as catalysts. This was investigated at two catalyst concentrations: high (68 mmole/l.) and low (1–1.5 mmole/l.) Table III and Table IV, respectively. The results are compared with those obtained with butyllithium (Table III and Table IV) in the same range of catalyst concentrations. It was found

TABLE IV
Polymerization by Various Catalysts at Low Catalyst Concentrations
Dependence of Molecular Weight on Monomer Concentration[a]

Run No.	Type of catalyst	[Monomer], mole/l.	Yield, %	$[\eta]$, dl/g.	$\bar{M}_w$
550	Cyclopentadienylsodium[b,d]	0.45	50	0.195	7,900
551	(1.0 mmole/l.)	0.45	60	0.204	8,400
588		1.80	50	0.318	15,100
589		1.80	55	0.311	14,700
590	Cyclopentadienyllithium[b,d]	0.45	65	0.195	7,900
591	(1.2 mmole/l.)	0.45	75	0.167	6,400
592		0.90	60	0.245	10,700
593		0.90	70	0.275	12,500
594		0.90	65	0.280	12,800
595		1.35	60	0.390	19,900
596		1.35	65	0.396	20,300
597		1.80	75	0.495	27,300
598		1.80	75	0.496	27,400
599		1.80	75	0.497	27,500
752	Fluorenyllithium[b]	0.45	30	0.111	3,700
753	(1.5 mmole/l.)	0.45	35	0.104	3,400
748		0.90	30	0.189	7,600
765		0.90	30	0.188	7,500
750		1.80	35	0.275	12,500
751		1.80	30	0.255	11,300
610	Butyllithium[c]	0.45	45	0.198	8,000
611	(1.12 mmole/l.)	0.45	40	0.198	8,000
606		0.90	60	0.392	20,000
607		1.80	40	0.642	38,600

[a] Experimental conditions: Catalyst solution was added in one portion to a solution of acrylonitrile in dimethylformamide. The total volume of the monomer, catalyst solvent (held always constant 2 ml.) and the solvent were kept constant (50 ml.). Polymerization temp. 0 ± 2°C., time 15 min.

[b] Catalyst solvent was tetrahydrofuran.

[c] Catalyst solvent was petroleum ether.

[d] The molecular weights of the polymers obtained by these catalysts are only a rough approximation as the polymers are branched.

(Table III) that contrary to butyllithium and fluorenyllithium, the molecular weights increased sharply with monomer concentration at the high catalyst concentrations on using cyclopentadienyllithium or cyclopentadienyl sodium. At low catalyst concentration (Table IV) the molecular weights increased with monomer concentration.

Effect of Catalyst Concentration

The molecular weights were found to be independent of catalyst concentration in tetrahydrofuran using fluorenyllithium (Table V) and phenyllithium (Table VI). In dimethylformamide using cyclopentadienyllithium

TABLE V
Polymerization by Fluorenyllithium
Dependence of Molecular Weight on Catalyst Concentration[a]

Run No.	Catalyst, mmole	[Catalyst], mole/l.	Yield, %	$[\eta]$, dl/g.	$\bar{M}_w$
711	0.6	12.0	30	0.100	3250
719	0.6	12.0	55	0.089	2750
704	1.2	24.0	35	0.098	3150
712	1.2	24.0	40	0.101	3300
720	1.2	24.0	35	0.089	2750
708	1.4	28.0	40	0.101	3300
701	2.2	44.0	60	0.096	3050
702	2.2	44.0	50	0.106	3500
721	3.0	60.0	60	0.089	2750
724	3.0	60.0	75	0.100	3250
745	3.0	60.0	85	0.087	2700[b]

[a] Experimental conditions: catalyst dissolved in tetrahydrofuran was added in one portion to a solution of acrylonitrile (0.90 mole/l.) in tetrahydrofuran. The total volume of the polymerization mixture was kept constant (50 ml.). Polymerization temp. 0 ± 2°C., time 15 min.

[b] The monomer was dropped into the polymerization mixture during 5 min.

TABLE VI
Polymerization by Phenyllithium
Dependence of Molecular Weight on Catalyst Concentration[a]

Run No.	Catalyst, mmole	[Catalyst], mole/l.	Yield, %	$[\eta]$ dl/g.	$\bar{M}_w$
435	1.8	36.0	55	0.111	3700
436	1.8	36.0	50	0.122	4200
401	4.2	84.0	65	0.095	3000
402	4.2	84.0	60	0.106	3500
417	4.2	84.0	70	0.101	3300
418	4.2	84.0	70	0.113	3800

[a] Experimental conditions: catalyst dissolved in diethyl ether (held always constant 3 ml.) was added in one portion to a solution of acrylonitrile (0.90 mole/l.) in tetrahydrofuran. The total volume of the polymerization mixture was kept constant (50 ml.). Polymerization temp. 0 ± 2°C., time 15 min.

(Table VII) in the catalyst range (1–10 mmole/l.) there was a small increase in molecular weight with decreasing catalyst concentration, the change being much smaller than that found with butyllithium.

TABLE VII

Polymerization by Cyclopentadienyllithium and Butyllithium
Dependence of Molecular Weight on Catalyst Concentration[a]

Run No.		Catalyst, mmole	[Catalyst], mole/l.	Yield %	[η], dl/g.	$\bar{M}_w$
574	Cyclopentadienyl-	0.060	1.2	75	0.245	10,700
575	lithium[b,d]	0.060	1.2	80	0.275	12,500
576		0.060	1.2	80	0.280	12,800
577		0.125	2.5	85	0.232	9,900
578		0.125	2.5	80	0.214	8,900
579		0.250	5.0	90	0.194	7,800
522		0.500	10.0	90	0.180	7,100
523		0.500	10.0	90	0.201	8,200
606	Butyllithium[c]	0.056	1.12	60	0.392	20,000
638		0.125	2.50	90	0.320	15,200
604		0.225	4.50	85	0.236	10,200
619		0.450	9.00	90	0.190	7,600

[a] Experimental conditions: catalyst solution was added in one portion to a solution of acrylonitrile (0.90 mole/l.) in dimethylformamide. The total volume of the monomer, the catalyst solvent (held always constant 2 ml.) and the solvent were kept constant (50 ml.). Polymerization temp. 0 ± 2°C., time 15 min.

[b] Catalyst dissolved in tetrahydrofuran.

[c] Catalyst dissolved in petroleum ether.

[d] The molecular weights of the polymers obtained by this catalyst are only a rough approximation as the polymers are branched.

Effect of Temperature

The effect of temperature was studied in tetrahydrofuran using fluorenyllithium in a temperature range (−50 to 20°C.) (Table VIII). Both the molecular weight and yield increased with lowering of temperature. A

TABLE VIII

Polymerization by Fluorenyllithium
Dependence of Yield and Molecular Weight on Temperature[a]

Run No.	Temperature, °C.	Yield, %	[η], dl/g.	$\bar{M}_w$
734	−50	65	0.269	12,200
743	−20	50	0.149	5,500
703	0	35	0.098	3,150
712	0	40	0.101	3,300
720	0	35	0.089	2,750
740	20	25	0.075	2,200
733	20	20	0.077	2,300
737	20	20	0.071	2,050

[a] Experimental conditions: catalyst 1.2 mmole (24 mmole/l.) dissolved in tetrahydrofuran was added in one portion to a solution of acrylonitrile 0.90 mole/l. in tetrahydrofuran. The total volume of the polymerization mixture was kept constant (50 ml.). Polymerization time 30 min.

semilogarithmic plot of molecular weight against the reciprocal of the polymerization temperature gave a straight line whose slope corresponds to a difference in activation energy between propagation and termination of 3.2 kcal./mole as calculated from the equation, $d \ln M/dT = \Delta E/RT^2$.

DISCUSSION

In the previous work[1] on the polymerization of acrylonitrile by cyclopentadienylsodium, it was found that the cyclopentadienyl anion acted as a polyfunctional catalyst capable of initiating polymerization at all places on the ring. This was due to the aromatic character of the cyclopentadienyl anion which has five equivalent resonance structures with a resonance energy even higher than benzene (42 kcal./mole)[5] and to the high acidity of the methylene hydrogen of cyclopentadiene ($pK_a = 16$),[6] comparable to that of methanol ($pK_a = 16.7$).[7] This behavior is similar to that known about the cyanoethylation reaction of cyclopentadiene when hexa-(β-cyanoethyl)-cyclopentadiene is formed even when the ratio of acrylonitrile to the cyclopentadiene used is only 2:1.[8]

The investigation of the acrylonitrile polymerization by butyllithium[2] on a wide range of catalyst concentrations, showed that at high catalyst concentrations termination was by chain transfer to monomer, and at low catalyst concentrations termination was monomolecular.

In the present work, the polymerization with the cyclopentadienyl anion was further investigated on a wide range of catalyst concentrations, and the dependence of molecular weight on monomer concentration was investigated at both high and low catalyst concentrations, and compared with the classical butyllithium catalyst. Investigations were carried out with fluorenyllithium which is similar to the cyclopentadienyl catalyst, to see if it behaves similarly as a polyfunctional catalyst, since it is known that acrylonitrile gives with fluorene *bis*-(9,9)-β-cyanoethyl fluorene.[8]

With cyclopentadienyllithium or sodium the molecular weights increased with increase in monomer concentration at both high (68 mmole/l.) (Table III) and low catalyst concentrations (1.12 mmole/l.) (Table IV). As compared to butyllithium (Table III and Table IV), it is seen that the molecular weights of the polymers obtained at high catalyst concentration were constant and independent of monomer concentration, while at the low butyllithium concentrations (1.12 mmole/l.) the molecular weights increased with increasing monomer concentration as was reported before .[2]

In principle the mechanism of the polymerization of acrylonitrile by both the cyclopentadienyl anion and butyllithium might be similar, and termination should be by transfer to monomer at the high catalyst concentration. The increase in molecular weight at high catalyst concentrations found with the cyclopentadienyl anion as compared to that obtained with butyllithium, should be therefore due to the special reactivity of the cyclopentadienyl anion, and as was found before, the increase in molecular weight is due to the fact that the cyclopentadienyl anion acts as a polyfunctional catalyst.

It was suggested[1] that there exists an equilibrium between a terminal cyclopentadiene group attached to a polymer chain and unreacted cyclopentadienyl sodium as follows:

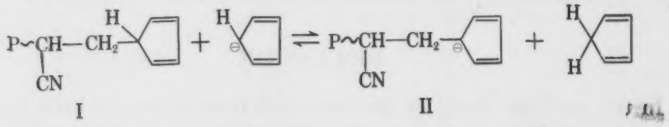

I II

This equilibrium is in favor of the formation of the cyclopentadienyl anion of the polymer (II), as the cyano group which is β to the hydrogen of the cyclopentadiene in I is a strong electron withdrawing group.

The fact that only with cyclopentadienyllithium or cyclopentadienyl sodium, the molecular weight increased strongly (about 300%) with monomer concentration at high catalyst concentration, supports this hypothesis, in that at high catalyst concentrations, this equilibrium should be in favor of the formation of II.

It is also possible that the hydrogen at position 1 in a terminal cyclopentadiene group on a polymer (due to its high acidity) acts as a terminator of the polymerization (chain transfer to polymer) as follows:

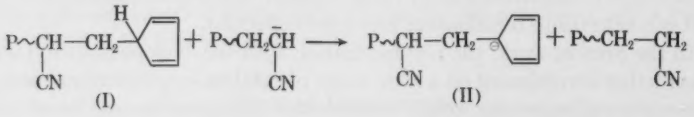

(I) (II)

Therefore the increase in molecular weight at the high catalyst concentrations is due to branching at the cyclopentadienyl end groups.

The results of the ozonolysis of the polymers (Table IX) show clearly that only the polymers obtained with cyclopentadienyl catalysts were degraded and not those with butyllithium. This is compatible with the results found earlier,[1] that the branched polymers are degraded by scission of the cyclopentadiene ring which is the center of branching.

With fluorenyllithium in tetrahydrofuran it is seen from Tables I and V that the molecular weights are independent of catalyst and monomer concentrations at the catalyst concentrations (12–60 mmole/l.) investigated, as consistent with chain transfer termination.

At lower catalyst concentration (1.5 mmole/l. in dimethylformamide the molecular weight increased with monomer concentration, but at high catalyst concentration (Table IV) the molecular weights remained constant and were of the same order as those obtained with butyllithium.

These results show clearly that the fluorenyl anion behaves similarly to the butyllithium but not to the cyclopentadienyl anion; i.e., with fluorenyl anion no branching occurs. The acidity of the methylene hydrogen of the fluorene endgroup is much smaller than that of cyclopentadiene ($pK_a = 25$ as compared to $pK_a = 16$),[6] and also smaller than that of acrylonitrile

TABLE IX
Degradation of Branched Polymers by Ozone[a]

Run no.	Catalyst	Before ozonolysis		After ozonolysis			Branching[c]	Decrease in molecular weight, %
		$[\eta]$, dl/g.	$\bar{M}_w$	$[\eta]$, dl/g.	$\bar{M}_w$	N, %[b]		
507[d]	Cyclopentadienylsodium	0.190	7,600	0.135	4,800	25.1	+	37
588[e]		0.318	15,100	0.248	10,900	24.8	+	28
511[d]	Cyclopentadienyllithium	0.221	9,300	0.160	6,100	24.5	+	33
598[e]		0.496	27,400	0.399	20,500	25.5	+	25
614	Butyllithium[f]	0.204	8,400	0.208	8,600	24.6	−	—
636		0.366	18,250	0.365	18,200	25.0	−	—

[a] Ozonolysis was carried out as previously described.[1]

[b] Analysis of the polymers before degradation gave nitrogen content in the range of 24.5–25.5%.

[c] (+) indicates branched polymers; (−) indicates unbranched polymers.

[d] (Table III).

[e] (Table IV).

[f] Polymerization conditions as in Table III; acrylonitrile concentration 1.80 mmole/l., butyllithium concentration: Run 614, 18 mmole/l.; Run 636, 4.5 mmole/l. Polymerization temp. 0°C.

($pK_a \sim 20$). This explains why termination by chain transfer to monomer would be preferred to that of chain transfer to polymer suggested for the case of cyclopentadiene mentioned above. Also, steric effects at position 9 of the fluorenyl endgroup (the only place where branching can occur) may hinder the possibility of branching.

The increase in molecular weight on increasing the monomer concentration with fluorenyllithium in dimethylformamide at very low catalyst concentrations is therefore due to the same cause as that earlier found with the butyllithium, i.e., monomolecular termination, where the molecular weight increased with monomer concentration according to $DP = K[M]$. On the other hand, with the cyclopentadienyl anion this increase in molecular weight at low catalyst concentrations can be due both to branching as was found earlier[1] and to monomolecular termination as found with the classical anionic catalyst butyllithium.[2]

Polymerization with Phenyllithium

From Tables II and IV it is seen that the molecular weights obtained are constant and independent of monomer and catalyst concentration, as is consistent with termination by chain transfer to monomer. It may be mentioned that the molecular weights obtained were of the same order as those obtained with fluorenyllithium.

Activity of the Catalyst

The catalysts butyl-, phenyl-, fluorenyl-, and cyclopentadienyl-lithium are derived from the following hydrocarbons arranged in order of increasing acidity:[9] butane > benzene > fluorene > cyclopentadiene.

The basic strength of the anions derived from these hydrocarbons would, of course, be in the opposite order, so that the cyclopentadienyl anion will be the weakest catalyst.

TABLE X
Catalyst Relative Activity[a]

Catalyst	Monomer		
	Acrylonitrile	Methyl methacrylate	Styrene
Butyllithium	+	+	+
Phenyllithium	+	−[b]	+
Fluorenyllithium	+	+	−[c]
Cyclopentadienyllithium	+	+[d]	−
Cyclopentadienylsodium	+	+[d]	−

[a] Plus (+) indicates polymerization, (−) indicates no polymerization.

[b] Schreiber[10] found that phenyl lithium does not polymerize methyl methacrylate as it reacts with its ester group.

[c] As found by Graham and Goode.[11]

[d] The monomer polymerized only under drastic conditions (in bulk and at temperature of about 40–50°C.).

As known the reactivity in anionic polymerization of the following vinyl monomers is in the order: acrylonitrile > methyl methacrylate > styrene.

Styrene needs a stronger base than acrylonitrile to be polymerized. From the investigation of the possibilities of the polymerization of these monomers by the above catalysts (Table X) it is seen that styrene was polymerized by butyllithium and phenyllithium but not by fluorenyllithium or cyclopentadienyl lithium; while methyl methacrylate was polymerized with difficulty by the cyclopentadienyl anion, showing that the order of reactivity of the catalysts decreases in the order: butyl $\simeq$ phenyl > fluorenyl > cyclopentadienyl as expected.

The phenyl anion, which has two more electrons (of the carbanion) than those required by the aromatic sextet, does not have the stability of an aromatic anion possessed by the fluorenyl or cyclopentadienyl anions, and is therefore more reactive and a stronger catalyst than these two.

References

1. Zilkha, A., and A. Ottolenghi, *J. Polymer Sci.*, **56**, 539 (1962).
2. Ottolenghi, A., and A. Zilkha, *J. Polymer Sci.*, **A1**, 687 (1963).
3. Zilkha, A., S. Barzakay, and A. Ottolenghi, *J. Polymer Sci.*, **A1**, 1813 (1963).
4. Cleland, R. L., and W. H. Stockmayer, *J. Polymer Sci.*, **17**, 473 (1955).
5. Todd, A., *Perspectives in Organic Chemistry*, Interscience, New York, 1956, p. 49.
6. Streitwieser, A., *Molecular Orbital Theory for Organic Chemists*, Wiley, New York, 1961, p. 414.
7. Ingold, C. K., *Structure and Mechanism in Organic Chemistry*, Bell, London, 1954 p. 726.
8. Bruson, H. A., *J. Am. Chem. Soc.*, **64**, 2457 (1942).
9. Coates, G. E., *Organo-Metallic Compounds*, Wiley, New York, 1960, p. 26.
10. Schreiber, H., *Makromol. Chem.*, **36**, 86 (1959).
11. Graham, R. K., D. L. Dunkelberger, and W. E. Goode, *J. Am. Chem. Soc.*, **82**, 400 (1960).

Résumé

On a étudié la polymérisation du nitrile acrylique en employant la cyclopentadiényl lithium et sodium, le fluorényl- et le phényllithium, et on a comparé l'effet de ces catalyseurs avec celui du butyllithium. Avec le phényl- et le fluorényllithium on constatait dans le tétrahydrofuranne une terminaison par transfert de chaîne sur le monomère. On a effectué la polymérisation homogène dans le diméthylformamide, à la fois des concentrations basses et élevées de catalyseur, et on a démontré que, en employnat des concentrations élevées de cyclopentadiényllithium et -sodium, les poids moléculaires augmentaient brusquement avec la concentration de monomère; contrairement à ceux qu'on obtenait avec le butyl- et le fluerényllithium. L'augmentation du poids moléculaire est due à ce qu'on avait trouvé précédemment, à savoir que l'anion cyclopentadiényle agit comme un catalyseur polyfonctionnel qui initie la polymérisation à plusieurs places du noyau. La basicité des catalyseurs examinés, déterminée sur la base de leur aptitude à polymériser des monomères d'acidité diminuante, était dans l'ordre: butyl $\simeq$ phényl > fluorényl > cyclopentadiényl.

Zusammenfassung

Die Polymerisation von Acrylnitril mit Cyclopentadienyllithium und -natrium sowie mit Fluorenyl- und Phenyllithium wurde untersucht und mit der butyllithium-angereg-

ten Polymerisation verglichen. Mit Phenyl- und Fluorenyllithium in Tetrahydrofuran wurden die Ketten durch Übertragung zum Monomeren abgebrochen. Die in Dimethylformamid bei hoher und niederer Katalysatorkonzentration durchgeführte homogene Polymerisation zeigte, dass bei Verwendung von Cyclopentadienyllithium und -natrium das Molekulargewicht bei hoher Katalysatorkonzentration mit der Monomerkonzentration scharf zunimmt; das steht in Gegensatz zu den Ergebnissen mit Butyl- und Fluorenyllithium. Die Molekular-gewichtszunahme ist durch die früher gefundene Tatsache bedingt, dass das Cyclopentadienylanion als polyfunktioneller Katalysator wirt und zum Polymerisationsstart an verschiedenen Stellen am Ring führt. Die aus der Fähigkeit zur Polymerisation von Monomeren mit abnehmender Acidität abgeleitete Reihenfolge der Basenstärke der untersuchten Katalysatoren war: Butyl $\simeq$ Phenyl > Fluorenyl > Cyclopentadienyl.

Received July 31, 1962
Revised October 2, 1962

JOURNAL OF POLYMER SCIENCE: PART A VOL. 1, PP. 3655–3664 (1963)

Oxine–Formaldehyde Polymers and Their Metallic Chelates

ROBERT H. HORROCKS and EUGENE C. WINSLOW, *University of Rhode Island, Kingston, Rhode Island*

Synopsis

Sulfuric acid, sodium hydroxide, formic acid, and oxalic acid were investigated as catalysts for the condensation of oxine with formaldehyde. All were found to promote the condensation in aqueous solution under conditions of reflux, although a variation in the time required was found. The condensation was effected without catalyst between 200–240°C. in a sealed container by intimately mixing oxine with paraformaldehyde. Oxine–formaldehyde condensation polymers are soluble in phenol and acids stronger than acetic acid. Chelation is obtained by dissolving the polymer in acid, adding a solution containing the ion to be chelated, and adjusting the pH of the mixture to a value sufficiently high so as to favor chelation but not so high as to precipitate the metallic hydroxide. Heat stability was determined by thermogravimetry and differential thermal analysis. All samples degraded (began to lose weight) at 270°C. or below. The mode of decomposition of the polymer chelates appears to be independent of the metallic ion, but the free polymer is different. Its initial weight loss (between 270 and 320°C.) is very gradual compared to the chelates. At 320°C. it reverts to a form similar to that of the chelate. A second difference of the free polymer is that the rate of decomposition is a function of temperature, while that of the polymer chelates is not. The chelates may therefore hold interest in use as ablative materials. A third difference is that the free polymer melts beginning at about 190°C. The chelates do not melt.

INTRODUCTION

Much research is being directed toward the preparation of polymeric chains which are propagated by the formation of metallic chelates. Some success has been achieved in formation of polymers through chelation but the physical properties of the resulting polymers leave something to be desired. This report discusses research which was aimed at producing conventional polymer chains of the phenol–formaldehyde type but which also had the capacity for formation of metallic ion chelated crosslinks. It is hoped that the polymer chain may give the desirable physical properties of conventional polymers and that the subsequently formed chelated crosslinks might impart additional desirable properties such as thermal stability. This report deals with the formation of oxine–formaldehyde (8-hydroxyquinoline–formaldehyde) polymers and their metallic chelates. Thermal stabilities as measured by thermogravimetry and differential thermal analysis are reported also.

DISCUSSION

Electrophilic substitution would be expected to take place on the 5 and 7 positions of oxine (8-hydroxyquinoline) which correspond to the *para* and *ortho* positions of phenol. Other reactions of oxine, such as halogenation, acetylation, and nitration, take place preferentially at the 5 and 7 positions. The fused ring of oxine reduces the possibility of crosslinking such as that experienced in phenol–formaldehyde condensation polymers. The oxine–formaldehyde polymers are linear, therefore, and are thermoplastic as compared with thermosetting phenol–formaldehyde polymers. If chelation with metallic ions were to occur between the oxine–formaldehyde chains, a thermosetting polymer would be produced by the chelated crosslinks.

An oxine–formaldehyde condensation polymer was easily formed using sulfuric acid as the catalyst. The polymer so produced was soluble in acids stronger than acetic and in phenol. It was not soluble in concentrated sodium hydroxide solution. It had a degree of polymerization $\bar{P}$ of 2.2.

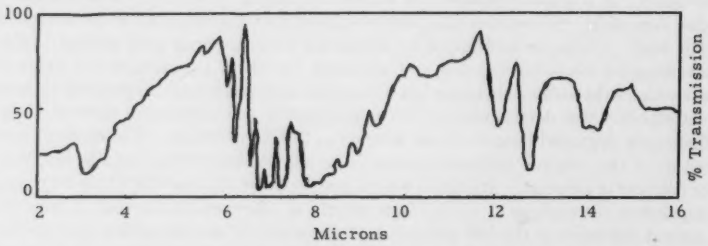

Fig. 1. IR spectra of oxine-formaldehyde condensation polymer.

Prolonged sulfuric acid catalyzed condensation over a period of several days produced a higher molecular weight material ($\bar{P}$ = 6.1). The polymer was washed in hot water.

Condensation of oxine with formaldehyde using sodium hydroxide as a catalyst gave a vigorous reaction at the melting point of oxine. Purification of the polymer was difficult because of chelation of the sodium ions. Because the polymer is not soluble in sodium hydroxide solution, precipitation occurs during polymer formation thus severely limiting the degree of polymerization.

Formic acid and oxalic acid catalysis was used because these catalysts can be removed after polymerization by virtue of their ability to pyrolyze to form volatile decomposition products. Oxalic acid is preferable because formic acid volatilizes as such during the polymerization. Because oxalic acid is somewhat weak, its catalytic activity requires a reaction time of as much as 100 hr. in order to produce polymers with $\bar{P}$ = 5.2.

An intimate mixture of oxine and paraform in the absence of catalyst yielded a polymer with $\bar{P}$ = 6.5. The reaction was carried out at 200–

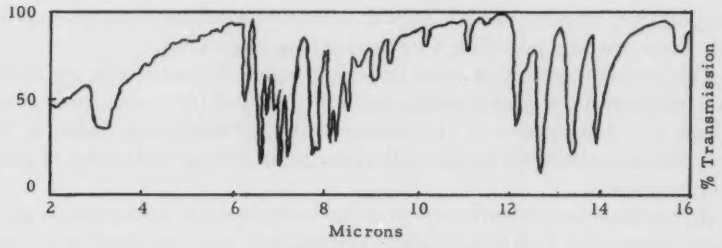

Fig. 2. IR spectra of oxine.

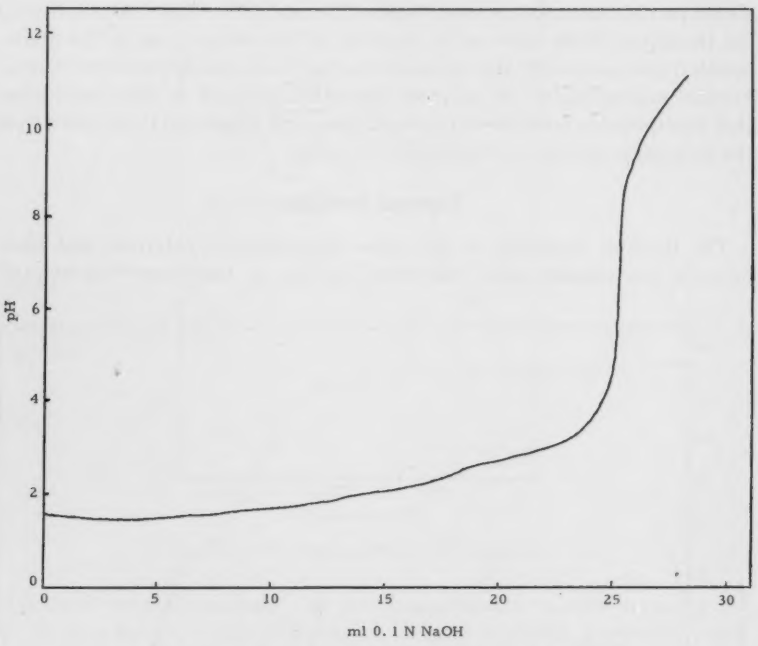

Fig. 3. Potentiometric titration of free polymer in 0.1*N* HCl.

240°C. in a sealed hydrogenation bomb. This polymer was the one used for heat stability studies.

Molecular weight measurements were made by bromination with bromate and bromide ions, allowing the excess bromine to convert iodide to iodine and titration with thiosulfate to a starch iodide end point. This method has been used with oxine for the quantitative determination of magnesium by forming the oxinate which is determined by bromination.[1] In this method bromine adds to the five and seven positions in the ring only. Since these are the positions blocked by the methylene groups in

the polymer, bromine can add only to the two end positions in a given polymer chain, thereby providing a method of counting chains.

The infrared spectra of both oxine and oxine–formaldehyde condensation polymer (oxalic acid-catalyzed) are included for comparison (Figs. 1 and 2). Absorptions in the carbon–hydrogen stretching region of the polymer are attributed to the methylene group and are indicative of polymer formation.

A potentiometric titration of an oxine–formaldehyde condensation polymer is plotted in Figure 3. Dilute hydrochloric acid was used as the solvent; therefore, an equivalence point occurred which corresponds to that of hydrochloric acid and sodium hydroxide at a pH of seven. Another equivalence point is apparent between a pH of 2.2 and 2.7. This is attributed to the transition of the polymer in the form of the cation going to the undissociated form similar to the behavior of oxine itself and substituted oxines.[2] Further substantiation of polymer formation is found in the observation that precipitation is seen to occur in the same pH range and it is known that the polymer is soluble in acid but not in water.

Thermal Stability

The thermal stabilities of the oxine–formaldehyde polymers and their metallic ion chelates were examined by use of thermogravimetry and

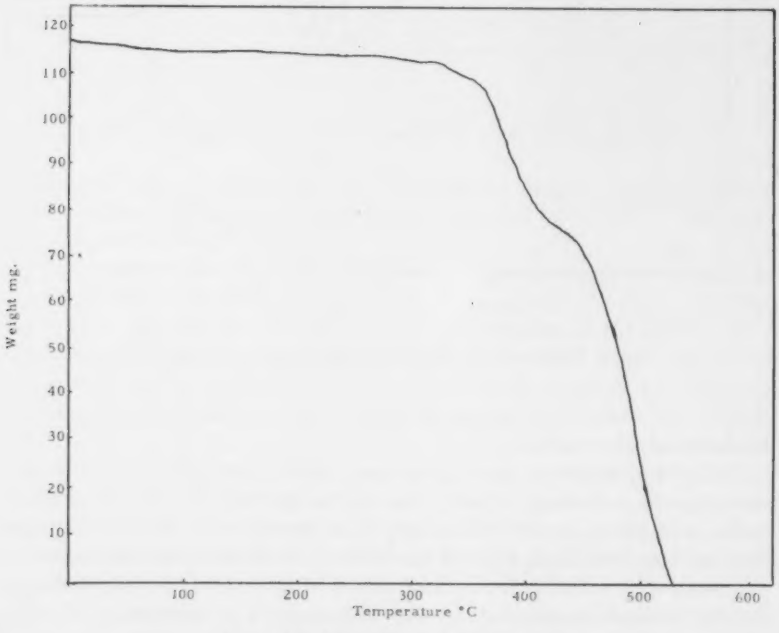

Fig. 4. TGA thermogram of free polymer.

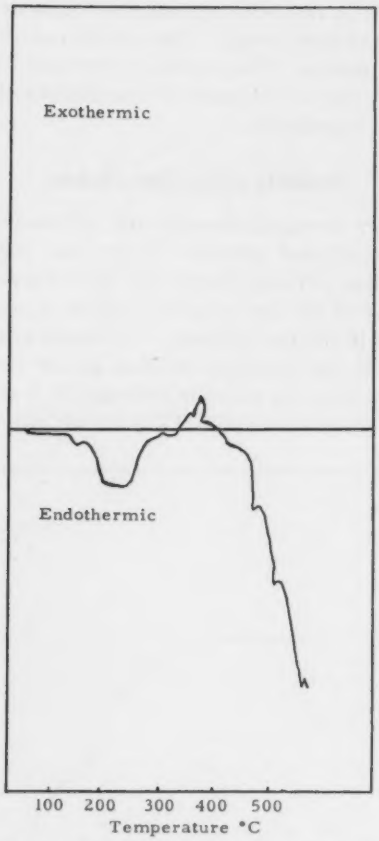

Fig. 5. DTA thermogram of free polymer.

differential thermal analysis. All thermogravimetric curves were run in an air atmosphere. The differential thermal analysis processes were carried out without using any effluent gas.

In the case of the unchelated oxine–formaldehyde polymer there is an excellent correlation between the TGA and the DTA curves. A very slight decrease in weight appears on the TGA curve (Fig. 4). This can be attributed to loosely held volatiles such as water. A very broad endotherm appears in this range on the DTA curve (Fig. 5). Significantly, no endotherm appears at the melting point of oxine. At 180°C. another endothermic reaction appears which persists to about 260–270°C. During this same range the TGA curve shows constant weight. A degradative reaction, accompanied by only a small weight loss, is suggested at 270°C. This reaction is possibly the formation of a xanthene adduct of a 7,7-*bis*(8-hydroxyquinoline) methane. The formation of this intermediate helps

explain why chelates do not exhibit analogous behavior. At 320° weight loss and exothermic change occurs. The erratic nature of the DTA curve suggests gaseous evolution. The excellent correlation between the TGA curve and the DTA curves indicates the probability that one particular route to degradation is preferred.

Stability of the Zinc Chelate

Figures 6 and 7 are thermogravimetric and differential thermal analysis curves showing the thermal stability of the zinc chelate of an oxine–formaldehyde polymer. Weight loss on the TGA curve (Fig. 6) begins at 270°C. as in the case of the free polymer. There is no initial "arresting" of the weight loss as in the free polymer. No break in the DTA curve occurs at 325°C. where the arresting reaction in the free polymer ceases. Both of these suggest that the phenolic hydrogen is involved in the arresting reaction such as would be needed for a xanthene adduct.

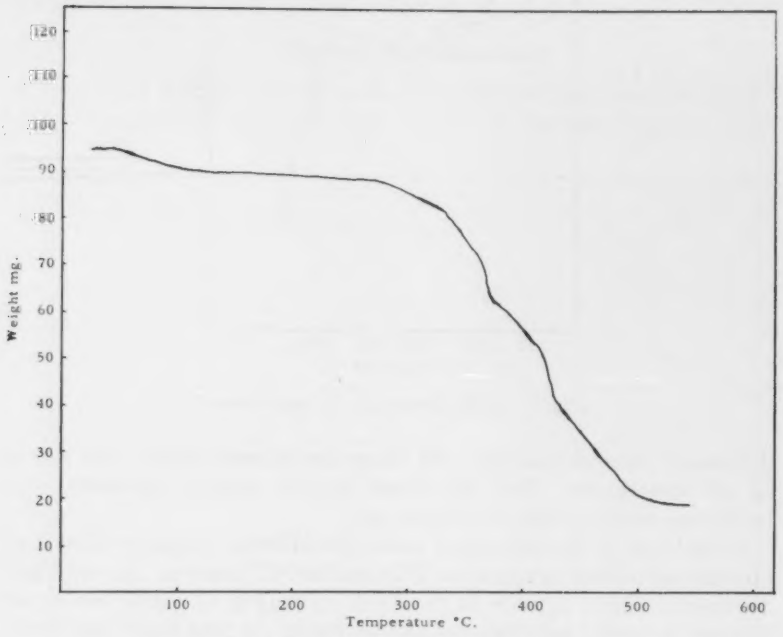

Fig. 6. TGA thermogram of zinc chelate.

The TGA curves indicate that the zinc chelate degrades at a lower initial temperature than that required to begin degradation of the free polymer. The rate of degradation, however, is slower for the zinc chelate. An increase in molecular weight caused by intermolecular chelation might be the means by which chelation slows the degradation of the polymer.

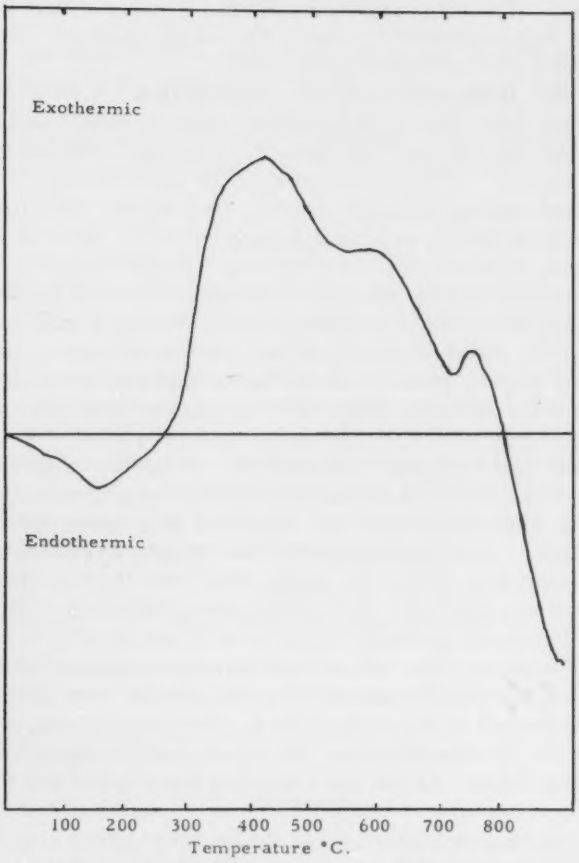

Fig. 7. DTA thermogram of zinc chelated polymer.

Chelates of oxine–formaldehyde polymers with ions of copper, lead, iron, antimony, and nickel were formed and tested by thermogravimetry and differential thermal analysis. The curves were essentially the same as those for zinc. In no case did chelation increase thermal stability over that of the free polymer.

EXPERIMENTAL

A. Condensations of Oxine and Formaldehyde

1. Sulfuric Acid-Catalyzed Condensation. A one-liter, three-necked flask was fitted with a reflux condenser, Teflon-bladed agitator, and thermometer and charged with oxine (77.0 g.) and formaldehyde (36.6 g., 37% formalin). This mixture was heated until the oxine melted. At this point the agitator was started and 2 ml. of concentrated sulfuric acid

were added. The temperature was increased to reflux. After $5^1/_2$ hr. the condenser was rearranged to remove the volatile material. The residue was recovered and used in subsequent steps.

2. Sodium Hydroxide-Catalyzed Condensation. A one-liter, three-necked flask fitted with a Teflon-bladed agitator, reflux condenser, and thermometer was charged with oxine (77.0 g.) and formaldehyde (53 g. of 37% formalin). This was heated until the oxine melted. A few drops of saturated sodium hydroxide solution were added. The temperature rose quickly to 100°C., and much fuming occurred. After about 1 min. the reaction subsided, and the temperature dropped to 94°C. The remaining portion of base was added, bringing the total to 3.3 g. The temperature was brought to gentle reflux. Within 5 min. globules of polymer were noted in the blood-red reaction mixture. After about 15 min. the polymer phases separated as one large globule which wound itself around the agitator. When 20 min. reaction time had elapsed the polymer was separated by decantation of the water phase.

3. Oxalic Acid-Catalyzed Condensation. A one-liter resin flask which was fitted with a Teflon-bladed agitator and a reflux condenser was charged with 800 g. water, 80 g. oxalic acid dihydrate, 40 g. oxine, and 26.6 ml. of 37% formalin. The reaction mixture was brought to reflux and held at that temperature for 75–100 hr., during which time the color changed from pale yellow to a dark red. Periodically during the course of the reaction additional amounts (generally 13 ml. twice a day) of 37% formalin were added. At the end of the reaction time the reflux condenser was rearranged to distil off the volatile portion. As the volatiles were distilled off, a point was reached at which there was a rather sharp change in viscosity. Within a few minutes after this, the viscous mass suddenly foamed into a fine orange foam. At this point agitation was stopped and the heating mantle was removed.

When the reaction mixture cooled the foam was placed in an open container which was placed in an oven at 170–180°C. until the foam structure was completely broken down and the gassing diminished.

4. Formic Acid-Catalyzed Condensation. A one-liter resin flask which was fitted with a Teflon-bladed agitator and reflux condenser was charged with 500 g. water, 40 g. oxine, 82.7 ml. formic acid, and 26.6 ml. of 37% formalin. The mixture was brought to reflux. Within 15 min. a reddish-brown material started to precipitate on the sides of the flask. Formic acid (13 ml.) was added, and the precipitate dissolved. Polymerization was continued another 36 hr., at which time the volatile portion was distilled off, leaving the product as a residue.

5. Noncatalyzed Condensation. A hydrogen bomb was charged with 50 g. oxine which had been intimately mixed with 13.6 g. of 91% paraformaldehyde. The inlet and exit ports of the bomb were sealed. The bomb was placed in the rocker heater and slowly brought to about 240°C. over a period of several hours and then allowed to cool. Excess formaldehyde and moisture were driven off by heating.

B. Zinc Chelate

The oxine–formaldehyde condensation polymer (0.1998 g.) was dissolved in about 25 ml. of 0.1*N* hydrochloric acid. To this 0.855 g. of zinc chloride was added and the pH adjusted to 4.5 with 0.1*N* NaOH. At a pH of 1.7 a bright yellow precipitate appeared. After standing overnight the pH had not changed from 4.5. The precipitate was filtered off and dried.

C. Molecular Weight

Approximately 0.1 g. of polymer which had been dried in an oven at 110°C. for 1 hr. was accurately weighed and dissolved in 50 ml. of 5*N* hydrochloric acid. Potassium bromide (1 g.) was added and two drops of a 0.1% solution of the sodium salt of methyl red. This solution was titrated with a 0.1 *N* solution of potassium bromate, stoppered, and allowed to stand for 2 min. Potassium iodide (1 g.) and starch indicator solution (2.5 ml.) were added and the solution titrated to the starch-iodide endpoint with a 0.1*N* solution of sodium thiosulfate which had been previously standardized against the potassium bromate solution used earlier. The degree of polymerization was calculated according to

$$\bar{P} = \frac{4000\,W}{(\text{meq. } BrO_3^- = \text{-meq. } S_2O_3^=)M}$$

where P is the degree of polymerization, W is the weight of polymer in grams, and M is the molecular weight of a repeating polymer unit (159.17).

This research was supported in part by a contract with the U. S. Army Quartermaster Research and Engineering Command, Natick, Massachusetts.

References

1. Kolthoff, I. M., and E. B. Sandell, *Textbook of Quantitative Inorganic Chemistry*, MacMillan, New York, 1948, p. 638.
2. Fernando, A., and J. P. Philips, *J. Am. Chem. Soc.*, **74**, 3103 (1952).

Résumé

L'acide sulfurique, l'hydroxyde de sodium, l'acide formique et l'acide oxalique ont été introduits comme catalyseurs pour la condensation de l'oxine avec le formaldéhyde. On a trouvé que tous favorisent la condensation dans une solution aqueuse sous reflux, bien que le temps requis soit variable. La condensation a été effectuée, sans catalyseur, entre 200°C et 240°C, dans un récipient scellé, en mélangeant d'une manière très intime l'oxine et le formaldéhyde. Les polymères de condensation oxine-formaldéhyde sont solubles dans le phénol et les acides plus forts que l'acide acétique. On obtient une chélation en dissolvant le polymère dans un acide, en ajoutant une solution qui contient l'ion qui doit être chélaté et en ajustant le pH du mélange à une valeur sufisamment élevée pour que la chélation soit favorisée sans que l'hydroxyde métallique ne précipite. La stabilité thermique a été déterminée par thermogravimétrie et par différentes analyses. Tous les échantillons dégradaient (commençaient à perdre du poids) à 270°C ou plus bas. La manière de décomposition des polymères chélatés semble être indépendante de l'ion métallique, mais le polymère libre est différent. Sa perte en poids initiale (entre 270°C

et 320°C) est très progressive si on la compare aux chélates. A 320°C elle retombe d'une forme similaire à cele du chélate. Une seconde différence avec le polymère libre est que la vitesse de décomposition est une fonction de la température, tandis que celle des polymères chélatés ne l'est pas. Ainsi les chélates peuvent être intéressants comme matériel ablatif. Une troisième différence est que le polymère libre commence à fondre à environ 190°C, alors que les chélates ne fondent pas.

Zusammenfassung

Schwefelsäure, Natriumhydroxyd, Ameisensäure und Oxalsäure wurden als Katalysatoren für die Kondensation von Oxin mit Formaldehyd untersucht. Alle erwiesen sich als Promotoren für die Kondensation in wässriger Lösung unter Rückfluss, die erforderliche Zeit war aber verschieden. Ohne Katalysator liess sich die Kondensation zwischen 200°C und 240°C in einem zugeschmolzenem Behälter durch innige Vermischung von Oxin und Paraformaldehyd durchführen. Oxin–Formaldehyd-Kondensationspolymere sind in Phenol und stärkeren Säuren als Essigsäure löslich. Chelatbildung wird durch Lösung des Polymeren in Säure, Zufügen einer Lösung des als Chelat zu bindenden Ions und Einstellen des pH der Mischung auf einen für die Chelatbildung genügend hohen, aber nicht zur Fällung des Metallhydroxyds führenden Wert erreicht. Wärmebeständigkeit wurde durch thermogravimetrische und differentialthermische Analyse bestimmt. Alle Proben zeigten einen Abbau (beginnenden Gewichtsverlust) bei 270°C oder darunter. Die Zersetzungsweise der polymeren Chelate scheint vom Metallion unabhängig zu sein, das freie Polymere verhält sich aber verschiedenartig. Sein Anfangsgewichtsverlust (zwischen 270° und 320°C) steigt im Vergleich zu dem der Chelate sehr langsam an. Bei 320°C nimmt er eine ähnliche Form wie bei den Chelaten an. Ein weiterer Unterschied des freien Polymeren besteht darin, dass die Zersetzungsgeschwindigkeit eine Temperaturfunktion ist, während das bei den Polymerchelaten nicht der Fall ist. Die Chelate können daher zur Verwendung als abtragende Stoffe von Interesse sein. Ein dritter Unterschied ist der, dass das freie Polymere von etwa 190°C an zu schmelzen beginnt. Die Chelate schmelzen nicht.

Received October 16, 1961
Revised October 11, 1962

BOOK REVIEW

N. G. GAYLORD, Editor

Makromolekulare Stoffe, Part II, Vol. XIV, Methoden der Organischen Chemie (Houben-Weyl), E. MÜLLER, Ed, Georg Thieme Verlag, Stuttgart, 1963. LXXII + 1251 pp., DM 272.00.

This book is Part II of the massive work entitled "Macromolecular Compounds" that comprises Volume XIV of the Houben-Weyl *Methoden der Organischen Chemie*. The review of the first part has previously appeared in the *Journal of Polymer Science*, **A1**, 1471 (1963). Whereas Part I dealt primarily with addition polymerization of vinyl and divinyl compounds, the subject matter of Part II is the preparation of macromolecular substances through polycondensation, ring-opening polymerization, and polymerization of the polyurethan-type. The latter methods are referred to in the German literature and in this text as "polyaddition reactions." The use of this term is most unfortunate since the terms "polyaddition" and "addition polymerization" should be considered synonymous, just as condensation polymerization and polycondensation are synonymous.

Specifically, Part II covers the preparation of polymers of the following types: polycarbonates, polyurethans, polyamides, amino resins, phenolic resins, acetal resins, and various polyacetals, as well as the polymerization of heterocyclic compounds. An additional large chapter is devoted to the reaction of natural and synthetic macromolecular substances, e.g., reactions of preformed synthetic polymers, natural rubber, cellulose, and starch. The final chapter deals with the proof of structure of macromolecular compounds. It covers chemical analysis and analysis of functional groups, and concludes with a 110-page listing of all publications dealing with the determination of polymer properties according to the type of analysis.

As in the case of Part I, the coverage is extensive and includes much recent work. Parts I and II of Volume XIV thus serve as a comprehensive survey of the entire literature of polymer preparation, and should prove to be of exceptional value to all chemists working in this area. The publication of this work represents a major addition to the literature of macromolecules and every laboratory concerned with polymers will find it extremely useful. Unfortunately, the high price of this book will allow few chemists to acquire personal copies.

Contributors to Part II are H. Herlinger, M. Hoffman, E. Husemann, E. Istel, W. Kern, H. Krimm, E. Müller, H. Rinke, R. Schmitz-Josten, P. Schneider, R. C. Schulz, G. Spielberger, R. Wegler, and R. Werner.

Fittingly, this book is dedicated to Otto Bayer on the occasion of his 60th birthday.

Norbert M. Bikales

Gaylord Associates, Inc.
Newark, New Jersey

ERRATA

Apparatus for Measuring the Dynamic Modulus of Thin Polymer Films

(article in *J. Polymer Sci.*, **A1**, 1585–1600, 1963)

By O. C. HANSEN, T. L. FABRY, L. MARKER, and O. J. SWEETING
Packaging Division, Film Operations, Olin Mathieson Chemical Corporation, New Haven, Connecticut

On p. 1586, lines 15 and 16, eq. (1), for $(1/2\pi)$ should read $(1/2\pi)$.
On p. 1586, last and penultimate lines, eq. (2), for $(1/2l)$ should read $(1/2l)$.
On p. 1587, line 6, eq. (3), for $(4\pi^2/g)$ should read $(16\pi^2/g)$.
On p. 1599, line 18, factor in parentheses should be $(1 - 4\pi^2 f_t^2 m/k)^{-1}$.

Molecular Weight Distribution by Velocity Ultracentrifugation

(article in *J. Polymer Sci.*, **62**, 179–196, 1962)

By M. WALES and S. J. REHFELD
Shell Development Company, Emeryville, California

On page 194 eq. (41) should read

$$M_{max} = M_p \exp \{p^2(a + 4)/6\}$$

Equation (42) should read

$$M_{sv} = M_p \exp \{p^2(a + 4)^2/24\}$$

AUTHOR INDEX, VOLUME 1

Abe, A., and Goodman, M.: Optical rotatory properties of polyaldehydes, 2193
Abdul-Karim, A.: see DeWinter, W.
Acker, T.: see Odian, G.
Acres, G. J. K., and Dalton, F. L.: Synthesis of styrene–methyl methacrylate nonrandom copolymers in emulsion systems with cobalt-60 gamma radiation, 2419
——, and Dalton, F. L.: On Co^{60} gamma ray-initiated emulsion polymerization, 3009
Alaniya, V. P.: see Topchiev, A. V.
Alexandrowicz, Z., and Katchalsky, A.: Colligative properties of polyelectrolyte solutions in excess of salt, 3231
——: see Katchalsky, A.
Alfred, L.: see Mattison, L. E.
Allcock, H. R., and Kugel, R. L.: Ionic polymerization of diphenylvinylphosphine oxide, 3627
Anderson, D. B., Burnett, G. M., and Gowan, A. C.: Some novel effects in solution polymerization, 1465
Anderson, E. W.: see McCall, D. W.
Arakawa, T.: see Wunderlich, B.
Arnett, R. L., Smith, M. E., and Buell, B. O.: An improved ebullioscope for high polymers, 2753
Avny, Y.: see Zilkha, A.
Azori, M.: see Tüdös, F.
Bacskai, R.: Polymerization of alicyclic epoxides with aluminum alkyl catalysts, 2777
——, and Lapporte, S. J.: The chemical structure of polyisobutylene obtained by Ziegler catalysis, 2225
Baer, E.: see Limbert, F. J.
Baer, M.: Anionic block polymerization. I. Block polymerization of styrene on polystyrene, 2171
Baker, W. P., Jr.: Polymerization of allene by organometallic initiation, 655
Baldwin, M. G.: Primary radical termination in methyl methacrylate polymerization, 3209
——, and Reed, S. F.: Polymerization studies on allylic compounds. I, 1919
Barrer, R. M., Barrie, J. A., and Rogers, M. G.: Heterogeneous membranes: diffusion in filled rubber, 2565
Barrie, J. A.: see Barrer, R. M.
Barzakay, S.: see Ottolenghi, A.
——: see Zilkha, A.
Bassett, D. C., Keller, A., and Mitsuhashi, S.: New features in polymer crystal growth from concentrated solutions, 763
Bassett, K. H., Liang, C. Y., and Marchessault, R. H.: The infrared spectrum of crystalline polysaccharides. IX. The near infrared spectrum of cellulose, 1687
Bataille, P., and Patterson, D.: An application of the Prigogine solution theory to intrinsic viscosities in polyisobutylene–*n*-alkane systems, 3265
Baumann, G. F., and Steingiser, S.: Rheological measurements on polycarbonate, 3395
Beck, K.: see Toggenburger, R.
Benerito, R. R., Berni, R. J., McKelvey, J. B., and Burgis, B. G.: Study of the base-catalyzed cellulose–*d,l*-butadiene diepoxide reaction, 3407
Berens, A. R.: see Krimm, S.
Berge, J. M.: see Shultz, A. R.
Berger, M.: Steric structures in copolymerization, 1601
——, and Buckley, D. J.: Structure effects and related polymer properties in polybutadiene. I. Preparation and characterization, 2945
Berni, R. J.: see Benerito, R. R.
Berry, J. P.: Fracture processes in polymeric materials. IV. Dependence of the fracture surface energy on temperature and molecular structure, 993
Bettelheim, F. A.: see DerSarKissian, V. M.
Beynon, K. I.: Monomers containing phosphorus. Part I. Copolymerization of phosphonates with *n*-lauryl methacrylate, 3343
——: Monomers containing phosphorus. Part II. Copolymerization of diallyl phenyl phosphine oxide with *n*-lauryl methacrylate, 3357
Billmeyer, F. W., Jr.: see De La Cuesta, M. O.
Binder, J. L.: The infrared spectra and structures of polyisoprenes, 37
——: The infrared spectra and structures of polybutadienes, 47
Bixler, H. J., Michaels, A. S., and Salame, M.: Gas transmission in irradiated polyethylene, 895
Bond, J., and Hobson, D. B.: The role of metal chelates in polymerization initiation. I. Chromous chelates, 2179
——, and ——: II. Cupric chelates, 2185
Boor, J. Jr., and Mitchell, J. C.: Kinetics of crystallization and a crystal-crystal transition in poly-1-butene, 59
Boryniec, A., and Łaszkiewicz, B.: Bulk copolymerization of methyl methacrylate with phenyldichlorophosphine, 1963
Bostick, E. E.: see Morton, M.
Bourne, M. C., Chichester, C. O., and Sterling, C.: Diffusion constants of a maltosaccharide series, 817

Bovey, F. A.: Polymer NMR spectroscopy. VIII. The influence of the pH of the polymerization medium on the stereochemical configuration of polymethacrylic acid, 843
——, and Tiers, G. V. D.: Polymer NMR spectroscopy. IX. Polyacrylamide and polymethacrylamide in aqueous solution, 849
——: see Tiers, G. V. D.
Bower, G. M., and Frost, L. W.: Aromatic polyamides, 3135
Bradley, L. J.: see Morton, M.
Bristow, G. M.: The mastication of elastomers. Part III. The solution properties of masticated synthetic *cis*-polyisoprene, 2261
Brockway, C. E., and Moser, K. B.: Grafting of poly(methyl methacrylate) to granular corn starch, 1025
Brodoway, N.: see Wich, G. S.
Brower, F. M., and McCormick, H. W.: Narrow molecular weight distribution polystyrenes, 1749
Brown, D. W.: see Florin, R. E.
Bruss, D. B., and Stross, F. H.: A comparison of dynamic methods for osmotic pressure measurements, 2439
——: see Burge, D. E.
Buckley, D. J.: see Berger, M.
Bueche, A. M.: Huggins, C. M.
Buell, B. O.: see Arnett, R. L.
Burge, D. E., and Bruss, D. B.: Preparation and properties of some poly-α-methylstyrenes, 1927
Burgis, B. G.: see Benerito, R. R.
Burke, W. J., and Higginbottom, H. P.: Nitrosation of linear phenol-formaldehyde polymers, 3617
Burkhart, R. D., and Zutty, N. L.: Copolymerization studies. III. Reactivity ratios of model ethylene copolymerizations and their use in *Q-e* calculations, 1137
Burnett, G. M.: see Anderson, D. B.
Cahill, J. W.: see Loconti, J. D.
Campbell, T. W., and McDonald, R. N.: Polymeric derivatives of 3,3-bis(aminomethyl)-oxetane and exoxysuccinyl chloride, 2525
Cappas, C.: see Pohl, H. A.
Carazzolo, G. A.: Structure of the normal crystal form of polyoxymethylene, 1573
——, and Mammi, M.: Crystal structure of a new form of polyoxymethylene, 965
Carmichael, J. B., and Kinsinger, J. B.: Unrestricted rotation in polymers with discrete rotational states, 2459
Carpenter, W. G.: see Pellon, J.
Cassidy, H. G.: see Kamogawa, H.
Chamberlain, N. F.: see Edwards, W. R.
Chappell, S. E., Sauer, J. A., and Woodward, A. E.: Effects of high energy irradiation on polypropylene, 2805
Charles, R. G.: Metal chelate polymers derived from tetraacetylethane, 267
Chen, C. S. H.: Polymerization induced by ionizing radiation at low temperatures. III. The effect of electron density on the polymerization of substituted styrenes, 1293
Chichester, C. O.: see Bourne, M. C.
Chiang, R.: Crystallization and melting behavior of polyacrylonitrile, 2765
Chien, J. C. W.: Kinetics of propylene polymerization catalyzed by α-titanium trichloride–diethylaluminum chloride, 425
——: Olefin polymerization and polyolefin molecular weight distribution, 1839
Chirkov, N. M.: see Firsor, A. P.
Chiv, T. T.: see Maron, S. H.
Chowdhury, F. H., and Neale, S. M.: Acid behavior of carboxylic derivatives of cellulose. Part I. Carboxymethylcellulose, 2881
——, and ——: Part II. Oxycellulose, 2893
Chu, B.: see Debye, P.
Chu, N. S., and Price, C. C.: Polyethers. XI. Polymerization of *dl*-propylene oxide with optically active catalyst systems, 1105
Clarke, R. G.: see Morton, M.
Clendinning, R. A.: see Garty, K. T.
Coleman, B. D., and Fox, T. G: General theory of stationary random sequences with applications to the tacticity of polymers, 3183
Contois, L. E.: see Dunham, K. R.
Cooper, W., Johnston, F. R., and Vaughan G.: Stereoregularity in polyvinyl alcohols and esters, 1509
——, and Smith, R. K.: Melting transitions in diene polymers, 159
Cotton, G. R., and Sacks, W.: Oxidative crosslinking of polyethylene by ultraviolet light, 1345
Crawford, G. H., Rice, D. E., and Landrum, B. F.: Nitroso fluorocarbon elastomers. Polymerization mechanism, 565
Crespi, G: see Natti, G.
Crompton, T. R., and Reid, V. M.: Unsaturation in high impact polystyrene analytical studies, 347
Czarnecki, S., and Kryszewski, M.: Some applications of afterglow studies of luminescent compounds in solid polymers, 3067
Dalton, F. L.: see Acres, G. J. K.
Dammont, F. R.: see Salovey, R.
Daniel, J.-C.: see Guyot, A.
Davis, B.: see Wiley, R. H.
Davis, P., and Tabor, B. E.: Kinetic study of the crosslinking of gelatin by formaldehyde and glyoxal, 799
Debye, P., Chu, B., and Kaufmann, H.: Molecular configuration of polystyrene in benzene, 2387
——, Chu, B., and Woermann, D.: Viscosity of critical mixtures, 249
——, Woermann, D., and Chu, B.: Critical opalescence of polystyrene in ethylcyclohexane, 255
De La Cuesta, M. O., and Billmeyer, F. W., Jr.: The molecular structure of

polyethylene. XII. Intrinsic viscosities of polyethylene solutions, 1721
DerSarKissian, V. M., and Bettelheim, F. A.: Strain birefringence of sodium hyaluronate films, 725
De Santis, P., Giglio, E., Liquori, A. M., and Ripamonti, A.: Stability of helical conformations of simple linear polymers, 1383
De Winter, W., Marvel, C. S., and Abdul-Karim, A.: Polydiacrylylmethane, 3261
Di Benedetto, A. T.: Molecular properties of amorphous high polymers. I. A cell theory for amorphous high polymers, 3459
——: II. An interpretation of gaseous diffusion through polymers, 3477
Dicyan, A. B.: see Wunderlich, B.
DiMarzio, E. A., and Gibbs, J. H.: Molecular interpretation of glass temperature depression by plasticizers, 1417
Dipietro, J.: see Zambelli, A.
Dole, M.: see Inokuti, M.
Douglass, D. C.: see McCall, D. W.
Drougas, J., Timnick, A., and Guile, R. L.: High frequency titrations of polydicarboxylic acid copolymers: polyitaconic acid-*Co*-styrene and polymaleic acid-*Co*-styrene, 1609
Dunham, K. R., VanDenBerghe, J., Faber, J. W. H., and Contois, L. E.: Effect of side-chain structure on poly-*d*-olefin properties, 751
Edwards, W. R., and Chamberlain, N. F.: Carbonium ion rearrangement in the cationic polymerization of branched alpha olefins, 2299
Ehrlich, P., and Kurpen, J. J.: Phase equilibria of polymer–solvent systems at high pressures near their critical loci: polyethylene with *n*-alkanes, 3217
Eirich, F. R: see Sabia, R.
Elden, H. R., and Feldman, M.: A kinetic analysis of swelling of rat tail tendon, 23
Ellis, K. C., and Warwicker, J. O.: Crystallite orientation in regenerated cellulose filaments. I. Measurement of orientation by x-ray methods, 1185
Enda, Y.: see Kishimoto, A.
Endrey, A. L.: see Rosen, I.
Faber, J. W. H.: see Dunham, K. R.
Fabry, T. L.: see Hansen, O. C., Jr.
Feitelson, J.: see Josephs, R.
Feldman, M.: see Elden, H. R.
Fetters, L. J.: see Morton, M.
Filipovich, G.: Nuclear magnetic resonance in solid polypyrrolidone, 2279
Firsor, A. P., Kashprov, B. N., Kissin, Yu. V., and Chirkov, N. M.: The dependence of the stereospecific action of the complex catalyst α-$TiCl_3$–$Me(C_2H_5)_n$ during the polymerization of α-olefins on the metal in the metalloorganic compound (article in *J. Polymer Sci.*, **62**, S104–S105, 1962), 1472
Fischer, H., Hellwege, K. H., and Neudorfl, P.: Elektronenspinresonanz-Utersuchungen an Peroxydradikalen in bestrahltem Polyproplen, 2109
Flisi, U: see Natti, G.
Flood, J. F.: see Wunderlich, B.
Florin, R. E., and Wall, L. A.: Electron spin resonance of gamma-irradiated cellulose, 1163
——, Wall, L. A., and Brown, D. W.: Electron spin resonance spectra of aged, γ-irradiated polystyrenes, 1521
Folt, V. L.: see Krimm, S.
Fort, R. J.: see Moore, W. R.
Foster, J. F.: see Rao, V. S. R.
Fox, R. B., Isaacs, L. G., and Stokes, S.: Photolytic degradation of poly(methyl methacrylate), 1079
Fox, T. G.: see Coleman, B. D.
Frey, D. A., Hasegawa, M., and Marvel, C. S.: Preparation and aromatization of poly-1,3-cyclohexadiene. II, 2057
Frost, L. W.: see Bower, G. M.
Fukui, K.: see Hayashi, K.
Fukutani, H.: see Iwasaki, K.
——: see Nakano, S.
Gager, W. B.: see Ungar, I. S.
Garty, K. T., Gibb, T. B., Jr., and Clendinning, R. A.: Cocatalysts for the linear polymerization of epoxides by dibutylzinc, 85
Gatti, G.: see Zambelli, A.
Gautron, R.: see Wippler, C.
Gershman, N. E.: see Winslow, E. C.
Gibb, T. B., Jr.: see Garty, K. T.
Gibbs, J. H.: see DiMarzio, E. A.
Gibbs, W. E.: see Morton, M.
Giglio, E.: see De Santis, P.
Gill, S. J.: see Toggenburger, R.
Glauz, R. D.: Transient analysis of a vibrating reed, 1693
Gogos, C. G.: see Pohl, H. A.
Golden, J. H., and Hazell, E. A.: Degradation of a polycarbonate by ionizing radiation, 1671
Goodman, M.: see Abe, A.
Gowan, A. C.: see Anderson, D. B.
Greenley, R. Z.: see Reichel, B.
Greyson, J., and Levi, A. A.: Calorimetric measurements of the heat of sorption of water vapor on dry swollen cellulose, 3333
Guha, T., and Palit, S. R.: Study of the rate of heterogeneous polymerization of methyl acrylate in aqueous solution, 877
Guile, R. L.: see Drougas, J.
Guillet, J. E.: Long-chain branching frequency in polyethylene, 2869
Gurnee, E. F.: see Rudd, J. F.
Gutowksy, H. S.: see Kusumoto, H.
Guyot, A., and Daniel, J.-C.: Étude de la polymerization des oléfines catalysée par les oxydes métalliques. I. Méthodes expérimentales d'étude cinétique; résultats preliminaires sur la polymérisation du propylène par le système catalytique Phillips, 2989
Haas, H. C., Husek, H., and Taylor, L. D.: On the ultraviolet absorption spectrum of polyvinyl alcohol, 1215
Haas, T. W.: see Sharma, M. G.

Hall, J. L.: see Morton, M.
Hansen, O. C., Jr., Fabry, T. L., Marker, L., and Sweeting, O. J.: Apparatus for measuring the dynamic tensile modulus of thin polymeric films, 1585
——, ——, ——, and ——: (article in *J. Polymer Sci.*, **A1**, 1585–1600, 1963), 3668
Hara, K.: see Tabata, Y.
Harrod, J. F.: Hydrogen bonding in amine-epoxide adducts, 385
Hartley, D. B.: see Tobolsky, A. V.
Hasegawa, M.: see Frey, D. A.
Havlik, A. J., Moacanin, J., and Otterness, I.: Ebulliometric and endgroup molecular weights of polyoxypropylene and polyoxyethylene glycols, 2213
Hawkins, W. L., and Sautter, Mrs. H.: Synergistic antioxidant combinations. Mechanism of stabilization with organosulfur compounds, 3499
——, and Worthington, Mrs. M. A.: Synergistic antioxidant combinations. Carbon black substitutes, 3489
Hayashi, K., Yonezawa, T., Okamura, S., and Fukui, K.: Molecular orbital theory of reactivity in radical polymerization. Part III, 1405
Hazell, E. A.: see Golden, J. H.
Heller, J., Tieszen, D. O., and Parkinson, D. B.: Polymerization of *N*-vinylcarbazole with Ziegler-type catalyst systems, 125
Hellwege, K. H.: see Fischer, H.
Heritage, K. J., Mann, J., and Roldan-Gonzalez, L.: Crystallinity and the structure of celluloses, 671
Hermans, J. J.: see Yamada, S.
Hewett, W. A., and Weir, F. E.: Dynamic properties of homo- and copolymers of 4-methyl-1-pentene, 1239
Higginbottom, H. P.: see Burke, W. J.
Hobson, D. B.: see Bond, J.
Hoeve, C. A. J., and O'Brien, M. K.: Specific diluent effects on polymer chain dimensions, 1947
Horrocks, R. H., and Winslow, E. C.: Oxine–formaldehyde polymers and their metallic chelates, 3655
Howard, G. J.: Turbidimetric titration of nylon 66, 2667
Hsiao, C. C., and Wu, T. S.: Orientation and strength of branched polymer systems, 1789
Hsu, B. S.: see Meredith, R.
Huang, R. Y.-M., Immergut, B., Immergut, E. H., and Rapson, W. H.: Grafting vinyl polymers onto cellulose by high energy radiation. I. High energy radiation-induced graft copolymerization of styrene onto cellulose, 1257
Huff, T., and Perry, E.: Reaction of polymeric radicals with organometallic compounds, 1553
Huggins, C. M., St. Pierre, L. E., and Bueche, A. M.: Further NMR studies of polydimethylsiloxanes: effects of radiation-induced crosslinking, 2731
Huntsberger, J. R.: The locus of adhesive failure, 1339
——: Adhesion. II. Relationships between viscoelasticity, interfacial equilibrium, and the temperature dependence of adhesion, 2241
Husek, H.: see Haas, H. C.
Iimura, K.: see Takeda, M.
Ikeda, S., Yamamoto, A., and Tanaka, H.: Stereoregulated polydideuteroethylene I. Polymers of *trans*-1,2-dideuteroethylene and *cis*-1,2-dideuteroethylene by a Ziegler catalyst, 2925
Immergut, B.: see Huang, R. Y.-M.
Immergut, E. H.: see Huang, R. Y.-M.
Inagaki, H., Kawai, S., and Nakazawa, A.: Application of the Archibald ultracentrifugal method for the study of dilute polymer solutions. II. Examination of two solution systems near the Flory temperature, 3303
Inokuti, M., and Dole, M.: Interpretation of the intrinsic viscosity of polymers undergoing simultaneous degradation and crosslinking, 3289
Inoue, M.: Nucleating effect on the kinetics of crystallization and the spherulites of nylon 6, 2013
——: Studies on crystallization of high polymers by differential thermal analysis, 2697
——: Properties of melt-blends of crystalline high polymers. Fusion and crystallization behaviors, 3427
Isaacs, L. G.: see Fox, R. B.
Iwasaki, K., Fukutani, H., and Nakano, S.: Polymerization of vinyl ethers with magnesium compounds. I. Catalytic reactivity of magnesium halides, 1937
——, Fukutani, H., Tsuchida, Y., and Nakano, S.: Polymerization of vinyl ether with magnesium compounds. II. Catalytic reactivity of magnesium compounds other than halides, 2371
——: see Nakano, S.
Iwasaki, M.: On the helical structure of polytetrafluoroethylene, 1099
Izumi, Z., Kiuchi, H., and Watanabe, M.: Copolymerization of acrylonitrile and *p*-sodium styrene sulfonate, 705
Jager, P., and Waight, E. S.: Solid state polymerization of methacrylamide and *N*-arylmethacrylamides, 1909
Jackson, J. F.: Crystallinity in ethylene–propylene copolymers, 2119
Jacobson, A. L.: The temperature dependence of magnesium chloride interaction with polyacrylic acid, 1955
——: see Redlich, O.
Johnson, D. R.: see Starkweather, H. W., Jr.
Johnston, F. R.: see Cooper, W.
Josephs, R., and Feitelson, J.: Interactions of polyelectrolytes. A turbidimetric method for the estimation of ionized polymers, 3385
Kalpagam, V., and Rao, M. R.: Effect of polar and nonpolar solvents on the

viscosity and the molecular weight of polymer solutions, 233
——, and ——: Depolarization measurements of polymer solutions in high dilutions. Part I, 517
——, and ——: Part II, 921
Kamei, T.-I.: see Tadokoro, H.
Kamogawa, H., and Cassidy, H. G.: Electron exchange polymers. XIX. Copolymerization behavior of vinylhydroquinone dibenzoate, 1971
Kaneko, M.: see Krigbaum, W. R.
Kashiwagi, M.: Radiation damage in oriented polyamides, 189
Kashprov, B. N.: see Firsor, A. P.
Katchalsky, A., and Alexandrowicz, Z.: On the addivity of osmotic properties of polyelectrolyte-salt solutions, 2093
——: see Alexandrowicz, Z.
Katz, D.: Polymerization and copolymerization of 1- and 9-vinylanthracenes and 9-vinylphenanthrene, 1635
——: see Tobolsky, A. V.
Kaufman, H.: see Debye, P.
Kawai, S.: see Inagaki, H.
Kazda, A.: see Zlámal, Z.
Ke, B.: Differential analysis of high polymers. VI. Comments on some material and experimental factors, 1453
Keller, A.: see Bassett, D. C.
Kende, I.: see Tüdös, F.
Kennedy, J. P., Kirshenbaum, I., Thomas, R. M., and Murray, D. C.: Fundamental studies on cationic polymerization. II. Mechanism and theory of inversion temperature, 331
——: see Kirshenbaum, I.
Ketley, A. D., and Moyer, J. D.: Competing side reactions in the polymerization of α-olefins by Ziegler-Natta catalysts, 2467
Kinsinger, J. B.: see Carmichael, J. B.
Kircher, J. F.: see Ungar, I. S.
Kirshenbaum, I., Kennedy, J. P., and Thomas, R. M.: Fundamental studies on cationic polymerization. III. Extension of mechanism studies to homogenous systems, 789
——: see Kennedy, J. P.
Kishimoto, A., and Enda, Y.: Diffusion of benzene in polyacrylates, 1799
Kissin, Yu. V.: see Firsor, A. P.
Kiuchi, H.: see Izumi, Z.
Kline, D. E.: Nuclear radiation effects in polytetrafluoroethylene, 1621
Klein, R.: see Odian, G.
Kobayashi, F., and Matsuya, K.: Copolymerization of α-pyrrolidone and ϵ-caprolactam, 111
Koral, J. N., and Smolin, E. M.: The preparation and polymerization of suberaldehyde, 2831
Kotera, A.: see Shima, M.
Kotliar, A. M.: Evaluation of molecular weight averages resulting from random crosslinking and chain scission processes for wide Schulz-Zimm distributions, 3175
Krigbaum, W. R., Kaneko, M., and Roig, A.: Dipole moments, stress relaxation, and birefringence of Viton fluoroelastomer, 1
——: see Roe, R.-J.
——: see Tokita, N.
Krimm, S., Folt, V. L., Shipman, J. J., and Berens, A. R.: Infrared spectra and assignments for polyvinyl chloride and deuterated analogs, 2621
Kryszewski, M., and Skorko, M.: Interactions of low molecular weight compounds with solid polymers, 2327
——: see Czarnecki, S.
Kugel, R. L.: see Allcock, H. R.
Kuhn, W., and Moser, P.: The dielectric relaxation time spectrum and the corresponding Cole-Cole diagram for methylcellulose in water, 151
Kulshrestha, V. K.: Studies on biocolloids and polyelectrolytes—the plant—gums viscosity of azrechtic acid, 1429
Kumins, C. A., and Roteman, J.: Effect of solid polymer interaction on transition temperature and diffusion coefficients, 527
——, Roteman, J., and Rolle, C. J.: Water sorption of titanium dioxide–poly(vinyl acetate–vinyl chloride) copolymer films, 541
Kuri, Z.: see Ueda, H.
Kurpen, J. J.: see Ehrlich, P.
Kusano, N.: see Sisido, K.
Kusumoto, H., and Gutowsky, H. S.: Proton magnetic resonance in natural rubber: comparison with dielectric measurements, 2905
Kuwahara, N.: On the polymer–solvent interaction in polymer solutions, 2395
Kwei, K.-P. S.: Graft copolymers of polyacrylic acid with desoxyribonucleic acid (DNA), 2309
Kwei, T. K.: Swelling of highly crosslinked network structure, 2977
Kwolek, S. L.: see Morgan, P. W.
Lakshminarayanaiah, N.: Activity coefficients of small ions in ion-exchange resins, 139
Landrum, B. F.: See Crawford, G. H.
Lang, J. L., Pavelich, W. A., and Clarey, H. D.: Homopolymerization of maleic anhydride. I. Preparation of the polymer, 1123
Lapporte, S. J.: see Bacskai, R.
Laszkiewicz, B.: see Boryniec, A.
Leininger, R. I.: see Ungar, I. S.
Levi, A. A.: see Greyson, J.
Levinson, G. S.: Molecular orbital calculation of monomer reactivity ratios (article in *J. Polymer Sci.*, **62**, 43–54, 1962), 1088
Lewin, M.: see Schmorak, J.
Liang, C. Y.: see Bassett, K. H.
Limbert, F. J., and Baer, E.: Kinetics of nucleation and growth of spherulites in homopolymers, 3317
Liquori, A. M.: see De Santis, P.
Litt, M.: Poly(4-methyl pentene): x-ray measurement of crystalline density and

observation of a structural anomaly, 2219
Livigni, R. A.: see Morton, M.
Lloyd, W. G.: The influence of transition metal salts in polyglycol autoxidations, 2551
Loconti, J. D., and Cahill, J. W.: Zone-refining fractionation of polymers, 3163
Loy, B. R.: Electron spin resonance of polypropylene, 2251
McCain, G. H.: see Rosen, I.
McCall, D. W., and Anderson, E. W.: Molecular motion in polyethylene. III, 1175
——, Douglass, D. C., and Anderson, E. W.: Self-diffusion and nuclear relaxation in polyisobutylene, 1709
McCormick, H. W.: Molecular weight distribution of linear polyethylene by sedimentation velocity analysis, 103
——: see Brower, F. M.
McDonald, R. N.: see Campbell, T. W.
McFadden, W. H.: see Redlich, O.
McIntosh, C. R., Stephens, W. D., and Taylor, C. O.: Changes in the stereospecificity of a Ziegler catalyst used in the polymerization of butadiene, 2003
McIntyre, D. B.: see Morton, M.
McKelvey, J. B.: see Benerito, R. R.
Mackie, J. S.: see Rudin, A.
Mammi, M.: see Carazzolo, G.
Manabe, Y.: see Yoshino, T.
Manley, R. St. J.: Growth and morphology of single crystals of cellulose triacetate, 1875
——: Hydrolysis of cellulose triacetate crystals, 1893
Mann, J.: see Heritage, K. J.
Marchese, B.: see Orsini, P. O.
Marchessault, R. H.: see Bassett, K. H.
Mark, H. F., and Ogata, N.: Copolymerization of aldehydes, 3439
Marker, L.: see Hansen, O. C., Jr.
Maron, S. H., and Chiu, T. T.: Study of entanglement of polymers in solution by viscosity measurements. II. Polymethyl methacrylate in various solvents, 2651
Marriott, J. A.: see Winslow, E. C.
Marvel, C. S.: see De Winter, W.
——: see Frey, D. A.
——: see Reichel, B.
——: see Shono, T.
——: see Vogel, H.
Matsuda, M.: see Tokura, N.
Matsuya, K.: see Kobayashi, F.
Mattison, L. E., Phipps, M. S., Alfred, L., Taylor, S., Thompson, J., and Saul, B.: Coordination compounds of *p*-nitrobenzeneazotyrosine, 3449
Mauer, J. J.: Particle size distribution in polymer solutions, 577
Mayberry, G. L.: see Wiley, R. H.
Mendelson, R. A.: Elution fractionation of crystalline polypropylene, 2361
Mercier, J., and Smets, G.: Copolymerization. I. Structure of polyacrylic anhydride, 1491
Meredith, R., and Hsu, B. S.: Dynamic bending properties of fibers: effect of temperature on nylon 66, terylene, orlon, and viscose rayon (article in *J. Polymer Sci.*, **61**, 271–292, 1962), 2240
Merrill, E. W., Mickley, H. S., Ram, A., and Stockmayer, W. H.: The second Newtonian viscosity number, 1201
Michaels, A. S.: see Bixler, H. J.
Mickley, H. S.: see Merrill, E. W.
Middleman, S.: A theory for surface elevation in the Weissenberg effect, 261
Milkovich, R.: see Morton, M.
Miller, A. A.: The reference point for liquid relaxation processes. I. Melt viscosity of polystyrene, 1857
——: II. Melt viscosity of polyisobutylene, 1865
Miller, S. M., Spindler, M. W., and Vale, R. L.: Use of dimaleimides as accelerators for the radiation-induced vulcanization of hydrocarbon polymers. Part II. Synthetic rubbers and saturated polymers, 2537
Mitchell, J. C.: see Boor, J., Jr.
Mitsuhashi, S: see Bassett, D. C.
Miyamichi, K.: see Overberger, C. G.
Moacanin, J.: see Havlik, A. J.
Moore, W. R., and Fort, R. J.: Viscosities of dilute solutions of polymethyl methacrylate, 929
——, and Shuttleworth, R.: Thermodynamic properties of solutions of cellulose acetate and cellulose nitrate, 733
——, and Shuttleworth, R.: Thermodynamic properties of solutions of cellulose triacetate, 1985
Mora, P. T.: see Wood, J. W.
Morgan, P. W., and Kwolek, S. L.: Interfacial polycondensation. XIII. Viscosity–molecular weight relationship and some molecular characteristics of 6–10 polyamide, 1147
Morris, R. J., Jr., and Persinger, H. E.: Molecular weight distribution in polypropylene glycol 2025, 1041
Morsi, M. K. S., and Sterling, C.: Crystallization in starch: the role of ions in the lyotropic series, 3547
Morton, M., Bostick, E. E., and Clarke, R. G.: Homogeneous anionic polymerization. III. Molecular weight of polyisoprene initiated by butyllithium, 475
——, Bostick, E. E., Livigni, R. A., and Fetters, L. J.: Homogeneous anionic polymerization. IV. Kinetics of butadiene and isoprene polymerization with butyllithium, 1735
——, and Gibbs, W. E.: The emulsion polymerization of 2,3-dimethylbutadiene-1,3, 2679
——, Milkovich, R., McIntyre, D. B., and Bradley, L. J.: Homogeneous anionic polymerization. I. Molecular weights of polystyrene initiated by sodium naphthalene, 443
——, and Piirma, I.: The branching reaction. III. Polymeric transfer con-

stants of vinyl acetate with styrene and methyl methacrylate, 3043
——, Rembaum, A. A., and Hall, J. L.: Homogeneous anionic polymerization. II. Molecular weight of polystyrene initiated by lithium alkyls, 461
Moser, P.: see Kuhn, W.
Mosher, H. P.: see Parks, G. S.
Moyer, J. D.: see Ketley, A. D.
Murahashi, S.: see Tadokoro, H.
Murakami, K.: see Sobue, H.
Murray, D. C.: see Kennedy, J. P.
Nakazawa, A.: see Inagaki, H.
Nakano, S., Iwasaki, K., and Fukutani, H.: Stereospecific polymerization of vinyl alkyl ethers, 3277
——: see Iwasaki, K.
Natta, G., Crespi, G., and Flisi, U.: Thermodynamic interpretations of the elastic properties of rubber obtained from ethylene–propylene copolymers, 3569
Neale, S. M.: see Chowdhury, F. H.
Neely, W. B.: Solution properties of polysaccharides. IV. Molecular weight and aggregate formation in methylcellulose solutions, 311
Neudorfl, P.: see Fischer, H.
Nielsen, L. E., and Stockton, F. D.: Theory of modulus of crystalline polymers, 1995
Nitta, I.: see Shioji, Y.
North, A. M., and Reed, G. A.: Diffusion-controlled polymerization of some alkyl methacrylates, 1311
Notley, N. T.: Molecular configuration of branched macromolecules, 227
Noyori, R.: see Sisido, K.
Nozaki, H.: see Sisido, K.
Nozaki, Y.: see Sisido, K.
Nozakura, S.: see Overberger, C. G.
O'Brien, M. K.: see Hoeve, C. A. J.
Odian, G., Sobel, M., Rossi, Klein, R., and Acker, T.: Radiation-induced graft polymerization of styrene to nylon, 639
Ogata, N.: Resonance effect of amide group on the polymerizability of lactam derivatives. III. Polymerization of many-membered lactams ring, 3151
——: see Mark, H. F.
Ogawa, Y.: see Tokura, N.
Ohnishi, S.-I., Sugimoto, S.-I., and Nitta, I: Electron spin resonance study of radiation oxidation of polymers. IIIA. Results for polyethylene and some general remarks, 605
——, ——, and ——: IIIB. Polypropylene and poly(vinyl chloride), 625
——: see Shioji, Y.
Okamura, S.: see Hayashi, K.
Oosawa, F.: Thermodynamic properties of rodlike polyelectrolyte solutions in the presence of salts, 1501
Orsini, P. O., Marchese, B., and Mazzarella, L.: Morphology of polyethylene single crystals, 1901
Otterness, I.: see Havlik, A. J.
Ottolenghi, A., Barzakay, S., and Zilkha, A.: Anionic polymerization of acrylonitrile by various catalysts, 3643
——, and Zilkha, A.: Termination of the anionic polymerization of acrylonitrile at low catalyst concentrations, 687
——: see Zilkha, A.
Overberger, C. G., and Miyamichi, K.: Copolymerization of styrene and aliphatic olefins, 2021
——, and Nozakura, S.: Copolymerization of styrene and styrene derivative with an aluminum alkyl-titanium trichloride catalyst, 1439
Owens, F. H., and Zimmerman, F. E.: Photochlorination of poly(methyl methacrylate) in aqueous suspension, 2711
Packter, A.: Conductivity and viscosity measurements on sodium polyacrylates of different molecular weights, 3021
Palit, S. R.: see Guha, T.
Palmer, K. J.: see Tomimatsu, Y.
Parkinson, D. B.: see Heller, J.
Parks, G. S., and Mosher, H. P.: Enthalpy and free energy changes in some simple polymerization processes, 1979
Patterson, D.: see Bataille, P.
Pellon, J.: Polyamides containing phosphorus. II. Structural effects on softening and glass transition temperatures, 3561
——, and Carpenter, W. G.: Polyamides containing phosphorus. I. Preparation and properties, 863
Persinger, H. E.: see Morris, R. J., Jr.
Perry, E.: see Huff, T.
Petree, M. C.: see Warfield, R. W.
Phipps, M. S.: see Mattison, L. E.
Piirma, I.: see Morton, M.
Pohl, H. A., Gogos, C. G., and Cappas, C.: Resistivity studies on polymer semiconductors, 2207
Poland, D.: see Wunderlich, B.
Polowinski, S.: see Turska, E.
Price, C. C.: see Chu, N. S.
Prins, W.: see Yamada, S.
Ram, A.: see Merrill, E. W.
Rao, M. R.: see Kalpagam, V.
Rao, V. S. R., and Foster, J. F.: Depolarization of scattered light in solutions of linear and branched polysaccharides, 289
Rapson, W. H.: see Huang, R. Y.-M.
Redlich, O., Jacobson, A. L., and McFadden, W. H.: On the fractionation of polypropylene by coacervation, 393
Reed, G. A.: see North, A. M.
Reed, S. F.: see Baldwin, M. G.
Rehfeld, S. J.: see Wales, M.
Reich, L., and Stivala, S. S.: A general kinetic scheme for Ziegler-type polymerization, 203
Riechel, B., Marvel, C. S., and Greenley, R. Z.: Transannular polymerization of 1,5-cyclooctadiene, 2935
Reid, V. M.: see Crompton, T. R.
Rembaum, A. A.: see Morton, M.
Rice, D. E.: see Crawford, G. H.
Ripamonti, A.: see De Santis, P.
Roe, R.-J., and Krigbaum, W. R.: A thermodynamic study of Viton elastomer, 2049

Rogers, M. G.: see Barrer, R. M.
Roig, A.: see Krigbaum, W. R.
Roldan-Gonzalez, L.: see Heritage, K. J.
Rolle, C. J.: see Kumins, C. A.
Rosen, B.: Some mechanical aspects of the swelling and shrinking of polymeric solids. Part I. External and internal restraints (article in *J. Polymer Sci.*, **58**, 821–837, 1962), 1472
Rosen, I., McCain, G. H., Endrey, A. L., and Sturm, C. L.: Syndiotactic polyvinyl formate and derived polyvinyl alcohol, 951
Rosenzweig, W.: see Salovey, R.
Rossi, A.: see Odian, G.
Roteman, J.: see Kumins, C. A.
Roth, P. I.: see Shultz, A. R.
Rubin, I. D.: Isomorphism in polycarbonates. Copolymers of hydroquinone and substituted hydroquinones, 1645
Rudd, J. F., and Gurnee, E. F.: The effect of molecular weight distribution on the optical properties of polystyrene in the transition region, 2857
Rudin, A., and Mackie, J. S.: Some anomalous brittleness temperatures of polyethylene, 2075
Rybnikar, F.: Mechanism of secondary crystallization in polymers, 2031
Saba, R. G., Sauer, J. A., and Woodward, A. E.: Dynamic shear behavior of poly-(γ-benzyl L-glutamate), poly(D,L-propylene oxide), and poly(ethyl vinyl ether), 1483
Sabia, R., and Eirich, F. R.: Viscoelastic behavior of plasticized polyvinyl chloride at large deformations. I. Stress relaxation, 2497
——, and ——: II. Creep, 2511
Sacks, W.: see Cotten, G. R.
St. Pierre, L. E.: see Huggins, C. M.
Sakurada, Y.: Polymerization of α-methylstyrene with $Al(C_2H_5)_3$–$TiCl_4$ catalyst, 2407
Salame, M.: see Bixler, H. J.
Salovey, R., and Dammont, F. R.: Irradiation of polyethylene oxide and polypropylene, 2155
——, and Rosenzweig, W.: Radiation dosimetry in polyethylene with silicon solar cells, 2145
Saltman, W. M.: Separated aluminum alkyl-titanium tetrachloride catalysts for isoprene polymerization, 373
Sauer, J. A.: see Chappell, S. E.
——: see Saba, R. G.
Saul, B.: see Mattison, L. E.
Sautter, Mrs. H.: see Hawkins, W. L.
Scanlan, J., and Thomas, D. K.: Cross-linking of natural rubber by dicumyl peroxide in the presence of oxidation inhibitors, 1015
Schmidt, P. G.: Polyethylene terephthalate structural studies, 1271
——: Polypropylene structure, 2317
Schmorak, J., and Lewin, M.: The chemical and physiochemical properties of wheat starch mildly oxidized with alkaline sodium hypochlorite, 2601
Schonhorn, H.: Generalized approach to adhesion via the interfacial deposition of amphiphatic molecules. I. Adhesion of polyethylene to aluminum, 2343
——: II. Adhesion of polyethylene to aluminum, 3523
Sekiguchi, H.: Mécanisme réactionnel de la polymérisation alcaline des lactames, 1627
Sharma, M. G., and Haas, T. W.: Some viscoelastic studies on Penton, 3079
Shashoua, V. E.: Static electricity in polymers. II. Chemical structure and antistatic behavior, 169
Shibano, H.: see Tabata, Y.
Shida, S.: see Ueda, H.
Shima, M., and Kotera, A.: Copolymerization characteristics of methyl acrylate and methyl methacrylate. I. Study of copolymerization kinetics by a deuterium tracer method, 1115
Shio i, Y., Ohnishi, S.-I., and Nitta, I.: ESR study of irradiated acrylic acid and reaction of the produced radical, 3373
Shipman, J. J., and Golub, M. A.: Infrared study of the reaction of polyisoprene and polybutadiene with sulfur by the use of deuterated polymers (article in *J. Polymer Sci.*, **58**, 1063–1082, 1962), 832
——: see Krimm, S.
Shono, T., and Marvel, C. S.: Polymers derived from unsaturated esters of hydronopoxyalkanols, 1543
——, and ——: Preparation and polymerization of vinyl 12-hydroxystearate, 2067
Shultz, A. R., Roth, P. I., and Berge, J. M.: Radiation degradation of polymethacrylates. Dose rate and medium effects, 1651
Shuttleworth, R.: see Moore, W. R.
Silverman, M. S.: see Soulen, J. R.
Simha, R.: see Utracki, L.
Simosaka, M.: see Sisido, K.
Sisido, K., Kusano, N., Noyori, R., Nozaki, Y., Simosaka, M., and Nozaki, H.: Polycondensation of xylylene dibromides by transition metals in water suspension, 2101
Skorko, M.: see Kryszewski, M.
Sliemers, F. A.: see Ungar, I. S.
Smets, G., and Van Humbeeck, W.: Reaction kinetics and tacticity of macromolecules. II. Acrylic acid copolymers, 1227
Smith, M. E.: see Arnett, R. L.
Smith, R. K.: see Cooper, W.
Smith, T. L.: Ultimate tensile properties of elastomers: I. Characterization by a time and temperature independent failure envelope, 3597
Smith, W. E., and Zelmer, R. G.: An interpretation of ethylene polymerization with alkyl-promoted transition-metal catalysts, 2587
Smolin, E. M.: see Koral, J. N.

Sobel, M.: see Odian, G.
Sobue, H., and Murakami, K.: Maximum relaxation time on polymers in the vicinity of critical molecular weight, 2039
——: see Tabata, Y.
Soulen, J. R., Silverman, M. S.: Polymerization of phosphonitrilic chloride trimer at high pressures and temperatures, 823
Spindler, M. W.: see Miller, S. M.
Starkweather, H. W., Jr., Whitney, J. F., and Johnson, D. R.: Crystalline order in nylon 66, 715
Stephens, W. D.: see McIntosh, C. R.
Stephenson, C. V., and Wilcox, W. S.: Ultraviolet irradiation of plastics. IV. Further studies of environmental effects on films and fibers, 2741
Stein, R.: see Van Leemput, R.
Steingiser, S.: see Baumann, G. F.
Sterling, C.: see Bourne, M. C.
——: see Morsi, M. K. S.
Stivala, S. S.: see Reich, L.
Stockmayer, W. H.: see Merrill, E. W.
Stockton, F. D.: see Nielsen, L. E.
Stokes, S.: see Fox, R. B.
Stross, F. H.: see Bruss, D. B.
Sturm, C. L.: see Rosen, I.
Sugai, S., and Woodward, A. E.: Counterion binding in partially neutralized copolymers of crotonic acid and vinyl alcohol, 2127
Sullivan, P.: see Wunderlich, B.
Sweeting, O. J.: see Hansen, O. C., Jr.
Symons, N. K. J.: Growth of single crystals of polytetrafluoroethylene from the melt, 2843
Tabata, Y., Shibano, H., Sobue, H., and Hara, K.: Radiation-induced cationic polymerization of ethylene, 1049
Tabor, B. E.: see Davis, P.
Tadokoro, H., Murahashi, S., Yamadera, R., and Kamei, T.-I.: Infrared absorption spectra of polyacrylonitrile and deuterated polyacrylonitriles, 3029
Takahashi, M.: see Tobolsky, A. V.
Takeda, M., and Iimura, K.: Studies on the configuration and conformation of vinyl-type polymers. II. Temperature dependence of the infrared spectrum of polyvinyl chloride in solution and stereoregularity (article in *J. Polymer Sci.*, **57**, 383–393, 1962), 1472
Takserman-Kroser, R.: Behavior of polymer solutions in the velocity field with parallel gradient. III. Molecular orientation in dilute solutions containing flexible chain macromolecules, 2477
——: IV. Viscosity of dilute solutions containing flexible chain macromolecules, 2487
——, and Ziabicki, A.: Behavior of polymer solutions in a velocity field with parallel gradient. I. Orientation of rigid ellipsoids in a dilute solution, 491
——, and ——: II. Viscosity of dilute solutions containing rigid ellipsoids, 507
Tanaka, H.: see Ikeda, S.
Tanner, D. D.: see Walling, C.
Taylor, C. O.: see McIntosh, C. R.
Taylor, L. D.: see Haas, H. C.
Taylor, S.: see Mattison, L. E.
Taylor, W. D., and Woodward, A. E.: Preparation and properties of copolymers of maleic anhydride and 2,2-dimethylaminoethyl methacrylate, 1473
Thomas, D. K.: see Scanlan, J.
Thomas, R. M.: see Kennedy, J. P.
——: see Kirshenbaum, I.
Thompson, J.: see Mattison, L. E.
Ticknor, L. B.: A thermodynamic method for the comparison of the order distribution in cellulose and other polymers, 243
Tiers, G. V. D., and Bovey, F. A.: Polymer NMR spectroscopy. VII. The stereochemical configuration of polytrifluorochloroethylene, 833
——: see Bovey, F. A.
Tieszen, D. O.: see Heller, J.
Timnick, A.: see Drougas, J.
Tobolsky, A. V.: Probability matrices, chain dimensions and statistical thermodynamics for semicrystalline macromolecules, 301
——, and Hartley, D. B.: Radical-anion polymerization, 15
——, Katz, D., and Takahashi, M.: Rheology of polytetrafluoroethylene, 483
——, ——, and ——: Rheology of polytetrafluoroethylene (article in *J. Polymer Sci.*, **A1**, 483–489, 1963), 1472
Toggenburger, R., Beck, K., and Gill, S. J.: Theoretical calculations of stress relaxation in concentrated solutions, 1779
——, and Gill, S. J.: Anisotropic properties of strained viscoelastic fluids. III. Birefringence of polystyrene solutions, 1765
Tokita, N., and Krigbaum, W. R.: Calculation of the displacement distance for a three-choice cubic lattic chain, 1069
Tokura, N., Matsuda, M., and Ogawa, Y.: Polymerization in liquid sulfur dioxide. Part XIII. Polymerization of styrene derivatives in liquid sulfur dioxide, 2965
Tomimatsu, Y., and Palmer, K. J.: Light-scattering studies on sugar beet arabans, 1005
Topchiev, A. V.: Some aspects of the production and study of semiconducting polymeric materials, 591
——, and Alaniya, V. P.: Synthesis of nitroolefins and an investigation of their ability to polymerize, 599
Tudos, F., Kende, I., and Azori, M.: Inhibition kinetics of the polymerization of styrene. II. Investigations on the effect of *s*-trinitrobenzene, 1353
——, ——, and ——: III. Investigations on the effect of substituted trinitrobenzenes, 1369
Turska, E., and Polowinski, S.: Examination of kinetics of graft copolymerization

on preirradiated polymethyl methacrylate, 2085
Tsuchida, Y.: see Iwasaki, K.
Ueda, H., Kuri, Z., and Shida, S.: Electron spin resonance studies of the reaction of gases with the radicals formed in irradiated polytetrafluoroethylene, 3537
Ungar, I. S., Kircher, J. F., Gager, W. B., Sliemers, F. A., and Leininger, R. I.: Radiolysis of the isomeric poly(butyl methacrylates), 277
Utracki, L., and Simha, R.: Corresponding state relations for the viscosity of moderately concentrated polymer solutions, 1089
Vale, R. L.: see Miller, S. M.
VanDenBerghe, J.: see Dunham, K. R.
Van Humbeeck, W.: see Smets, G.
Van Leemput, R. and Stein, R.: Experimental data on dilute polymer solutions. I. Hydrodynamic properties and statistical coil dimensions of poly(*n*-butyl methacrylate), 985
Vaughan, G.: see Cooper, W.
Vogel, H., and Marvel, C. S.: Polybenzimidazoles. II, 1531
Vogelsong, D. C.: Crystal structure studies on the polymorphic forms of nylons 6 and 8 and other even nylons, 1055
Waight, E. S.: see Jager, P.
Wales, M., and Rehfeld, S. J.: Molecular weight distribution by velocity ultracentrifugation (article in *J. Polymer Sci.*, **62**, 179–196, 1962), 3668
Wall, L. A.: see Florin, R. E.
Walling, C., and Tanner, D. D.: Organic reactions under high pressure. IX. The effect of pressure on the stereochemistry of methyl methacrylate polymerization, 2271
Walters, M. H.: Fibrous structure in stretched crystalline elastomers, 3091
Warfield, R. W., and Petree, M. C.: Thermodynamic properties of polymethyl methacrylate and methyl methacrylate, 1701
Warwicker, J. O.: The diffusion of chyrsophenine G into viscose sheet, 3105
——: see Ellis, K. C.
Watanabe, M.: see Izumi, Z.
Weir, F. E.: see Hewett, W. A.
Welch, F. T.: see Zutty, N. L.
Westerman, L.: The molecular weight distribution in polypropylene, 411
White, E. F. T., and Zissell, M. J.: Polymerization of acrylonitrile in dimethylsulfoxide, 2189
Whitney, J. F.: see Starkweather, H. W., Jr.
Wich, G. S., and Brodoway, N.: Relative reactivity ratios for two new 2-chloro-1,3-butadiene systems, 2163
Wilcox, W. S.: see Stephenson, C. V.
Wiley, R. H., and Davis, B.: Tracer techniques for the determination of monomer reactivity ratios. V. Monomer reactivity ratios for styrene–isoprene copolymerization, 2819
——, and Mayberry, G. L.: Tracer techniques for the determination of monomer reactivity ratios. IV. Copolymerization characteristics of some divinyl monomers, 217
Wilson, C. W., III: NMR study of molecular chain structure of polyvinylidine fluoride, 1305
Winslow, E. C., and Gershman, N. E.: Phthalocyanine-crosslinked polyvinylphthalic acid, 2383
——, and Marriott, J. A.: Effect of crystallization on the thermal stability of polyvinylphthalic acid and its methyl ester, 321
Winslow, E. C.: see Horrocks, R. H.
Wippler, C., and Gautron, R.: Étude de l'influence du tetrahydrofurane sur la radioreticulation du chlorure de polyvinyle, 943
Woermann, D.: see Debye, P.
Wood, J. W., and Mora, P. T.: Preparation and biological application of highly substituted cationic derivatives of polysaccharides, 3511
Woodward, A. E.: see Chappell, S. E.
——: see Saba, R. G.
——: see Sugai, S.
——: see Taylor, W. D.
Worthington, Mrs. M. A.: see Hawkins, W. L.
Wu, T. S.: see Hsiao, C. C.
Wunderlich, B.: The effect of pressure on the crystallization of polyethylene from dilute solution, 1245
——, and Poland, D.: Thermodynamics of crystalline linear high polymers. II. The influence of copolymer units on the thermodynamic properties of polyethylene, 357
——, Sullivan, P., Arakawa, T., Dicyan, A. B., and Flood, J. F.: Thermodynamics of crystalline linear high polymers. III. Thermal breakdown of the crystalline lattice of polyethylene, 3581
Yakashima, S.: Effect of ions on the dielectric dispersion of ovalbumin solution, 2791
Yamada, S., Prins, W., and Hermans, J. J.: Determination of number-average molecular weights by elastoosmometry, 2335
Yamadera, R.: see Tadokoro, H.
Yamamoto, A.: see Ikeda, S.
Yoda, N.: Syntheses of polyanhydrides. XII. Crystalline and high melting polyamidepolyanhydride of methylenebis(*p*-carboxyphenyl)amide, 1323
Yonezawa, T.: see Hayashi, K.
Yoshino, T., and Manabe, Y.: Photosensitivity of dry-heated polyacrylonitrile, 2135
Zambelli, A., Dipietro, J., and Gatti, G.: The nature of active components in catalytic systems prepared from $TiCl_3$, monoalkylaluminum dihalides, and

electron-donor substances, in the polymerization of propylene, 403
Zelmer, R. G.: see Smith, W. E.
Ziabicki, A.: see Takserman-Krozer, R.
Zilkha, A., and Avny, Y.: Polymerization of acrylonitrile by electron transfer catalysts, 549
——, Barzarkay, S., and Ottolenghi, A.: Effect of solvents on the anionic polymerization of styrene by phenyllithium, 1831
——: see Ottolenghi, A.
Zimmerman, F. E.: see Owens, F. H.
Zissell, M. J.: see White, E. F. T.
Zlámal, Z., and Kazda, A.: Donor–acceptor interaction in cationic polymerization. V. Influence of some alcohols on the molecular weight of polyisobutylene in polymerization catalyzed by aluminum trichloride, 3199
Zutty, N. L.: Copolymerization studies. IV. Transannular copolymerization of bicyclo[2.2.1] hepta-2,5-diene, 2231
——, and Welch, F. J.: Synthesis of vinyl polymers containing α-substituted γ-butyrolactone groups in their backbones, 2289
——: see Burkhart, R. D.

SUBJECT INDEX, VOLUME 1

Acrylic acid copolymers, 1227
Acrylonitrile, anionic polymerization of, 3643
  copolymerization of, 705
  polymerization by electron transfer catalysts, 549
  polymerization in dimethylsulfoxide, 2189
  termination of anionic polymerization at low catalyst concentrations, 687
Adhesion, relationships between viscoelasticity, interfacial equilibrium, and the temperature dependence of, 2241
  via the interfacial deposition of amphiphatic molecules, 2343, 3523
Adhesive failure, locus of, 1339
Afterglow studies, luminescent compounds in solid polymers, 3067
Aldehydes, copolymerization of, 3439
Alicyclic epoxides, polymerization with aluminum alkyl catalysts, 2777
Alkyl methacrylates, diffusion-controlled polymerization of, 1311
Allene, polymerization, by organometallic initiation, 655
Allylic compounds, polymerization studies on, 1919
Aluminum alkyl catalysts, polymerization of alicyclic epoxides with, 2777
Aluminum alkyl–titanium trichloride catalyst, copolymerization with, 1439
Amine-epoxide adducts, hydrogen bonding, 385
3,3-Bis(aminomethyl)-oxetane, polymeric derivatives of, 2525
Amorphous high polymers, 3459, 3477
Amphipathic molecules, adhesion via the interfacial deposition of, 2343, 3523
Anionic block polymerization, styrene on polystyrene, 2171
Anionic polymerization, homogeneous, 443, 461, 475
  of acrylonitrile, 3643
  of styrene, effect of solvents on, 1831
  termination, of acrylonitrile, 687
Antistatic behavior, 169
Archibald ultracentrifugal method, study of dilute polymer solutions, 3303
Aromatic polyimides, 3135
N-Arylmethacrylamides, solid state polymerization of, 1909
Azrechtic acid, gums viscosity of, 1429
Bicyclo[2.2.1]hept-2,5-diene, transannular copolymerization of, 2231
Biocolloids, 1429
Birefringence, of Viton fluoroelastomer, 1
Branched macromolecules, molecular configuration of, 227
Bulk copolymerization, methyl methacrylate with phenyldichlorophosphine, 1963
Butadiene, stereospecificity of a Ziegler catalyst used in the polymerization of, 2003
Butyllithium, 475
  kinetics of butadiene and isoprene polymerization with, 1735
γ-Butyrolactone, synthesis of vinyl polymers containing α-substituted, 2289
ε-Caprolactam, copolymerization of, 111
Carbon black substitutes, 3489
Carbonium ion rearrangement, in cationic polymerization of branched alpha olefins, 2299
Carboxymethylcellulose, 2881
Catalysts, electron transfer, 549
  separated aluminum alkyl–titanium tetrachloride, for isoprene polymerization, 373
Cationic polymerization, donor–acceptor interaction in, 3199
  fundamental studies, 331, 789
  radiation-induced, of ethylene, 1049
Cell theory, amorphous high polymers, 3459
Cellulose, acid behavior of carboxylic derivatives of, 2881, 2893
  crystallinity and structure, 671
  dry swollen, calorimetric measurements of heat of sorption of water vapor on, 3333
  filaments, regenerated, crystallite orientation in, 1185
  grafting vinyl polymers onto, 1257
  γ-irradiated, electron spin resonance of, 1163
Cellulose–*d,l*-butadiene diepoxide reaction, 3407
Cellulose acetate, thermodynamic properties of solutions of, 733
Cellulose nitrate, thermodynamic properties of solutions of, 733
Cellulose triacetate, crystals, hydrolysis of, 1893
  growth and morphology of single crystals of, 1875
  thermodynamic properties of solutions of, 1985
Chain dimensions, for semicrystalline macromolecules, 301
Chain scission processes, evaluation of molecular weight averages resulting from, 3175
2-Chloro-1,3-butadiene systems, relative reactivity ratios, for, 2163
Chrysophenine G, diffusion into viscose sheet, 3105
Coacervation, fractionation of polypropylene by, 393
Cole–Cole diagram, for methylcellulose in water, 151
Conformations, helical, stability of, 1383

Counterion binding, in partially neutralized copolymers of crotonic acid and vinyl alcohol, 2127
Critical molecular weight, 2039
Crosslinking, kinetic study of, 799
radiation-induced, 2731
Crystal–crystal transition, in poly-1-butene, 59
Crystal structure studies, on polymorphic forms of nylons 6 and 8 and other even nylons, 1055
Crystalline high polymers, properties of melt-blends, 3427
linear, thermodynamics of, 3579
Crystalline lattice of polyethylene, thermal breakdown of, 3579
Crystalline order, in nylon 66, 715
Crystalline polymers, theory of the modulus of, 1995
Crystallite orientation, in regenerated cellulose filaments, 1185
Crystallization, of high polymers, studies by differential thermal analysis, 2697
mechanism of secondary, 2031
of polyacrylonitrile, 2765
Cubic lattice chain, three-choice, calculation of displacement distance, 1069
1,5-Cyclooctadiene, transannular polymerization of, 2935
Diallyl phenyl phosphine oxide, copolymerization of, with *n*-lauryl methacrylate, 3357
Depolarization measurements, of polymer solutions in high dilutions, 517, 921
Dibutylzinc, cocatalysts for the linear polymerization of epoxides by, 85
Dicumyl peroxide, crosslinking of natural rubber by, 1015
trans-1,2-Dideuteroethylene, and *cis*-1,2-dideuteroethylene by a Ziegler catalyst, 2925
Dielectric dispersion, effect of ions on, 2791
Diene polymers, melting transitions, 159
Differential thermal analysis, crystallization of high polymers by, 2697
of high polymers, material and experimental factors, 1453
Diffusion coefficients, effect of solid polymer interaction on, 549
Diffusion constants, of a maltosaccharide series, 817
Dimaleimides, accelerators for radiation-induced vulcanization of hydrocarbon polymers, 2537
2,2-Dimethylaminoethyl methacrylate, preparation and properties of copolymers of, 1473
2,3-Dimethylbutadiene-1,3, emulsion polymerization of, 2679
Dimethylsulfoxide, polymerization of acrylonitrile in, 2189
Diphenylvinylphosphine oxide, ionic polymerization of, 3627
Dipole moments, of Viton fluoroelastomer, 1
Distribution, order of, in cellulose, 243
particle size, in polymer solutions, 577
DNA, graft copolymer of polyacrylic acid with, 2309
Dynamic modulus, tensile, apparatus for measuring, 1585; *erratum*, 3668
Ebullioscope, for high polymers, 2753
Elastomers, mastication of, 2261
nitroso fluorocarbon, 565
tensile properties of, 3595
Elastoosmometry, determination of number-average molecular weights by, 2335
Electron-donor substances, catalytic systems prepared from, 403
Electron exchange polymers, 1971
Electron spin resonance, of gamma-irradiated cellulose, 1163
of polypropylene, 2251
Electron spin resonance studies, reaction of gases with radicals formed in irradiated polytetrafluoroethylene, 3537
of peroxide radicals in irradiated polypropylene, 2109
Ellipsoids, rigid, orientation in a dilute solution, 491
rigid, viscosity of dilute solutions containing, 507
Elution fractionation, crystalline polypropylene, 2361
Emulsion polymerization, Co^{60} gamma ray initiated, 3009
Epoxides, linear polymerization, 85
Ethylcyclohexane, 255
Ethylene, cationic copolymerization, radiation-induced, 1049
model copolymerizations, reactivity ratios of, 1137
polymerization with alkyl-promoted transition metal catalysts, 2587
Ethylene–propylene copolymers, crystallinity in, 2119
properties of rubber obtained from, 3567
Exoxysuccinyl chloride, polymeric derivatives of, 2525
Failure envelope, characterization of elastomer by, 3595
Fibers, dynamic bending properties of, 2240
Fracture processes, in polymeric materials, 993
Gas transmission, in irradiated polyethylene, 895
Gaseous diffusion, through polymers, 3477
Gelatin, kinetic study of the crosslinking of, by formaldehyde and glyoxal, 799
Glass temperature depression, by plasticizers, molecular interpretation of, 1417
Graft copolymers, of polyacrylic acid with DNA, 2309
Graft, copolymerization, high energy radiation-induced, 1257
kinetics of, on preirradiated polymethyl methacrylate, 2085
radiation-induced, of styrene to nylon, 639
Heterogeneous polymerization, rate study of methyl acrylate in aqueous solution, 877
High polymers, crystalline, linear, 357

Homogeneous anionic polymerization, 1735
Homopolymers, kinetics of nucleation and growth of spherulites in, 3317
Hydrogen bonding, in amine-epoxide adducts, 385
Hydronopoxyalkanols, polymers derived from unsaturated esters of, 1543
Intrinsic viscosity, in polyisobutylene–*n*-alkane systems, 3265
of polymers undergoing simultaneous degradation and crosslinking, 3289
Inversion temperature, theory of, 331
Ion-enchange resins, activity of small ions in, 139
Ionic polymerization, of diphenylvinylphosphine oxide, 3627
Ionized polymers, turbidimetric method for estimation of, 3385
Irradiated acrylic acid, ESR study of, 3373
Isoprene, polymerization, catalysts, 373
Lactames, reaction mechanism of the alkaline polymerization of, 1627
Lactam derivatives, effect of amide group on the polymerizability of, 3151
n-Lauryl methacrylate, copolymerization of diallyl phenyl phosphine oxide with, 3357
copolymerization of phosphonates with, 3343
Light scattering studies, on sugar beet arabans, 1005
Lithium alkyls, 461
Lyotropic series, role of ions in, 3547
Macromolecules, flexible chain, molecular orientation in dilute solutions containing, 2477
flexible chain, viscosity of dilute solutions containing, 2487
reaction kinetics and tacticity of, 1227
Magnesium halides, catalytic reactivity of, 1937
Maleic anhydride, homopolymerization of, 1115
preparation and properties of copolymers of, 1473
Maltosaccharide series, diffusion constants of, 817
Membranes, heterogeneous, 2565
Metallic chelates, of oxine–formaldehyde polymers, 3655
role in polymerization initiation, 2179, 2185
Metal chelate polymers, from tetraacetylethane, 267
Methacrylamide, solid state polymerization of, 1909
Methyl acrylate, study of rate of heterogeneous polymerization, 877
Methylcellulose, in water, dielectric relaxation time spectrum, 151
Methylcellulose solutions, molecular weight and aggregate formation in, 311
Methylenebis(*p*-carboxyphenyl)amide, crystalline and high melting polyamidepolyanhydrides of, 1323
Methyl methacrylate, bulk copolymerization of, 1963
polymerization, effect of pressure on the stereochemistry of, 2271
polymerization, primary radical termination in, 3209
thermodynamic properties of, 1701
4-Methyl-1-pentene, dynamic properties of homo- and copolymers of, 1239
α-Methylstyrene, polymerization with $Al(C_2H_5)_3$–$TiCl_4$ catalyst, 2407
Molecular orbital theory, of reactivity, in radical polymerization, 1405
Molecular weight averages, evaluation for wide Schulz–Zimm distributions, 3175
Molecular weight distribution, by velocity ultracentrifugation (*erratum*), 3668
Monoalkylaluminum dihalides, catalytic systems prepared from, 403
Monomer reactivity ratios, molecular orbital calculation (*erratum*), 1088
tracer techniques for the determination of, 2819
Natural rubber, crosslinking by dicumyl peroxide, 1015
proton magnetic resonance in, 2905
Newtonian viscosity number, the second, 1201
p-Nitrobenzeneazotyrosine, coordination compounds, 3449
Nitroolefins, synthesis, and ability to polymerize, 599
Nitrosation, of linear phenol–formaldehyde polymers, 3615
Nonpolar solvents, effect on viscosity and molecular weight, 233
Nonrandom copolymers, synthesis of styrene–methyl methacrylate, in emulsion solutions, 2419
Nuclear magnetic resonance, in polypyrrolidone, 2279
Nuclear magnetic resonance study, of molecular chain structure of polyvinylidene fluoride, 1305
of polydimethylsiloxanes, 2731
Nucleating effect, on the kinetics of crystallization, 2013
Number-average molecular weights, determination by elastoosmometry, 2335
Nylon, graft polymerization of, to styrene, 639
Nylon 6, spherulites of, 2013
Nylons 6 and 8, crystal structure studies on polymorphic forms, 1055
Nylon 66, crystalline order in, 715
turbidimetric titration of, 2667
Olefins, aliphatic, and styrene, copolymerization of 2021
α-Olefins, carbonium ion rearrangement in the cationic polymerization of branched, 2299
competing side reactions in the polymerization of, 2467
Olefin polymerizations, 1839
Organometallic compounds, reaction of polymeric radicals with, 1553
Organo-sulfur compounds, mechanism of stabilization, 3499
Osmotic pressure measurements, 2439
Ovalbumin solution, effect of ions on the dielectric dispersion of, 2791

Oxine–formaldehyde polymers, and their metallic chelates, 3655
Oxycellulose, 2893
Penton, viscoelastic studies, 3079
Peroxide radicals, electron spin resonance study of, in polypropylene, 2109
Phenol–formaldehyde polymers, nitrosation of, 3615
Phenyldichlorophosphine, bulk copolymerization of methyl methacrylate with, 1963
Phenyllithium, effect of solvents on the anionic polymerization of styrene by, 1831
Phosphonates, copolymerization of, with *n*-lauryl methacrylate, 3343
Phosphonitrilic chloride trimer, polymerization at high pressures and temperatures, 823
Photochlorination, of polymethyl methacrylate, 2711
Photolytic degradation, of polymethyl methacrylate, 1079
Plastics, ultraviolet irradiation of, 2741
Polar solvents, effect on viscosity and molecular weight, 233
Polyacrylamide, in aqueous solution, 849
Polyacrylates, diffusion of benzene in, 1799
Polyacrylic acid, graft copolymers of, with DNA, 2309
  temperature dependence of magnesium chloride interaction with, 1955
Polyacrylic anhydride, structure of, 1491
Polyacrylonitrile, crystallization and melting behavior of, 2765
  deuterated, infrared absorption spectra of 3029
  dry-heated, photosensitivity of, 2135
Polyaldehydes, optical rotatory properties of, 2193
Polyamides, containing phosphorus, 863
  oriented, radiation damage, 189
6–10 Polyamide, viscosity–molecular weight relationship and some molecular characteristics of, 1147
Polyanhydrides, synthesis of, 1323
Polybenzimidazoles, 1531
Poly(γ-benzyl L-glutamate), dynamic shear behavior, 1483
Polybutadienes, infrared spectra and structures of, 47
  structure effects and related polymer properties in, 2945
Poly-1-butene, kinetics of crystallization, 59
Polybutyl methacrylates, radiolysis of isomeric, 277
Poly(*n*-butyl methacrylate), hydrodynamic properties and statistical coil dimensions, 985
Polycarbonate, degradation of, by ionizing radiation, 1671
  isomorphism in, 1645
  rheological measurements on, 3395
Polycondensation, interfacial, 1147
Poly-1,3-cyclohexadiene, preparation and aromatization, 2057
Polydiacrylylmethane, 3261
Polydicarboxylic acid copolymers, high frequency titration, 1609
Polydideuteroethylene, stereoregulated, 2925
Polydimethylsiloxanes, NMR studies of, 2731
Polyelectrolytes, 1429
Polyelectrolyte–salt solutions, additivity of osmotic properties of, 2093
  rodlike, thermodynamic properties of, 1501
Polyelectrolyte solutions, colligative properties, 3231
Polyethylene, adhesion to aluminum, 2343, 3523
  with *n*-alkanes, 3217
  anomalous brittleness, temperatures of, 2075
  effect of pressure on the crystallization of, 1245
  electron spin resonance study of radiation oxidation of, 605
  influence of copolymer units on the thermodynamic properties of, 357
  irradiated, gas transmission, 895
  linear, molecular weight distribution, 103
  long-chain branching frequency in, 2869
  molecular motion in, 1175
  molecular structure, 1721
  oxidative crosslinking of, by ultraviolet light, 1345
  radiation dosimetry in, 2145
  single crystals, morphology of, 1901
Polyethylene oxide, irradiation of, 2155
Poly(ethyl vinyl ether), dynamic shear behavior of, 1483
Polyglycol autoxidations, influence of transition metal salts in, 2551
Polyisobutylene, melt viscosity, 1865
Polymethyl methacrylate, in aqueous suspension, photochlorination of, 2711
  grafting to granular corn starch, 1025
  photolytic degradation, 1079
  preirradiated, examination of kinetics of graft copolymerization on, 2085
  thermodynamic properties, 1701
  in various solvents, 2651
  viscosities of dilute solutions, 929
  molecular structure obtained by Ziegler catalysis, 2225
  self-diffusion and nuclear relaxation in, 1709
Polyisobutylene–*n*-alkane systems, application of Prigogine solution theory to intrinsic viscosities in, 3265
Polyisoprene, infrared spectra and structures of, 37
  molecular weight of, initiated by butyllithium, 475
cis-Polyisoprene, masticated, synthetic, solution properties of, 2261
Polyitaconic acid-*Co*-styrene, 1609
Polymaleic acid-*Co*-styrene, 1609
Polymer chain dimensions, diluent effects, 1947
Polymer crystal growth, from concentrated solutions, 763

Polymer semiconductors, resistivity studies on, 2207
Polymer solutions, behavior in velocity field, 2477, 2487
polymer–solvent interaction, 2395
Polymer–solvent systems, phase equilibria of, 3217
Polymer systems, branched, orientation and strength, 1789
Polymeric solids, mechanical aspects of swelling and shrinking (*erratum*), 1472
Polymeric transfer constants, of vinyl acetate, 3043
Polymerization processes, enthalpy and free energy changes in, 1979
Polymethacrylamide, in aqueous solution, 849
Polymethacrylates, radiation degradation of, 1651
Polymethacrylic acid, influence of pH of polymerization medium on stereochemical configuration, 843
Poly (4-methyl pentene), x-ray measurement of crystalline density and observation of a structural anomaly, 2219
Poly-α-methylstyrenes, preparation and properties of, 1927
Polyolefin, molecular weight distribution, 1839
Poly-α-olefin, properties, effect of side-chain structure on, 751
Polyoxyethylene glycols, ebulliometric and endgroup molecular weights of, 2213
Polyoxymethylene, crystal structure of new form, 965
structure of normal crystal form, 1573
Polyoxypropylene glycols, ebulliometric and endgroup molecular weights of, 2213
Polypropylene, crystalline, elution fractionation of, 2361
effects of high energy irradiation on, 2805
electron spin resonance of, 2251
electron spin resonance study of radiation oxidation of, 625
electron spin resonance study of peroxide radicals in, 2109
fractionation by coacervation, 393
irradiation of, 2155
molecular weight distribution, 411
polymerization, kinetics of, 425
structure, 2317
Polypropylene glycol 2025, molecular weight distribution in, 1041
Poly(D,L-propylene oxide), dynamic shear behavior, 1483
Polypyrrolidone, solid, nuclear magnetic resonance in, 2279
Polysaccharides, crystalline, infrared spectrum, 1687
highly substituted cationic derivatives of, 3511
linear, branched, depolarization of scattered light in solutions of, 289
solution properties, 311
Polystyrene, in benzene, molecular configuration of, 2387
Polystyrene, effect of molecular weight distribution on the optical properties in the transition region, 2857
in ethylcyclohexane, critical opalescence, 255
γ-irradiated, electron spin resonance spectra of, 1521
high impact, unsaturation in, 347
melt viscosity of, 1857
molecular weight of, initiated by lithium alkyls, 461
molecular weights of, initiated by sodium naphthalene, 443
narrow molecular weight distribution, 1749
solutions, birefringence of, 1765
Polytetrafluoroethylene, growth of single crystals from the melt, 2843
Polytrifluorochloroethylene, stereochemical configuration, 833
Polyvinyl alcohol, derived from syndiotactic polyvinyl formate, 951
stereoregularity in, 1509
ultraviolet absorption spectrum, 1215
Poly(vinyl chloride), electron spin resonance study of radiation oxidation of, 625
influence of tetrahydrofurane on the radioreticulation of, 943
infrared spectra and assignments for, 2621
plasticized, viscoelastic behavior of, creep, 2511
plasticized, viscoelastic behavior of, stress relaxation, 2497
Polyvinyl formate, syndiotactic, and derived polyvinyl alcohol, 951
Polyvinylidene fluoride, NMR study of molecular chain structure of, 1305
Polyvinylphthalic acid, effect of crystallization on thermal stability, 321
phthalocyanine-crosslinked, 2383
Prigogine solution theory, application to intrinsic viscosities, 3265
helical structure, 1099
radiation effects in, 1621
reaction of gases with the radicals formed in irradiated, 3537
rheology of, 483; *erratum*, 1472
Probability matrices, for semicrystalline macromolecules, 301
Propylene, polymerization by the Phillips catalytic system, 2989
polymerization, nature of active components in catalytic systems, 403
dl-Propylene oxide, polymerization of, with optically active catalyst systems, 1105
α-Pyrrolidone, copolymerization of, 111
Q-e calculations, reactivity ratios used in, 1137
Radiation dosimetry, in polyethylene with silicon solar cells, 2145
Radiation oxidation of polymers, electron spin resonance study of, 605, 625
Radical-anion, polymerization, 15
Radiolysis, of isomeric poly(butyl methacrylates), 277
Random crosslinking, evaluation of

molecular weight averages resulting from, 3175
Rat tail tendon, kinetic analysis of swelling of, 23
Reactivity ratios, monomer, determination, 217
of model ethylene copolymerizations and their use in Q-e calculations, 1137
Relaxation processes, liquid, reference point for, 1857, 1865
Relaxation time, on polymers in vicinity of critical molecular weight, 2039
Rheology, of polytetrafluoroethylene, 483; *erratum*, 1472
Rotation, unrestricted, in polymers, 2459
Rubber, elastic properties of, 3567
filled, diffusion in, 2565
synthetic, 2537
Schulz–Zimm distributions, wide, 3175
Sedimentation velocity analysis, 103
Semiconducting polymeric materials, production and study, 591
Semicrystalline macromolecules, 301
Side-chain structure, effect on poly-α-olefin properties, 751
Sodium hyaluronate films, strain birefringence, 725
Sodium naphthalene, 443
Sodium polyacrylates, conductivity and viscosity measurements of, 3021
p-Sodium styrene sulfonate, copolymerization of, 705
Solid polymers, interactions of low molecular weight compounds with, 2327
Solution polymerization, some novel effects of, 1465
Spectroscopy, polymer NMR, 833, 843, 849
Starch, crystallization in, 3547
State relations, corresponding, for viscosity of moderately concentrated polymer solutions, 1089
Static electricity, in polymers, 169
Stationary random sequences, general theory of, 3183
Statistical thermodynamics, for semicrystalline macromolecules, 301
Stereospecific polymerization, of vinyl alkyl ethers, 3277
Steric structures, in copolymerization, 1601
Strain birefringence, of sodium hyaluronate films, 725
Stress relaxation, of Viton fluoroelastomer, 1
theoretical calculations of, 1779
Stretched crystalline elastomers, fibrous structure in, 3091
Styrene, and aliphatic olefins, copolymerization of, 2021
copolymerization with aluminum alkyl–titanium trichloride catalyst, 1439
graft polymerization of, to cellulose, 1257
graft polymerization of, to nylon, 639
inhibition kinetics of the polymerization of, 1353, 1369
Styrene derivatives, polymerization in liquid sulfur dioxide, 2965
Styrene–isoprene copolymerization, monomer reactivity ratios for, 2819
Suberaldehyde, preparation and polymerization of, 2831
Synergistic antioxidant combinations, 3489, 3499
Tetraacetylethane, metal chelate polymers derived from, 267
Tetrahydrofurane, influence on the radioreticulation of polyvinyl chloride, 943
Thin polymer films, apparatus for measuring dynamic tensile modulus, 1585; *erratum*, 3668
Titanium dioxide–poly(vinyl acetate–vinyl chloride), copolymer films, 541
α-Titanium trichloride—diethylaluminum chloride kinetics of polypropylene polymerization catalyzed by, 425
α-Titanium trichloride-methyl polyethyl complex, stereospecific action (*erratum*), 1472
Tracer techniques, determination of reactivity ratios by, 217
Transannular polymerization, of 1,5-cyclooctadiene, 2935
Transition metal catalysts, ethylene polymerization with alkyl-promoted, 2587
Transition metal salts, influence in polyglycol autoxidations, 2551
Transition temperature, effect of solid polymer interaction on, 549
Trinitrobenzene, substituted, effect on polymerization of styrene, 1369
s-Trinitrobenzene, effect on the polymerization of styrene, 1353
Turbidimetric titration, of nylon 66, 2667
Unsaturation, in high impact polystyrene, 347
Velocity field, behavior of polymer solutions in, 491, 507
Velocity ultracentrifugation, molecular weight distribution by (*erratum*), 3668
Vibrating reed, transient analysis, 1693
Vinyl alkyl ethers, stereospecific polymerization of, 3277
9-Vinylanthracenes, and 1-, polymerization of, 1635
N-Vinylcarbazole, polymerization with Zeigler-type catalyst systems, 125
Vinyl ethers, polymerization with magnesium compounds, 1937, 2371
Vinylhydroquinone dibenzoate, copolymerization behavior of, 1971
Vinyl 12-hydroxystearate, preparation and polymerization of, 2067
Vinyl polymers, containing α-substituted γ-butyrolactone groups in their backbones, 2289
Vinyl-type polymers, studies on configuration and conformation (*erratum*), 1472
Viscoelastic behavior, of polyvinyl chloride, 2497, 2511
Viscoelastic fluids, anisotropic properties of, 1765
Viscosity, of critical mixtures, 249

Viton elastomer, thermodynamic study of, 2049
Viton fluoroelastomer, 1
Vulcanization, radiation-induced, 2537
Water sorption, 541
Weissenberg effect, theory for surface elevation, 261
Wheat starch, chemical and physicochemical properties of, 2601
Xylylene dibromides, polycondensation by transition metals in water suspension, 2101
Zone-refining fractionation, 3163
Ziegler catalyst, changes in the stereospecificity of, 2003
Ziegler-type catalyst systems, 125
Ziegler-type polymerizations, a kinetic scheme for, 203

Journal of Polymer Science

PART A: GENERAL PAPERS

Volume 1, 1963

Editorial Board: R. M. FUOSS · J. J. HERMANS · H. MARK
H. W. MELVILLE · C. G. OVERBERGER · G. SMETS

N. G. GAYLORD, Book Review Editor

Advisory Board:

T. ALFREY, JR.
Midland, Mich.

W. O. BAKER
Murray Hill, N. J.

H. BENOIT
Strasbourg

C. J. BEVINGTON
Birmingham

J. W. BREITENBACH
Vienna

A. M. BUECHE
Schenectady, N. Y.

C. W. BUNN
Welwyn Garden City

G. M. BURNETT
Aberdeen

F. S. DAINTON
Leeds

P. DEBYE
Ithaca, N. Y.

F. EIRICH
Brooklyn, N. Y.

P. J. FLORY
Pittsburgh, Pa.

J. FURUKAWA
Kyoto

G. GEE
Manchester

A. KATCHALSKY
Rehovoth

A. KELLER
Bristol

G. M. KLINE
Washington, D. C.

M. MAGAT
Paris

C. S. MARVEL
Tucson, Ariz.

G. NATTA
Milan

S. OKAMURA
Kyoto

A. PETERLIN
Durham, N. C.

C. C. PRICE
Philadelphia, Pa.

CH. SADRON
Strasbourg

G. V. SCHULZ
Mainz

H. M. SPURLIN
Wilmington, Del.

A. J. STAVERMAN
Leiden

J. K. STILLE
Iowa City, Iowa

W. H. STOCKMAYER
Hanover, N. H.

M. SZWARC
Syracuse, N. Y.

A. V. TOBOLSKY
Princeton, N. J.

K. UEBERREITER
Berlin

INTERSCIENCE PUBLISHERS

Copyright © 1963, by John Wiley & Sons, Inc.

Statement of ownership, management, and circulation (Act of October 23, 1962: Section 4369, Title 39 United States Code)

1. Date of filing: September 30, 1963

2. Title of Publication: JOURNAL OF POLYMER SCIENCE

3. Frequency of issue: monthly

4. Location of known office of publication: 20th and Northampton Streets, Easton, Pennsylvania, 18042

5. Location of headquarters of general business offices of publisher: 605 Third Avenue, New York 16, New York, 10016

6. The names and addresses of publisher, editor, and managing editor:
Publisher: Eric S. Proskauer, John Wiley & Sons, Inc., 605 Third Avenue, New York 16, New York
Editor: Herman Mark, Polytechnic Institute of Brooklyn, 333 Jay Street, Brooklyn 1, New York
Managing Editor: None

7. Owner: John Wiley & Sons, Inc., 605 Third Avenue, New York 16, New York.
Stockholders owning or holding 1 per cent or more of total amount of John Wiley & Sons, Inc., stock as of September 30, 1963:

Cynthia W. Darby, 23 Farrington St., Newburgh, N. Y.; Maurits Dekker, 511 West 232nd St., Bronx, N. Y.; Rozetta S. Dekker, 511 W. 232nd St., Bronx, N. Y.; Julia W. Gilbert, Box 1191, Carmel, Calif.; Edward P. Hamilton, c/o John Wiley & Sons, Inc., 605 Third Avenue, New York 16, N. Y.; Elizabeth W. Hamilton, c/o John Wiley & Sons, Inc., 605 Third Avenue, New York 16, N. Y.; W. Bradford Wiley and Francis Lobdell, Trustees of Elizabeth W. Hamilton Trust, dated 12/23/52, c/o John Wiley & Sons, Inc., 605 Third Avenue, New York 16, N. Y.; I. M. Kolthoff, University of Minnesota, School of Chemistry, Minneapolis, Minn.; Willy Levinger, 336 Central Park West, New York, N. Y.; R. R. Pennywitt, Box 211, Mantaloking, N. J.; R. C. Runyon, Jr., 130 East End Ave., New York 28, N. Y.; Francis Lobdell and William J. Seawright, Trustees f/b/o Deborah Elizabeth Wiley, u/a dated 6/2/58, c/o John Wiley & Sons, 605 Third Avenue, New York 16, N. Y.; Kate R. Q. Wiley, 1192 Park Avenue, New York 28, N. Y.; Edward P. Hamilton, Trustee f/b/o Kate R. Q. Wiley, u/a dated 6/6/38, c/o John Wiley & Sons, Inc., 605 Third Avenue, New York 16, N. Y.; Francis Lobdell and William J. Seawright, Trustees f/b/o Peter Booth Wiley, u/a dated 6/2/58, c/o John Wiley & Sons, Inc., 605 Third Avenue, New York 16, N. Y.; K. R. Q. Wiley, E. P. Hamilton, and Cynthia W. Darby, Executors of the will of W. O. Wiley, c/o E. P. Hamilton, 605 Third Avenue, New York 16, N. Y.; Francis Lobdell and William J. Seawright, Trustees f/b/o William Bradford Wiley, 2nd, u/a dated 6/2/58, c/o John Wiley & Sons, Inc., 605 Third Avenue, New York 16, N. Y.; Adele E. Windheim, 8 Dundee Rd., Larchmont, N. Y.; W. Bradford Wiley and E. P. Hamilton, Trustees for Edward P. Hamilton Foundation, u/a dated 12/23/57, c/o John Wiley & Sons, Inc., 605 Third Avenue, New York 16, N. Y.; Powers & Co., P. O. Box 1479, Church St. Station, New York 8, N. Y.; Reing & Co., P. O. Box 491, Church St. Station, New York 8, N. Y.; Eric S. Proskauer & Charles H. Lieb, as Trustees U-A Dated 11/27/62, 220 Central Park South, New York 19, New York.

8. Known bondholders, mortgagees, and other security holders owning or holding 1 per cent or more of total amount of bonds, mortgages, or other securities: None

9. Paragraphs 7 and 8 include, in cases where the stockholder or security holder appears upon the books of the company as trustee or in any other fiduciary relation, the name of the person or corporation for whom such trustee is acting, also the statements in the two paragraphs show the affiant's full knowledge and belief as to the circumstances and conditions under which stockholders and security holders who do not appear upon the books of the company as trustees, hold stock and securities in a capacity other than that of a bona fide owner. Names and addresses of individuals who are stockholders of a corporation which itself is a stockholder or holder of bonds, mortgages or other securities of the publishing corporation have been included in paragraphs 7 and 8 when the interests of such individuals are equivalent to 1 per cent or more of the total amount of the stock or securities of the publishing corporation.

10. This item must be complete for all publications except those which do not carry advertising other than the publishers own and which are named in Sections 132.231, 132.232, and 132.233, Postal Manual (Sections 4355a, 4355b, and 4356 of Title 39, United States Code)

I certify that the statements made by me above are correct and complete:

Eric S. Proskauer
Publisher

CONTENTS

Vol. 1, Issue Nos. 1–12

Journal of Polymer Science
Part A: General Papers

ISSUE NO. 1, JANUARY

W. R. KRIGBAUM, M. KANEKO, and A. ROIG: Dipole Moments, Stress Relaxation, and Birefringence of Viton Fluoroelastomer.. 1

A. V. TOBOLSKY and D. B. HARTLEY: Radical-Anion Polymerization..... 15

HARRY R. ELDEN and MARSHA FELDMAN: A Kinetic Analysis of Swelling of Rat Tail Tendon..... 23

JOHN L. BINDER: The Infrared Spectra and Structures of Polyisoprenes..... 37

JOHN L. BINDER: The Infrared Spectra and Structures of Polybutadienes..... 47

J. BOOR, JR., and J. C. MITCHELL: Kinetics of Crystallization and a Crystal-Crystal Transition in Poly-1-Butene..... 59

K. T. GARTY, T. B. GIBB, JR., and R. A. CLENDINNING: Cocatalysts for the Linear Polymerization of Epoxides by Dibutylzinc 85

H. W. MCCORMICK: Molecular Weight Distribution of Linear Polyethylene by Sedimentation Velocity Analysis..... 103

FUMIO KOBAYASHI and KOICHI MATSUYA: Copolymerization of α-Pyrrolidone and ϵ-Caprolactam..... 111

JORGE HELLER, D. O. TIESZEN, and D. B. PARKINSON: Polymerization of *N*-Vinylcarbazole with Ziegler-Type Catalyst Systems 125

N. LAKSHMINARAYANAIAH: Activity Coefficients of Small Ions in Ion-Exchange Resins..... 139

W. KUHN and P. MOSER: The Dielectric Relaxation Time Spectrum and the Corresponding Cole-Cole Diagram for Methylcellulose in Water..... 151

W. COOPER and R. K. SMITH: Melting Transitions in Diene Polymers..... 159

VICTOR E. SHASHOUA: Static Electricity in Polymers. II. Chemical Structure and Antistatic Behavior..... 169

MICHIO KASHIWAGI: Radiation Damage in Oriented Polyamides.. 189

LEO REICH and S. S. STIVALA: A General Kinetic Scheme for Ziegler-Type Polymerizations..... 203

RICHARD H. WILEY and GERALD L. MAYBERRY: Tracer Techniques for the Determination of Monomer Reactivity Ratios.

IV. Copolymerization Characteristics of Some Divinyl Monomers 217
N. T. Notley: Molecular Configuration of Branched Macromolecules 227
V. Kalpagam and M. Ramakrishna Rao: Effect of Polar and Nonpolar Solvents on the Viscosity and the Molecular Weight of Polymer Solutions 233
L. B. Ticknor: A Thermodynamic Method for the Comparison of the Order Distribution in Cellulose and in Other Polymers 243
P. Debye, B. Chu, and D. Woermann: Viscosity of Critical Mixtures 249
P. Debye, D. Woermann, and B. Chu: Critical Opalescence of Polystyrene in Ethylcyclohexane 255
Stanley Middleman: A Theory for Surface Elevation in the Weissenberg Effect 261
Robert G. Charles: Metal Chelate Polymers Derived from Tetraacetylethane 267
Israel S. Ungar, John F. Kircher, William B. Gager, Francis A. Sliemers, and Robert I. Leininger: Radiolysis of the Isomeric Poly(butyl Methacrylate) 277
V. S. R. Rao and Joseph F. Foster: Depolarization of Scattered Light in Solutions of Linear and Branched Polysaccharides 289
Arthur V. Tobolsky: Probability Matrices, Chain Dimensions and Statistical Thermodynamics for Semicrystalline Macromolecules 301
W. Brock Neely: Solution Properties of Polysaccharides. IV. Molecular Weight and Aggregate Formation in Methylcellulose Solutions 311
Eugene C. Winslow and Jean A. Marriott: Effect of Crystallization of the Thermal Stability of Polyvinylphthalic Acid and Its Methyl Ester 321
J. P. Kennedy, I. Kirshenbaum, R. M. Thomas, and D. C. Murray: Fundamental Studies on Cationic Polymerization. II. Mechanism and Theory of Inversion Temperature 331
T. R. Crompton and V. W. Reid: Unsaturation in High Impact Polystyrene Analytical Studies 347
Bernard Wunderlich and Douglas Poland: Thermodynamics of Crystalline Linear High Polymers. II. The Influence of Copolymer Units on the Thermodynamic Properties of Polyethylene 357
William M. Saltman: Separated Aluminum Alkyl-Titanium Tetrachloride Catalysts for Isoprene Polymerization 373
J. F. Harrod: Hydrogen Bonding in Amine-Epoxide Adducts 385
O. Redlich, A. L. Jacobson, and W. H. McFadden: On the Fractionation of Polypropylene by Coacervation 393
A. Zambelli, J. Dipietro, and G. Gatti: The Nature of Active Components in Catalytic Systems Prepared from $TiCl_2$, Mono-

alkylaluminum Dihalides, and Electron-Donor Substances, in the Polymerization of Propylene 403
LOWELL WESTERMAN: The Molecular Weight Distribution in Polypropylene 411
JAMES C. W. CHIEN: Kinetics of Propylene Polymerization Catalyzed by α-Titanium Trichloride–Diethylaluminum Chloride .. 425
MAURICE MORTON, RALPH MILKOVICH, D. B. MCINTYRE, and L. J. BRADLEY: Homogeneous Anionic Polymerization. I. Molecular Weights of Polystyrene Initiated by Sodium Naphthalene 443
MAURICE MORTON, A. A. REMBAUM, and J. L. HALL: Homogeneous Anionic Polymerization. II. Molecular Weight of Polystyrene Initiated by Lithium Alkyls 461
MAURICE MORTON, E. E. BOSTICK, and R. G. CLARKE: Homogeneous Anionic Polymerization. III. Molecular Weight of Polyisoprene Initiated by Butyllithium 475
A. V. TOBOLSKY, D. KATZ, and M. TAKAHASHI: Rheology of Polytetrafluoroethylene 483
RACHELA TAKSERMAN-KROZER and ANDRZEJ ZIABICKI: Behavior of Polymer Solutions in a Velocity Field with Parallel Gradient. I. Orientation of Rigid Ellipsoids in a Dilute Solution 491
RACHELA TAKSERMAN-KROZER and ANDRZEJ ZIABICKI: Behavior of Polymer Solutions in a Velocity Field with Parallel Gradient. II. Viscosity of Dilute Solutions Containing Rigid Ellipsoids .. 507
V. KALPAGAM and M. RAMAKRISHNA RAO: Depolarization Measurements of Polymer Solutions in High Dilutions. Part I 517
CHARLES A. KUMINS and JEROME ROTEMAN: Effect of Solid Polymer Interaction on Transition Temperature and Diffusion Coefficients 527
CHARLES A. KUMINS, JEROME ROTEMAN, and CLIFFORD J. ROLLE: Water Sorption of Titanium Dioxide–Poly(vinyl Acetate–Vinyl Chloride) Copolymer Films 541
ALBERT ZILKHA and YAIR AVNY: Polymerization of Acrylonitrile by Electron Transfer Catalysts 549
G. H. CRAWFORD, D. E. RICE, and B. F. LANDRUM: Nitroso Fluorocarbon Elastomers. Polymerization Mechanism 565

ISSUE NO. 2, FEBRUARY

JOHN J. MAURER: Particle Size Distribution in Polymer Solutions .. 577
A. V. TOPCHIEV: Some Aspects of the Production and Study of Semiconducting Polymeric Materials 591
A. V. TOPCHIEV and V. P. ALANIYA: Synthesis of Nitroolefins and an Investigation of Their Ability to Polymerize 599
SHUN-ISHI OHNISHI, SHUN-ICHI SUGIMOTO, and ISAMU NITTA: Electron Spin Resonance Study of Radiation Oxidation of Polymers. IIIA. Results for Polyethylene and Some General Remarks .. 605
SHUN-ISHI OHNISHI, SHUN-ICHI SUGIMOTO, and ISAMU NITTA: Elec-

tron Spin Resonance Study of Radiation Oxidation of Polymers. IIIB. Polypropylene and Poly(Vinyl Chloride) 625
GEORGE ODIAN, MARJORIE SOBEL, ALBERT ROSSI, ROBERT KLEIN, and TERESE ACKER: Radiation-Induced Graft Polymerization of Styrene to Nylon 639
WILLIAM P. BAKER, JR.: Polymerization of Allene by Organometallic Initiation 655
K. J. HERITAGE, J. MANN, and L. ROLDAN-GONZALEZ: Crystallinity and the Structure of Celluloses 671
ARIEL OTTOLENGHI and ALBERT ZILKHA: Termination of the Anionic Polymerization of Acrylonitrile at Low Catalyst Concentrations 687
Z. IZUMI, H. KIUCHI, and M. WATANABE: Copolymerization of Acrylonitrile and *p*-Sodium Styrene Sulfonate 705
HOWARD W. STARKWEATHER, JR., JOHN F. WHITNEY, and DONALD R. JOHNSON: Crystalline Order in Nylon 66 715
VAHAK M. DERSARKISSIAN and FREDERICK A. BETTELHEIM: Strain Birefringence of Sodium Hyaluronate Films 725
W. R. MOORE and R. SHUTTLEWORTH: Thermodynamic Properties of Solutions of Cellulose Acetate and Cellulose Nitrate 733
K. R. DUNHAM, J. VANDENBERGHE, J. W. H. FABER, and L. E. CONTOIS: Effect of Side-Chain Structure on Poly-α-Olefin Properties 751
D. C. BASSETT, A. KELLER, and S. MITSUHASHI: New Features in Polymer Crystal Growth from Concentrated Solutions 763
I. KIRSHENBAUM, J. P. KENNEDY, and R. M. THOMAS: Fundamental Studies on Cationic Polymerization. III. Extension of Mechanism Studies to Homogeneous Systems 789
P. DAVIS and B. E. TABOR: Kinetic Study of the Crosslinking of Gelatin by Formaldehyde and Glyoxal 799
M. C. BOURNE, C. O. CHICHESTER, and C. STERLING: Diffusion Constants of a Maltosaccharide Series 817
J. R. SOULEN and M. S. SILVERMAN: Polymerization of Phosphonitrilic Chloride Trimer at High Pressures and Temperatures ... 823

Book Reviews

Polyamino Acids, Polypeptides and Proteins. MARK A. STRAHMANN, ed. Reviewed by H. MORAWETZ 831
Direct Analysis of Diffraction by Matter. R. HOSEMANN and A. N. BAGCHI. Reviewed by H. S. KAUFMAN 831

Erratum

J. J. SHIPMAN and M. A. GOLUB: Infrared Study of the Reaction of Polyisoprene and Polybutadiene With Sulfur by the Use of Deuterated Polymers (article in *J. Polymer Sci.*, **58**, 1063–1082, 1962) 832

Issue No. 3, March

G. V. D. Tiers and F. A. Bovey: Polymer NMR Spectroscopy. VII. The Stereochemical Configuration of Polytrifluorochloroethylene 833
F. A. Bovey: Polymer NMR Spectroscopy. VIII. The Influence of the pH of the Polymerization Medium on the Stereochemical Configuration of Polymethacrylic Acid 843
F. A. Bovey and G. V. D. Tiers: Polymer NMR Spectroscopy. IX. Polyacrylamide and Polymethacrylamide in Aqueous Solution 849
Joseph Pellon and W. G. Carpenter: Polyamides Containing Phosphorus. I. Preparation and Properties 863
Tilak Guha and Santi R. Palit: Study of the Rate of Heterogeneous Polymerization of Methyl Acrylate in Aqueous Solution 877
Harris J. Bixler, Alan S. Michaels, and Morris Salame: Gas Transmission in Irradiated Polyethylene 895
V. Kalpagam and M. Ramakrishna Rao: Depolarization Measurements of Polymer Solutions at High Dilutions. Part II 921
W. R. Moore and R. J. Fort: Viscosities of Dilute Solutions of Polymethyl Methacrylate 929
C. Wippler et R. Gautron: Étude de l'Influence du Tetrahydrofurane sur la Radioreticulation du Chlorure de Polyvinyle 943
Irving Rosen, G. H. McCain, A. L. Endrey, and C. L. Sturm: Syndiotactic Polyvinyl Formate and Derived Polyvinyl Alcohol 951
Gianalvise Carazzolo and Mario Mammi: Crystal Structure of a New Form of Polyoxymethylene 965
R. Van Leemput and R. Stein: Experimental Data on Dilute Polymer Solutions. I. Hydrodynamic Properties and Statistical Coil Dimensions of Poly(*n*-Butyl Methacrylate) 985
J. P. Berry: Fracture Processes in Polymeric Materials. IV. Dependence of the Fracture Surface Energy on Temperature and Molecular Structure 993
Yoshio Tomimatsu and K. J. Palmer: Light-Scattering Studies on Sugar Beet Arabans 1005
J. Scanlan and D. K. Thomas: Crosslinking of Natural Rubber by Dicumyl Peroxide in the Presence of Oxidation Inhibitors .. 1015
C. E. Brockway and K. B. Moser: Grafting of Poly(methyl Methacrylate) to Granular Corn Starch 1025
R. J. Morris, Jr. and H. E. Persinger: Molecular Weight Distribution in Polypropylene Glycol 2025 1041
Yoneho Tabata, Hiroshi Shibano, Hiroshi Sobue, and Kiyoshi Hara: Radiation-Induced Cationic Polymerization of Ethylene 1049
Donald C. Vogelsong: Crystal Structure Studies on the Polymorphic Forms of Nylons 6 and 8 and Other Even Nylons 1055

NOBORU TOKITA and W. R. KRIGBAUM: Calculation of the Displacement Distance for a Three-Choice Cubic Lattice Chain.. 1069
ROBERT B. FOX, LAWRENCE G. ISAACS, and SUZANNE STOKES: Photolytic Degradation of Poly(methyl Methacrylate)..... 1079

Book Review

Advances in Spectroscopy. Vol. II. H. W. THOMPSON, ed. Reviewed by R. P. BAUMAN..... 1087

Erratum

G. S. LEVINSON: Molecular Orbital Calculation of Monomer Reactivity Ratios (article in *J. Polymer Sci.*, **60**, 43–54, 1962) 1088

ISSUE NO. 4, APRIL

L. UTRACKI and ROBERT SIMHA: Corresponding State Relations for the Viscosity of Moderately Concentrated Polymer Solutions 1089
MACHIO IWASAKI: On the Helical Structure of Polytetrafluoroethylene..... 1099
NAN SHIEH CHU and CHARLES C. PRICE: Polyethers. XI. Polymerization of *dl*-Propylene Oxide with Optically Active Catalyst Systems..... 1105
MIKIKO SHIMA and AKIRA KOTERA: Copolymerization Characteristics of Methyl Acrylate and Methyl Methacrylate. I. Study of Copolymerization Kinetics by a Deuterium Tracer Method..... 1115
JOHN L. LANG, W. A. PAVELICH, and H. D. CLAREY: Homopolymerization of Maleic Anhydride. I. Preparation of the Polymer..... 1123
R. D. BURKHART and N. L. ZUTTY: Copolymerization Studies. III. Reactivity Ratios of Model Ethylene Copolymerizations and Their Use in *Q-e* Calculations..... 1137
PAUL W. MORGAN and STEPHANIE L. KWOLEK: Interfacial Polycondensation. XIII. Viscosity-Molecular Weight Relationship and Some Molecular Characteristics of 6–10 Polyamide.. 1147
ROLAND E. FLORIN and LEO A. WALL: Electron Spin Resonance of Gamma-Irradiated Cellulose..... 1163
DAVID W. MCCALL and ERNEST W. ANDERSON: Molecular Motion in Polyethylene. III..... 1175
K. C. ELLIS and J. O. WARWICKER: Crystallite Orientation in Regenerated Cellulose Filaments. I. Measurement of Orientation by X-Ray Methods..... 1185
E. W. MERRILL, H. S. MICKLEY, A. RAM, and W. H. STOCKMAYER: The Second Newtonian Viscosity Number..... 1201
HOWARD C. HAAS, HELEN HUSEK, and LLOYD D. TAYLOR: On the Ultraviolet Absorption Spectrum of Polyvinyl Alcohol.... 1215

G. Smets and W. Van Humbeeck: Reaction Kinetics and Tacticity of Macromolecules. II. Acrylic Acid Copolymers.... 1227
W. A. Hewett and F. E. Weir: Dynamic Properties of Homo- and Copolymers of 4-Methyl-1-Pentene..... 1239
Bernhard Wunderlich: The Effect of Pressure on the Crystallization of Polyethylene from Dilute Solution..... 1245
R. Y.-M. Huang, B. Immergut, E. H. Immergut, and W. H. Rapson: Grafting Vinyl Polymers onto Cellulose by High Energy Radiation. I. High Energy Radiation-Induced Graft Copolymerization of Styrene onto Cellulose..... 1257
P. G. Schmidt: Polyethylene Terephthalate Structural Studies.. 1271
Catherine S. Hsia Chen: Polymerization Induced by Ionizing Radiation at Low Temperatures. III. The Effect of Electron Density on the Polymerization of Substituted Styrenes..... 1293
Chas. W. Wilson, III: NMR Study of Molecular Chain Structure of Polyvinylidene Fluoride..... 1305
A. M. North and G. A. Reed: Diffusion-Controlled Polymerization of Some Alkyl Methacrylates..... 1311
Naoya Yoda: Syntheses of Polyanhydrides. XII. Crystalline and High Melting Polyamidepolyanhydride of Methylenebis-(*p*-carboxyphenyl)amide..... 1323
J. R. Huntsberger: The Locus of Adhesive Failure..... 1339
G. R. Cotten and W. Sacks: Oxidative Crosslinking of Polyethylene by Ultraviolet Light..... 1345
Ferenc Tüdös, Imre Kende, and Mária Azori: Inhibition Kinetics of the Polymerization of Styrene. II. Investigations on the Effect of *s*-Trinitrobenzene..... 1353
Ferenc Tüdös, Imre Kende, and Mária Azori: Inhibition Kinetics of Polymerization of Styrene. III. Investigations on the Effect of Substituted Trinitrobenzenes..... 1369
P. De Santis, E. Giglio, A. M. Liquori, and A. Ripamonti: Stability of Helical Conformations of Simple Linear Polymers.. 1383
K. Hayashi, T. Yonezawa, S. Okamura, and K. Fukui: Molecular Orbital Theory of Reactivity in Radical Polymerization. Part III..... 1405
Edmund A. DiMarzio and Julian H. Gibbs: Molecular Interpretation of Glass Temperature Depression by Plasticizers.... 1417
V. K. Kulshrestha: Studies on Biocolloids and Polyelectrolytes—The Plant—Gums Viscosity of Azrechtic Acid..... 1429
C. G. Overberger and S. Nozakura: Copolymerization of Styrene and Styrene Derivative with an Aluminum Alkyl-Titanium Trichloride Catalyst..... 1439
Bacon Ke: Differential Analysis of High Polymers. VI. Comments on Some Material and Experimental Factors..... 1453
D. B. Anderson, G. M. Burnett, and A. C. Gowan: Some Novel Effects in Solution Polymerization..... 1465

Book Review

Makromolekulare Stoffe. Part I, Vol. XIV, Methoden der Organischen Chemie (Houben-Weyl), E. MÜLLER, Ed. Reviewed by NORBERT M. BIKALES 1471

Errata

A. P. FIRSOR, B. N. KASHPROV, YU. V. KISSIN, and N. M. CHIRKOV: The Dependence of the Stereospecific Action of the Complex Catalyst α-$TiCl_3$–$Me(C_2H_5)_n$ during the Polymerization of α-Olefins on the Metal in the Metalloorganic Compound (article in *J. Polymer Sci.*, **62**, S104–S105, 1962) 1472

A. V. TOBOLSKY, D. KATZ, and M. TAKAHASHI: Rheology of Polytetrafluoroethylene (article in *J. Polymer Sci.*, **A1**, 483–489, 1963) 1472

MASATAMI TAKEDA and KAZUYOSHI IIMURA: Studies on the Configuration and Conformation of Vinyl-Type Polymers. II. Temperature Dependence of the Infrared Spectrum of Polyvinyl Chloride in Solution and Stereoregularity (article in *J. Polymer Sci.*, **57**, 383–393, 1962) 1472

B. ROSEN: Some Mechanical Aspects of the Swelling and Shrinking of Polymeric Solids. Part I. External and Internal Restraints (article in *J. Polymer Sci.*, **58**, 821–837, 1962) 1472

ISSUE NO. 5, MAY

W. D. TAYLOR and A. E. WOODWARD: Preparation and Properties of Copolymers of Maleic Anhydride and 2,2-Dimethylaminoethyl Methacrylate 1473

R. G. SABA, J. A. SAUER, and A. E. WOODWARD: Dynamic Shear Behavior of Poly(γ-benzyl L-Glutamate), Poly(D,L-Propylene Oxide), and Poly(ethyl Vinyl Ether) 1483

J. MERCIER and G. SMETS: Copolymerization. I. Structure of Polyacrylic Anhydride 1491

FUMIO OOSAWA: Thermodynamic Properties of Rodlike Polyelectrolyte Solutions in the Presence of Salts 1501

W. COOPER, F. R. JOHNSTON, and G. VAUGHAN: Stereoregularity in Polyvinyl Alcohols and Esters 1509

R. E. FLORIN, L. A. WALL, and D. W. BROWN: Electron Spin Resonance Spectra and Aged, γ-Irradiated Polystyrenes 1521

HERWARD VOGEL and C. S. MARVEL: Polybenzimidazoles. II .. 1531

TOSHIYUKI SHONO and C. S. MARVEL: Polymers Derived from Unsaturated Esters of Hydronopoxyalkanols 1543

T. HUFF and ELI PERRY: Reaction of Polymeric Radicals with Organometallic Compounds 1553

GIAN ALVISÉ CARAZZOLO: Structure of the Normal Crystal Form of Polyoxymethylene 1573

ORIN C. HANSEN, JR., THOMAS L. FABRY, LEON MARKER, and ORVILLE J. SWEETING: Apparatus for Measuring the Dynamic Tensile Modulus of Thin Polymeric Films 1585
M. BERGER: Steric Structures in Copolymerization 1601
J. DROUGAS, A. TIMNICK, and R. L. GUILE: High Frequency Titrations of Polydicarboxylic Acid Copolymers: Polyitaconic Acid-*Co*-Styrene and Polymaleic Acid-*Co*-Styrene 1609
D. E. KLINE: Nuclear Radiation Effects in Polytetrafluoroethylene 1621
HIKARU SEKIGUCHI: Mécanisme réactionnel de la Polymérisation alcaline des Lactames 1627
DOV KATZ: Polymerization and Copolymerization of 1- and 9-Vinylanthracenes and 9-Vinylphenanthrene 1635
ISAAC D. RUBIN: Isomorphism in Polycarbonates. Copolymers of Hydroquinone and Substituted Hydroquinones 1645
A. R. SHULTZ, P. I. ROTH, and J. M. BERGE: Radiation Degradation of Polymethacrylates. Dose Rate and Medium Effects .. 1651
J. H. GOLDEN and E. A. HAZELL: Degradation of a Polycarbonate by Ionizing Radiation 1671
K. H. BASSETT, C. Y. LIANG, and R. H. MARCHESSAULT: The Infrared Spectrum of Crystalline Polysaccharides. IX. The Near Infrared Spectrum of Cellulose 1687
R. D. GLAUZ: Transient Analysis of a Vibrating Reed 1693
R. W. WARFIELD and M. C. PETREE: Thermodynamic Properties of Polymethyl Methacrylate and Methyl Methacrylate 1701
DAVID W. MCCALL, DEAN C. DOUGLASS, and ERNEST W. ANDERSON: Self-Diffusion and Nuclear Relaxation in Polyisobutylene 1709
M. O. DE LA CUESTA and F. W. BILLMEYER, JR.: The Molecular Structure of Polyethylene. XII. Intrinsic Viscosities of Polyethylene Solutions 1721
MAURICE MORTON, E. E. BOSTICK, R. A. LIVIGNI, and L. J. FETTERS: Homogeneous Anionic Polymerization. IV. Kinetics of Butadiene and Isoprene Polymerization with Butyllithium .. 1735
F. M. BROWER and H. W. MCCORMICK: Narrow Molecular Weight Distribution Polystyrene 1749
ROBERT TOGGENBURGER and STANLEY J. GILL: Anisotropic Properties of Strained Viscoelastic Fluids. III. Birefringence of Polystyrene Solutions 1765
R. TOGGENBURGER, K. BECK, and S. J. GILL: Theoretical Calculations of Stress Relaxation in Concentrated Solutions 1779
C. C. HSIAO and T. S. WU: Orientation and Strength of Branched Polymer Systems 1789
A. KISHIMOTO and Y. ENDA: Diffusion of Benzene in Polyacrylates 1799
ALBERT ZILKHA, SAMUEL BARZAKAY, and ARIEL OTTOLENGHI: Effect of Solvents on the Anionic Polymerization of Styrene by Phenyllithium 1813

JAMES C. W. CHIEN: Olefin Polymerizations and Polyolefin Molecular Weight Distribution 1839

ISSUE NO. 6, JUNE

A. A. MILLER: The Reference Point for Liquid Relaxation Processes. I. Melt Viscosity of Polystyrene 1857
A. A. MILLER: The Reference Point for Liquid Relaxation Processes. II. Melt Viscosity of Polyisobutylene 1865
R. ST. JOHN MANLEY: Growth and Morphology of Single Crystals of Cellulose Triacetate 1875
R. ST. JOHN MANLEY: Hydrolysis of Cellulose Triacetate Crystals 1893
P. GIORDANO ORSINI, B. MARCHESE, and L. MAZZARELLA: Morphology of Polyethylene Single Crystals 1901
P. JÄGER and E. S. WAIGHT: Solid State Polymerization of Methacrylamide and *N*-Arylmethacrylamides 1909
M. G. BALDWIN and SAMUEL F. REED: Polymerization Studies on Allylic Compounds. I 1919
DAVID E. BURGE and DOUGLAS B. BRUSS: Preparation and Properties of Some Poly-α-Methylstyrenes 1927
K. IWASAKI, H. FUKUTANI, and S. NAKANO: Polymerization of Vinyl Ethers with Magnesium Compounds. I. Catalytic Reactivity of Magnesium Halides 1937
C. A. J. HOEVE and M. K. O'BRIEN: Specific Diluent Effects on Polymer Chain Dimensions 1947
ADA L. JACOBSON: The Temperature Dependence of Magnesium Chloride Interaction with Polyacrylic Acid 1955
ATANAZY BORYNIEC and BOGUMIŁ ŁASZKIEWICZ: Bulk Copolymerization of Methyl Methacrylate with Phenyldichlorophosphine 1963
HIROYOSHI KAMOGAWA and HAROLD G. CASSIDY: Electron Exchange Polymers. XIX. Copolymerization Behavior of Vinylhydroquinone Dibenzoate 1971
GEORGE S. PARKS and HELENE P. MOSHER: Enthalpy and Free Energy Changes in Some Simple Polymerization Processes 1979
W. R. MOORE and R. SHUTTLEWORTH: Thermodynamic Properties of Solutions of Cellulose Triacetate 1985
LAWRENCE E. NIELSEN and FRED D. STOCKTON: Theory of the Modulus of Crystalline Polymers 1995
CHARLES R. MCINTOSH, WILLIAM D. STEPHENS, and CURTIS O. TAYLOR: Changes in the Stereospecificity of a Ziegler Catalyst Used in the Polymerization of Butadiene 2003
MASAKAZU INOUE: Nucleating Effect on the Kinetics of Crystallization and the Spherulites of Nylon 6 2013
C. G. OVERBERGER and KAZUO MIYAMICHI: Copolymerization of Styrene and Aliphatic Olefins 2021
F. RYBNIKÁŘ: Mechanism of Secondary Crystallization in Polymers 2031

HIROSHI SOBUE and KENKICHI MURAKAMI: Maximum Relaxation Time on Polymers in the Vicinity of Critical Molecular Weight 2039
RYONG-JOON ROE and WILLIAM R. KRIGBAUM: A Thermodynamic Study of Viton Elastomer 2049
D. A. FREY, MASAKI HASEGAWA, and C. S. MARVEL: Preparation and Aromatization of Poly-1,3-Cyclohexadiene. II 2057
TOSHIYUKI SHONO and C. S. MARVEL: Preparation and Polymerization of Vinyl 12-hydroxystearte 2067
A. RUDIN and J. S. MACKIE: Some Anomalous Brittleness Temperatures of Polyethylene 2075
E. TURSKA and S. POŁOWIŃSKI: Examination of Kinetics of Graft Copolymerization on Preirradiated Polymethyl Methacrylate 2085
A. KATCHALSKY and Z. ALEXANDROWICZ: On the Additivity of Osmotic Properties of Polyelectrolyte–Salt Solutions 2093
KEIITI SISIDO, NOBUO KUSANO, RYÔZI NOYORI, YÔKO NOZAKI, MASATOSI SIMOSAKA, and HITOSI NOZAKI: Polycondensation of Xylylene Dibromides by Transition Metals in Water Suspension 2101
H. FISCHER, K.-H. HELLWEGE, und P. NEUDÖRFL: Elektronenspinresonanz-Untersuchungen an Peroxydradikalen in bestrahltem Polypropylen 2109
J. F. JACKSON: Crystallinity in Ethylene–Propylene Copolymers 2119
S. SUGAI and A. E. WOODWARD: Counterion Binding in Partially Neutralized Copolymers of Crotonic Acid and Vinyl Alcohol 2127
TSUNEO YOSHINO and YASUO MANABE: Photosensitivity of Dry-Heated Polyacrylonitrile 2135
R. SALOVEY and ROSENZWEIG: Radiation Dosimetry in Polyethylene with Silicon Solar Cells 2145
R. SALOVEY and F. R. DAMMONT: Irradiation of Polyethylene Oxide and Polypropylene 2155
G. S. WICH and N. BRODOWAY: Relative Radioactivity Ratios for Two New 2-Chloro-1,3-Butadiene Systems 2163
M. BAER: Anionic Block Polymerization. I. Block Polymerization of Styrene on Polystyrene 2171
JOAN BOND and D. B. ROBSON: The Role of Metal Chelates in Polymerization Initiation. I. Chromous Chelates 2179
JOAN BOND and D. B. ROBSON: The Role of Metal Chelates in Polymerization Initiation. II. Cupric Chelates 2185
E. F. T. WHITE and M. J. ZISSELL: Polymerization of Acrylonitrile in Dimethylsulfoxide 2189
AKIHIRO ABE and MURRAY GOODMAN: Optical Rotatory Properties of Polyaldehydes 2193
H. A. POHL, C. G. GOGOS, and C. CAPPAS: Resistivity Studies on Polymer Semiconductors 2207
A. J. HAVLIK, J. MOACANIN, and I. OTTERNESS: Ebulliometric and Endgroup Molecular Weights of Polyoxypropylene and Polyoxyethylene Glycols 2213

MORTON LITT: Poly(4-methyl Pentene): X-Ray Measurement of Crystalline Density and Observation of a Structural Anomaly 2219
R. BACSKAI and S. J. LAPPORTE: The Chemical Structure of Polyisobutylene Obtained by Ziegler Catalysis 2225
N. L. ZUTTY: Copolymerization Studies. IV. Transannular Copolymerization of Bicyclo[2.2.1]hepta-2,5-diene 2231

Book Reviews

Radiation Chemistry of Polymeric Systems High Polymers, A. CHAPIRO, Ed. Reviewed by G. ADLER 2237
Introduction to Polymer Chemistry. J. K. STILLE. Reviewed by ROBERT W. LENZ 2237
Soviet Research on Organo-Silicon Chemistry, 1959, Parts I and II, Consultants Bureau. Reviewed by EUGENE G. ROCHOW 2238
Unsolved Problems in Polymer Science, FRANK R. MAYO, Ed. Reviewed by C. G. OVERBERGER and E. H. IMMERGUT 2239

Erratum

R. MEREDITH and BAY-SUNG HSU: Dynamic Bending Properties of Fibers: Effect of Temperature on Nylon 66 Terylene, Orlon, and Viscose Rayon (article in *J. Polymer Sci.*, **61**, 271–292, 1962) 2240

ISSUE NO. 7, JULY

J. R. HUNTSBERGER: Adhesion. II Relationships between Viscoelasticity, Interfacial Equilibrium, and the Temperature Dependence of Adhesion 2241
B. R. LOY: Electron Spin Resonance of Polypropylene 2251
G. M. BRISTOW: The Mastication of Elastomers. Part III. The Solution Properties of Masticated Synthetic *cis*-Polyisoprene 2261
CHEVES WALLING and DENNIS D. TANNER: Organic Reactions under High Pressure. IX. The Effect of Pressure on the Stereochemistry of Methyl Methacrylate Polymerization 2271
G. FILIPOVICH: Nuclear Magnetic Resonance in Solid Polypyrrolidone 2279
N. L. ZUTTY and F. J. WELCH: Synthesis of Vinyl Polymers Containing α-Substituted γ-Butyrolactone Groups in their Backbones 2289
W. R. EDWARDS and N. F. CHAMBERLAIN: Carbonium Ion Rearrangement in the Cationic Polymerization of Branched Alpha Olefins 2299
KWEI-PING SHEN KWEI: Graft Copolymers of Polyacrylic Acid with Desoxyribonucleic Acid (DNA) 2309
PAUL G. SCHMIDT: Polypropylene Structure 2317
MARIAN KRYSZEWSKI and MARTA SKORKO: Interactions of Low Molecular Weight Compounds with Solid Polymers 2327

S. YAMADA, W. PRINS, and J. J. HERMANS: Determination of Number-Average Molecular Weights by Elastoosmometry..... 2335
HAROLD SCHONHORN: Generalized Approach to Adhesion Via the Interfacial Deposition of Amphiphatic Molecules. I. Adhesion of Polyethylene to Aluminum..... 2343
ROBERT A. MENDELSON: Elution Fractionation of Crystalline Polypropylene..... 2361
K. IWASAKI, H. FUKUTANI, Y. TSUCHIDA, and S. NAKANO: Polymerization of Vinyl Ether with Magnesium Compounds. II. Catalytic Reactivity of Magnesium Compounds Other than Halides..... 2371
EUGENE C. WINSLOW and NANCY E. GERSHMAN: Phthalocyanine-Crosslinked Polyvinylphthalic Acid..... 2383
P. DEBYE, B. CHU, and H. KAUFMANN: Molecular Configuration of Polystyrene in Benzene..... 2387
NOBUHIRO KUWAHARA: On the Polymer–Solvent Interaction in Polymer Solutions..... 2395
YUTAKA SAKURADA: Polymerization of α-Methylstyrene with $Al(C_2H_5)_3$–$TiCl_4$ Catalyst..... 2407
G. J. K. ACRES and F. L. DALTON: Synthesis of Styrene–Methyl Methacrylate Nonrandom Copolymers in Emulsion Systems with Cobalt-60 Gamma Radiation..... 2419
D. B. BRUSS and F. H. STROSS: A Comparison of Dynamic Methods for Osmotic Pressure Measurements..... 2439
JACK B. CARMICHAEL and JACK B. KINSINGER: Unrestricted Rotation in Polymers with Discrete Rotational States..... 2459
A. D. KETLEY and J. D. MOYER: Competing Side Reactions in the Polymerization of α-Olefins by Ziegler-Natta Catalysts... 2467
RACHELA TAKSERMAN-KROZER: Behavior of Polymer Solutions in the Velocity Field with Parallel Gradient. III. Molecular Orientation in Dilute Solutions Containing Flexible Chain Macromolecules..... 2477
RACHELA TAKSERMAN-KROZER: Behavior of Polymer Solutions in the Velocity Field with Parallel Gradient. IV. Viscosity of Dilute Solutions Containing Flexible Chain Macromolecules 2487

Book Reviews

Physik der Kunstoffe, WERNER HOLZMULLER and KURT ALTENBERG, Editors. Reviewed by MAURICE L. HUGGINS..... 2495
Advances in Petroleum Chemistry and Refining, Vol. IV, JOHN J. MCKETTA, JR, Editor. Reviewed by HERBERT N. FRIEDLANDER..... 2495

ISSUE NO. 8, AUGUST

RAFFAELE SHIBA and F. R. EIRICH: Viscoelastic Behavior of Plasticized Polyvinyl Chloride at Large Deformations. I. Stress Relaxation..... 2497

RAFFAELE SABIA and F. R. EIRICH: Viscoelastic Behavior of Plasticized Polyvinyl Chloride at Large Deformations. II. Creep 2511
TOD W. CAMPBELL and RICHARD N. MCDONALD: Polymeric Derivatives of 3,3-Bis(aminomethyl)-Oxetane and of Exoxysuccinyl Chloride 2525
S. M. MILLER, M. W. SPINDLER, and R. L. VALE: Use of Dimaleimides as Accelerators for the Radiation-Induced Vulcanization of Hydrocarbon Polymers. Part II. Synthetic Rubbers and Saturated Polymers 2537
W. G. LLOYD: The Influence of Transition Metal Salts in Polyglycol Autoxidations 2551
R. M. BARRER, J. A. BARRIE, and M. G. ROGERS: Heterogeneous Membranes: Diffusion in Filled Rubber 2565
WAYNE E. SMITH and RALPH G. ZELMER: An Interpretation of Ethylene Polymerization with Alkyl-Promoted Transition-Metal Catalysts 2587
J. SCHMORAK and M. LEWIN: The Chemical and Physicochemical Properties of Wheat Starch Mildly Oxidized with Alkaline Sodium Hypochlorite 2601
S. KRIMM, V. L. FOLT, J. J. SHIPMAN, and A. R. BERENS: Infrared Spectra and Assignments for Polyvinyl Chloride and Deuterated Analogs 2621
SAMUEL H. MARON and THOMAS T. CHIU: Study of Entanglement of Polymers in Solution by Viscosity Measurements. II. Polymethyl Methacrylate in Various Solvents 2651
G. J. HOWARD: Turbidimetric Titration of Nylon 66 2667
MAURICE MORTON and WILLIAM E. GIBBS: The Emulsion Polymerization of 2,3-Dimethylbutadiene-1,3 2679
MASAKAZU INOUE: Studies on Crystallization of High Polymers by Differential Thermal Analysis 2697
F. H. OWENS and F. E. ZIMMERMAN: Photochlorination of Poly(methyl Methacrylate) in Aqueous Suspension 2711
C. M. HUGGINS, L. E. ST. PIERRE, and A. M. BUECHE: Further NMR Studies of Polydimethylsiloxanes: Effects of Radiation-Induced Crosslinking 2731
C. V. STEPHENSON and W. S. WILCOX: Ultraviolet Irradiation of Plastics. IV. Further Studies of Environmental Effects on Films and Fibers 2741

ISSUE NO. 9, SEPTEMBER

RAYMOND L. ARNETT, MELVIN E. SMITH, and BARRY O. BUELL: An Improved Ebullioscope for High Polymers 2753
R. CHIANG: Crystallization and Melting Behavior of Polyacrylonitrile 2765
R. BACSKAI: Polymerization of Alicyclic Epoxides with Aluminum Alkyl Catalysts 2777
SHIRO YAKASHIMA: Effect of Ions on the Dielectric Dispersion of Ovalbumin Solution 2791

S. E. Chappell, J. A. Sauer, and A. E. Woodward: Effects of High Energy Irradiation on Polypropylene 2805
Richard H. Wiley and Burns Davis: Tracer Techniques for the Determination of Monomer Reactivity Ratios. IV. Monomer Reactivity Ratios for Styrene–Isoprene Copolymerization 2819
Jerry N. Koral and Edwin M. Smolin: The Preparation and Polymerization of Suberaldehyde 2831
N. K. J. Symons: Growth of Single Crystal of Polytetrafluoroethylene from the Melt 2843
J. F. Rudd and E. F. Gurnee: The Effect of Molecular Weight Distribution on the Optical Properties of Polystyrene in the Transition Region 2857
J. E. Guillet: Long-Chain Branching Frequency in Polyethylene 2869
F. H. Chowdhury and S. M. Neale: Acid Behavior of Carboxylic Derivatives of Cellulose. Part I. Carboxymethylcellulose .. 2881
F. H. Chowdhury and S. M. Neale: Acid Behavior of Carboxylic Derivatives of Cellulose. Part II. Oxycellulose 2893
Hazime Kusumoto and H. S. Gutowsky: Proton Magnetic Resonance in Natural Rubber: Comparison with Dielectric Measurements 2905
Sakuji Ikeda, Akio Yamamoto, and Hiroshi Tanaka: Stereoregulated Polydideuteroethylene I. Polymers of *trans*-1,2-Dideuteroethylene and *cis*-1,2-Dideuteroethylene by a Ziegler Catalyst 2925
Bernd Reichel, C. S. Marvel, and R. Z. Greenley: Transannular Polymerization of 1,5-Cyclooctadiene 2935
M. Berger and D. J. Buckley: Structure Effects and Related Polymer Properties in Polybutadiene. I. Preparation and Characterization 2945
Niichiro Tokura, Minoru Matsuda, and Yasuo Ogawa: Polymerization in Liquid Sulfur Dioxide. Part XIII. Polymerization of Styrene Derivatives in Liquid Sulfur Dioxide 2965
T. K. Kwei: Swelling of Highly Crosslinked Network Structure .. 2977
Alain Guyot et Jean-Claude Daniel: Etude dela Polymérisation des Oléfines catalysée par les Oxydes métalliques. I. Méthodes expérimentales d'Etude cinétique; Résultats préliminaires sur la Polymérisation du Propylene par le Systéme catalytique Phillips 2989

Issue No. 10, October

G. J. K. Acres and F. L. Dalton: On Co^{60} Gamma-Ray-Initiated Emulsion Polymerization 3009
A. Packter: Conductivity and Viscosity Measurements on Sodium Polyacrylates of Different Molecular Weights 3021
Hiroyuki Tadokoro, Shunsuke Murahashi, Reizô Yamadera, and Tei-Ichi Kamei: Infrared Absorption Spectra of Polyacrylonitrile and Deuterated Polyacrylonitriles 3029

MAURICE MORTON and IRJA PIIRMA: The Branching Reaction. III. Polymeric Transfer Constants of Vinyl Acetate with Styrene and Methyl Methacrylate 3043
STEFAN CZARNECKI and MARIAN KRYSZEWSKI: Some Applications of Afterglow Studies of Luminescent Compounds in Solid Polymers 3067
M. G. SHARMA and T. W. HAAS: Some Viscoelastic Studies on Penton 3079
M. H. WALTERS: Fibrous Structure in Stretched Crystalline Elastomers 3091
J. O. WARWICKER: The Diffusion of Chrysophenine G into Viscose Sheet 3105
G. M. BOWER and L. W. FROST: Aromatic Polyimides 3135
NAOYA OGATA: Resonance Effect of Amide Group on the Polymerizability of Lactam Derivatives. III. Polymerization of Many-Membered Lactams Ring 3151
JOSEPH D. LOCONTI and JOHN W. CAHILL: Zone-Refining Fractionation of Polymers 3163
A. M. KOTLIAR: Evaluation of Molecular Weight Averages Resulting from Random Crosslinking and Chain Scission Processes for Wide Schulz-Zimm Distributions 3175
BERNARD D. COLEMAN and THOMAS G FOX: General Theory of Stationary Random Sequences with Applications to the Tacticity of Polymers 3183
Z. ZLÁMAL and A. KAZDA: Donor–Acceptor Interaction in Cationic Polymerization. V. Influence of Some Alcohols of the Molecular Weight of Polyisobutylene in Polymerization Catalyzed by Aluminum Trichloride 3199
M. G. BALDWIN: Primary Radical Termination in Methyl Methacrylate Polymerization 3209
PAUL EHRLICH and JOHN J. KURPEN: Phase Equilibria of Polymer–Solvent Systems at High Pressures Near Their Critical Loci: Polyethylene with *n*-Alkanes 3217
Z. ALEXANDROWICZ and A. KATCHALSKY: Colligative Properties of Polyelectrolyte Solutions in Excess of Salt 3231
W. DEWINTER, C. S. MARVEL, and AZIZ ABDUL-KARIM: Polydiacrylylmethane 3261

ISSUE NO. 11, NOVEMBER

P. BATAILLE and D. PATTERSON: An Application of the Prigogine Solution Theory to Intrinsic Viscosities in Polyisobutylene–*n*-Alkane Systems 3265
S. NAKANO, K. IWASAKI, and H. FUKUTANI: Stereospecific Polymerization of Vinyl Alkyl Ethers 3277
MITIO INOKUTI and MALCOLM DOLE: Interpretation of the Intrinsic Viscosity of Polymers Undergoing Simultaneous Degradation and Crosslinking 3289

HIROSHI INAGAKI, SYUJI KAWAI, and ATSUSHI NAKAZAWA: Application of the Archibald Ultracentrifugal Method for the Study of Dilute Polymer Solutions. II. Examination of Two Solution Systems near the Flory Temperature 3303
FRANK J. LIMBERT and ERIC BAER: Kinetics of Nucleation and Growth of Spherulites in Homopolymers 3317
J. GREYSON and A. A. LEVI: Calorimetric Measurements of the Heat of Sorption of Water Vapor on Dry Swollen Cellulose 3333
K. I. BEYNON: Monomers Containing Phosphorus. Part I. Copolymerization of Phosphonates with *n*-Lauryl Methacrylate .. 3343
K. I. BEYNON: Monomers Containing Phosphorus. Part II. Copolymerization of Diallyl Phenyl Phosphine Oxide with *n*-Lauryl Methacrylate 3357
YŪJI SHIOJI, SHUN-ICHI OHNISHI, and ISAMU NITTA: ESR Study of Irradiated Acrylic Acid and Reaction of the Produced Radical 3373
R. JOSEPHS and J. FEITELSON: Interactions of Polyelectrolytes. A Turbidimetric Method for the Estimation of Ionized Polymers 3385
GERT F. BAUMANN and SAMUEL STEINGISER: Rheological Measurements on Polycarbonate 3395
RUTH R. BENERITO, RALPH J. BERNI, JOHN B. MCKELVEY, and BEVERLY G. BURGIS: Study of the Base-Catalyzed Cellulose —*d,l*-Butadiene Diepoxide Reaction 3407
MASAKAZU INOUE: Properties of Melt-Blends of Crystalline High Polymers. Fusion and Crystallization Behaviors 3427
H. F. MARK and N. OGATA: Copolymerization of Aldehydes 3439
LOUIS E. MATTISON, MARTHA S. PHIPPS, LILLIAN ALFRED, SALLY TAYLOR, JOHN THOMPSON, and BARRY SAUL: Coordination Compounds of *p*-Nitrobenzeneazotyrosine 3449
A. T. DIBENEDETTO: Molecular Properties of Amorphous High Polymers. I. A Cell Theory for Amorphous High Polymers 3459
A. T. DIBENEDETTO: Molecular Properties of Amorphous High Polymers. II. An Interpretation of Gaseous Diffusion Through Polymers 3477
W. L. HAWKINS and MRS. M. A. WORTHINGTON: Synergistic Antioxidant Combinations. Carbon Black Substitutes 3489
W. L. HAWKINS and MRS. H. SAUTTER: Synergistic Antioxidant Combinations. Mechanism of Stabilization with Organo-Sulfur Compounds 3499
J. W. WOOD and PETER T. MORA: Preparation and Biological Application of Highly Substituted Cationic Derivatives of Polysaccharides 3511

Book Reviews

Analytical Chemistry of Polymers, Vol. XII, Part II., G. M. KLINE, Ed., Reviewed by H. S. KAUFMAN 3519
Physical Properties of Polymers, F. BUECHE, and Mechanical Properties of Polymers, L. E. NIELSEN. Reviewed by R. S. STEIN 3519

ISSUE NO. 12, DECEMBER

Editorial 3251

HAROLD SCHONHORN: Generalized Approach to Adhesion Via the Interfacial Deposition of Amphipathic Molecules. II. Adhesion of Polyethylene to Aluminum 3523

HISASHI UEDA, ZENICHIRO KURI, and SHOJI SHIDA: Electron Spin Resonance Studies of the Reaction of Gases with the Radicals Formed in Irradiated Polytetrafluoroethylene 3537

M. KHAIRY, S. MORSI, and CLARENCE STERLING: Crystallization in Starch: The Role of Ions in the Lyotropic Series 3547

JOSEPH PELLON: Polyamides Containing Phosphorus. II. Structural Effects on Softening and Glass Transition Temperatures 3561

G. NATTA, G. CRESPI, and U. FLISI: Thermodynamic Interpretations of the Elastic Properties of Rubbers Obtained from Ethylene–Propylene Copolymers 3569

BERNHARD WUNDERLICH, PETER SULLIVAN, TAMIO ARAKAWA, A. B. DICYAN, and J. F. FLOOD: Thermodynamics of Crystalline Linear High Polymers. III. Thermal Breakdown of the Crystalline Lattice of Polyethylene 3581

THOR L. SMITH: Ultimate Tensile Properties of Elastomers. I. Characterization by a Time and Temperature Independent Failure Envelope 3597

WILLIAM J. BURKE and HAROLD P. HIGGINBOTTOM: Nitrosation of Linear Phenol-Formaldehyde Polymers 3617

H. R. ALLCOCK and R. L. KUGEL: Ionic Polymerization of Diphenylvinylphosphine Oxide 3627

ARIEL OTTOLENGHI, SAMUEL BARZAKAY, and ALBERT ZILKHA: Anionic Polymerization of Acrylonitrile by Various Catalysts .. 3643

ROBERT H. HORROCKS and EUGENE C. WINSLOW: Oxine–Formaldehyde Polymers and Their Metallic Chelates 3655

Book Review

Makromolekulare Stoffe, Part II, Vol. XIV, Methoden der Organischen Chemie (Houben-Weyl), E MÜLLER, Ed. Reviewed by NORBERT M. BIKALES 3665

Errata

O. C. HANSEN, T. L. FABRY, L. MARKER, and O. J. SWEETING: Apparatus for Measuring the Dynamic Modulus of Thin Polymer Films (article in *J. Polymer Sci.*, **A1,** 1585–1600, 1963) 3666

M. WALES and S. J. REHFELD: Molecular Weight Distribution by Velocity Ultracentrifugation (article in *J. Polymer Sci.*, **62,** 179–196, 1962) 3666

Author Index Volume 1 3667

Subject Index Volume 1 3678

Manuscripts should be submitted to one of the members of the Editorial Board or to the Editorial Office, c/o H. Mark, Polytechnic Institute of Brooklyn, 333 Jay Street, Brooklyn 1, New York. Those in Europe should be submitted to Professor G. Smets, University of Louvain, Louvain, Belgium, and those in the United Kingdom to Sir Harry W. Melville, Department of Scientific and Industrial Research, 5–11 Regent Street, London, S. W. 1, England. Address all other correspondence to Interscience Publishers, a Division of John Wiley & Sons, Inc., 605 Third Avenue, New York 16, New York.

WILEY BOOKS

Two Important New Interscience Books for the Polymer Chemist . . .

MORPHOLOGY of POLYMERS

Edited by T. G. Rochow, *American Cyanamid Company*. Includes the papers presented at the American Chemical Society Symposium, held at Los Angeles, California, April 4–5, 1963. The symposium was organized to consider the parameters of morphology, composition, and properties on four levels of *macromolecular organization*. The book offers unique and comprehensive coverage of macromolecular domains, morphology of surfaces, the crystalline phase, and the polyphase systems. (Journal of Polymer Science, Part C: POLYMER SYMPOSIA, No. 3).

1963. Approx. 144 pages. Prob. $6.00.

An INTRODUCTION to CLAY COLLOID CHEMISTRY

By H. Van Olphen, *Exploration and Production Research Division of Shell Development Company, A Division of Shell Oil Company*. This book develops a thorough understanding of modern concepts in colloid and surface chemistry and their applications to specific clay systems. It considers not only the effect of changes in fluid composition on the forces acting between suspended clay particles, but also the consequences of these changes on the bulk physical and mechanical properties of important clay suspensions. Mathematical formulations of modern colloid science are avoided in the main text, and only the gist of the theoretical approach is discussed. For the benefit of those engaged in physicochemical clay research, however, the author has provided an appendix offering a survey of electric double-layer computations as they apply to clay systems.

1963. 301 pages. $10.00.

send for on-approval copies

INTERSCIENCE PUBLISHERS

a division of

JOHN WILEY & SONS, Inc.

605 Third Avenue **New York, N. Y., 10016**